Spring 5-14-2016

Functionalization of Metal Oxide Surfaces through Chemical Reactions and Physical Adsorption

Gabriel C. Graffius
gabriel.graffius@student.shu.edu

Functionalization of Metal Oxide Surfaces through Chemical Reactions and Physical Adsorption

By:

Gabriel C. Graffius

Dissertation submitted to the Department of Chemistry and Biochemistry of Seton Hall University in fulfillment of the requirements for the degree of

Doctor of Philosophy

March 2016

South Orange, New Jersey

We certify that we have read this dissertation and that in our opinion it is sufficient in scientific scope and quality as a dissertation for the degree of Doctor of Philosophy.

APPROVED

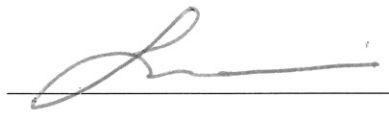

Alexander Y. Fadeev, Ph.D.
Research Mentor

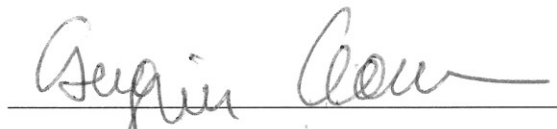

Sergiu M. Gorun, Ph.D.
Member of Dissertation Committee

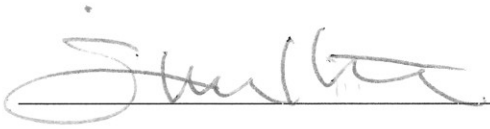

Stephen P. Kelty, Ph.D.
Member of Dissertation Committee

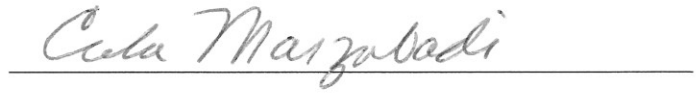

Cecilia H. Marzabadi, Ph.D.
Chair, Department of Chemistry and Biochemistry

Abstract

The synthesis of high surface area metal oxides is an area of extensive research with potential applications in catalysis, adsorption, and materials chemistry. The functionalization of a material's surface can dramatically change its physical and chemical properties. The research described herein is built on the foundation of traditional techniques used for synthesis, characterization, and functionalization of metal oxides and develops new mechanisms and materials for the functionalization of surfaces.

We began with Methyl-terminated poly(dimethylsiloxanes) (PDMSs), which are typically considered to be inert and not suitable for surface functionalization reactions because of the absence of readily hydrolysable groups. Nevertheless, these siloxanes do react with silica and other oxides, producing chemically grafted organic surfaces. Whether ignored or simply forgotten, this reaction provides a versatile, yet simple method for the covalent functionalization of inorganic surfaces. In this research, we explored the reactions of linear methyl-terminated and cyclic PDMS as well as bis-fluoroalkyl disiloxanes for the surface functionalization of mesoporous silica. FTIR and chemical analysis, as well as contact angle measurements and water adsorption confirmed the formation of high quality hydrophobic surfaces. An additional study of the reactions of silica with different degrees of hydration demonstrated the critical role of water in initiating the grafting of the siloxanes. We proposed a mechanism for the reaction that involved the hydrolysis of the adsorbed siloxanes by the Lewis acidic centers, followed by the coupling of silanols to the surface to produce grafted siloxanes.

We then explored Phthalocyanines (Pcs), an interesting class of catalytically active molecules with unique spectroscopic, photoelectric, and sometimes magnetic properties. This research involved a systematic study of the solution adsorption of two series perfluorinated Pcs on various surfaces to generate heterogeneous Pc materials for several applications. Initial adsorption studies focused on metal oxides and functionalized silicas in acetone. Characterization of the adsorption was performed by solution UV/Vis, solid-state reflectance UV/Vis/NIR, and elemental analysis. Additional mechanistic studies focused on the role of Lewis acid/base interactions between the electron donating surfaces and electron deficient Pcs. Comparison studies were completed in a moderately polar, non-coordinating solvent, methylene chloride. Our results demonstrated solution adsorption as a viable technique for the production of phthalocyanine thin films on metal oxide surfaces.

To my family:

My wife, Adrienne

My Parents, Donald and Linda

"It is evident that an acquaintance with natural laws means no less than an acquaintance with the mind of God therein expressed."

-James Joule

Acknowledgements

I would like to sincerely thank the following individuals for their support and guidance; their willingness to always help made my tenure at Seton Hall University most enjoyable.

Dr. Alexander Y. Fadeev: For teaching me to go beyond 'good enough' in my research. His supervision kept me focused and his mentorship taught me many things, directly and indirectly related to my research. I am forever grateful of the time he dedicated to increasing my abilities as a scientist.

Dr. Sergiu M. Gorun: For investing much of your time into my work at SHU, for introducing me to phthalocyanines and expanding the scope of my research. His support and energy helped drive me to seek out unique solutions as problems arose and ask 'why?' at each new discovery.

Dr. Francis Bernardoni: For introducing me to the graduate program at Seton Hall University and being my Merck-based mentor. Thank you for all of the training, discussions, and input in the area of surface science.

Dr. Naijun Wu, Theresa Natishan, and Rebecca Evans: For supporting my academic aspirations. Each has contributed greatly to my growth as a chemist.

I would also like to thank my friends in Dr. Fadeev's research group who provided friendship and support during my tenure: **Kyle Eckenroad, Karthik Jayaraman, and Dr. Edwin Vega**.

I would also like to acknowledge Dr. Gorun's research group for their input into the phthalocyanine studies. Specifically, **Dr. Hemantbhai Patel** and **Erik Carrion** for synthesis and isolation of the phthalocyanines, as well as **Ryan Cohen** for purification and NMR characterization of zinc phthalocyanines.

Table of Contents

List of Figures

List of Tables

Chapter 1 : Synthesis, Modification and Characterization of Porous Materials

Image reproduced from ref 45 with permission from Elsevier, 2011

1.1 Introduction

The focus of this work was the functionalization of metal oxide surfaces through chemical reactions and physical adsorption. It is, therefore, important to provide a summary of the methods and theory used throughout this work. The first steps in each process described herein, were synthesis and characterization the metal oxide materials that were to be modified. Adsorption or covalent functionalization were then used to modify the surfaces. Finally the resulting materials were characterized mechanisms used to obtain them.

In this chapter, the methods for synthesis of high surface area metal oxide materials, specifically silicas, will be summarized. The techniques commonly used to characterize these materials will then be described. A discussion of methods used for the modification of surfaces will also be included. Finally, the methods used for the characterization of the modified hydrophobic surfaces will be detailed. This collection of procedures and theory provides the foundation for understanding the research we have conducted.

1.2 Metal Oxides: Surfaces and Characterization

Metals and Metal oxides are abundant materials with countless applications in daily life. As solids, these materials are beneficial for their rigidity and resistance to stress.[1] The more common of the two in nature are metal oxides; a mixture of at least one oxygen and one metal. Even 'pure' metals become oxidized quickly when exposed to air, causing the properties of the surface and the bulk to vary in these materials.[2] A simple description of metal oxide bulk crystal structure is based on a close-packed or nearly

close packed array of oxygen anions, in which metal cations occupy interstitial sites. For example, in the close-packed corundum (α-Al_2O_3) structure, cations occupy two thirds of the octahedral sites available in the hexagonal-close-packed (h.c.p.) oxygen anion array. In the rutile (TiO_2) structure, half of the octahedral sites are filled with oxygen in the h.c.p. structure.[3]

In this work, however, we focus on the surface structure of the bulk materials being studied, as this is where interactions with the environment (e.g. adsorption and chemical reactions) occur. Surfaces, in fact, are energetically unfavorable. The surfaces of metal oxides differ from the bulk because they represent the termination of the crystal lattice and the point of exposure to chemical reactions with environment. The surface of solids are generally not flat, in fact, real solid surfaces are made up of a combination of flat regions, structural defects, and point defects. The arrangement of surface atoms depends on the plane preferentially exposed during the formation of the surface and according to the preparation or post-synthesis conditions of the bulk material.[4]

Of particular interest in this work are high surface area to volume (bulk) materials with a large interfacial region. High surface areas are achieved using nanoparticles or porous materials.[5] Some materials, like charcoal and silica-alumina, have irregular pores with widely variable diameters in a normal shape. Conversely, other materials such as zeolites and clay minerals have pores that are entirely uniform. [6] It is, in fact, quite difficult to synthesize materials that are not at least superficially porous.[7]

Though some of our studies utilized porous α-Al_2O_3 and TiO_2 nanoparticles, the majority of the work centered on synthesis, functionalization, and characterization of porous silicas (SiO_2). Specific properties of α-Al_2O_3 and TiO_2 used in solution

adsorption studies will be discussed in 0 3, but in-depth discussion of SiO_2 and its characterization is applicable to all areas of this research. Silica, therefore, will be used as the model material for a more detailed discussion of synthesis, characterization, and modification of metal oxides.

1.1.1 Synthesis of Porous Silicas

Silica and silicates are abundant materials, with the earth's crust being largely composed of these materials in some form. It is the principle constituent in rocks and its degradants: sands, clays, and soils. It is frequently utilized in building materials as natural silicate stones or as a component in manufactured materials such as cement, concrete, and glass.[8] Additionally, it has been a major component of technological advances as a semiconductor and microchip component.[2] As one can deduce from these uses, Si containing materials are generally highly stable materials available in many forms. Of particular interest is silica (SiO_2), which possesses a lattice structure of tetrahedral SiO_4 building blocks. Each unit is connected to the next by sharing an oxygen atom to give Si-O-Si bridges.[8]

Silicas have arguably been one of the most important substrates for surface functionalization, due to the myriad of reagents available that utilize various chemistries. The majority of our work also focused on porous silicas; materials with many applications that include drying agents, drug delivery, sensors, chromatography, and heterogeneous catalysis.[2,8,9] These versatile materials have been the focus of much study due to the variety of pore structure and particle morphology that can be produced. The synthesis and characterization of these materials will be discussed in further detail.

1.1.1.1 The Sol-Gel Process

The most commonly used process to produce porous silicas is the sol-gel process. It involves the complete hydrolysis of tetraalkoxysilanes under highly controlled conditions. It is also used for production of specialty metal oxide glasses and ceramics. The sol-gel process can be reduced to three basic stages: partial hydrolysis of metal alkoxides to form reactive monomers, the polycondensation of these monomers to form colloid-like oligomers (sol formation), and additional hydrolysis to promote polymerization and cross-linking to produce a three-dimensional gel.[8] More specifically, an example of initiation of the polymerization involves acid catalyzed hydrolysis of tetraethylortho silicate (TEOS):

$$H_3O^+ + Si(OC_2H_5)_4 \rightarrow HO - Si(OC_2H_5)_3 + C_2H_5OH + H^+ \qquad \textbf{(1 - 1)}$$

Continued hydrolysis would ultimately produce $Si(OH)_4$ (mono silicic acid), however, in this reaction it is more likely that rapid condensation of the mono silicic acid will occur as the reaction proceeds, due to its instability:

$$Si(OC_2H_5)_3OH + HOSi(OC_2H_5)_3 \rightarrow (C_2H_5O)_3Si - O - Si(OC_2H_5)_3 + H_2O \textit{ or,}$$

$$Si(OC_2H_5)_3OH + Si(OC_2H_5)_4 \rightarrow (C_2H_5O)_3Si - O - Si(OC_2H_5)_3 + C_2H_5OH$$

(1 - 2)

Multiple simultaneous reactions taking place in this system make controlling the polymerization highly complicated. The rate can be controlled by pH and ionic means. The rate of polymerization is proportional to the concentration of H^+ with pH < 2 and of OH^- with pH > 2.[8] Uncondensed SiOH groups quickly react to form siloxane bonds (Si-O-Si) and results in the formation of ring-like structures which further react and condense to form spherical units. The spheres in solution, known as the sol, can further combine to

form larger particles of a size that can be controlled by the pH of the solution. A pH of ~2 is the isoelectric point of silica, when it has no net charge. Below the isoelectric point the particles will not grow larger than 2-4 nm but can aggregate to form gel networks. At a pH above 7, particles will partially dissolve and be redeposited to form larger particles in a process called Ostwald ripening.[8] The negative charge of the particles at high pH will prevent aggregation of the gel beyond the desired size. Factors affecting the characteristics of the silica gel include: the size of the primary particle at the moment of aggregation, the concentration of particles in solution, the compactness of the network, the pH, salt concentration, and the temperature and time during which the gel is aged or treated.[8]

The sol-gel process can consistently deliver porous spherical particles of a uniform size distribution. However, the pores are simply the voids left between solid spheres in contact with one another. This leads to pores of different shape, a wide pore size distribution and high interconnectivity as demonstrated in Figure 1-1. Changes may be made to the process to deliver more consistency in the pores, but this may come at the expense of the spherical particles and uniform size distribution. The control of porosity is of great industrial importance in applications such as the design of heterogeneous catalysts, industrial adsorbents, membranes and ceramics. Furthermore, porosity is one of the factors which influence the chemical reactivity of solids and the physical interaction of solids with gases and liquids.[7]

Figure 1-1: Schematic of the Sol-Gel Process

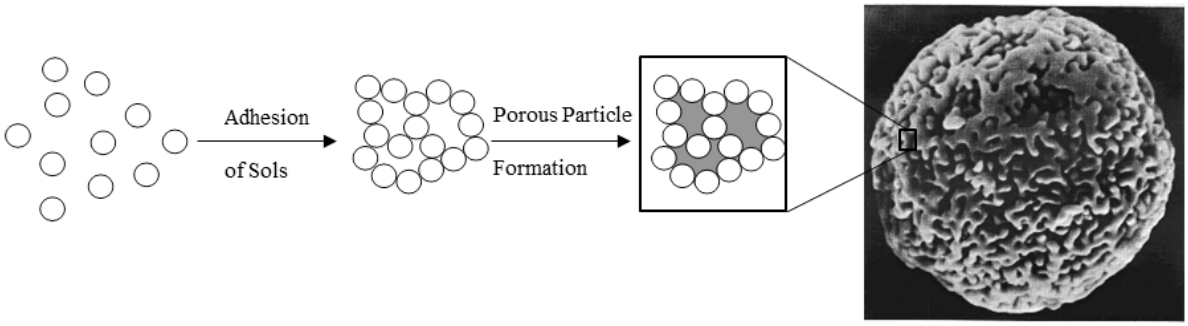

Figure 1-1: Formation of silica pores by the sol-gel process creates a porous with a pores of irregular shape within the particle *Picture reproduced from ref 11 with permission from Elsevier, 1979.*

1.1.1.2 Templated Mesoporous Silicas

Technical advances in various fields such as adsorption, separation, catalysis, drug delivery, sensors, photonics, and nano-devices all require development of ordered porous materials with controllable structures and systematically tailored pore architecture.[9] Structural changes to the pores of only a few nanometers can be impactful for growing number of applications. The IUPAC has defined cylindrical pores as *micropores*: pore internal width less than 2 nm; *mesopores*: pore of internal width between 2 and 50 nm; and *macropores*: pore of internal width greater than 50 nm.[7]

Ordered mesoporous silicas have been the focus of much attention since the discovery of the M41 family of materials by the Mobil corporation in 1992.[12] Since their discovery, ordered mesoporous particles have attracted much attention because of their various potential applications. These materials are stable structures with well-controlled and extremely narrow pore size distributions. They are highly porous, with high specific surface areas (500-1500 m^2/g). Formation of these particles was adapted from the sol-gel process, involving the hydrolysis and condensation of silica material in the presence of a micellular template. The proposed mechanisms are that the silica framework can

hydrolyze around a pre-formed liquid crystal mesophase (Figure 1-2, A) or by a cooperative self-assembly process (Figure 1-2, B).[13] Since then, various surfactants and reaction conditions have been optimized to produce a variety of mesoporous structures.[12]

Various ionic and non-ionic surfactants or water-soluble polymers have been used to prepare ordered mesoporous silica with pore sizes typically ranging between 2 and 10 nm. MCM-41[14] (MCM = Mobil Composition of Matter) and MCM-48,[15] for example, utilize the quaternary cationic surfactant under basic reaction conditions. The reaction is run at basic pH, taking advantage of the ionic interactions between the cationic surfactant and the anionic silica. In the MCM-41 reactions that we used, an additional restructuring step was included.[16] Briefly, 3.6 g of Aerosil, 6.0 g H_2O, 6.2 g of 25% tetramethylammonium hydroxide$_{(aq)}$ were combined in a flask and stirred. Separately, a

Figure 1-2: Synthesis of Templated Mesoporous Silicas

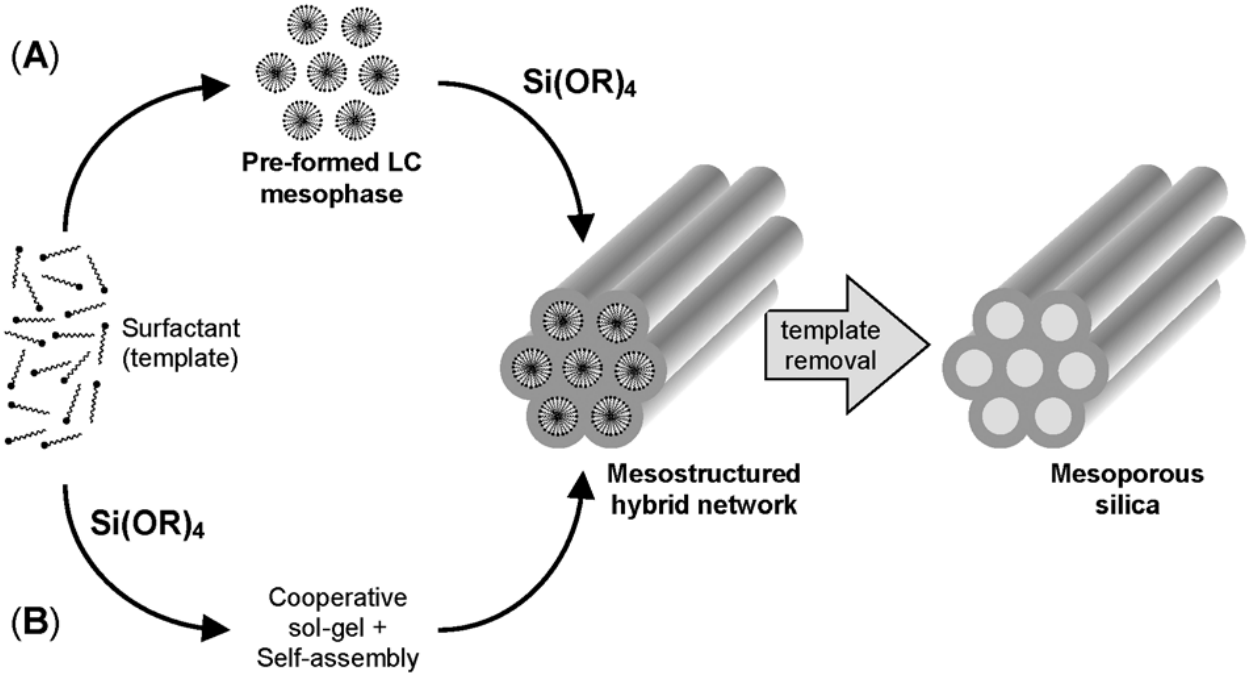

Figure 1-2: Schematic pathway for preparing surfactant-templated mesoporous silicas, illustrating a formation mechanism based on a preformed liquid crystal mesophase (A) or a cooperative process (B). *Reproduced from ref 13 with permission of the Royal Society of Chemistry*.

solution of cetyltrimethylammonium bromide (CTAB), 6.6 g of H_2O and 1.2 g of 30% ammonium hydroxide was prepared. The two solutions were combined and stirred at room temperature for 30 minutes. The solution was then transferred to an oven and aged at 70°C for 3 days. Prior to characterization (Figure 1-5a), the product was filtered and washed with water and acetone before being calcinated at 600°C for 6 hours.

Non-ionic surfactants are available in a wide variety of chemical structures. First introduced by Stucky *et al*[17] with SBA-15 (Santa Barbara Amorphous, Figure 1-3) and SBA-16. They are widely used to produce mesophases with different geometries and reagents. In this reaction, the pH is kept below 2 to ensure that the silica particles are in their cationic state to balance Coulombic, hydrogen bonding, and van der Waals interactions to enhance long range periodic order of the material. For example, in a typical SBA-15 (48/80) synthesis,[17,18] 5 g of the triblock copolymer, pluronic P123 [poly(ethylene oxide)$_{20}$–poly(propylene oxide)$_{70}$–poly(ethylene oxide)$_{20}$], was combined with 37.5 g of H_2O and 150 g of 2N $HCl_{(aq)}$ and stirred with heating at 35°C until the solution was opaque. The silica source, 10.6 g of TEOS, is added drop-wise to the solution. The reaction is allowed to proceed at 35°C for 20 hours. At this point the stirring is stopped and the batch is placed in an oven at 80°C for 48 hours. The resulting solid is filtered and washed with copious amounts of 2N $HCl_{(aq)}$, water, and then acetone. Calcination at 500°C for 6 hours removes excess water and surfactant, yielding the final product with S_{BET} ~500-700 m^2/g (Figure 1-5b). Pore size and surface area can be modified by adjusting concentration, oven temperature, and age time. We also noted that calcination time and temperature had an impact on surface hydroxyl groups and final S_{BET}. The greater hydrothermal stability and overall mechanical strength offered by the

thick pore walls, as well as large surface area and tunable pore size, give SBA-15 an advantage is many applications over MCM-41.

Figure 1-3: TEM Image of SBA-15 Particles

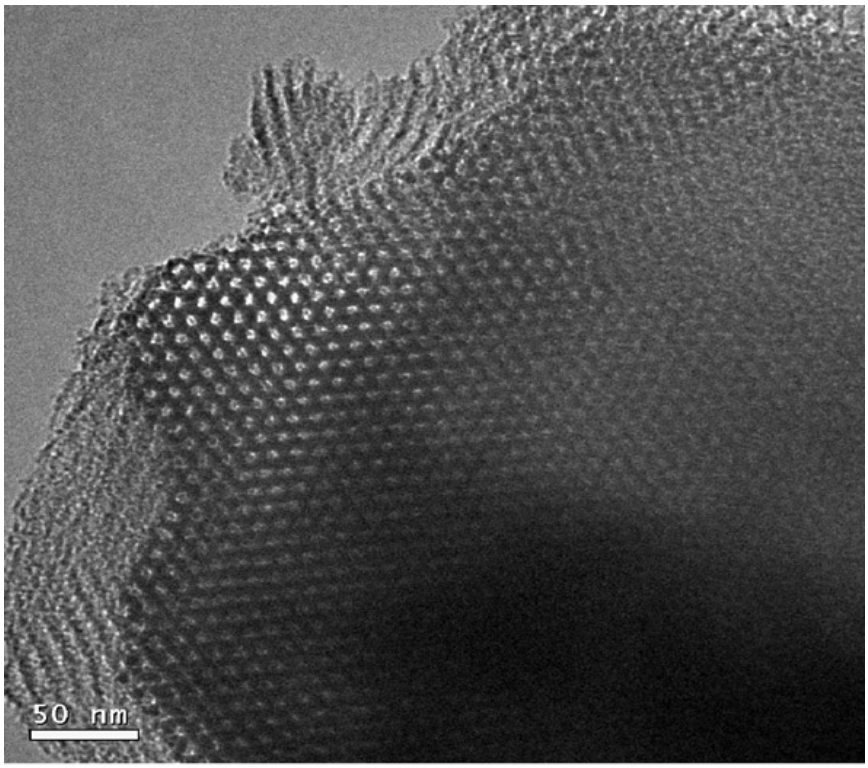

Figure 1-3: TEM image of an SBA-15 particle cross-section, demonstrating the hexagonal shape and ordered packing of the pores. *Reproduced from ref 19 with permission from the American Chemical Society, 2011.*

Finally, anionic surfactants, such as carboxylates, sulfates and sulfonates, can also be used in templated synthesis. They are often used in combination with the assistance of aminosilanes or quaternary aminosilanes such as 3-aminopropyltrimethoxysilane (APS) as co-structure-directing agents. As an excellent example, we experimented with the formation of helical mesoporous silicas with an anionic amino acid-based surfactant. In a typical synthesis,[19] a mixture of 9.4 g TEOS and 0.6 g APS was added to a solution of 1.3 g myristoyl alanine (C_{14}-L-Alanine), 1.2 g L-arginine, and 23 g deionized water with stirring at 30^{o}C. The mixture is allowed to react with stirring for 7 minutes and then

static conditions for 2 hours. The product is then placed in an oven at 80°C for 15 hours. The products are separated by centrifugation and dried at 100°C followed by calcination at 600°C for 8 hours. Based upon the intended application and desired properties of the material, the choice of procedure and synthesis conditions can be made.

1.1.2 Surface Area and Porosity

Most materials, to some extent, are porous. In fact, it is quite difficult to prepare a truly flat, non-porous solid. The presence of pores and surface defects will have an impact on several physical properties such as density, thermal conductivity, and strength.[7] The importance of controlling the porosity in many applications was discussed earlier in this chapter. There are several major methods for the characterization of pores including; stereology, radiation scattering, pycnometry, intrusion, adsorption-desorption from the gas phase, fluid flow, and calorimetry. Of these techniques, gas adsorption-desorption is the most popular. It is also the primary technique we used to characterize the materials we synthesized (Note: adsorption isotherms and adsorption-desorption isotherms are used interchangeably to describe the same technique). It is from adsorption that we obtain surface area, average pore diameter, total volume of the pores, surface energy, and hydrophobicity (from water adsorption). A detailed discussion of this technique is important to understand the materials we synthesize.

When characterizing a porous material, one should first obtain its surface area. This is most commonly measured by gas adsorption-desorption isotherms. Adsorption is the process whereby molecules from a gas or liquid are taken up by a solid surface via energetic interactions. Desorption is the reverse process in which adsorbed molecules are removed from a solid surface. Adsorption is distinguished from absorption which refers

to molecules entering into the lattice (bulk) of the solid material. Adsorption is governed by either physical (physisorption) or chemical (chemisorption) forces.[6] Gas adsorption for surface area measurements is physisorption at the critical temperature (T_c) at which the adsorbate is in equilibrium between the vapor and liquid phase at a particular pressure. A known quantity of the adsorbate gas is released to the sample (previously degassed with heat and vacuum to remove other adsorbed liquids and gases) and adsorption onto the sample occurs until equilibrium is reached. The difference between the amount of gas dosed and amount remaining is the quantity adsorbed, which is plotted versus the equilibrium pressure. Adsorbates commonly used in gas adsorption experiments include N_2, CO, CO_2, O_2, and the noble gases. Additional energetic information about a surface can be obtained with NH_3, CH_4 CH_3OH, H_2O, and C_6H_6 as adsorbates.[20] One can see that the adsorbate-adsorbent interactions would vary greatly, depending on the adsorbate utilized.

Nitrogen (N_2) adsorption at 77K and standard pressure is by far the most commonly used adsorption technique because of its availability, cost, and relative inertness. To simplify the descriptions in this discussion, the technique and theory for N_2 will be described, as it also applies to other adsorbates and conditions. In the adsorption experiments, the material being adsorbed (N_2) is called the adsorbate, and the solid is the adsorbent. Adsorption occurs by the physical forces acting between the solid and the gas molecules.[1] Depending on the nature of both the adsorbate and the adsorbent, the strength of these forces may vary. In a N_2 isotherm, the interactions are relatively weak and uniform, and the measurement of accumulated nitrogen on the surface of the material provides the surface area.

The initial theory to understand adsorption isotherms was developed by Irving Langmuir in 1918.[21] His assumptions, that most notably include adsorption of only a monolayer, make the equation not applicable to porous solids. Yet, the Langmuir equation serves as the foundation of adsorption theory:

$$\frac{1}{n} = \frac{1}{Kn_m}\left(\frac{1}{P}\right) + \frac{1}{n_m} \qquad \textbf{(1 - 3)}$$

where p (p/p_o) is the adsorbate equilibrium pressure, and n and n_m are the adsorbed weight and monolayer weight. Though still applied today to chemisorption and type I isotherms, the Langmuir equation has largely been superseded by other equations.[22]

The Brunauer-Emmett-Teller theory is an extension of the Langmuir theory, but applies to the presence of multilayer adsorption. Among their assumptions, it is important to note that an adsorbed molecule can act as an adsorption site for a subsequent adsorption layer. This means that a point of the formation of a distinct monolayer does not occur. Rearranged to its linear form, the BET equation yields a straight line from approximately $0.05 \leq p/p_o \leq 0.35$, thus enabling the calculation of the quantity of N_2 present in a monolayer (n_m) without a distinct monolayer actually being formed:

$$\frac{1}{n\left[\frac{P}{P_0}-1\right]} = \frac{1}{n_m C} + \frac{C-1}{n_m C}\left(\frac{P}{P_0}\right) \qquad \textbf{(1 - 4)}$$

Imbedded within the BET equation is the C constant, an expression of the heat of adsorption throughout the experiment. This constant can be determined from the y-intercept when plotting the isotherm as a linear function. A C constant of approximately 100-200 would imply high surface energies, indicative of a large number of silanol groups on the surface of bare silica. A low C constant (~10-30) implies lower surface energies, often due to the presence of CH_2 and CH_3 functionalities, with increasingly more ordered alkylsilane groups providing lower C constant values. The C constant can

also be used as an indication of the presence of micropores due to the contribution of the energetic interaction of the adsorbate with pore walls.[23]

Furthermore, from the value we obtain for n_m the specific surface area (S_{BET}) can be calculated by

$$\boldsymbol{S_{BET} = \omega n_m N_A} \qquad \textbf{(1 - 5)}$$

when N_A is Avogadro's number and $\boldsymbol{\omega}$ is the cross-sectional area of molecular nitrogen. It is important to carefully determine the cross-sectional area of the adsorbate. When using N_2 one must consider that the molecule is not spherical, as is generally assumed for adsorbates. The cross-sectional area of N_2 is highly dependent on the surface energy of the material to which it is adsorbing. It has been determined, that on highly energetic surfaces, such as SiO_2, the orientation of N_2 is upright with a cross-sectional area of 13.5 $Å^2$. For a low energy surface, such as C_{18} modified silicas, a cross-sectional area of 16.2 $Å^2$ is used because it will lay flat on the surface.[24]

Adsorption-desorption isotherms can be further applied to characterize the pores of materials. The pores of particles can have many different sizes and shapes, as is demonstrated in Figure 1-1 and Figure 1-3. It was Dubinin, who first observed that the mechanism of physisorption differed between very narrow pores, wider pores, and the open surface. This is due to the energy of interaction between the adsorbate and the pore walls.[25] For the sake of consistency, the IUPAC has defined pore sizes by the diameter of an assumed cylindrical pore as its pore-width. *Micropores* have widths less than 2 nm and adsorption is dominated by interactions of the adsorbates with the walls, *macropores* have widths larger than 50 nm, and they are so wide that they act as flat surfaces during adsorption. *Mesopores* are 'just right' and have widths between 2 and 50 nm and have

both types of interactions present as well as the occurrence of pore condensation,[7] which will be discussed in further detail.

The IUPAC has also established six classifications for adsorption isotherms, demonstrated in Figure 1-4. The Type I isotherm is referred to as the Langmuir isotherm because it appears to represent monolayer coverage, however, it also applies to multilayer adsorption on microporous adsorbents. Type II isotherms (S-shaped) are monolayer-multilayer isotherms obtained with nonporous or macroporous adsorbents. Type IV is the isotherm of greatest interest to us, it includes the presence of a hysteresis loop because of capillary condensation of the adsorbate within mesoporous materials. The SBA-15, MCM-41, and Davisil silica materials that we utilized all present Type IV isotherms in N_2 adsorption experiments. Types III and V isotherms are materials with weak adsorbate-adsorbent interactions, with Type V displaying capillary condensation. Finally, Type VI isotherms represent mixed materials with a high degree of surface uniformity in stepwise groupings.[20]

Similar to the energetic interactions described for a vapor with a solid surface, a liquid can interact with a solid and 'wet' the surface. The energy of this interaction can be visualized by capillary action and formation of a meniscus. This phenomenon is present in porous materials at capillary condensation because the vapor pressure of the curved surface is higher than that of a flat surface. Thus, condensation of the adsorbate in pores occurs at a pressure lower than atmospheric pressure, correlating to the pore size. This is expressed in the Kelvin equation;

$$\ln\left(\frac{P}{P^o}\right) = \frac{-2\gamma V_L}{RT} \cdot \frac{1}{r_m} \quad \textbf{(1 - 6)}$$

when P/P^o is the partial pressure of vapor in equilibrium with a meniscus having a radius of curvature r_m, γ is the surface tension of the liquid and V_L is the molar volume of the liquid. Macropores will not demonstrate capillary condensation due to a pore size too large for this phenomenon.[22]

Figure 1-4: Classifications for Adsorption Isotherms and Hysteresis Loops

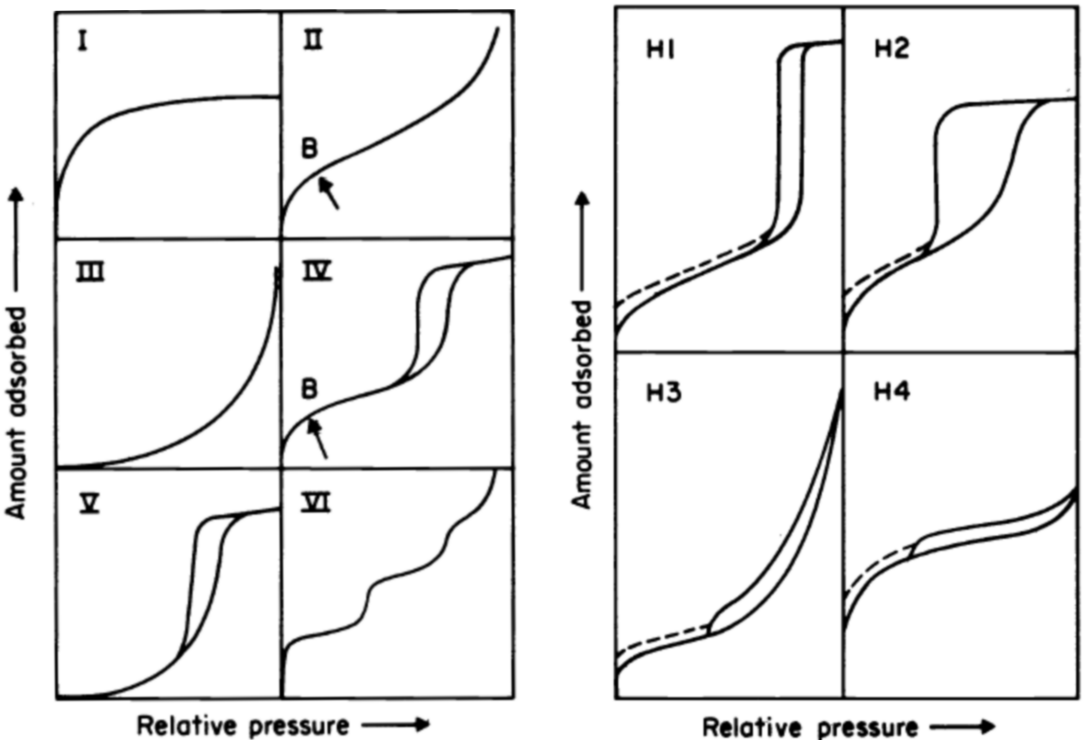

Figure 1-4: IUPAC System of Classification for adsorption isotherms (a) and hysteresis loops (b). *Reproduced from ref 22 with permission from Springer, 2004.*

It is important to carefully consider the assumptions made in both the BET equation and the Kelvin equation and understand their limitations. Several adjustments have been made to the basic theory that are not included in this review, references [20] and [22] are excellent sources for this information. It is, however, noted that the Kelvin equation does not account for fluid-wall interactions or the existence of the multilayer

film already present in the pores at capillary condensation. If these factors are accounted for, the modified Kelvin equation is obtained

$$\ln\left(\frac{P}{P^o}\right) = \frac{-2\gamma cos\theta}{RT\Delta\rho(r_p - t_c)} \qquad (1 - 7)$$

where t_c describes the statistical thickness of the multilayer prior to the capillary condensation. These values were obtained experimentally by the analysis of standard isotherms of nonporous materials in what is called a t-plot.[20] The modified Kelvin equation is used for pore size analysis of mesoporous materials in the Barrett-Joyner-Halenda (BJH) method.[26] Though detailed analysis is limited to mesoporous materials, the micropore volume can also be determined using the t-plot. There are several other pore analysis techniques with various advantages and disadvantages not included in this discussion.

A limiting factor in determination of the pores is the cross sectional area of the adsorbate. Adsorbates such as Argon and water vapor can be used for the analysis of pores smaller than those for which N_2 can be used. For example, Naono *et al*[27,28] determined pore size distribution curves for various adsorbents from the isotherms of both water and nitrogen gas. They showed that when water was used, pore size distribution can be calculated for pores with a radius of 0.9 to 1.1 nm while the limit for N_2 was 1.7 nm.[27]

In addition to being able to determine the pore size, the steepness of the capillary condensation and the shape of the hysteresis loop is an indication of the pore size distribution, pore geometry, and pore connectivity. The hysteresis loop present in a porous material is further categorized in four groups by the IUPAC, as displayed in Figure 1-4b. Type H1 is associated with porous materials with well-defined cylindrical-

like pore channels, like the SBA-15 silicas displayed in Figure 1-3. Type H2 is associated with disordered pores with a wide distribution of pore size and shape. Davisil silicas are an excellent example of materials with an H2 hysteresis. Type H3 is not common, but is associated with slit-shaped pores. Finally, Type H4 isotherms are associated with microporous region slit-shaped pores.[20]

The hysteresis loop is a very important part of the adsorption curve and the source of some disagreement when calculating the pore size. Hysteresis is present because of non-ideality of the meniscus in either the adsorption or desorption. It was initially suggested that the pore condensation occurred by a cylindrical meniscus, while the evaporation occurred from a hemispherical meniscus.[22] However, recent theory, confirmed by Non-Local Density Functional Theory (NLDFT), suggests that metastable states may exist between the vapor-like state and formation of the liquid phase. In the independent pore model, pore condensation is delayed to a higher p/p_o resulting in artificially large pore sizes, this does not occur with evaporation by a receding meniscus. This theory applies well to a uniform, cylindrical-like porous material with an H1 hysteresis (Figure 1-4b) like SBA-15, but may not be ideal for materials with H2 hysteresis. For these materials, calculations of the pore size should use the adsorption because evaporation (desorption) in the non-uniform and interconnected pores is driven by the smaller bottlenecks present in the pores. In 'inkbottle' pores the desorption does not occur at the thermodynamic equilibrium and is, therefore, delayed.[20]

The total pore volume can be calculated at the point of maximum adsorption, the flat portion of the isotherm near saturation pressure (Figure 1-8). The rise in the isotherm

after this point is inter-particle condensation at saturation pressure. Here, the total pore volume (per gram of adsorbent) can be calculated as

$$\boldsymbol{V_{pore} = a_{max} V_L} \qquad \textbf{(1 - 8)}$$

when a_{max} is the point of maximum adsorption in mol/g and V_L is the molar volume of liquid nitrogen in mL/mol.

Figure 1-5: Nitrogen Adsorption-Desorption Isotherms of Mesoporous Silicas

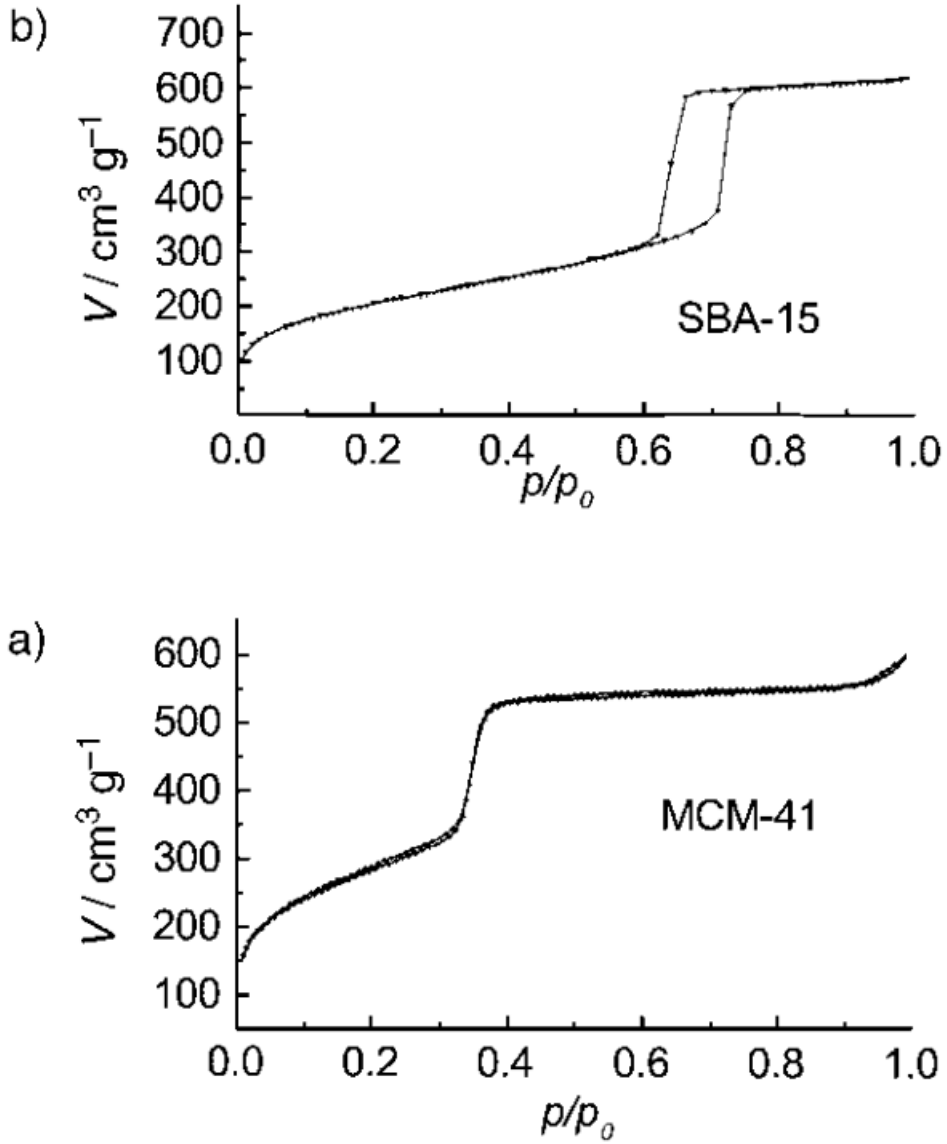

Figure 1-5: Nitrogen adsorption-desorption isotherms for MCM-41 (a) and SBA-15 (b). *Reproduced from ref* 29 *with permission from John Wiley and Sons, 2004.*

The gas adsorption techniques described herein are excellent for characterization of mesoporous materials. A common method for characterization of macroporous materials or inter-particle packing is intrusion, specifically mercury porosimetry. The accuracy of this method relies on knowledge of the contact angle (wetting) of mercury on the surface of the analyte material. Briefly, an external pressure is applied to the system to force mercury into the pores of the solid. The required pressure is inversely proportional to the size of the pores. The limiting factor in the analysis is the external pressure required for the analysis, limiting the breadth of materials for which this technique can be used.[20]

Careful control and understanding of the process of the formation of porous metal oxide solids is important for their varied applications. Of particular interest are ordered mesoporous materials, with uniform cylindrical-like pores. The variety of analyses used to characterize these materials aid the production of these materials and build an understanding of the chemistry present at the interface. The chemistry of the surface, however, may not be ideal for the application or long-term stability of the interface. Therefore, functionalization of the surface may be necessary.

1.2 Functionalization of Surfaces

The surface of a metal or metal oxide material is unique when compared to the bulk. Within the bulk, the physical arrangement of atoms and chemical bonding is mostly uniform, as the material has arranged itself into a thermodynamically stable conformation for the conditions under which it was synthesized. The surface, on the other hand, represents the abrupt termination of this order, and is subsequently exposed to the atmosphere, creating opportunities for new chemical bonds. The surface of inorganic solids, metal oxides in particular, is highly polar and exhibits high surface energies. They

often have a strong affinity for water present in the atmosphere, resulting in surface hydroxyl groups and/or layers of strongly bound water. 'Defects' in the surfaces can also create Lewis acid/base centers with different characteristics depending on the surrounding chemical bonds.[30] These features can be an advantage or a disadvantage, depending on the intended function of the material. However, the interfacial surface energy or reactivity of a solid can be modified simply by the functionalization of its surface. This changes the energy of solid-solid, solid-liquid, and solid-vapor interactions. Physical adsorption and a wide range of selective chemical reactions are used for modification of a bulk solid's surface.

The terms 'lyophilic' and 'lyophobic,' derived from the Greek words to describe a love (philos) or fear (phobos) of dissolving or mixing with (Lyo), as well as 'hydrophobic' and hydrophilic' (also Greek for "water fearing" and "water loving", respectively) are words that help to qualitatively describe the energy and intensity of interactions at the interface between a solid and liquid. Strong interactions with a lyophilic/hydrophilic material describe a polar surface. Weak interactions with a lyophobic/hydrophobic material describe non-polar surfaces. Hydrophobic surfaces are often prepared by modifying the surfaces with hydrocarbons (alkanes), fluorinated alkanes, and methylsiloxanes.[30] Herein, we will describe adsorption and covalent attachment as effective ways to modify the surface of metals and metal oxides.

In this discussion, two main ways in which the surface of a solid can be modified will be discussed. We will first detail physical adsorption – specifically strong or even irreversible adsorption (as opposed to the weak/reversible adsorption of gases we discussed in section 1.1.2) to produce relatively robust surfaces. Self-assembled

monolayers will be introduced as an interesting phenomenon that involves both physical adsorption and covalent attachment. Finally, covalent attachment is discussed, with a focus on organosilicon chemistry. At times, adsorption and covalent attachment may be occurring simultaneously. Disagreements in these mechanisms have arisen as a result of this cooperative functionalization, as is highlighted in chapter 2.

1.2.1 Physical Adsorption on Surfaces

All three states of matter can be adsorbed at a solid surface: gases (as discussed in section 1.1.2), liquids, and dissolved solids. The last two are adsorbed from a liquid solution, liquids from a composite liquid, and solids as a solute and represents a more simple system than that of a solution.[31] In general, adsorption can be an effective means of modifying surfaces with thin films. Adsorption is often divided into two sub-classes: physisorption and chemisorption, based upon the presence of absence electronic perturbation. Due to the formation of a chemical bond in chemisorption, we will discuss 'adsorption' to include only physisorption as we discuss covalent attachment separately. Within the discussion, one will observe that some monolayer formation is not fully understood, and the mechanism is either adsorption, covalent attachment, or a combination of both.

Techniques for the application of thin films include vacuum sublimation, painting, spray drying, dispersion in a polymeric binder, and mechanical rubbing. However, the ability to form uniform monolayers on surfaces often requires more elegant techniques. Adsorption of solute from solvent can be an effective way to form uniform surfaces, allowing the intermolecular forces to aide in the organization of the adsorbate on the

surface. Solute adsorption is used in many applications, such as chromatography, detergents, dyeing, pollution control, photography, and laboratory measurements.

Figure 1-6: Classification of Solute Adsorption Isotherms

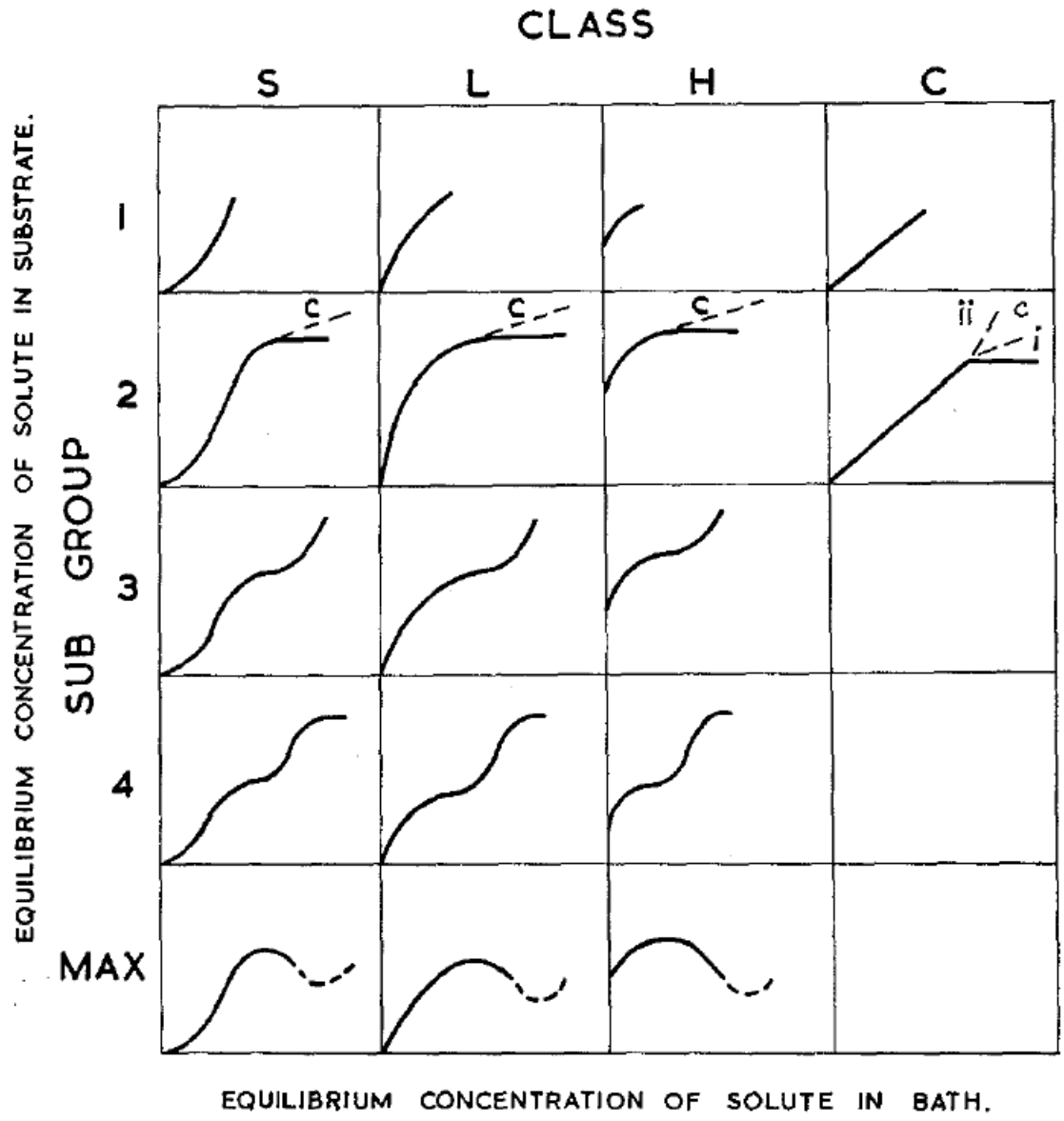

Figure 1-6: System of classification for solute adsorption isotherms. The four main classes: S, L, H, and C are shown along with the 5 subgroups. *Reproduced from ref 31 with permission from the Royal Society of Chemistry, 1969.*

Adsorption of solute from solution is a more complex system than that of gas adsorption under vacuum. Solute adsorption is most common when solubility is low, and the volume of the solvent is kept constant. Similar to vapor adsorption, the adsorption isotherms of solution adsorption present a powerful tool for understanding the interactions between the solute and the solid. At equilibrium, the quantity adsorbed (Γ) is plotted against the concentration (C_e) (as opposed to pressure, though both represent surface 'bombardment').[31]

Just as gas adsorption isotherms are carefully classified, so too are the solute adsorption isotherms.[31] Some of the classifications overlap, due to the similar interactions present in the two systems. Solute adsorption is divided into four main classes based upon the shape of the initial adsorption: S (S-shaped), L (Langmuir), H (High affinity), and C (constant partition). Subgroups further classify the adsorption isotherms at the latter part of the isotherm.[31] A comparison of the solute classification system is provided in Figure 1-6.

Adsorption of solute from solution is a more complex system than that of gas adsorption under vacuum. In solution adsorption the effect of solute-solute, solute-solvent, solute-substrate, and solvent-substrate interactions must be considered. Solution adsorption studies can be characterized by the equation[32]

$$\boldsymbol{\Gamma = \frac{\Gamma_{max} K_L C_e}{1 + K_L C_e}} \qquad \textbf{(1 - 9)}$$

with the Langmuir constant (K_L) defined as

$$\boldsymbol{K_L = \frac{N e^{E/RT}}{\Gamma_{max} \nu \sqrt{(2\pi MRT)}}} \qquad \textbf{(1 - 10)}$$

when Γ is the equilibrium concentration of the adsorbent, C_e is the equilibrium concentration of adsorbate in solution, Γ_{max} is the maximum monolayer adsorption

capacity. For K_L, N is Avogadro's number, E is the energy of activation for the removal of solute from the substrate, v is the frequency of oscillation of the adsorbate molecules perpendicular to the surface, M is the molecular weight of the adsorbate, R is the gas constant, and T is the temperature.

Some factors to consider when obtaining E are that the solute is a dilute solution in the solvent '*B'* (if a mixture, the additional component is 'C'). The solvent may be adsorbed to the substrate in competition with the solute, so the energy of activation of its removal (E_B) should also be taken into account. Thus the energy of activation for the removal of the solute 'A' should be expressed as[30]

$$\boldsymbol{E = E_A^0 - E_B - E_C} \qquad \textbf{(1 - 11)}$$

It is important to note that the interactions between adsorbed molecules can impact the energy of activation for the removal of solute. Such is specifically the case with S-type adsorption isotherms. If the molecule is strongly attracted to the surface, but has negligible interaction with neighboring solute, the E_A is independent of the presence of neighboring adsorbed molecules. This would be the case for L-type adsorption. However, if the solute-solute forces are significant relative to the solute-substrate forces, then the E_A will increase with the presence of neighboring solute and 'cooperative adsorption' occurs. In this situation, E_A varies with Γ to the power (n) during the adsorption study.[30]

$$\boldsymbol{E_A = E_A^0 + \Delta E_A \Gamma^n - E_B - E_C} \qquad \textbf{(1 - 12)}$$

If we consider both the L-type and S-type isotherms, when Γ approaches Γ_{max} the slope of the adsorption curve begins to shallow to a 'knee' shape as the number of sites remaining for adsorption decreases. However, in the special case of the C-type isotherm the linear shape indicates that the number of available sites remains constant throughout

the solute concentrations up to saturation. This means that the surface available expands proportionally with Γ. The other special case is the H-type isotherm when adsorbate-substrate affinity is very high ($E_A^0 >> (E_B + E_C)$), thus the resulting $\delta \Gamma/\delta C_e$ is very high.[30]

In subgroup 1, the adsorbate monolayer has not been reached, likely due to experimental difficulties related to solubility. In subgroup 2 and higher, the plateau of "Point B" is reached, signifying the completion of the first monolayer. The subsequent rise (subgroup 3) represents the development of a second layer which is completed in subgroup 4. This trend could continue with additional layers. Energetically, the 'surface' is not solely made up of the solute particles, as opposed to the substrate, and are generally weaker, often producing an s-type curve. The final subgroup, *max*, often occurs when solutes associate in solution (often aqueous solutions) during the adsorption process. With an increase in solution concentration a point is reached at which the solute-solute interactions overcome the solute-substrate interactions so that some solute is desorbed form the surface.[31]

1.2.2 Self-Assembled Monolayers

The process of formation of closely packed monolayers, often via cooperative adsorption with relatively high ordering is referred to as surface self-assembly, and the monolayers prepared as self-assembled monolayers (SAMs).[30] In nature, self-assembly results in super-molecular hierarchical organization of interlocking components that provide very complex systems.[33] The anatomy of a SAM material includes a surface-active head-group, an alkyl chain, and a unique interface group. Spontaneous formation

of the assembly includes surface interaction at the head-group and intermolecular interactions of the tail group.

The earliest works of preparation and wettability studies of these ordered monolayers of long-chained amphiphylic molecules supported on metals and metal oxides were first described by Zisman in 1946.[30] SAMs on metals and metal oxides are the most studied, best characterized and most easily controllable. They produce a range of materials that are flat and stable, and can be highly ordered or disordered.[34] Further research on SAMs were those derived from alkyl-trichlorosilanes on glass and from di-n-alkyl disulfides compounds in dilute solutions adsorbed on gold and other metals.[33] Since these early studies, there have been thousands of publications on synthesis, characterization, and applications of SAMs. Good SAMs can be prepared via reactions or adsorption of various long-chain aliphatic acids (carbonic, phosphonic, phosphoric, hydroxamic, thiocarbonic, etc.) with metals and metal oxides.[30]

SAMs are differentiated from covalently attached monolayers (CAMs) because each molecule does not have a chemical bond with the surface, allowing closer packing and alignment as demonstrated in Figure 1-7. Stability is achieved by intermolecular interaction, cross-linking bonds, and periodic covalent attachment or ionic or hydrogen bonding of the head group.[35] The molecular structure of SAMs is influenced by the metal substrate, the type of bonding with surface, and the chain length of the alkyl group.

The reactions of alkyl-trichloro and alkyl-trimethoxysilanes are well studied and produce SAMs on a variety of solids. The self-assembly process is reasonably well understood, and the importance of temperature, solvent, and surface water has been examined. The reaction proceeds via hydrolysis of $RSiX_3$ with the formation of

Figure 1-7: Surface Functionalization with Chlorosilanes

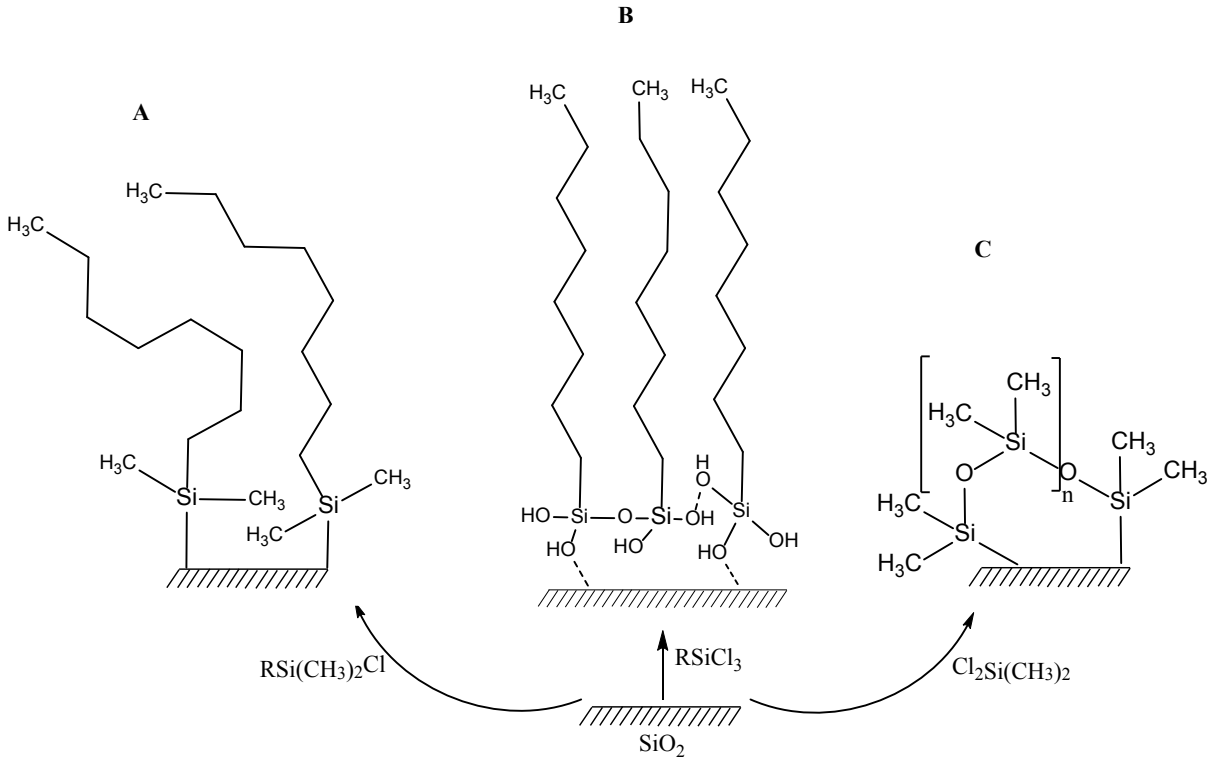

Figure 1-7: Different synthetic strategies for surface functionalization using organosilicon chemistry. Using (A) monofunctional alkylsilanes to produce CAMs; (B) trifunctional alkylsilanes to produce SAMs; (C) difunctional alkylsilanes to produce oligo(dimethylsiloxane) layers.

$RSi(OH)_3$ intermediates. Upon formation, trisilanols assemble on the surface into a closely packed monolayer, which is stabilized by 'vertical' (Si_s-O-Si and Si_s-OH…HO-Si) linkages, and by van der Waals interactions between alkyl chains. The best $RSiX_3$ monolayers are composed of closely packed close-to-vertical chains in an extended all-trans conformation.[30]

The reaction temperature and the amount of adsorbed water are, potentially, the most critical parameters for the preparation of the most closely packed and ordered SAMs. If conditions are not carefully controlled, polymerization and distortion of the SAM occurs. Surface bound water initiates the reactions and temperature is used to

control the kinetics of formation of the SAMs and the rate at which surface reactions take place. SAMs are generally formed at close to room temperature conditions. An excess of water leads to disordered surfaces, while insufficient water leads to low grafting densities. Rigorously dried surfaces may not react at all at room temperature. It has been suggested that surface water acts as a lubricating layer and a source of hydrogen bonding to produce ordered SAMs. Surface water accounts for surface interactions and SAM formation on materials that are not reactive with the head group.[30]

Stable SAMs have been formed on many metal and metal oxide surfaces. Lateral binding between head groups and van der Waals forces between hydrophobic tails play an important role in the self-assembly process. Head groups are immobilized to the surface by adsorption or ionic or covalent attachment at periodic sites on the solid or by hydrogen bonding stabilization with surface bound water. SAMs represent one of the most complex and elegant areas of study in surface science.

Another interesting adsorption method is the Langmuir-Blodgett technique, which is used in the preparation of uniform thin films with controllable thickness and packing. Very simply, a thin layer of amphyphilic solute dissolved in a volatile solvent is allowed to assemble evenly on the surface of a liquid, usually water. The substrate is then slowly immersed in the liquid and the solute is transferred onto its surface and the solvent evaporates, leaving a deposited layer for solute. Subsequent emersion steps add layers to the surface of the substrate. Though the technique produces uniform thin films, often these films are easily distorted or displaced by external forces. To increase stability, a post-formation treatment may be implemented to 'cure' the materials. Langmuir-

Blodgett films have been explored for applications in electronics, optics, chemical sensors and biochemical probes.[36]

Adsorption plays an important role in the functionalization of materials, either as the direct method or by being utilized in a cooperative function. Stable, uniform surfaces can be obtained by multiple adsorption techniques. However, covalent attachment may be necessary for the long-term stability of the surface.

1.2.3 Covalent Functionalization of Surfaces

The covalent functionalization of surfaces is widely utilized in various applications due to production of stable and reproducible monolayers with excellent stability provided by covalent bonds. These materials have obvious advantages over SAMs or adsorbed layers in applications which would cause prolonged stress at the surface, such as pressure and pH stress in chromatography, or wide temperature ranges for protective coatings. A variety of reactive head groups are used for covalent attachment including; silanes, phosphonates, carboxylates, catechol, and amines.[37] Our work focuses specifically on organosilicon chemistry.

Under certain conditions, surface functionalization is initiated when the readily hydrolysable group reacts with water to produce silanols that are highly reactive with M-OH groups. The silanols begin to align by hydrogen bonding with the M-OH prior to covalent bonding with the surface. Robust surfaces are produced with silicas due to the strength of the Si_s-O-Si bond. The reaction proceeds well with other metal oxides, though the M-O-Si bond is not as strong.[37] The packing of molecules in CAMs on silica are relatively high (0.36-0.45 nm^2/molecule, monofunctional), indicating production of

uniform monolayers. SAMs, by comparison, obtain monolayers with spacing of only 0.2-0.22 nm^2/molecule.

For lyophobization, only a limited number of groups are utilized, and the grafting density is important to determine the exposed functionality. The lowest surface energy materials are composed of perfluoroalky groups (CF_3), $\gamma_{SV} < 12$ mJ/m^2. Next are surfaces of fluoromethylene (CF_2), methyl (CH_3), dimethylsiloxane (DMS) [$OSi(CH_3)_2$] groups at $\gamma_{SV} \sim 20\text{-}22$ mJ/m^2, followed by exposed CH_2 at $\gamma_{SV} \sim 25$ mJ/m^2. One reason that SAMs can have superior hydrophobicity to CAMs is the exposed CH_3 at the interface instead of a mixture with CH_2 (Figure 1-7). The presence of virtually any other non-fluorinated functionality increases the surface energy of the solid relative to these examples.[38]

Organosilicon chemistry is widely used due to the variety of reagents and the production of strong, covalent bonding on the surface of solids. Specifically, organosilanes with the general formula $R_{4-n}SiX_n$ (n = 1, 2, 3), when X is a readily hydrolysable group (X = Cl, OR, NR_2 H, etc.), are powerful reagents for chemical surface functionalization for several reasons. First, organosilanes with a large variety of R groups are available commercially, enabling the preparation of surfaces with all of the major organic functionalities. Second, the resulting surfaces have good thermal and chemical stability due to strong Si-O linkages with the surface. Third, the silanes have high synthetic versatility by varying the number of reactive 'X' groups. Mono (n = 1), di (n = 2), and trifunctional (n = 3) silanes obtain monolayers with similar functional groups but varied molecular organization. For example, monofunctional silanes will produce

covalently attached monolayers (CAMs), while trifunctional silanes will produce SAMs (Figure 1-7).[30]

Similar to the formation of SAMs, temperature and surface bound water also play an important role when producing CAMs. Side reactions may occur when using organosilanes, as the reactive alkylsilanols can react with one another to form larger polymers on the surface or terminate the reaction. This is why difunctional and trifunctional organosilanes are not used as frequently to produce CAMs. Addition of an 'R' group with functionality other than an alkane influences the conditions necessary for control of the reaction. For example, fluoroalkylsilanes currently produce the lowest energy (most lyophobic) surfaces. Several reactions for fluoroalkyl (X= Cl, OR, H, NH_2) have been reported, though special care is taken to control the reaction. The presence of the fluorinated moiety in the molecule affects the surface reactions in several ways: due to its electron withdrawing properties, the Si-X group has higher reactivity; high reactivity but poor solubility in solvents used for silanization improves adsorption prior to reaction, explaining their higher reactivity with surfaces; fluoroalkylsilanes react more quickly with moisture and, therefore, must be handled with great care to avoid aggregation and deposition of polymeric layers on the surface.[30]

Dimethylsiloxanes (DMS) groups present an alternative to the CH_x and CF_x groups in constructing hydrophobic surfaces. Polydimethylsiloxane (PDMS) has a flexible backbone, and superior thermal properties. These properties set them apart from other materials and provide attractive features for using siloxane chemistry for the design of low-energy surfaces with non-aliphatic architecture. Solid supported PDMS surfaces can be prepared via vapor-phase and solution phase reactions of $(CH_3)_2Cl_2$ (Figure 1-7) and

($Cl[Si(CH_3)_2O]^n$-$Si(CH_3)_2Cl$, n=1-4) with minerals in the presence of adsorbed water. Reactions are also strongly influenced by the degree of hydration on the surface.[30]

Reactions with dry silicas yielded surfaces with, approximately a single layer of PDMS chains grafted to the surface via two Si_s-O-Si bonds. The average area per $[OSi(CH_3)_2]$ unit was 0.42 nm^2, indicating a horizontal orientation. When saturated with vapors, PDMS layers had 11 dms/nm2 indicating 'vertical' orientation. Studies conducted with FTIR indicated formation of linear OH-terminated oligomeric DMS units. These units react with the surface (and each other), forming a surface of cyclic oligo-(DMS) grafted to silica via two Si_s-O-Si bonds containing more than 6 DMS units.[39] The amount of grafted DMS can be controlled with high precision by varying the amount of water pre-adsorbed on silica. In chapter 2, we will introduce an alternative means of producing DMS modified surfaces using methyl-terminated PDMS.

The large variety of R groups available in organosilicon chemistry allows functionalization beyond hydrophobization. It is important to choose an R group with a reactive moiety that is not reactive with the surface or Si-O bonds. Once the surface is protected by the monolayer, subsequent reactions may be performed at the new interface. For example, catalysts may be attached in a post-functionalization reaction and create a recyclable heterogeneous catalyst for use in flow chemistry.[40] Functionalization has also been used to immobilize silica nanoparticles on cellulose, simply by introducing the proper reactive functionalization via a cyanate reaction.[41]

In the synthesis of modified surfaces using organosilicon chemistry, some of the problems with the reagents have only been briefly discussed. Undesired reactions with the moisture in air lead to undesired products. Additionally, byproducts of the reactions,

such as HCl from chlorosilanes, can corrode some substrates and disrupt the uniformity of the resulting surface. When X is H or alkoxy, the by-products are more benign (H_2 or alcohols). In chapter 2, we propose a reaction with methyl-terminated PDMS with H_2O as the only by-product.

1.2.4 Characterization of the Functionalized Materials

After the modified materials have been produced, a very important step is the characterization of the resulting functionalized materials. One must first obtain the extent of the surface functionalization, followed by the characteristics of the new surface. There are various techniques for the characterization of functionalized materials, the most attention will be placed on the techniques used frequently in this work.

Fourier transformed infrared spectra (FTIR) of the solids before and after modification can provide a wealth of information about the new surface. The main features of bare silica are well established and studied. These include a sharp peak at ~3750 cm^{-1} for surface silanols (Si_s-OH), two broad peaks at 3400-3550 and ~1650 cm^{-1} for adsorbed water and hydrogen bonded silanols, and several bands at ~1100, 820, and 450 cm^{-1} for siloxane network bonds.[42] After surface modification, the use of a subtracted spectrum and analysis of the unique peaks from the 'neat' chemical modifier help determine changes in the features of the surface of silica. For example, disappearance of the broad bands representing surface adsorbed water and hydrogen bonded silanols indicates removal of water from the surface. Another very important observation would be the disappearance of the band at 3740 cm^{-1} with concurrent appearance of a broad peak at 1085 cm^{-1}, providing evidence of covalent attachment via a

reaction at Si_s-OH to form Si_s-O-Si bonds.[39] Further detailed assessments will be discussed as necessary in the forthcoming chapters.

Chemical analysis (CHN analysis) of modified materials is performed by microchemical combustion analysis. Briefly, the material is oxidized to CO_2, H_2O, and NO_2 at high temperature. The levels of the resulting compounds are separated by gas chromatography and analyzed by thermal conductivity. The method has the advantage of quantifying only the organic compounds present with only a few milligrams of sample.[43] From the %C results, the grafting density (ρ, groups/nm^2) of the monolayers on silica is calculated via the following equation:

$$\boldsymbol{\rho = \frac{6\times10^5\cdot(\%C)}{[1200\times n_C - MW\times(\%C)]}\cdot\frac{1}{S_{BET}}} \qquad \textbf{(1 - 13)}$$

where n_C is the number of carbons in the grafted group, MW is the molecular weight of the grafted group, and S_{BET} is the BET surface area of the underlying bare silica.[44]

Thermal properties and grafting density of the alkylated silicas were also assessed through thermogravimetric analysis (TGA). In this technique, a few milligrams of each sample are gradually heated to 1000^{o}C under an atmosphere of nitrogen with the mass constantly measured. Weight loss for modified silicas is well studied. For alkylated silicas, the first significant weight loss occurs below 100^{o}C, and is attributed to desorption of the weakly bound surface water and solvents. The extent of this weight loss correlated with the hydrophobicity of the material. At temperatures greater than 200^{o}C, the weight loss is attributed to the thermal destruction of the organic moieties in alkylated silicas. The temperature of the onset of the weight loss and the temperature of the maximum rate of the weight loss T_{MAX} (DTGA) were characteristic of the method of

Figure 1-8: Characterization of Materials by Nitrogen Adsorption

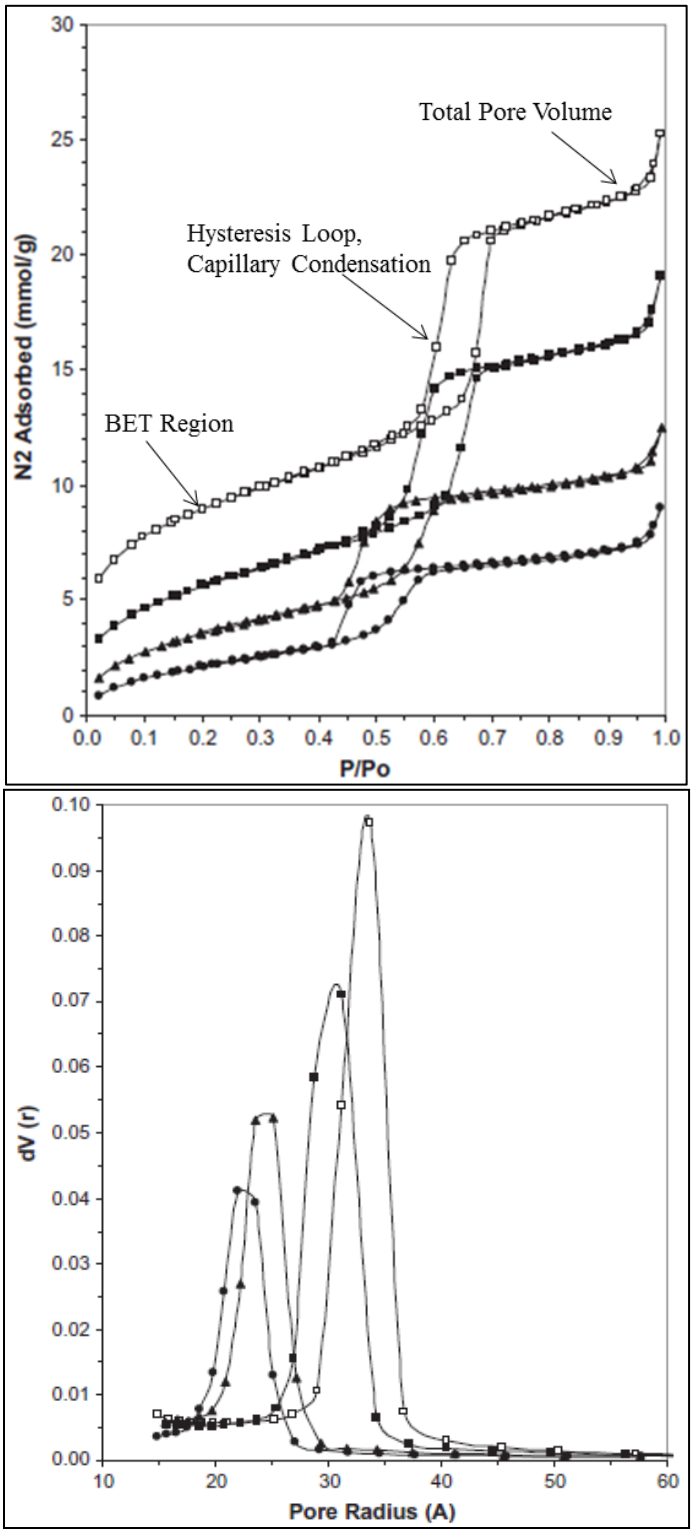

Figure 1-8: Example of nitrogen adsorption isotherms (top) and pore size distributions for SBA-15 silica grafted with SAMs of $C_nH_{2n+1}Si(Oet)_3$. Bare SBA (□); n=1 (■); n=8 (▲) n=18 (●). *Adapted from ref* 45 *with permission from Elsevier, 2011.*

preparation of alkylated silicas. For studies discussed here-in, the weight loss in the 200-800^{o}C region was compared to the approximate carbon percent in the sample (%C = 0.85x[%WeightLoss(200-800^{o}C)]).[44] Other analysis with these theories is discussed in detail in the coming chapters.

As with bare porous silicas, adsorption-desorption studies can be a powerful tool for the characterization of functionalized materials. Changes to the C constant, surface area, pore shape, and pore size distribution are carefully analyzed after surface modification. A *C* constant of approximately 100-200 would imply high surface energies, indicative of a large number of silanol groups on the surface of bare silica. A low C constant (~10-30) implies lower surface energies, often due to the presence of CH_2 and CH_3 functionalities, with more ordered alkylsilane groups providing lower C constant values. Most monolayer coverage will 'block' any micropores from analyte adsorption, and this must be taken into account as part of the analysis.

Of great interest after surface modification is the change in the total volume of the pores and the surface area. Changes to the pores can be used in the experimental determination of the bonded layer thickness (Figure 1-8). When the pore volume is corrected relative to 1 gram of bare silica, thickness of the grafted layer (*h*) is calculated as follows:[46]

$$\boldsymbol{h = \frac{V_{SiO_2} - V_{mod}}{S_{BET}}} \qquad \textbf{(1 - 14)}$$

when V_{SiO2} and V_{mod} are the total pore volumes of bare silica and modified silica, respectively and S_{BET} is the surface area of bare silica. Similarly, the change in pore diameter (D_{pore}) after modification can be used to calculate the thickness of the grafted layer by the equation

$$h = 0.5 \times (D_{pore}^{SiO2} - D_{pore}^{mod}) \qquad (1 - 15)$$

The experimentally determined bonded layer thickness in the pores can be used to characterize the orientation of the monolayer. For example, in a SAM of n-alkyl-trichlorosilanes, a linear increase in thickness observed with the addition of each carbon (n) in the alkyl group fitting the equation:

$$h(nm) = 0.126n + 0.478 \qquad (1 - 16)$$

indicates all-trans alkyl chains oriented approximately perpendicular to the surface. A CAM will have a thickness lower than the all-trans oriented SAM because the alkyl chains are not as closely packed and ordered.

Numerous studies have investigated the adsorption of various molecules on silica. Vapor adsorption of molecules other than N_2 can also be a helpful tool in analysis of modified materials.[27] A unique application involves choosing an adsorbing molecule with a high affinity for the bare surface, but very low affinity for the modified surface to show the significant change in the hydrophobicity of the surface at the molecular level. In our work (chapter 2), water adsorption was used to characterize the change in hydrophobicity of silica after surface

modification. A dramatic change in the quantity of water adsorbed and a lack of capillary condensation demonstrated that the reaction obtained a uniform hydrophobic surface.

Though far more technologically advanced methods may be available, 'wetting' has proven to continue to be a useful and sensitive method for characterization of surface functionality and structure of modified materials. Contact angle measurements are an important technique for probing the character of solid-liquid interfaces when spectroscopic methods may be limited. Wetting methods compliment the usual

spectroscopic approaches to characterizing the solid-liquid interface. Wetting is uniquely valuable in characterizing surfaces for its combination of high surface sensitivity and applicability to disordered surfaces.[34]

The contact angle (θ) is measured at the three-phase contact between a liquid, solid, and vapor. Young[47] characterized this as the balance of the free surface energies at the liquid-vapor (γ_{LV}), solid-vapor (γ_{SV}), and solid-liquid (γ_{SL}) as indicated in Figure 1-9.[34]

$$\boldsymbol{\gamma_{LV}cos\theta = \gamma_{SV} - \gamma_{SL}} \qquad \textbf{(1 - 17)}$$

However, the equilibrium contact angle is more often expressed as a balance of the work of adhesion ($W_A = \gamma_{SV} + \gamma_{LV} + \gamma_{SL}$) and the work of cohesion ($W_C = 2\,\gamma_{LV}$) and is written as:

$$\boldsymbol{cos\theta = \frac{2W_A - W_C}{W_C}} \qquad \textbf{(1 - 18)}$$

When the $W_A \geq W_C$, the contact angle approaches zero as the liquid spreads over the surface (complete wetting, Figure 1-10). An example of this would be water on a freshly cleaned glass, which would be considered hydrophilic. Covalent attachment of closely packed alkyl groups to the surface of glass, however, would result in a decrease in the W_A and a higher contact angle for water. On a hydrophobic surface such as this, when W_A is less than 0.5 W_C, the contact angle will be > 90°. Theoretically, when W_A approaches zero, the contact angle approaches 180°, but this situation is not observed for smooth surfaces.[1]

Figure 1-9: Illustration of Interfacial Energies with Wetting

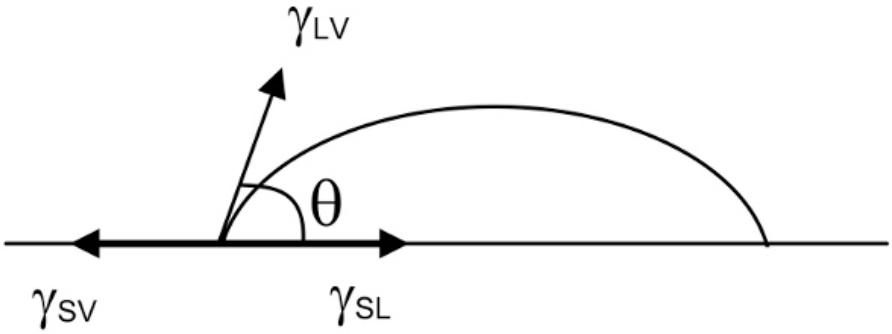

Figure 1-9: Illustration of a liquid droplet on a solid surface demonstrating the balance of free surface energies at the liquid-vapor (γ_{LV}), solid-vapor (γ_{SV}), and solid-liquid (γ_{SL}) interfaces. *Reproduced from ref 34 with permission from the American Chemical Society, 1990***.**

As this equation represents an ideal surface with all surface energies being accurately measurable, several models have been used to expand this theory. An excellent review of these approaches is provided by Fadeev.[30] These models assume a homogeneous, non-deformable, and unreactive solid surface. In practice, however, most real surfaces have some level of heterogeneity that causes a wetting hysteresis. Hysteresis, in this case, refers to the difference between the advancing (θ_A, as wetted area increases) and receding (θ_R, as wetted area decreases) contact angles. Due to this phenomenon, full characterization of the hydrophobicity of materials requires evaluation of both advancing and receding contact angles.[38] Hysteresis demonstrates the useful sensitivity of wetting to the depth of functional groups below the organic-water interface. Examples of techniques used to obtain contact angle values include the telescope-goniometer, Wilhelmy balance, and the capillary rise method.[48]

The difference between the advancing and receding contact angle is far from zero for most systems. A large value in hysteresis is commonly taken to indicate a system not at equilibrium. Contact angle measurements rely heavily on comparisons of

measurements in similar systems rather than on interpretation of absolute values obtained from only one system.[1] Thus, we use contact angles because they are convenient, very sensitive to obtain details of interfacial structure even at the angstrom scale, and because they are applicable to the characterization of solid-liquid interfaces. These measurements at least correlate with thermodynamically significant measures of surface and interfacial free energies.

Figure 1-10: Contact Angle Measurements for Pressed Pellets

Figure 1-10: Contact angle measurements for pressed pellets of different wettability. Examples include: wetting (left), intermediate (middle), and non-wetting (right) materials. (*Reproduced from ref 45 with permission from Elsevier, 2011.*) Note: that roughness introduced by the pressed powders caused different contact angles to comparable smooth surfaces.

For materials such as the pressed pellets of porous materials that were used in our work, containing a rough and heterogeneous topography, a correction to a 'mixed' surface must be made (Figure 1-10). The relationship between the contact angle of a liquid on a smooth surface (θ) and the apparent contact angle, $\theta_{\#}$, on a mixed surface of the same material is described by the Cassie-Baxter equation[38,49]:

$$\boldsymbol{cos\theta_{\#} = f_1\, cos\theta - f_2} \qquad \textbf{(1 - 19)}$$

where f_1 is the fraction of the surface are made up of solid material and f_2 ($f_2 = 1 - f_1$) is the fraction of open area (pores, air-liquid interface). Additional complexity is added if the surface chemistry of the measured surface is not uniform. In this case, a study on

smooth, flat surfaces is recommended for evaluation of the uniformity in the surface chemistry of a particular reaction using the same equation.

Herein, the methods and underlying theory for the techniques commonly used for characterization of modified surfaces have been reported. A combination of the FTIR, adsorption, and wetting provided the basis of our understanding for the materials we synthesized. The mechanism of the reaction, thickness of the grafted layer, uniformity and hydrophobicity of the material can be obtained.

1.3 Conclusions

In this chapter, the methods for synthesis and characterization of porous metal oxide materials, specifically silicas, have been reviewed. The modification of surfaces by adsorption, self-assembled monolayers, and covalent attachment were described. Additionally, the methods typically used for the characterization of the modified porous materials were discussed. This collection of theories and procedures provides the foundation of the work we have undertaken.

Continuing to chapter 2, a new method for the modification of the silica surface is introduced. The reactions of previously considered inert poly(dimethylsiloxane)s to obtain uniform hydrophobic surfaces is described. In chapter 3, functionalization of surfaces by solution adsorption with a variety of fluorinated phthalocyanines is examined. Our study focused on the forces that dominate the adsorption of these materials to different surfaces as changes to the molecule were made.

Chapter 2 : Covalent Functionalization of Silica Surfaces Using "Inert" Poly(dimethylsiloxanes)

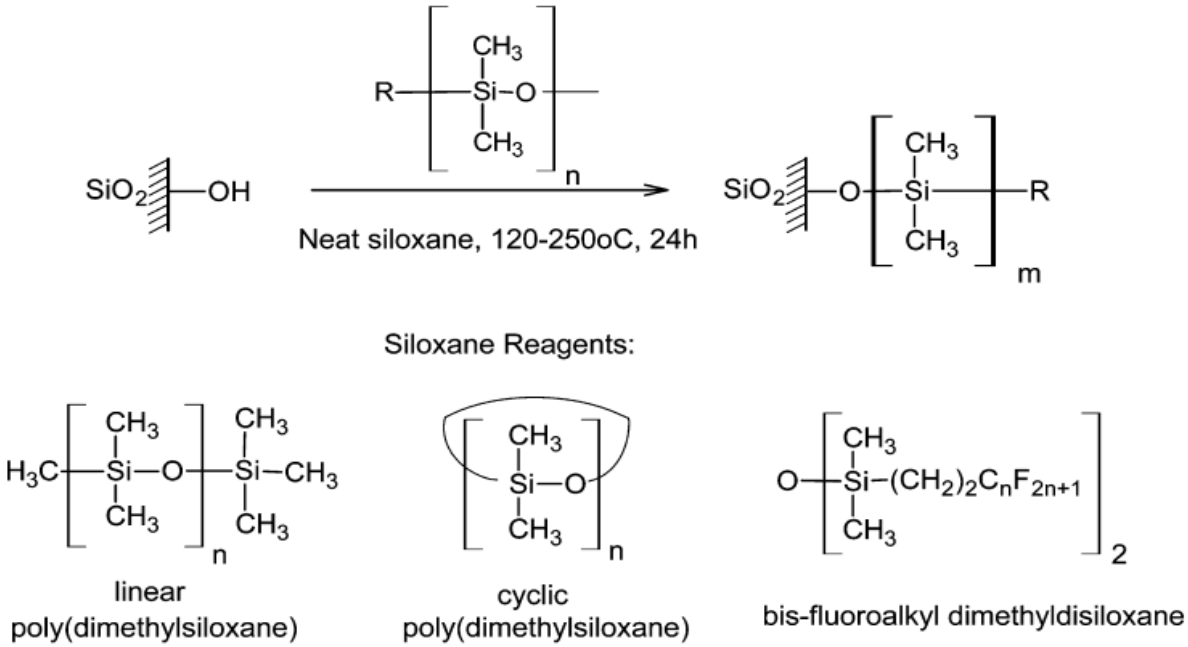

Reprinted (adapted) from ref 101 with permission from Langmuir. Copyright 2014, American Chemical Society.

2.1 Abstract

Methyl-terminated poly(dimethylsiloxanes) (PDMSs) are typically considered to be inert and not suitable for surface functionalization reactions because of the absence of readily hydrolysable groups. Nevertheless, these siloxanes do react with silica and other oxides, producing chemically grafted organic surfaces. Known since the 1970s and then forgotten and recently rediscovered, this reaction provides a versatile yet simple method for the covalent functionalization of inorganic surfaces. In this work, we have explored the reactions of linear methyl-terminated and cyclic PDMS and bis-fluoroalkyl disiloxanes for the surface functionalization of mesoporous Davisil ($D_{pore} \approx$ 30–35 nm) and SBA-15 silicas ($D_{pore} \approx$ 6-7 nm). The optimal reaction conditions included 24 h of contact of neat siloxane liquids and silica at 120–250°C (depending on the siloxane). A study of the reactions of silicas with different extents of hydration demonstrated the critical role of water in facilitating the grafting of the siloxanes. The proposed reaction mechanism involved the hydrolysis of the adsorbed siloxanes by the Lewis acidic centers (presumably formed by water adsorbed onto surface defects) followed by the coupling of silanols to the surface to produce grafted siloxanes. For rigorously dehydrated silicas (calcination ~1000°C), an alternative pathway that did not require water and involved the reaction of the siloxanes with the strained siloxane rings was also plausible. According to FTIR and chemical analysis, the reactions of bis-fluoroalkyl disiloxanes and cyclic PDMS (D_3–D_5) produced covalently attached monolayer surfaces, and the reactions of high-MM methyl-terminated PDMS produced polymeric grafted silicas with a PDMS mass content of up to 50%. As evidenced by the high contact angles of ~130°/100° (adv/rec) and the negligible amount of water adsorption over the entire range of relative

pressures, including saturation ($p/p^0 \rightarrow 1$), the siloxane-grafted porous silicas show uniform, high-quality hydrophobic surfaces. An overall comparison of siloxanes with classical silane coupling agents (i.e., silanes with readily hydrolysable functionalities such as chloro, amino, etc.) demonstrated that the reactions of siloxanes produced surfaces of similar quality and, although requiring higher temperatures, used noncorrosive, less hazardous reagents, thereby providing an environmentally benign alternative to the chemical functionalization of metal oxide surfaces.

2.2 Introduction

Organosilanes, with the general formula $R_{4-n}SiX_n$ (n = 1, 2, 3), where X = Cl, OC(O)R′, OR′, NR'_2, or H, are the most widely used reagents for the chemical functionalization of mineral surfaces that find numerous applications as materials for adsorption, separations, catalysis, wetting and adhesion control, hydrophobic and superhydrophobic coatings, polymer fillers and composites, the immobilization of biological molecules, sensors, modified electrodes, and others.[50-56] Organosilanes with a large variety of R groups are available commercially, enabling the preparation of surfaces of nearly all major organic functionalities either through direct deposition or subsequent modification reactions. Robust Si–O linkages between the silane and the surface (covalently attached monolayers, CAMs) and between neighboring silane molecules (self-assembled monolayers, SAMs) ensure good thermal and chemical stability of the silane-modified surfaces. Many of the surface reactions of organosilanes "work" with a wide range of substrates of different geometries (single crystals, fibers, fine particles, porous solids) and chemistries (silicas, metals and metal oxides, polymers, etc.). The principles of silane coupling have been extensively covered in the literature.[50-54,57,58]

Organosiloxanes ($R_3Si–O–SiR_3$) are typically not regarded as silane coupling agents because of the absence of readily hydrolysable groups. The siloxanes, however, do react with surfaces in a similar fashion as do the "reactive" organosilanes, which was recognized in pioneering works on covalent surface functionalization in the 1970s and 1980s. The reactions of hexamethyldisiloxane and linear and cyclic poly(dimethylsiloxane) (PDMS) producing silica-supported grafted siloxane surfaces have been reported.[59-64] Although the direct cleavage of Si−O−Si bond by surface

silanols occurred only at high at temperatures[62,63] of ~300–350°C, the reactions were facilitated greatly by adsorbed water.[59-61] The irreversible adsorption (chemisorption) of hexamethyldisiloxane on silica in the presence of physisorbed water was observed at room temperature.[59] The mechanism of siloxane bond cleavage on silica involving the six-membered ring formed by surface silanol, siloxane, and molecular water has been proposed.[61] In more recent works,[65,66] the use of the siloxanes for the covalent functionalization of surfaces has been rediscovered. With solid-state NMR and DSC it was demonstrated[65] that the reaction of linear PDMS with silica produced surfaces of chemically grafted PDMS loops of four to eight repeat units. The use of methyl-terminated PDMS and PDMS copolymers as a general method for the covalent functionalization of inorganic surfaces (Si, Ti, Al, and Ni) has been reported.[66]

The adsorption of PDMS on silica and the local structure of the PDMS–silica interface have received significant attention because of the importance of this interface in applications of the silica-reinforced composites and silicone coatings. It should be noted, however, that despite the significant research effort there is no general agreement in the literature on the adsorption mechanism and the type of molecular interactions at the PDMS–silica interface. On the basis of ellipsometry, contact angles, adsorption kinetics, and rheological studies, the authors[67-69] concluded that the PDMS adsorption on silica was governed by the H-bonding between siloxane oxygen and surface silanols, yet no direct evidence of such H-bonding was ever demonstrated. Some chemical grafting during the adsorption of methyl-terminated PDMS on glass was mentioned;[70] however, the major adsorption interaction of PDMS with the surface was attributed to H-bonding, and the chemical grafting was attributed to the presence of OH-terminated PDMS as a

contaminant. Alternatively, comprehensive studies[71-73] using inelastic neutron scattering, IR, quantum chemistry, and MD simulations demonstrated that interactions of PDMS with silica were similar to those in bulk PDMS (i.e., weak, nonspecific van der Waals type). In terms of interaction energies, classical H-bonding made only a minor contribution, and van der Waals forces mainly governed the system.[72,73]

In this article, we explored the reactions of methyl-terminated linear and cyclic PDMS and bis-fluoroalkyl disiloxanes (bis-R_f) for the covalent surface functionalization of mesoporous silicas. The main focus of our work was placed on (1) the optimization of the reaction conditions for the covalent functionalization of porous silicas using siloxanes with different structures, (2) the clarification of the role of silica surface hydration in its reactivity toward siloxanes, and (3) the characterization of the grafting density, surface hydrophobicity, and thermal stability of the siloxane-grafted porous silicas.

2.3 Experimental

2.3.1 Chemicals

All solvents, unless stated otherwise, were purchased from Thermo Fisher Scientific (Waltham, MA). The siloxanes were obtained from Gelest (Morrisville, PA) and used as received.

2.3.2 Silicas

Wide-pore silica gel Davisil 250 was obtained from Grace (Columbia, MD). The pore structure of Davisil 250 was assessed by nitrogen adsorption (77 K) using an ASAP 2020 analyzer (Micromeritics, Norcross, GA): specific surface area S(BET) = 252 m^2/g, total pore volume V_{pore}= 1.82 cm^3/g, and average pore diameter D_{pore} ≈ 30–35 nm.

SBA-15 was synthesized by a method adapted from Stucky *et al*.[17] In a typical synthesis 5 g of the surfactant Pluronic P123 [poly-ethylene-glycol-*block*-polypropylene-glycol-*block*-polyethylene-glycol ($EO_{20}PO_{70}EO$)] was placed in a 250 mL pressure bottle and dissolved, with stirring, in 190 mL of 1.4 N HCl (aq) at a temperature of 35°C. Upon dissolution, 51 mmol of tetraethyl orthosilicate (TEOS) was added drop wise and then allowed to stir at 35°C for 20 h. The resultant mixture was placed in an oven at 80°C and allowed to age (without stirring) for a period of 48 hours. Once completed, the slurry solution was filtered using a medium porosity fritted glass filter. The silica was first washed with 1 N HCL (aq), followed by water, acetone, toluene, and acetone again. After initial drying at 60°C, the solid SBA-15 is then calcinated at 600°C for 6 hours to remove any remaining surfactant. The nitrogen adsorption results of the materials used are summarized in Table 0-3.

2.3.3 Reaction of Siloxanes with Silicas

Silica (~0.5 g) was placed in a glass vial, and neat silicone oil was added to the vessel drop wise in an amount sufficient to soak through and fully cover the powder (~1 mL). Hexamethylcyclotrisiloxane (D_3), a solid at room temperature, was melted in the vessel by heating to 80 °C prior to the addition of silica. The vials were capped and placed in an oven at the desired temperature for the desired amount of time (generally 24 h). After the completion of the reaction, the reactors were allowed to cool and the silicas were transferred to a glass filter and rinsed with toluene (three to five times with 30 mL), acetone (three to five times with 30 mL), water–acetone, and acetone again (two to three times with 30 mL). The silicas were air dried on the filter and then dried in an oven at 60°C for 1 h.

To study the effect of surface hydration (silanol content) on the reaction, a series of progressively dehydrated silicas were prepared by calcination at 400–1000°C overnight. After calcination, the silicas were cooled to room temperature in nitrogen and used immediately in the reactions with siloxanes. To study the effect of atmospheric moisture, a series of reactions were carried out in pressure Ace glass sealed reactors and in sealed glass ampules. The rest of the procedure was the same as described above. For the majority of the reaction conditions, the reactions were repeated at least twice. The results of chemical analysis for independent runs were within 10% (or better) agreement.

2.3.4 Material Analysis

The extent of surface reactions was quantified through chemical analysis (%C, %H, and %F when present), which was performed by Robertson Microlit Laboratories (Ledgewood, NJ). To allow direct comparison between the reactions using linear and cyclic PDMS of different molecular masses, the grafting density was calculated as the number of dimethylsiloxane (DMS) repeat units per nm^2 using equation

$$\boldsymbol{\rho_{DMS}} = \frac{\mathbf{6} \times \mathbf{10^5} \times (\%\boldsymbol{C})}{[\boldsymbol{n_C} \times \mathbf{1200} - \boldsymbol{MM} \times (\%\boldsymbol{C})]} \cdot \frac{\mathbf{1}}{\boldsymbol{S_{BET}}} \qquad \textbf{(2 - 1)}$$

where MM and n_C represent the molecular mass and number of carbons in the DMS group (74 g/mol and 2), %C is the carbon weight percentage in the modified silica, and S_{BET} is the BET surface area of bare silica (m^2/g). For silicas reacted with fluoroalkyl disiloxanes, the grafting density was calculated as the number of monomer fluoroalkyl siloxy groups per nm^2. The grafting density was determined separately from %C and from %F

$$\boldsymbol{\rho} = \frac{\mathbf{6} \times \mathbf{10^5} \cdot (\%\boldsymbol{C})}{[\mathbf{1200} \times \boldsymbol{n_C} - \boldsymbol{MW} \times (\%\boldsymbol{C})]} \cdot \frac{\mathbf{1}}{\boldsymbol{S_{BET}}} \qquad \textbf{(1 - 13)}$$

$$\rho_F = \frac{6 \times 10^5 \times (\%F)}{[n_F \times 1900 - MM \times (\%F)]} \cdot \frac{1}{S_{BET}} \qquad \textbf{(2 - 2)}$$

where MM is the molecular mass of grafted group $-OSi(CH_3)_2(CH_2)_2C_nF_{2n+1}$ and n_C and n_F represent the number of carbon and fluorine atoms in it. The ρ and ρ_F data are in close agreement. Typical standard deviations in carbon analysis and surface area measurements were ~0.05% C and ~5–10 m^2/g (for silicas), respectively, which translated to ~0.05 group/nm^2 standard deviation for the grafting density of the siloxane-modified silicas.

Thermogravimetric analysis (TGA) was performed using a TA Instruments thermogravimetric analyzer operated between room temperature and 1000°C at a heating rate 10°C/min in a flow of dry nitrogen (20 cm^3/min).

FTIR measurements were performed using a PerkinElmer Spectrum One instrument with a Harrick Seagull accessory as well as a Thermo Nicolet iS50 equipped with an ATR accessory. For the Spectrum One, samples of bare and siloxane-grafted silica were packed tightly in the sample compartment, and the spectra were collected in reflectance mode. Collection parameters were 128 scans at a resolution of 4 cm^{-1}. The subtraction of spectra was completed using the vendor software.

Water contact angles for the modified silicas were measured using a Rame-Hart contact angle goniometer with pressed silica pellets. Eight-millimeter-diameter pellets of modified silicas were prepared using a hand press. The probe fluid (DI water) was added/withdrawn using a Gilmont microsyringe.

Nitrogen adsorption-desorption isotherms (77 K) were measured using an ASAP 2020 analyzer (Micromeritics, Norcross, GA, USA). The adsorption isotherms were measured over a relative pressure p/p_o range extending from 10^{-2} to 0.995. Desorption

isotherms were measured over a relative pressure range from 0.995 to 0.2-0.3. Prior to analysis, the materials were outgassed at 100^{o}C overnight using the out-gassing port of the instrument. A relatively low out-gassing temperature was chosen to avoid degradation of the siloxanes bound to silica. The specific surface area was measured via the BET method in the range of relative pressure from 0.06 to 0.20. The cumulative volume of the pores was determined from adsorption at 0.98 p/p_o. The micropore volume was determined using the t-plot method using software provided by the instrument's vendor. The pore size distribution and average pore diameter was calculated with the BJH algorithm (desorption for SBA-15, adsorption for Davisil).

Water vapor adsorption–desorption isotherms (293 K) were obtained using a Quantachrome Autosorb One automatic volumetric adsorption instrument (Boynton Beach, FL). Prior to the analysis, samples were outgassed at 100°C overnight. The surface area was calculated via the BET method in the range of relative pressure p/p_o from 0.05 to 0.25.

2.4 Results and Discussion

The main focus of this work was to investigate the reactions of poly(dimethylsiloxanes) of different structures for the covalent surface functionalization of mesoporous silicas (Davisil 250 and SBA-15). By using the mesoporous silica, we intended to explore the potential of the siloxane reagents for the surface functionalization of porous materials for applications in adsorption and separations, water purification, catalysis, and energy storage, among others. Three groups of siloxanes were evaluated: (1) a series of methyl-terminated linear PDMSs with molecular mass (MM) ranging from 0.4 to 225 kDa, (2) cyclic PDMS (D_3, D_4, and D_5), and (3) bis-fluoroalkyl disiloxanes

(bis-C_nF_{2n+1}, n = 1, 6, 8). The reaction schematics, the structure of the siloxanes, and their notation are summarized in Figure 0-1 and Table 0-1.

2.4.1 Reaction of Siloxanes with Silica by IR

The presence of the methylsiloxane species on the siloxane-grafted silicas was confirmed by FTIR spectroscopy. As a representative example, Figure 0-2 shows an overlay of a spectrum of neat PDMS T23 and a spectrum of silica reacted with PDMS T23 (after the subtraction of the spectrum of bare silica). The absorption bands at 1261 and 786 cm^{-1} were attributed to bending and rocking modes of the Si–CH_3 groups. The bands at 2961 and 1420 cm^{-1} (weak) were stretching and deformation modes of the CH_3 groups in PDMS. Similar spectral changes that were consistent with the structure of the siloxanes used for the reactions were also observed for silicas reacted with cyclic PDMS and bis-R_f (Figure 0-3 and Figure 0-4).

Figure 2-1: Reaction of Siloxanes with the Silica Surface

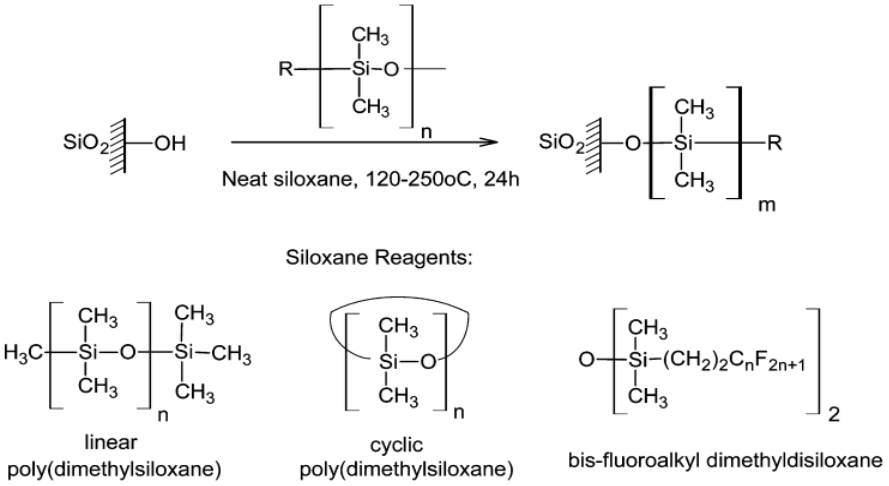

Figure 2-1: Schematics of the reaction of siloxanes with the silica surface and structures of the siloxane reagents studied.

The changes in the spectra in the 3000–3800 cm^{-1} region (OH stretching) provided insight into the surface chemical bonding mode. For silicas pretreated at room temperature, however, the picture was not very informative because the 3000–3800 cm^{-1} region was dominated by the strong absorption from physisorbed water. After the reactions with siloxanes, the subtraction spectra (Figure 0-2, top) showed only broad negative peaks at ~3400 and 1620 cm^{-1}, which was attributed to the removal of physisorbed water, consistent with the hydrophobic nature of the siloxane-grafted silicas. For silicas pretreated at elevated temperatures, physisorbed water was largely removed and the spectra showed bands from the isolated (3747 cm^{-1}) and hydrogen-bonded (~3550 cm^{-1}) silanols. After the reaction with siloxanes, the intensity of these bands was significantly reduced (Figure 0-2, bottom), indicating the involvement of the surface silanol groups in the reactions with siloxanes and suggesting the formation of surface covalent bonds Si_S–O–Si.

The analysis of the Si–O stretching region (1000−1100 cm^{-1}) of the spectra provided additional insight into the structure of the grafted PDMS chains (Figure 0-3). For the silicas reacted with the linear PDMS of high MM (≥1.25 kDa), two prominent bands at ~1010 and 1080 cm^{-1} were present in the spectra, whereas for the silicas reacted with the cyclic PDMS (D_3, D_4, and D_5) and linear PDMS with MM = 0.4 and 0.75 kDa, a single band at ~1003 cm^{-1} was

observed. These bands were assigned to the stretching of Si–O (ν_{AS}) in the grafted PDMS species. From the literature, it is known that the Si–O mode is present as a single band in the spectra for cyclic dimethylsiloxanes with small rings ($n < 5$), whereas for larger siloxane rings ($n \geq 6$) and/or linear PDMS this band splits in two.[74] The analysis of

Table 2-1: Structure and Properties of the Siloxanes Studied in This Work

Chemical structure	Molecular mass, Da	# of repeat units[b]	b.p., ^{o}C	Des.
cyclic PDMS				
$[OSi(CH_3)_2]_3$	222	3	134	D_3
$[OSi(CH_3)_2]_4$	296	4	176	D_4
$[OSi(CH_3)_2]_5$	371	5	210	D_5
linear PDMS[a]				
$-[OSi(CH_3)_2]_n-$	400	5	-	T02
–»–	750	10	-	T05
–»–	1250	16	-	T11
–»–	2000	27	-	T12
–»–	3750	50	-	T15
–»–	13500	182	-	T23
–»–	52500	710	-	T35
–»–	115000	1550	-	T46
–»–	250000	3400	-	T53
bis(perfluoroalkyl)tetramethyl-disiloxane				
$O[Si(CH_3)_2(CH_2)_2CF_3]_2$	326	2	195	bis-CF_3
$O[Si(CH_3)_2(CH_2)_2C_6F_{13}]_2$	826	2	342	bis-C_6F_{13}
$O[Si(CH_3)_2(CH_2)_2C_8F_{17}]_2$	966	2	>400	bis-C_8F_{17}

[a]Linear PDMS were mixtures of oligomers.
[b]The molecular mass and number of repeat units were provided by the manufacturer and represent average values.

Figure 2-2: FTIR Monitoring of Reactions with Linear PDMS

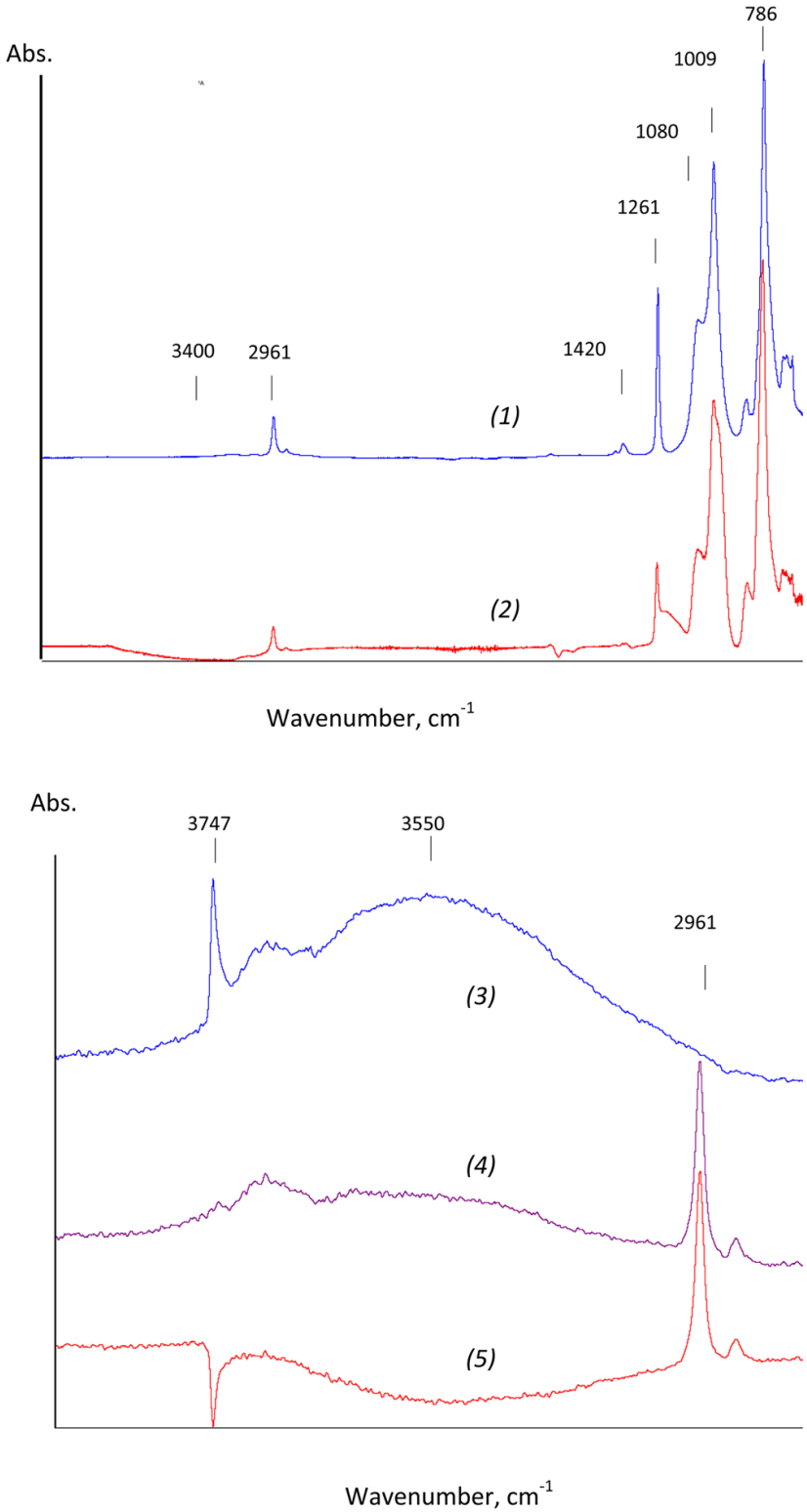

Figure 2-2: FTIR spectra of Davisil 250 reacted with PDMS T23. Top: Spectrum of neat PDMS T23 (1) and difference spectrum of Davisil 250 (prepared at room temperature) reacted with T23 (2). Bottom: The OH-stretching region for bare Davisil 250 prepared at 400 °C (3), spectra of this silica reacted with T23 (4), and difference spectrum (5).

Figure 2-3: FTIR Overlay of Neat Siloxanes and Modified Silicas

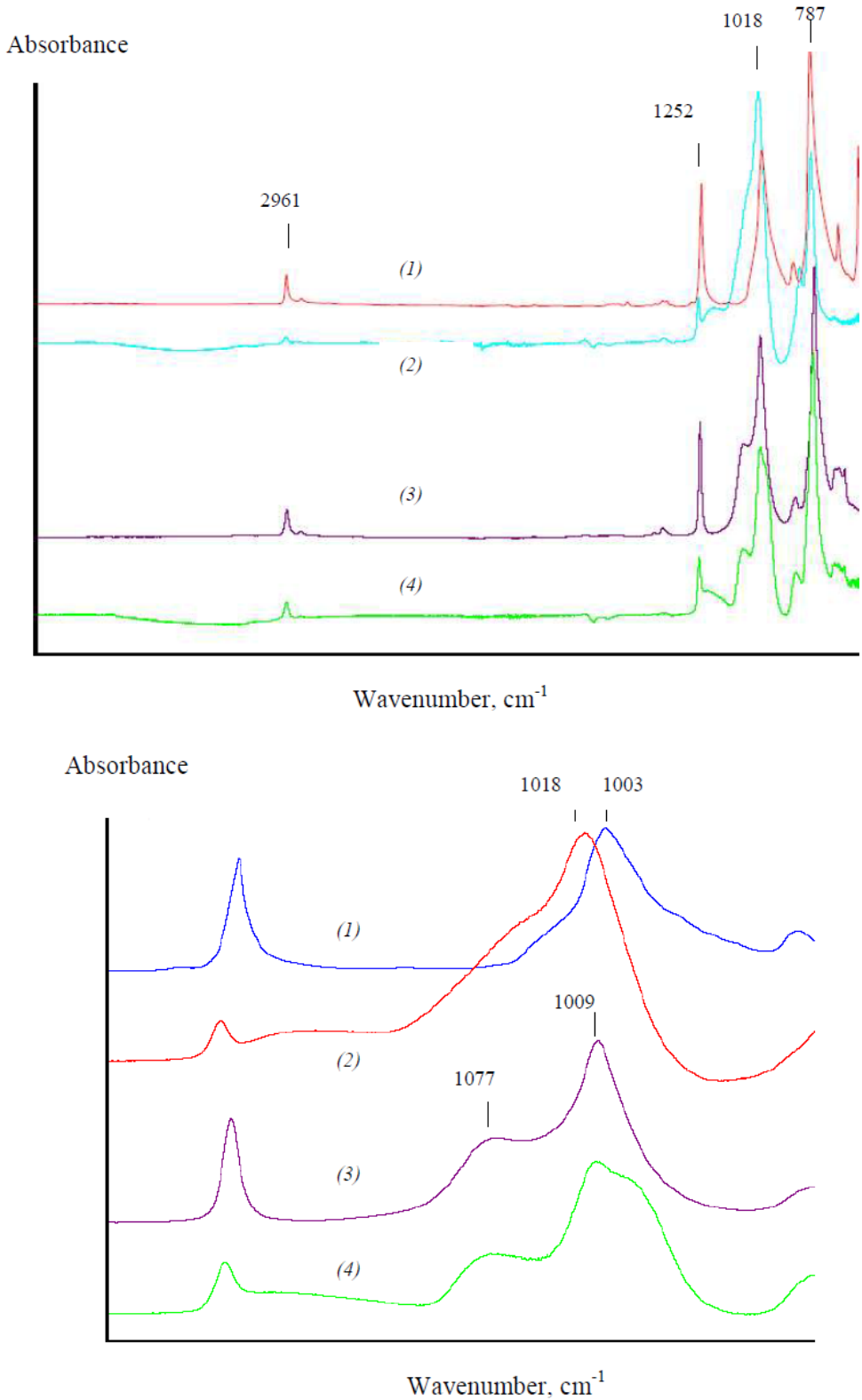

Figure 2-3: Top: FTIR of neat D_3 (*1*) and difference spectrum of Davisil 250 (prepared at room temperature) reacted with D_3 (*2*); neat T23 (*3*) and difference spectrum of Davisil 250 (prepared at room temperature) reacted with T23 (4). Bottom: Close up at the 1000-1100 cm^{-1} region (siloxane stretching).

Figure 2-4: FTIR Overlay of Neat Bis-CF_3 and Modified Silica

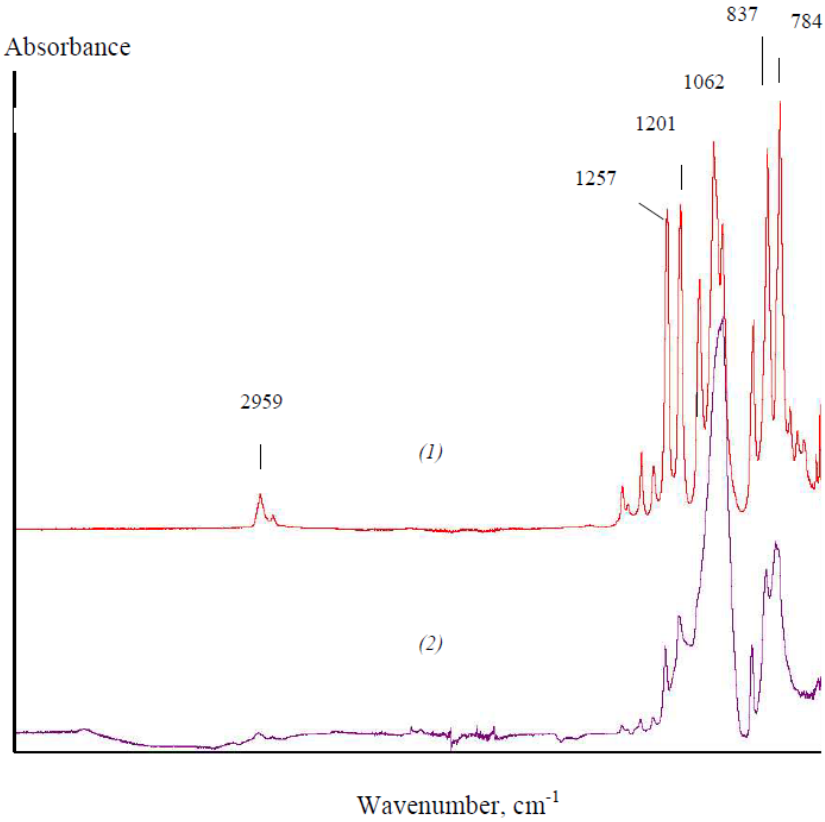

Figure 2-4: FTIR of neat bis-CF_3 (*1*) and difference spectrum of Davisil 250 (prepared at room temperature) and reacted with bis-CF_3 (*2*).

this spectral region for the PDMS-grafted silicas led us to conclude that the major products of the reaction of the high-MM PDMS were linear PDMS chains and/or larger PDMS loops ($n \geq 6$), whereas for the reactions of cyclic and low-MM PDMS the major products were PDMS cycles with smaller rings ($n < 5$). The characteristic bands for $Si(CH_3)_2OH$ groups (970 and 840 cm^{-1}, Si–OH stretching) were not noted in the spectra for silicas reacted with either linear or cyclic PDMS, which argued that the presence of the OH-terminated PDMS species was insignificant, thereby further supporting the conclusion that the major products for the reaction were PDMS loops grafted to the surfaces by two ends. In our previous work,[39] we studied the reactions of α,ω-dichloro-terminated PDMS with hydrated silicas that produced PDMS loops covalently attached to

silica by two Si_S–O–Si bonds. A comparison of the results[39] with the results of the present work showed that the IR spectra for silicas reacted with methyl-terminated PDMS and silicas reacted with α,ω-dichloro-terminated PDMS[39] were nearly identical, demonstrating the similarity in composition of these grafted layers.

2.4.2 Role of Reaction Temperature and Structure of Siloxane

The effect of the reaction temperature was studied for all three types of siloxanes by assessing the number of grafted siloxanes, which was quantified through chemical analysis (%C, H, F). The results are summarized in Figure 0-5. First, we noted that for all of the siloxanes tested, the reactions required elevated temperature. Very low organic loadings were observed at room temperature, arguing for thermally activated chemical bonding of the siloxanes on the silica surface. Depending on the structure of the siloxane, however, the optimal reaction temperatures that ensured maximal grafting were different. Linear PDMSs, with an average MM greater than 1.25 kDa, were clearly the most active siloxanes studied in this work: the maximal grafting was observed at 120°C. The reactions of cyclic PDMS and bis-R_f disiloxanes required higher temperatures: ~200°C (bis-R_f) and ~250°C (cyclic PDMS). Further increases in temperature resulted in lower grafting or gave rise to side reactions, e.g., bulk polymerization of cyclic PDMS at temperatures exceeding 275°C. The relatively high reactivity of the high-MM PDMS was attributed to the molecular mass effect: the higher-MM polymer adsorbed more strongly and therefore was conceivably more available for the surface reactions. We cannot, however, completely rule out the probability of the presence of OH-terminated PDMS in the samples as contaminants. The OH-terminated PDMSs are known to be much more active[67,70] than CH_3-terminated PDMSs in their reactions with silica, and their

Figure 2-5: Effect of Reaction Temperature

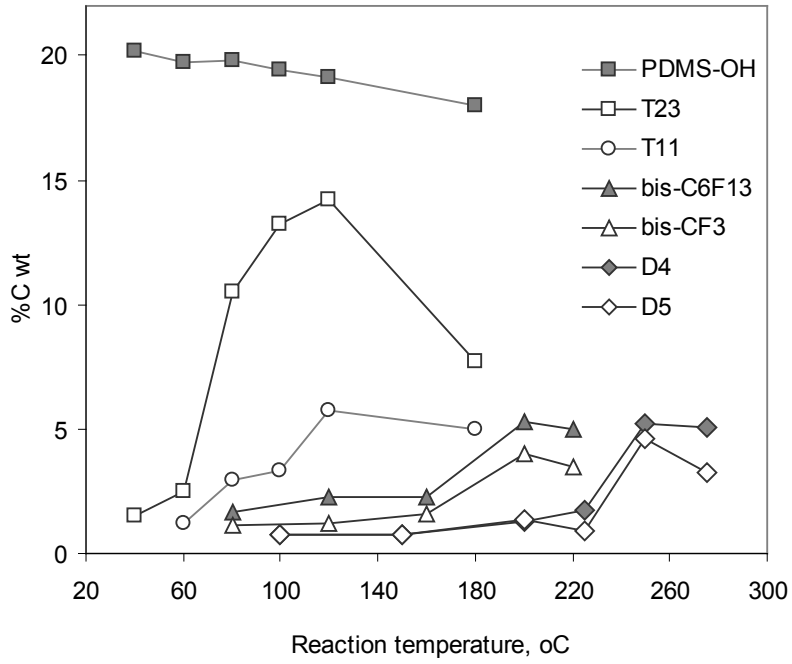

Figure 2-5: Effect of reaction temperature on the amount of grafted siloxane (%C, wt). For the designation of siloxanes, see **Table 2-1**. The points are connected to guide the eyes; some points are omitted for clarity.

presence, even in small quantities, would affect the surface grafting. For comparison, Figure 0-5 shows data for the OH-terminated PDMS. The reaction of the OH-terminated PDMS with silica occurred at room temperature and resulted in notably larger grafting compared to that for methyl-terminated PDMS. The higher reactivity of bis-R_f disiloxanes versus that of cyclic PDMS was attributed to the electron-withdrawing effect of the fluoroalkyl group that made the siloxane bond more reactive.[74]

2.4.3 Grafting Density for the Siloxane-Modified Silicas: Comparison with Other Silane Coupling Agents

The effectiveness of the surface functionalization reactions is primarily determined by the extent of surface coverage or the maximal achievable grafting density

ρ_{max}, group/nm^2. Also, such parameters as the ease of the procedure, the reproducibility of the reaction, and the hazards of the reagents play an important role when the effectiveness of different reactions is evaluated. To compare the effectiveness of the siloxanes, we examined their maximal grafting densities along with the other reaction parameters with respect to those for chloro- and alkoxysilanes, the most studied class of organosilicon reagents used for the surface functionalization of silicas and other substrates. The most straightforward comparison was possible between bis-R_f disiloxanes (this work) and R_f monofunctional and trifunctional silanes[30] because they reacted with silica surfaces in a similar fashion to produce chemically grafted monolayers of the R_f groups (Table 2-2).

Table 2-2: Grafting Density Comparison of Coupling Reagents

Reagent, n=1-6	$\rho_{\max}, group/nm^2$	Comments and References
$[C_nF_{2n+1}(CH_2)_2Si(CH_3)_2]_2O$	1.4-2.3[a]	Non-corrosive reagents. Effective in vapor phase or with neat liquids. T~200°C. Works well for single and porous surfaces [this work].
$C_nF_{2n+1}(CH_2)_2Si(CH_3)_2X$ X=Cl, $N(CH_3)_2$, CH_3O, C_2H_5O	1.6-2.4[a]	Best results obtained for X=Cl and $N(CH_3)_2$ that are corrosive. Effective in solution, vapor phase, and with neat liquids. T ~60-100°C. Works well for single and porous surfaces. [30]
$C_nF_{2n+1}(CH_2)_2SiX_3$, X=Cl, CH_3O, C_2H_5O	2.7-3.5[a]	Best results obtained for X=Cl that are highly corrosive. Poor reproducibility due to high sensitivity to reaction conditions. T ~25°C. Solvent is needed, ρ_{max} can be achieved only for flat surfaces. Does not work well for porous silicas.[30]

Table 2-2: Comparison of $[C_nF_{2n+1}(CH_2)_2Si(CH_3)_2]_2O$, $C_nF_{2n+1}(CH_2)_2Si(CH_3)_2X$ and $C_nF_{2n+1}(CH_2)_2SiX_3$ as reagents for surface functionalization of silicas. ([a] For all of the reagents, grafting density decreased as the size of fluoroalkyl component increased. The low number corresponds to the reagent with n=6 and the high number corresponds to the reagent with n=1.)

Figure 2-6: Grafting Density and Thickness of the PDMS Layer

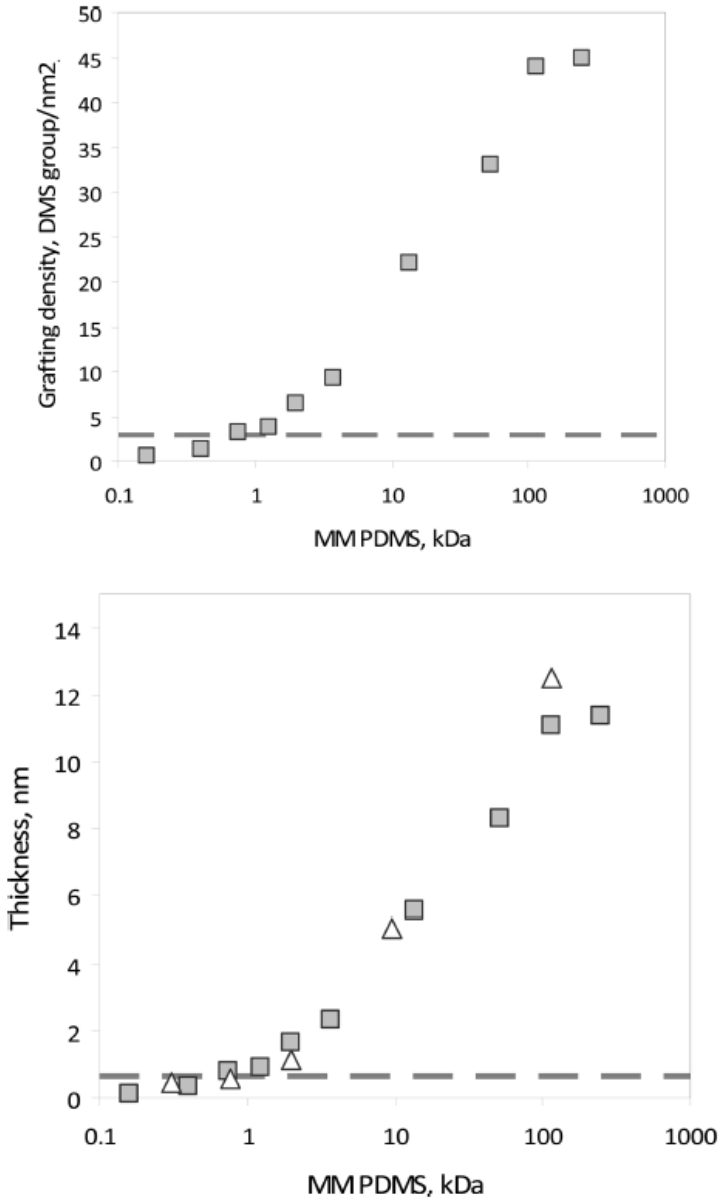

Figure 2-6: Top: the effect of average molecular mass of linear PDMS on grafting density (DMS group/nm^2). Reaction conditions: 24 h at 100^{o}C. Bottom: Squares - thickness of PDMS layers calculated from the grafting density and diameter of the PDMS chain [this work]. Triangles - ellipsometric thickness of PDMS grafted on Si wafers.[66] Dashed line corresponds to a single layer of PDMS lying flat on the surface.

The analysis in Table 2-2 shows that the ρ_{max} values obtained for the disiloxanes were similar to those reported for the best-quality monolayers derived from chloro- and aminosilanes.[30] We noted that the reaction of siloxanes, although it required a higher temperature, used noncorrosive reagents and produced water as the only byproduct, thereby providing a cleaner and less hazardous environment than amino- and chlorosilanes.

For silicas reacted with cyclic PDMS, the maximal grafting densities were in the range of five to six dimethylsiloxane (DMS) repeat units per nm^2, which was consistent with the monomolecular grafting and thereby ruled out continuous reaction by ring-opening polymerization. A minor decrease in the grafting density was observed in the range of $D_3 > D_5 \approx D_4$. The somewhat higher reactivity of D_3 was attributed to the strained ring effect.[75]

As opposed to the reactions of bis-R_f disiloxanes and cyclic PDMS, the reactions of high-MM PDMS produced polymeric surfaces. The data in Figure 0-6 shows that the grafting density on Davisil 250 increased as the MM of PDMS increased and then leveled off. The saturation was observed for PDMS of 115 kDa and was higher with the grafting density plateau at ~45 DMS group/nm^2. Using the grafting density data and the molecular dimensions of the DMS group, the average thickness of the PDMS grafted layers was estimated as follows. The area occupied by the DMS group grafted onto silica has been reported[39] to be $\sigma = 0.40$ nm^2. This value was close to the molecular cross-section of the PDMS chain in PDMS crystals,[76] $\sigma = 0.36$ nm^2. When 0.40 nm^2 was used for the molecular cross-section, the maximal grafting density for a monolayer of DMS groups on silica was obtained as $\rho_{max} = \sigma^{-1} = 2.50$ group/nm^2, which served as an upper

Figure 2-7: Comparison of Grafting Densities for Davisil 250 and SBA-15

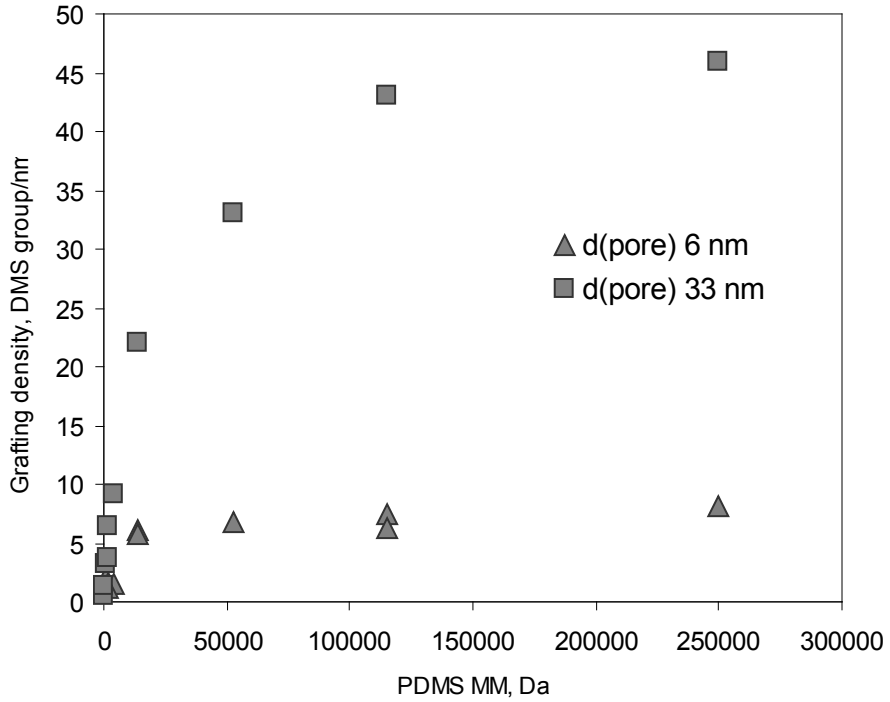

Figure 2-7: The effect of average molecular mass of linear PDMS on grafting density (DMS group/nm^2) for two mesoporous silicas: Davisil 250, d_{pore} = 33 nm (squares) and SBA-15, d_{pore} = 6 nm (triangles). Reaction conditions: 24 h at 100^{o}C.

limit for a closely packed single layer of PDMS lying flat on the surface. The diameter of the DMS group was determined to be $(4\sigma/\pi)^{1/2}$ = 0.71 nm (spherical shape), which was used as an estimate of the thickness of a single layer of PDMS. Assuming uniformly packed layers, the average thickness of the PDMS surface with the grafting density ρ was calculated to be $h = (\rho/\rho_{max}) \times 0.71$ nm. The plot of the calculated thickness on Davisil 250 for silicas reacted with PDMS as a function of their MM is shown at the bottom of Figure 0-6. From that graph, we determined that the amount of grafted PDMS that was equivalent to a single layer of PDMS was observed for the reaction of 0.75 kDa PDMS. The saturation grafting density of 45 DMS group/nm^2 corresponded to ~18 layers of PDMS with a total thickness of ~12.8 nm. Figure 0-6 also shows the ellipsometric

Figure 2-8: Nitrogen Adsorption Isotherms for SBA-15 Reacted with Linear PDMS

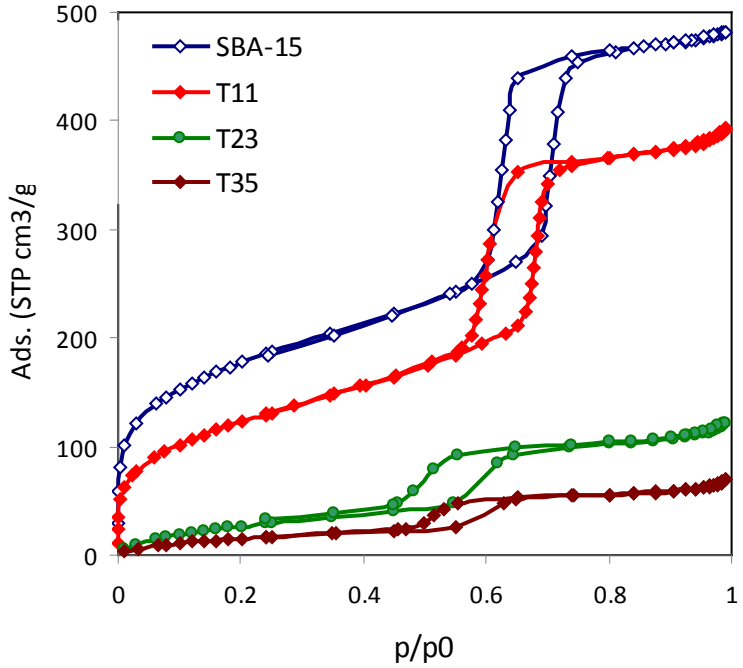

Figure 2-8: Nitrogen adsorption-desorption isotherms (77K) for the SBA-15 reacted with linear PDMS (See Table 0-3 for the full data set).

thickness data reported for the PDMS layers grafted onto Si wafers.[65] The reaction conditions (24 h at 100°C) used in ref. [65] were similar to those used in this work, thus allowing for a direct comparison of the results. As seen in Figure 0-6, two sets of data matched, thereby demonstrating that the reactions of PDMS with Davisil 250 worked as well as with smooth silica (Si wafer), producing surfaces of similar thickness (amount of grafted PDMS). The difference between a flat surface substrate (Si wafer) and porous silica becomes notable for PDMS with MM ≥ 115 kDa when the thickness of porous silica reached the plateau, which was attributed to space limitations for the reactions inside the pores as compared to the reaction with smooth substrates. The average thickness at the plateau (12.8 nm) was ~80% of the average pore radius of Davisil 250, ~15–17.5 nm.

Table 2-3: Pore Structure and Surface Properties of SBA-15 Grafted with Siloxanes

Siloxane	ρ^a, group/nm^2	S_{BET}, m^2/g	V_{pore}, cm^3/g	D_{pore}, nm	C_{BET}	h^b, nm
none (batch I)	-	532	0.74	7.2	135	-
D3	3.05	258	0.58	6.3	42	0.45
T05	2.08	489	0.64	6.5	70	0.35 (0.58)
T11	1.61	452	0.60	6.6	69	0.30 (1.15)
T23	6.02	115	0.18	4.6	15	1.30 (5.05)
T35	6.80	64	0.10	4.7	19	1.25
T46	7.50	63	0.10	4.8	20	1.20 (12.48)
none (batch II)		712	1.04	6.1	147	-
bis-CF_3	1.76	438	0.58	5.0	39	0.55
bis-C_6F_{13}	1.33	288	0.38	4.3	33	0.90
bis-C_8F_{17}	0.76	337	0.44	5.1	50	0.50

[a] calculated as number of dimethylsiloxy repeat units per nm^2,
[b] in parenthesis – data from ref. [66] for the PDMS surfaces on Si wafers prepared under comparable conditions

2.4.4 Nitrogen Adsorption-Desorption Analysis of SBA-15 Silicas

The SBA-15 procedure was selected as the representative ordered mesoporous silica material in this study due to its greater hydrothermal stability, large surface area and larger pore size. We immediately observed that despite the smaller pore size, the reaction does occur with linear PDMS within the pore of the SBA-15 material as demonstrated by the decrease in pore size (D_{pore}), pore volume (V_{pore}) and surface area with increasing chain length (Table 0-3, Figure 0-8). Similar to Davisil 250, grafting

density for linear PDMS reached a plateau and even decreased slightly when high MM PDMS reacted with SBA-15. As is clearly demonstrated in Figure 0-7, the saturation was reached at ~ 7 DMS groups/nm^2, a much lower level than that of

Davisil 250. The more uniform shape of the SBA-15 pores allows for a more detailed analysis of the data as provided in Table 0-3. To obtain thickness of the grafted layer (*h*, nm), we used the pore diameter (D_{pore}) valued and applied equation (1-15).

$$\boldsymbol{h = 0.5 \times (D_{pore}^{SiO2} - D_{pore}^{mod})} \qquad \textbf{(1 - 15)}$$

The thickness values obtained (e.g. T35 = 1.25 nm) at the plateau represent only 36% of the average pore radius of SBA-15 (~3.5 nm). The lower relative grafting density and grafted layer thickness can be attributed, at least partially, to the increased confinement in the pores of the SBA-15 relative to Davisil 250.

Figure 2-9: Pore Size Distributions for SBA-15 Reacted with Cyclic PDMS

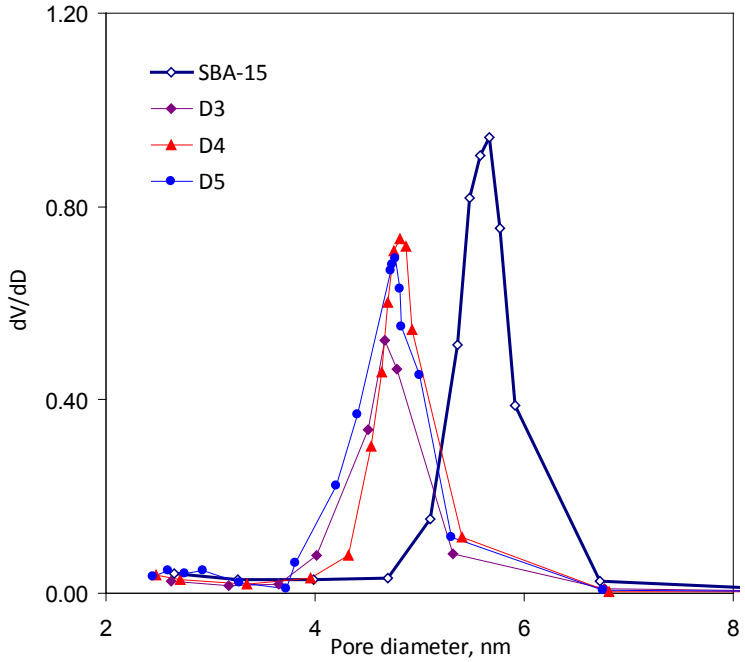

Figure 2-9: Pore size distributions for SBA-15 reacted with D_3, D_4, and D_5 collected from the desorption curve of the nitrogen isotherm (77K). See Table 2-3 for numerical data.

The same trend of lower grafting density for SBA-15 relative to Davisil 250 occurs, albeit to a lesser extent, for bis-R_f disiloxanes and cyclic PDMS (Table 0-3, Figure 0-9). The bis-R_f disiloxanes and cyclic PDMS, though lacking a plateau because of their small size, had lower grafting densities than equivalent Davisil 250 experiments. For example, bis-CF_3 obtained grafting density of 1.8 groups/nm^2 on SBA-15 (Table 0-3) and 2.3 groups/nm^2 on Davisil 250 (Table 0-2). Further investigation was necessary to understand these differences. Additional factors we considered were the synthetic and structural differences between the materials. Specifically, as will be discussed in more detail, we investigated the difference in level of hydration of the SBA-115 surfaces due to the 600^{o}C calcination step.

2.4.5 Role of Surface Water

The importance of the physisorbed water for the reactions of siloxanes with silicas has been highlighted in early work.[59-61] To investigate further, we have studied the reactions of siloxanes with a series of progressively dehydrated silicas. It is well documented[76] that the amount of water on the silica surface can be thoroughly controlled through the thermal treatment of silica at different temperatures. According to the Zhuravlev model,[76] the initial dehydration of silica involved the removal of physically adsorbed water, most of which was completed by ~200°C. The subsequent loss of water in the 200–1000°C range was attributed to the process of dehydroxylation of surface silanols with the formation of siloxane bridges. We note that this was a rather simplified description of the dehydration process because it does not differentiate between the various kinds of silanol groups (isolated, vicinal, geminal) nor does it take into account their accessibility (internal vs. external silanols). Nevertheless, this model accurately

Table 2-4: Physisorbed Water and Total Silanols on Davisil 250 Prepared at Different Temperatures

Calcination T, ^{o}C	S_{BET} (N_2), m^2/g	[a] H_2O, molecule/nm^2	[a] SiOH, group/nm^2
100	252	2.3	5.5
500	273	0	2.5
600	253	0	1.2
800	232	0	0.5
1000	118	0	0.2

[a]Experimental results were compared to those found in the literature.[76]

described the overall dehydration process and provided a simple method to determine the amount of physisorbed water and the number of silanol groups by TGA.[76,77] To determine the surface concentration of physisorbed water and silanol groups, the BET surface areas were assayed for each silica dehydrated at different temperature. The results are shown in Table 2-4. Davisil 250 dehydrated at 100°C had 2.3 molecules of physisorbed water per nm^2 and 5.5 silanols per nm^2, indicating a fully hydroxylated surface.[76] Calcination at $T \geq$ 500°C produced silicas that were free from molecularly adsorbed water with a gradually decreasing population of silanols as the calcination temperature increased, in a good agreement with the literature.[76]

Figure 0-10 presents grafting densities plotted as functions of silica (Davisil 250) calcination temperature. The grafting density data are shown as a percentage of the maximal value (observed for silica pretreated at 100°C), thereby allowing for direct

Figure 2-10: The Effects of Silica Calcination Temperature on Reactions with Siloxanes

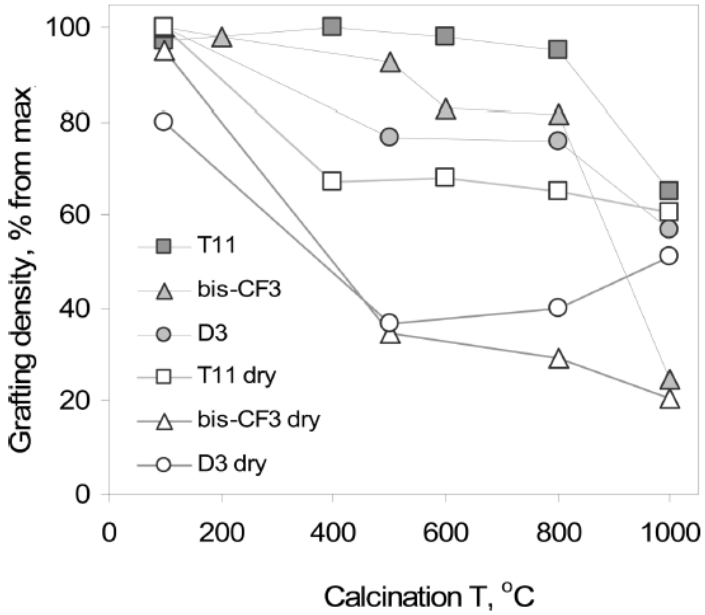

Figure 2-10: The effects of silica calcination temperature on the reactions with different siloxanes. Grafting density data (y-axes) is shown as a % from the maximal value grafting density observed for a given siloxane. Closed symbols represent data for the reactions carried out at atmospheric pressure using siloxanes "as received" (containing 60-100 ppm of water). Open symbols stand for the reactions carried out under rigorously dry conditions. The temperature and time of all the reactions were 100°C and 24 h. The points are connected to guide the eyes.

comparison of the reactions of the siloxanes of different structures. As anticipated, for all of the siloxanes the grafting density decreased as the temperature of silica calcination increased. The decrease in grafting density, however, was not consistent with the decreased number of surface silanols. Indeed, for silicas pretreated at 800 °C, the number of silanols was less than 10% of that for fully hydroxylated silica, yet only a minor decrease in grafting density was observed (Figure 2-10). The removal of physisorbed water (treatment at 200°C) did not seem to have any significant impact on the reactions. Only for silicas calcinated at 1000°C did the number of grafted siloxanes show a notable decrease reflecting the nearly complete removal of silanols. However, even for these

silicas, the grafting densities were unusually high. Initially puzzled by these results, we later realized that silica was not the only source of water for the reaction.

Normally, the reactions of silica with siloxanes were carried out in capped vials at atmospheric pressure, so there was a possibility of atmospheric moisture entering the reaction media. We also found that a notable amount of water could be introduced into the reaction

system with the siloxanes. According to chemical analysis (Oven Karl Fischer), the equilibrium amount of water present in all of the siloxanes "as received" was ~60–100 ppm. The use of dried siloxanes (heating in vacuum) did show some reduction of the grafting density, but the effect was not significant. Therefore, our next experiments were aimed at eliminating the possible impact of atmospheric moisture by carrying out the reactions under rigorously dry conditions. These included thorough outgassing of both silica and siloxane at elevated temperature and running the reactions under vacuum (using nonvolatile siloxanes). The results are also shown in Figure 2-10 with open symbols. The difference in the reactivity for the systems in vacuum versus being exposed to the atmosphere was remarkable: the grafting densities for the reactions carried out in vacuum were reduced greatly as compared to the reactions exposed to the atmosphere, confirming that atmospheric moisture did play an important role in the mechanism, facilitating the reaction of siloxanes with silica. Although the reduction of grafting under dry conditions was observed for all types of siloxanes, the effect was more prominent for low-MM siloxanes (bis-CF_3 and D_3) than for high-MM PDMS. We attributed this to differences in the surface reactions for monomers (one grafting point per molecule) and polymers, where multiple grafting points per molecule were possible. In

the case of low-MM siloxanes (bis-CF_3 and D_3), grafting was directly related to the concentration of the surface reaction centers (physisorbed water and silanols) that were reduced significantly as the dehydration temperature increased. For high-MM PDMS, the decrease in the number of reaction centers probably decreased the number of grafting points per molecule, but it had less of an effect on the total number of grafted molecules, which remained approximately constant at ~65–70% from the maximum for silicas dehydrated at $T > 400$°C.

The results presented above further supported the critical role of physisorbed water for the reaction of siloxanes with silicas, as first proposed in ref [61]. We believe that the reactions of siloxanes with silica are initiated by the Lewis acid centers formed by water molecules adsorbed on the silica surface defects. The acidic centers are known to catalyze the hydrolysis of the siloxane bond.[74] The silanols produced after the hydrolysis of the siloxane further react with surface silanols, yielding grafted siloxanes:

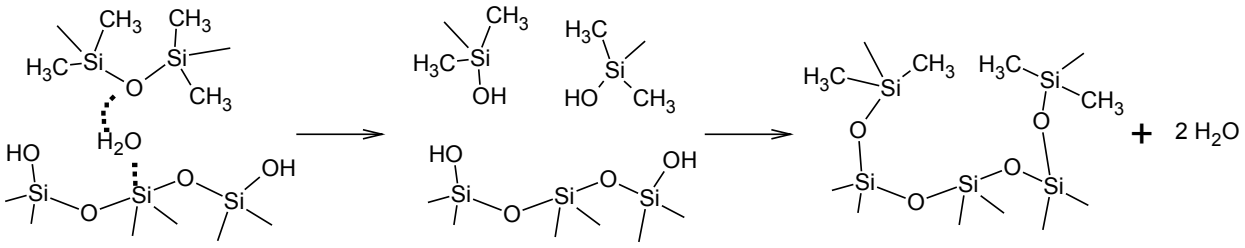

According to the reaction scheme shown above, one molecule of surface water is consumed and two water molecules are produced per two grafting points. To examine this further, we ran the reactions in open vessels while monitoring the total weight of the reaction system over time using TGA. By using silicas and nonvolatile PDMS T23 (both dried to a constant weight at the temperature of the reaction, 100°C, prior to mixing), the weight loss observed was associated with the removal of the water byproduct of the

surface grafting reaction. The corresponding weight loss curves shown in Figure 2-11 demonstrate that the weight loss was

Figure 2-11: Isothermal Weight Loss Kinetic Plots of the Reaction

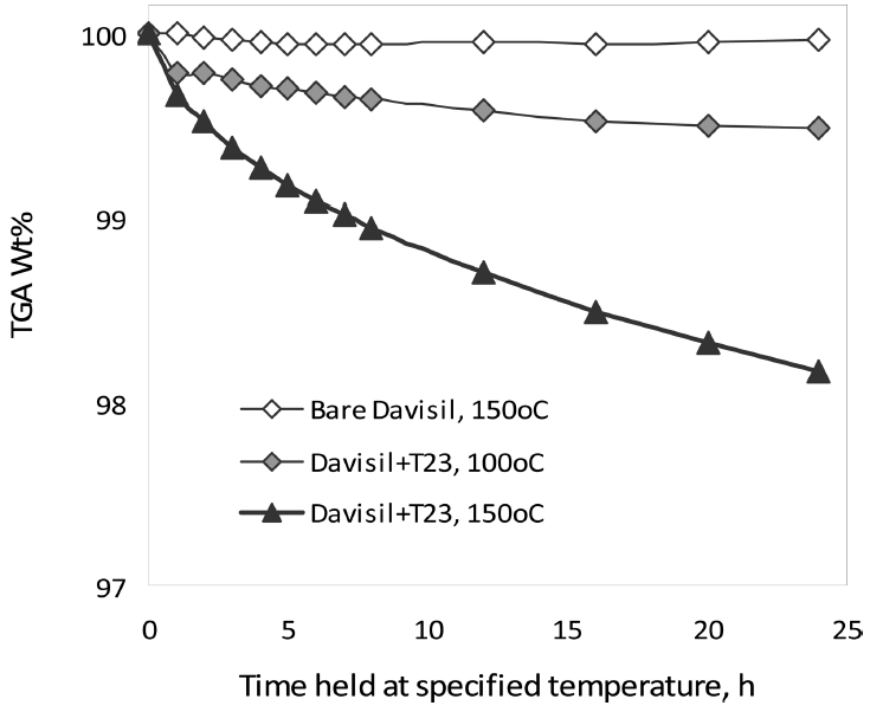

Figure 2-11: Isothermal weight loss kinetic plots observed for bare Davisil 250 (open symbols) and Davisil 250 mixed with PDMS T23 (closed symbols).

notable after the first hour of contact of silica with PDMS, indicating that the reaction was fast. Interestingly, the reaction was not complete after 24 h because the weight loss curve did not level off (Figure 2-11). In this regard, we point out that according to chemical analysis (%C, H), the reactions of T23 PDMS were completed by 12 h because no further increase in carbon loading was observed after that time. When comparing these two sets of kinetic data, we speculate that the initial stage (minutes to hours) of the reaction included the hydrolysis of the siloxanes into silanols and the immediate strong adsorption of these silanols on the silica surface through H-bonding. These processes

resulted in the immobilization of the siloxanes on the surface but did not release any water and therefore were not reflected in the weight loss curves shown in Figure 0-11. In a later stage (many hours and possibly days, depending on the temperature) of the reaction, the adsorbed silanols reacted with surface silanols to release water, which was observed in the weight loss curves. We surmised that (especially for the high-MM PDMS) the rearrangements of the adsorbed silanol-terminated siloxanes on the surface, possibly including their further hydrolysis and subsequent reactions with surface silanols and with each other (cross-linking) continue to take place well after the reactions are quenched and considered to be terminated.

To investigate this further, we conducted post-reaction annealing studies. For example, a fully characterized sample of SBA-15 modified with PDMS T35 was placed in an oven for 24 hours at temperature while exposed to the atmosphere. The samples were then analyzed by nitrogen adsorption and compared to the original material. This cycle was repeated multiple times. Specifically for the high-MM PDMS, we observed only minor changes to the D_{pore}, but significant decreases in V_{pore} and S_{BET}. This demonstrated that further hydrolysis and reactions, specifically cross-linking, may occur to completely 'block' the already significantly confined pores.

Table 2-5: Characterization of SBA-15 Silica Modified with T35 and Annealed

Cycle	Initial	1 (80°C, 24 h)	2 (100°C, 24 h)
$S_{BET,}$ m^2/g	64	50	18
V_{pore}, cm^3/g	0.10	0.08	0.04
D_{pore}, nm	4.7	5.1	4.9

The data presented in Figure 2-10 also demonstrated that the reaction of siloxanes with silica did occur, albeit to a lesser extent, even with silica dehydrated at 1000°C and under dry conditions (i.e., when supposedly no water was present in the system). The residual reactivity observed even for rigorously dried systems deserves special explanation. According to the reaction scheme proposed above, the reaction of siloxanes with silica produced water, so, with respect to water, the reaction was autocatalytic. It was therefore plausible to assume that even residual traces of water would be sufficient to initiate the reaction. Although we cannot completely rule out the presence of trace amounts of water in the reactions, we would like to offer an alternative explanation for the reactivity of dehydrated silicas with siloxanes that did not require water. This involves the reaction of the siloxanes with dehydrated silica surface via the opening of strained siloxane rings:

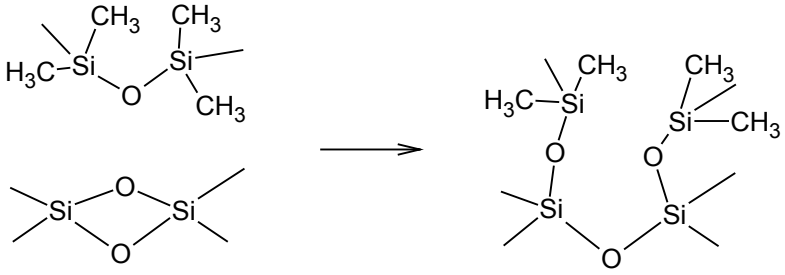

The dehydration of silicas at high temperatures (~400–1000°C) produced surfaces containing strained siloxane rings.[78,79] These strained rings readily participated in various reactions and could be used as reactive centers for the covalent functionalization of surfaces. The reaction of siloxanes with strained siloxane rings was first described in ref [59]. The reactions of strained siloxane rings with water, alcohols, amines, silanes, and siloxanes have also been reported.[78-82] For the concentration of the siloxane rings, the following numbers have been reported (with the temperature of the

Table 2-6: Hydrophobic Surface Properties of Silicas Grafted with Siloxanes

Siloxane	Davisil 250			SBA-15	
	ρ^a, group/nm^2, Davisil 250	θ (adv/rec), deg., Davisil 250 (pressed pellets)	Water vapor adsorption at p/p^0 = 0.3, mg/g gram of Davisil 250	ρ^a, group/nm^2, SBA-15	θ (adv/rec), deg., SBA-15 (pressed pellets)
none	-	spreads	36.19	-	spreads
D_3	9.3	126/95	4.26	3.05	151/141
bis-C_6F_{13}	1.8	130/105	6.02	1.33	157/144
T11	6.5	110/10	13.86	1.61	23/0
T23	22	115/70	12.26	6.02	121/93
T35	33	115/84	11.98	6.80	124/96

[a]Calculated as the number of dimethylsiloxy groups per nm^2,
[b]Bis-C_6F_{13} disiloxane was calculated as the number of C_6F_{13} groups per nm^2

silica treatment in parentheses): 0.15 nm^{-2} (1200°C),[80] 0.2–0.4 nm^{-2} (1080°C),[79] 0.04–-0.13 nm^{-2} (900°C),[81] and 0.004–0.024 nm^{-2} (300–700°C).[82] In this work, for the reaction of dried bis-CF_3 siloxane with silica dehydrated at 1000°C, the grafting density of the CF_3 groups was 0.26 nm^{-2}. Assuming that the reaction occurred exclusively through the strained rings, this corresponded to a concentration of 0.13 siloxane rings per nm^2, which is well within the range reported in the literature. This result indicated that the reaction of siloxanes with rigorously dehydrated silicas could be explained solely by the strained ring centers, thereby demonstrating an alternative pathway for the reaction of siloxanes with surfaces that did not require water.

Figure 2-12: Contact Angel Measurement Image

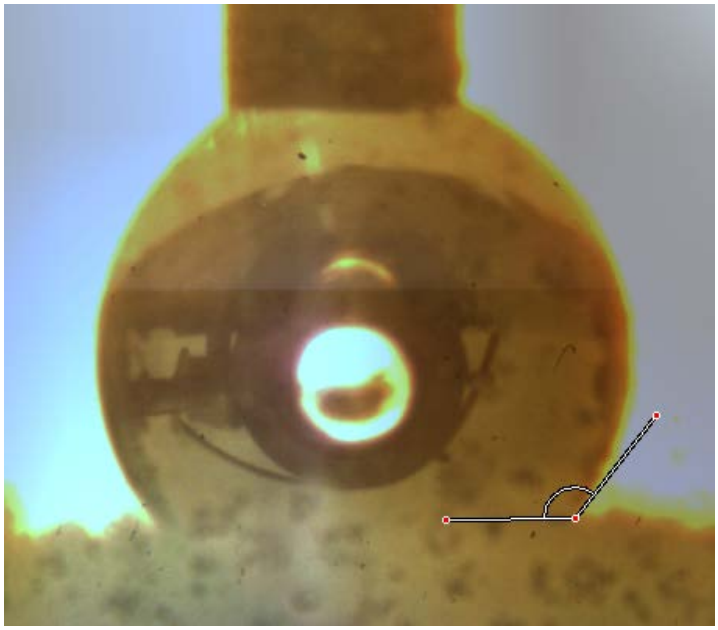

Figure 2-12: Image of a contact angle measurement for a pressed pellet of Davisil 250 modified with bis-C_6F_{13}. The roughness introduced by the pressed powders caused higher different contact angles than that of a comparable smooth surfaces.

Figure 2-13: Water Vapor Adsorption-Desorption Isotherm Comparison

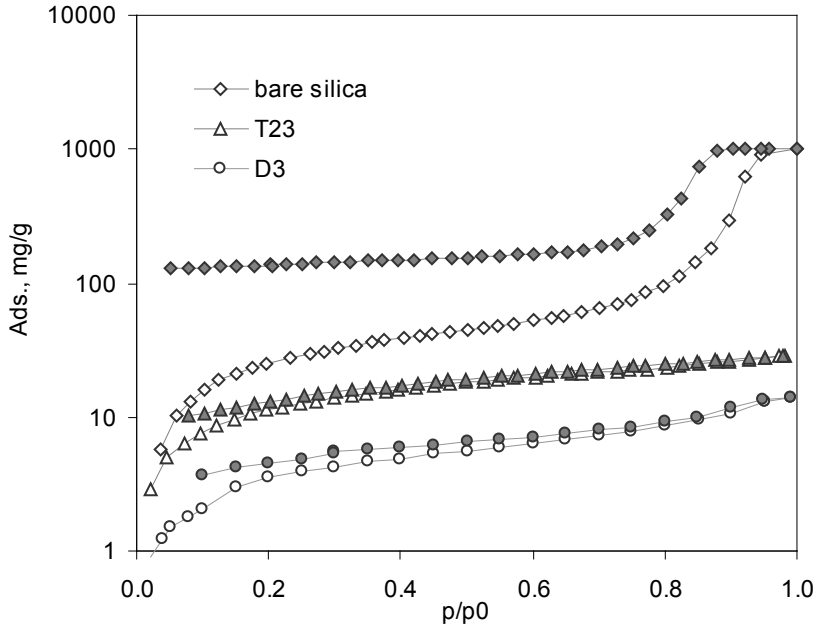

Figure 2-13: The adsorption-desorption isotherms of water vapor (293K) for bare Davisil 250 silica and silica reacted with T23 and D_3 siloxanes. Open symbols, adsorption; closed symbols, desorption.

2.4.6 Surface Properties

To gain insight into the uniformity of the coatings, the hydrophobic surface properties of the siloxane-modified silicas were examined next. Two methods were used to assess the hydrophobicity of the surfaces prepared: (1) water contact angles using silica pressed pellets and (2) adsorption isotherms of water vapor at room temperature (293 K). The data is summarized in Table 0-6 and demonstrated for Davisil 250 in Figure 0-12 and Figure 0-13.

Water spreads over the surface of bare silica, indicating highly polar surfaces of silanol groups. The grafting of nonpolar organosiloxanes on silica produced hydrophobic surfaces that were evidenced by a remarkable increase in the water contact angles. The best-quality hydrophobic surfaces were obtained for silicas reacted with cyclic PDMS and bis-fluoroalkyl disiloxanes. The water contact angles for these surfaces were as high as 157°/144° (adv/rec), indicating low-energy surfaces with nonpolar functionalities. The high values of both advancing and receding angles were characteristic of densely packed uniform surfaces that provided efficient blockage of polar centers of bare silica. We attribute the higher contact angles and decreased hysteresis for SBA-15 relative to Davisil 250 to its more uniform packing of the pellets due to their much smaller particle size. For both materials, we consistently observed that the water contact angles for the pressed powders were a bit higher (~5–10°) than those reported for surfaces of covalently attached and self-assembled monolayers of similar chemical composition supported on smooth (Si wafer) substrates,[30] which was attributed to the surface roughness of the pressed pellets (Figure 0-13). The contact angles for the silicas reacted with linear PDMS were strongly affected by the MM of the PDMS used (Table 0-6). For the

surfaces derived from low-MM PDMS (≤3.75 kDa), the advancing contact angles were high (>100°) yet the receding angles were particularly low (~0–40°), indicating a substantial presence of uncovered silanols. For PDMS with MM greater than 13.5 kDa, the hydrophobicity of the surfaces greatly improved with the advancing angles leveling off ~115°. The receding angles, however, were less than 90°, which was consistent with the hydrophobic surfaces of grafted PDMS chains and, possibly, a small number of polar groups available to water (Si–OH).

The adsorption isotherms of water vapor corroborated the contact angle data. Figure 0-13 presents the water adsorption isotherms for bare Davisil silica and silicas grafted with various siloxanes. As demonstrated by the remarkable reduction of the water adsorption observed over the entire range of pressures, including the saturation ($p/p_0 \rightarrow 1$), the reactions of siloxanes produced high-quality hydrophobic surfaces. According to the adsorption of nitrogen (Figure 0-8), all of the modified silicas demonstrated type IV isotherms, i.e., the silica pore space was largely preserved albeit the pore volume was notably reduced by the grafting. Even though the pore space was available, no pore filling was observed by water. The adsorbed amounts of water at saturation corresponded only to a small fraction (~2-5%) of the available pore volume. Assuming a uniform distribution and 0.106 nm^2 for the cross-section of the adsorbed water molecule,[83] these adsorbed amounts corresponded to approximately one-third of the monolayer capacity. Such a low value of water adsorption and the absence of pore filling at saturation were indicative of uniform, hydrophobic surfaces of the pores. The absence of pore filling by water was observed, not only for silicas reacted with bis-R_f disiloxanes and cyclic PDMS (where only monomolecular grafting was possible) but

also for silicas reacted with the high-MM PDMS arguing for the uniform distribution of grafted polymers over the pore surfaces. As shown in Figure 0-12, the desorption was always incomplete, and small residual amounts of water were retained by the silicas. This water, however, was adsorbed reversibly because it was completely removed upon outgassing at elevated temperature. On the basis of the amount of water adsorbed at $p/p_0 = 0.3$, the hydrophobicity of the siloxane-grafted silicas was as follows:

$$Cyclic\ PDMS\ \approx bis - R_f\ siloxane\ \geq high\ MM\ linear\ PDMS$$

$$> low\ MM\ linear\ PDMS$$

We noted that this range of hydrophobicity was consistent with that obtained by contact angles (Table 0-6). The agreement between the two techniques in the characterization of the surface hydrophobicity of porous silicas was remarkable, considering that the contact angles probe the external surfaces of the particles and the vapor adsorption isotherms probe the entire surface, ~98% of which is the surface of the pores.

2.4.7 Thermogravimetric Analysis

One of the superior qualities of the siloxanes as surface functionalization agents is related to the excellent thermal stability of the siloxane-grafted silicas as assessed by TGA. The representative TGA plots for bare silica and silica reacted with different siloxanes are shown in Figure 0-14. For all siloxane-grafted silicas, the main weight loss feature was observed above ~300°C, which was attributed to the degradation of grafted organic groups. The temperature of the onset of the weight loss and the temperature of the maximal rate of the weight loss (T_{max}) showed some variation for different siloxanes. The total weight loss varied significantly, reflecting the difference in mass fraction of

Figure 2-14: TGA Plots of Grafted Silicas

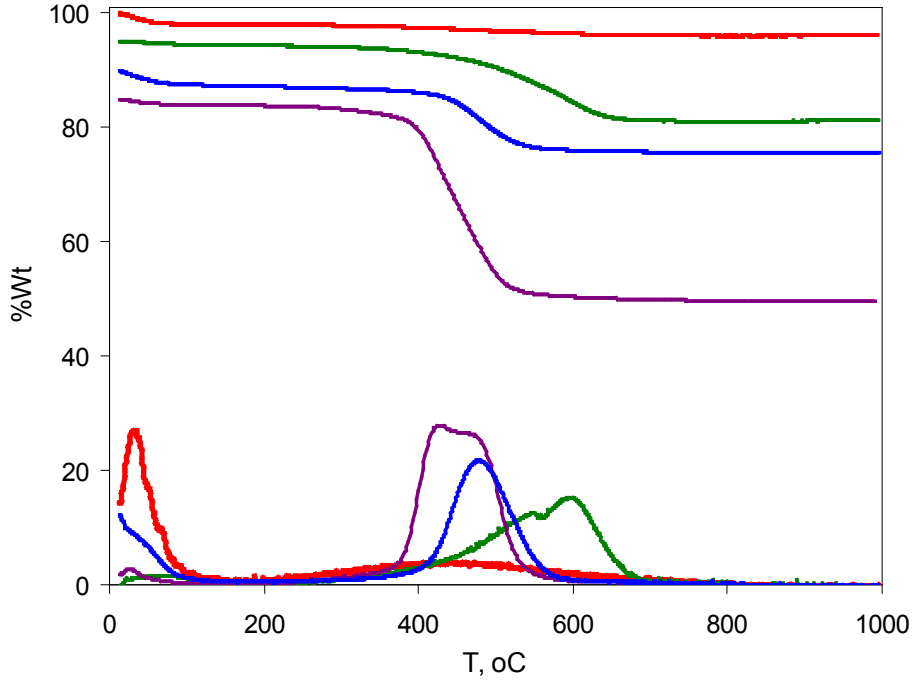

Figure 2-14: TGA plots for bare silica (---) and silica grafted with D_3 (---, offset by 5 wt%), bis-CF_3 (---, offset by 10 wt%), and T23 (---, offset by 15 wt%).

grafted siloxanes: from ~10% for silicas reacted with cyclic PDMS and bis-fluoroalkyl disiloxanes up to ~50% for silicas reacted with the high-MM PDMS. For silicas reacted with cyclic PDMS, the weight loss occurred over a wide range of temperature (~340–670°C), with T_{max} centered at ~550–600°C. For silicas grafted with high-MM PDMS, the weight loss occurred in a similar range (~300–600°C) yet at a notably lower T_{max} ~ 450°C. From the literature on the thermal degradation of PDMS,[84] the mechanism of this process involved depolymerization via scission of the Si–O–Si backbone with the formation of volatile cyclic siloxanes (D_3 and higher). For the PDMS chains grafted to silica,[39] the degradation mechanism was proposed to be similar; however, the process was affected by the grafting points, where the depolymerization of grafted PDMS was interrupted by the silica matrix. For monolayers of DMS groups grafted to silica, the

Figure 2-15: Weight Fraction of Carbon in the TGA Weight Loss for Grafted Silicas

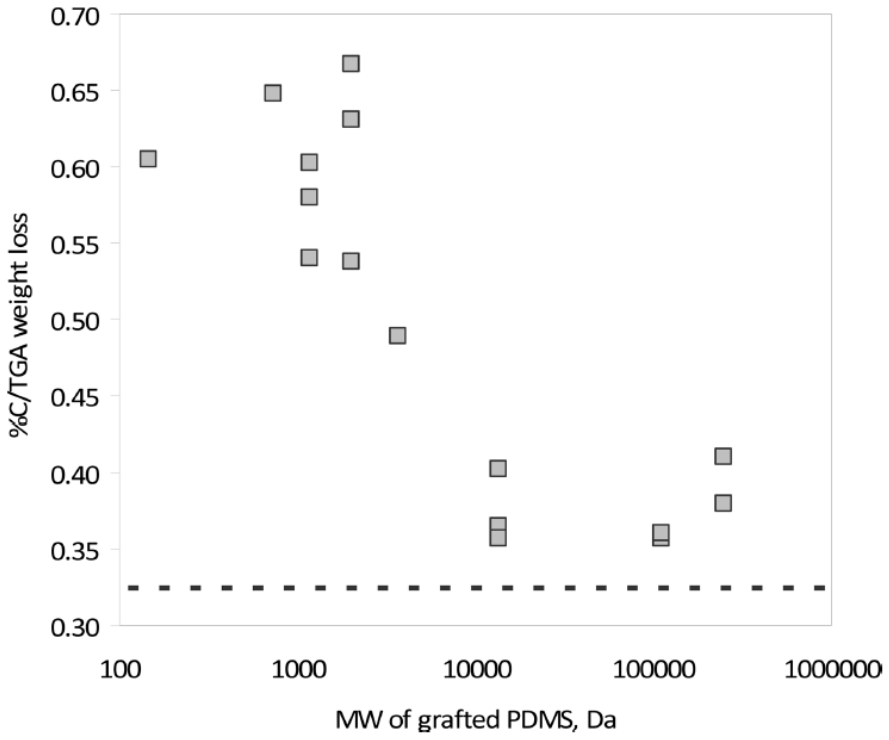

Figure 2-15: Weight fraction of carbon in the TGA total weight loss (200-600°C region) for silicas grafted with a linear PDMS of different molecular mass. The dashed line is at 0.32, the weight fraction of carbon in pure PDMS.

degradation pathway was different because it involved breaking the Si–CH_3 bonds rather than the desorption of dimethylsiloxy species via breaking the Si–O–Si_S bonds.[39] The T_{max} for PDMS-silicas was ~450°C, whereas for DMS-silicas T_{max} was higher,[39] ~550°C. With this data, the differences in TGA curves observed for silicas reacted with high- and low-MM PDMS can be explained by different numbers of grafts per molecule and therefore different contributions of different degradation mechanisms. We tried to differentiate these processes based on the analysis of the carbon percent (determined separately via chemical analysis) in the total weight loss. For the thermal degradation occurring mainly through depolymerization, the carbon fraction in the weight

loss would approach 0.32, the value for pure PDMS. As the number of grafts per chain increased, the contribution from the pyrolysis of Si–CH_3 groups would also be increasing, leading to an increase in the percentage of carbon in the total weight loss. The experimental data (Figure 2-15) demonstrated a notable decrease in the percentage of carbon in the total weight loss as the MM of grafted PDMS increased. This supported the conclusion of fewer attachment points (per PDMS chain) for silicas reacted with high-MM PDMS. For silicas reacted with bis-R_f disiloxanes, the total weight loss increased with the size of the fluoroalkyl group, reflecting an increase in the grafted amount, and onset and T_{max} were similar at ~490–500°C for all of the bis-R_f disiloxanes studied.

2.5 Conclusions

The reactions of bis-R_f disiloxanes, cyclic PDMS (D_3–D_5), and linear methyl-terminated PDMS (MM 0.4–250 kDa) with Davisil silica ($D_{pore} \approx$ 30–35 nm) and SBA-15 silica ($D_{pore} \approx$ 6-7 nm) were investigated. According to FTIR and chemical analysis, the reactions of bis-R_f and cyclic PDMS produced closely packed monomolecular surfaces of chemically grafted fluoroalkyl groups and small PDMS cycles ($n < 5$), respectively. Using linear methyl-terminated PDMS of high-MM (≥1.25 kDa) produced chemically grafted polymeric surfaces. As assessed by water contact angles and adsorption isotherms (293 K) of water vapor, quality hydrophobic surfaces were obtained for silicas grafted with bis-R_f disiloxanes, D_3–D_5, and linear PDMS of MM ≥ 13.5 kDa. According to TGA, the siloxane-grafted silicas showed superior thermal stability: the temperatures of the maximal weight loss rate were ~450°C (PDMS), ~500 °C (bis-R_f), and ~575 °C (D_3–D_5).

A study of the reactions of silicas with different extents of hydration and controlled moisture content in the system demonstrated the critical role of water in facilitating the grafting of the siloxanes. The proposed reaction mechanism involved the hydrolysis of the siloxanes by the Lewis acid centers formed by the adsorbed water (presumably on surface defects). According to this scheme, the hydrolysis of the siloxanes produced silanols that further reacted with surface silanols to yield the siloxane-grafted surfaces. For the rigorously dehydrated silicas (calcination ~1000°C), an alternative pathway that involved the reaction of the siloxanes with the strained siloxane rings and did not require water was also plausible.

An overall comparison of siloxanes and classical silane coupling agents (i.e., silanes with readily hydrolysable functionalities such as chloro, amino, etc.) demonstrated that the reactions of siloxanes with silicas produced surfaces of similar quality and, although they required higher temperatures, used noncorrosive reagents and generated only water as a byproduct, thereby providing a viable and environmentally benign alternative to the chemical functionalization of mesoporous metal oxides.

Chapter 3 : Solution Adsorption of Phthalocyanines on Solids Surfaces

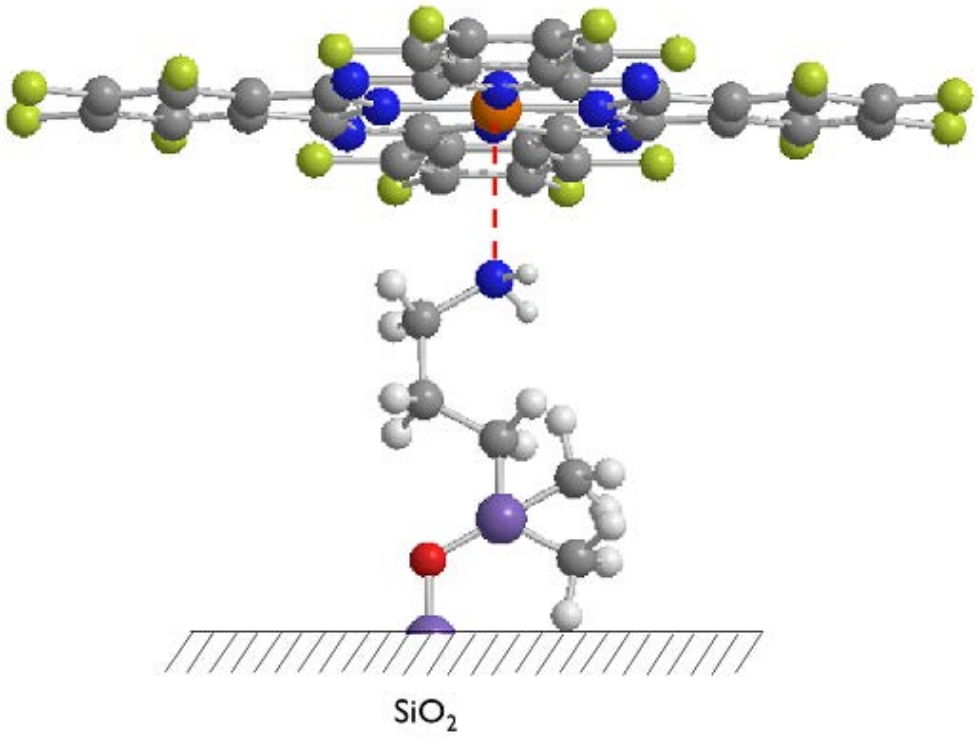

3.1 Abstract

In this study, the adsorption of two series of phthalocyanines (Pcs) from acetone and methylene chloride on the surface of bare and functionalized metal oxides was studied. The two Pc series were: (1) zinc phthalocyanines with the sixteen hydrogens substituted with F and/or i-C_3F_7; the naming convention is F_nPcZn, where n = 16, 40, 52 and 64 and (2) peripherally *i*-C_3F_7 substituted phthalocyanines with varied central metals, F_{64}PcM, where M = Zn, Ru, Cu, Co, Fe and VO. The Pcs were also assessed for thermal stability by TGA. Adsorption of the phthalocyanines readily occurred on the surface of Al_2O_3 and aminated silicas. The most reproducible monomolecular thin films were produced on both surfaces with F_{64}PcM (M=Zn, Ru) aged in acetone for two days at room temperature. Fairly consistent bilayers were produced using F_nPcZn (n = 16, 40) in acetone, a result of these Pc's propensity to form cofacial dimers. Pc multilayers were produced via adsorption from methylene chloride after two days at room temperature, despite the lower solubility of the phthalocyanines in this solvent.

Mechanistic studies indicated that the adsorption of phthalocyanines on the surface of both metal oxides and functionalized metal oxides was largely determined by three factors: (1) the electron deficiency of the phthalocyanine metal center, (2) the Lewis basicity of the substrate surface, and (3) the interactions of the solvent with the phthalocyanine molecule and the substrate surface. A mechanism was proposed in which strong adsorption occurred via axial coordination of the phthalocyanine metal center to basic moieties on the substrate surface. Solution adsorption of fluorinated phthalocyanines was demonstrated to be a simple and reproducible technique for the formation of phthalocyanine thin films on certain metal oxide surfaces.

3.2 Introduction

Phthalocyanines (Pcs) are an interesting class of molecules that are catalytically active dyes with unique spectroscopic, photoelectric, and sometimes magnetic properties. Some Pcs are also highly chemically and thermally stable.[85] Phthalocyanines are chemically versatile because of the numerous possibilities of modifications to both the coordinated central group and the macrocycle. This versatility has led to many technological applications such as photoactive dyes,[85] semiconductors,[86] photovoltaic cells,[87] electrophotography,[86] photosensitizers,[88] gas sensors,[89] low-dimensional metals, photodynamic therapy,[90] Langmuir-Blodgett films,[36,89,91] liquid crystals,[92] and optics.[93]

Phthalocyanines are planar aromatic macrocycles, the synthetic analogs of porphyrins, consisting of four isoindole units presenting an 18 π-electron aromatic cloud delocalized over an arrangement of alternated carbon and nitrogen atoms (Figure 3-1).[94] The properties of Pc compounds can be tuned through relatively straightforward chemical procedures.[95] Physical and chemical properties of phthalocyanines are most impacted by a change in their central atom, peripheral modification, or a structural change to the macrocycle.[96] A change in the central metal will impact the catalytic activity and electronic, spectroscopic, and physical properties.[88] In fact, The two hydrogen atoms of the central cavity have been replaced by more than 70 metallic species.[94] Replacement of H-atoms in all α and β positions of the ring (Figure 3-1) has been studied for various applications. Changes to the periphery, β for example, have been used to increase solubility,[97] change the electronic structure,[86] or covalent attachment to a solid support.[98]

Figure 3-1: Nomenclature of Phthalocyanine Molecules

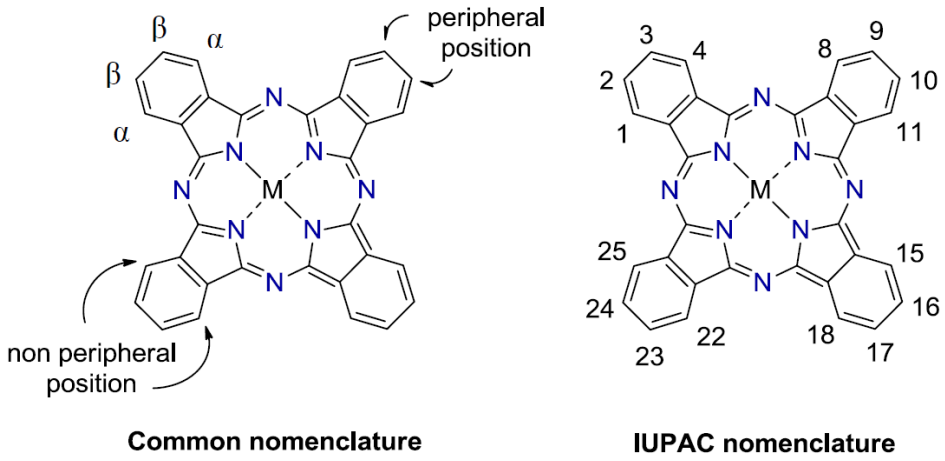

Figure 3-1: Numbering scheme and labeling of outer-ring positions (α, β) of the phthalocyanine molecule core.[98] Note the 16 C-H bonds present in an unsubstituted molecule, M = Metal.

Many potential applications (photovoltaic cells, gas sensors, electrochromic displays, electroluminescent devices, etc.) require Pcs to be present in the solid state as thin films.[36] The formation of Pc thin films has been achieved primarily by sublimation, evaporation, chemical

vapor deposition, molecular beam epitaxy, electrochemical deposition, spin coating, thin film casting, and self-assembled monolayer techniques.[94] Many of these techniques are necessary due to the low solubility of Pcs in organic solvents, while also taking advantage of their chemical and thermal stability. Enhanced solubility can be achieved by incorporation of ligand groups in the Pc α and β positions during chemical synthesis.[91] Generally speaking, the insertion of bulky groups bonded to the periphery of the macrocycle improves the solubility and prevents aggregation because of steric hindrance.[99] Additionally, a selected isoindole units can be modified with alkyl chains to be used with the Langmuir-Blodgett technique.[36]

Of particular interest to this work, photoexcited Pcs develop a very short-lived singlet excited state that, through intersystem crossing, gives rise to a longer-lived triplet state. The efficient production of singlet oxygen from this triplet state has led to applications in photodynamic therapy and photocatalysis.[90] Photoexcited Pcs have been used for the oxidative degradation of sulfur-containing compounds, phenols, and chlorinated phenols as well as oxidation of secondary alcohols and aromatic compounds, allylic amination, and epoxidation of olefins.[94]

Peripheral substituents have also been used to tune the steric and electronic features of phthalocyanines, yielding both electron rich and electron poor species, the latter including the important class of halogenated phthalocyanines.[97] The focus of our groups' work has been the replacement of α and β hydrogens with fluorine and *i*-C_3F_7 groups to increase the relative stability and catalytic activity of Pcs.[90] Addition of the electron withdrawing fluorine groups leads to a molecule with increased ionization potential, thereby protecting the catalyst from oxidative destruction by the singlet oxygen it produces.[100] One drawback of this substitution is poor solubility and an increased propensity for aggregation in solution.[93] However, further substitution of the β position with bulky *i*-C_3F_7 demonstrated a further increase in stability with a simultaneous increase in solubility and decrease in aggregation.[97]

With increased stability and solubility, solution adsorption presented a more viable alternative for the preparation of phthalocyanine thin films. We focused on previously described F_{64}PcM and F_nPcZn series. The F_{64}PcZn complex is common to both series. The structures of F_{16}PcZn, F_{28}PcZn, F_{40}PcZn, F_{52}PcZn, and F_{64}PcZn dyes produced by microwave synthesis are shown in Figure 3-2 (Note: H_{16}PcZn is not shown,

but was included in our work for direct comparison).[98] The pictured dyes constituted a systematic series of isoelectronic Zn complexes in which only peripheral modifications were performed to alter the electronic density of the common aromatic macrocycle and metal center.[90] In this series, the electronic deficiency of the metal center increased in the order of H_{16}PcZn < < F_{16}PcZn < F_{28}PcZn < F_{40}PcZn < F_{52}PcZn < F_{64}PcZn.[97] The addition of the bulky *i*-C_3F_7 groups dramatically increased the solubility of the phthalocyanines and significantly decreases aggregation of the compounds in solution.

Figure 3-2: Synthesis and Structures of Phthalocyanines

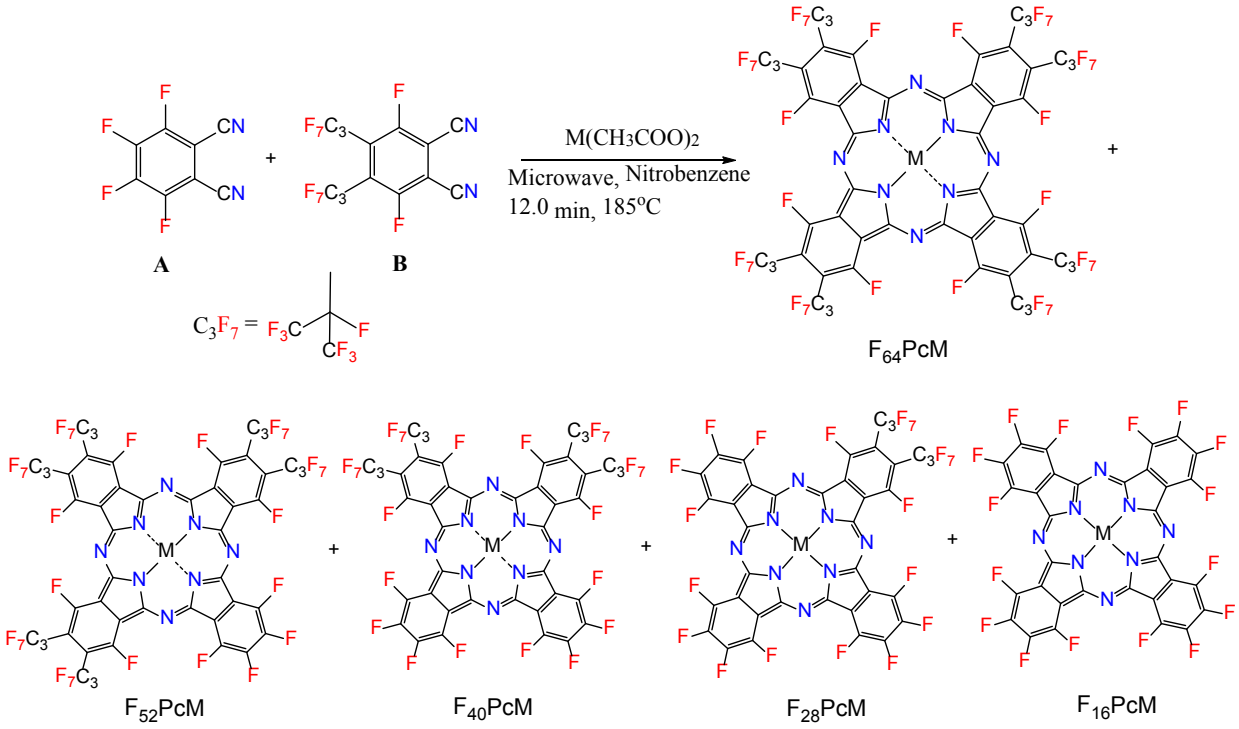

Figure 3-2: General synthetic scheme for the preparation of fluorinated phthalocyanines. Varying the ratios of phthalonitrile reactants, **A** and **B,** preferentially targets production of one of the five products shown. A reaction with only **A** will produce F_{16}PcZn. A reaction with only **B** will produce F_{64}PcZn. Ratios for **A** to **B** of 3:1, 1:1, and 1:3 are used for the synthesis of F_{28}PcZn, F_{40}PcZn (*cis* and *trans*, only *cis* displayed), F_{52}PcZn, respectively.

A simplified description of the factors impacting adsorption from solution involves solute-solute, solute-solvent, solute-substrate, and solvent-substrate interactions. The changes to the solute (phthalocyanine) substituents and metal center we have described should have an impact on its interactions with the solvent and substrates. We can gain further insight into these interactions with changes to the surface of the substrate. A change in solvent will also provide the final piece of information necessary to fully understand the solution adsorption of phthalocyanines.

Thus, in this work, we have undertaken a systematic study of the solution adsorption of fluorinated phthalocyanines on a variety of surfaces, taking advantage of the enhanced solubility of many of these materials. The end-goal of this work was the production of stable phthalocyanine thin films for use as recyclable, solid-supported heterogeneous catalysts. We report the solution adsorption of the two series on several substrates. To gain deeper understanding, adsorption of each series from acetone and methylene chloride was compared on several unique adsorbents. Additionally, we explored the interactions that facilitate adsorption and discuss a potential mechanism of adsorption.

3.3 Experimental

3.3.1 Chemicals

All solvents and chemicals necessary for the synthesis of the phthalocyanines were purchased from VWR (Randor, PA) (List of chemical companies includes Alfa Aesar (Ward Hill MA), Fisher Scientific (Pittsburgh, PA), Sigma-Aldrich (Saint Louis, MO), TCI Co. Ltd. America (Portland, OR) etc.). (Waltham, MA). Commercially available

phthalocyanines were purchased from Sigma-Aldrich (St. Louis, MO). The silanes and siloxanes were obtained from Gelest (Morrisville, PA) and used as received (unless stated otherwise).

3.3.2 Metal Oxides

Wide-pore silica gel, Davisil 500, was obtained from Grace (Columbia, MD). The pore structure of Davisil 500 was assessed by nitrogen adsorption (77 K) using an ASAP 2020 analyzer (Micromeritics, Norcross, GA), some of the properties are summarized in Table 3-1. SBA-15 silicas were synthesized, characterized and used as described in Chapter 2.

All aluminum oxides (alumina, α-Al_2O_3) were purchased from Sigma-Aldrich (St. Louis, MO). The majority of the studies for alumina were performed on these superficially porous materials. Separately, we purchased acidic, basic and neutral porous activated aluminas (γ-Al_2O_3) with Brockmann activity I. The properties of the different aluminas are summarized in Table 3-1.

Table 3-1: Summary of the Metal Oxide Material Properties

	S_{BET} (m^2/g)	D_{pore} (nm)
SiO_2 (Davisil 500)	67	42 - 53
SiO_2 (SBA-15)	532	7.2
TiO_2 (P25)	62	-
α-Al_2O_3	48	-
Al_2O_3 (Activated)	150	5.8

Titanium (IV) oxide (TiO_2) P25 nanopowder (Anatase/Rutile at ~70:30) was obtained from Nippon Aerosil (Tokyo, Japan). The nonporous nanopowder had ~12 nm primary particles with S_{BET} = 62 m^2/g.

3.3.3 Functionalization of the Silica Surface

Silicas with PDMS and trifluoromethyl functionality (bis-CF_3) were synthesized according to the procedure described in detail in Chapter 2.[101] PDMS modification was performed at 100°C for 24 hours (PDMS) while modification with bis-CF_3 was performed at 200°C for 72 hours (bis-CF_3).

All other silicas were synthesized from alkoxysilanes by traditional methods. Silica was dried at 100 °C for a period of three hours. Once complete, the silane was diluted to 20% in toluene and added to a vessel in a sufficient amount to cover the silica material. The mixture was then placed in an oven at 60 °C for 72 hours. The functionalized silica material was allowed to cool prior to filtration and washing with toluene, acetone, water-acetone, and acetone once again. The modified silicas were air dried on the filter and then dried in an oven at 60 °C for 1 h. The materials were then characterized by nitrogen adsorption-desorption (77K) isotherms and used for the adsorption studies.

The grafting density of modified silicas was obtained from carbon analysis performed by Robertson Microlit Laboratories (Ledgewood, NJ) using the ASTM method. Grafting density of PDMS modified silicas was calculated as the number of dimethylsiloxane (DMS) repeat units per nm^2 using the equation:

$$\boldsymbol{\rho_{DMS}} = \frac{\mathbf{6} \times \mathbf{10^5} \times (\%\boldsymbol{C})}{[\boldsymbol{n_C} \times \mathbf{1200} - \boldsymbol{MM} \times (\%\boldsymbol{C})]} \cdot \frac{\mathbf{1}}{\boldsymbol{S_{BET}}} \qquad \textbf{(2 - 1)}$$

where MM is the molecular mass of the DMS group, n_C is the number of carbon atoms in the DMS group, S_{BET} is the surface area of the bare silica, and % C is the carbon weight percent. Nitrogen adsorption–desorption isotherms (77 K) were measured using an ASAP 2020 analyzer (Micromeritics, Norcross, GA, USA). For all other silicas, the grafting density was calculated as the number of monomer siloxy groups per nm^2. The grafting density was determined from % C:

$$\boldsymbol{\rho = \frac{6\times10^5\cdot(\%C)}{[1200\times n_C - MW\times(\%C)]}\cdot\frac{1}{S_{BET}}} \qquad \textbf{(1 - 13)}$$

where MM is the molecular mass of the grafted group and n_C represents the number of carbon atoms present in it.

3.3.4 Synthesis of Perfluorinated Phthalocyanines

Synthesis of the perfluorinated phthalonitrile precursor and phthalocyanines was completed by our co-research group at Seton Hall using a previously developed procedure (Figure 3-2).[98,102] Briefly, the fluorinated precursor, tetrafluorophthalonitrile, (**A**) was purchased from TCI Co., Ltd. Perfluoro (4,5-diisopropyl)phthalonitrile (**B)** was synthesized from **A** by nucleophilic substitution as described in the literature.[102] The fluorinated phthalonitriles (**A, B**) at proper mole ratios were melted with a metal acetate using a microwave at 185 °C to yield a blue-green solid.[102,103] Synthesis using only **A** yielded F_{16}PcM. Synthesis using only **B** yielded F_{64}PcM. Synthesis of fluorinated phthalocyanines using mixed starting materials could yield, in principle, four additional organic scaffolds: F_{28}PcM, F_{40}PcM (*cis* and *trans*), F_{52}PcM. Chromatographic

purification of the products yielded the purified blue-green material. The structure and purity of the material was confirmed by ^{13}C and ^{19}F NMR spectra.[103]

3.3.5 Thermogravimetric Analysis

Thermogravimetric analysis (TGA) was performed using a TA Instruments thermogravimetric analyzer operated between room temperature and 1000°C at a heating rate 10°C/min with ambient (air exposure) or a flow of dry nitrogen (20 cm^3/min). Stability of the adsorbed phthalocyanines was assessed by heating materials to set temperatures (200-400°C) and analyzing the TGA weight loss and solid state spectra.

3.3.6 Solution Adsorption of Phthalocyanines

Small scale experiments were carried out to study the adsorption behavior of phthalocyanines on varied surfaces. Typically, a fixed amount of adsorbent (25 mg) was added into vials containing 2 ml of dye solution at known concentrations. The vials were briefly agitated and stored, protected from light, at room temperature for two days until equilibrium was reached. UV/Vis analysis samples were collected by decanting to avoid evaporation during a filtration process. The dye concentration was determined on a Varian Cary 300 (Palo Alto, CA) double beam UV/Vis spectrometer by measuring absorbance maximum for each dye. The quantity of adsorption at equilibrium, Γ (μmol/m^2), was calculated by the equation:

$$\boldsymbol{\Gamma = \frac{(C_0 - C_e)V}{W} \cdot \frac{1}{S_{BET}}} \qquad \textbf{(3 - 1)}$$

where C_0 and C_e were the liquid phase concentrations of Pc at initial and equilibrium conditions, respectively. V (L) was the volume of the Pc solution and W (g) was the

mass of dry sorbent used. S_{BET} (m^2/g) is the surface area of the adsorbent as measured by nitrogen adsorption.

The Langmuir isotherm model[32] was employed to describe the sorption behavior of phthalocyanines on surfaces. The Langmuir model is based on assumptions that monolayer coverage of adsorbate occurs over homogeneous sites and that a saturation point is reached when no further adsorption can occur. The isotherm model is represented as follows:

$$\boldsymbol{\Gamma = \frac{\Gamma_{max} K_L C_e}{1 + K_L C_e}} \qquad \textbf{(1 - 9)}$$

where Γ_{max} is the maximum monolayer adsorption capacity (μmol/m^2); and K_L (Eq. **1 - 10**) is the Langmuir adsorption equilibrium constant related to the affinity of the binding sites and energy of adsorption (L/μmol). Based upon the dimensions of the phthalocyanine molecules studied, the Γ_{max} was estimated to allow us to compare orientation and quantify how closely the coverage approached a monolayer.

The equation is rearranged to its linear form to calculate the Langmuir constants Γ_{max} and K_L. A plot of $1/\Gamma$ versus $1/C_e$ will obtain a slope of $1/\Gamma_{max}$ and intercept $1/(\Gamma_{max}K_L)$:

$$\boldsymbol{\frac{1}{\Gamma} = \left(\frac{1}{\Gamma_{max} K_L}\right)\left(\frac{1}{C_e}\right) + \frac{1}{\Gamma_{max}}} \qquad \textbf{(3 - 2)}$$

To determine the enthalpy of adsorption of model perfluorinated phthalocyanines, a study was designed to obtain the temperature effect on the adsorption kinetics in acetone. Adsorption isotherms were obtained at 283, 297, and 313K and plotted at selected points with the linearized Clausius-Clapeyron equation:

$$\boldsymbol{Ln(C_e) = \frac{\Delta H_{ads}}{R}\left(\frac{1}{T}\right)} \qquad \textbf{(3 - 3)}$$

C_e is the equilibrium concentration at each T, temperature (K) at a constant Γ (mol/L), the constant, R, is 8.314 J/mol*K; to obtain ΔH_{ads} in J/mol. Only negligible values for ΔH_{ads} (< 1 kJ/mol) were obtained for the materials studied and thus will not be discussed in further detail.

The orientation of the phthalocyanines on the surface after adsorption was an important property to understand and was determined, partially, by comparison of the experimental and theoretical Γ_{max}. Due to the generally planar shape of the molecule, the Γ_{max} for densely packed molecules would be quite different for the vertical (on edge) versus the horizontal orientation (face down), as shown in Table 3-2 and Figure 3-3. The dimensions of F_{16}PcZn and F_{64}PcZn were calculated using published XRPD data focused on a single molecule with the assistance of Mercury software. We then compared these results to manually calculated values using bond lengths, angles, and van der Waals radii obtained for unsubstituted Pcs.[104] Using the cross-sectional area (ω), a square/rectangular molecular shape was assumed to calculate theoretical Γ_{max} ($\mu mol/m^2$) of a tightly packed monolayer. The phthalocyanines without four-fold symmetry, such as F_{40}PcZn, would have a ω and resulting Γ_{max} that is intermediate to those of F_{16}PcZn and F_{64}PcZn.

The UV/Vis quantitation technique was verified by chemical analysis of (%C, %H, %N and %F, when present) of the filtered, washed, and dried samples, which was performed by Robertson Microlit Laboratories (Ledgewood, NJ). The %C data was converted to $\mu mol/m^2$ to allow direct comparison to UV/Vis results.

Figure 3-3: Space-Filling Model of F_{64}PcZn Shown at Different Orientations

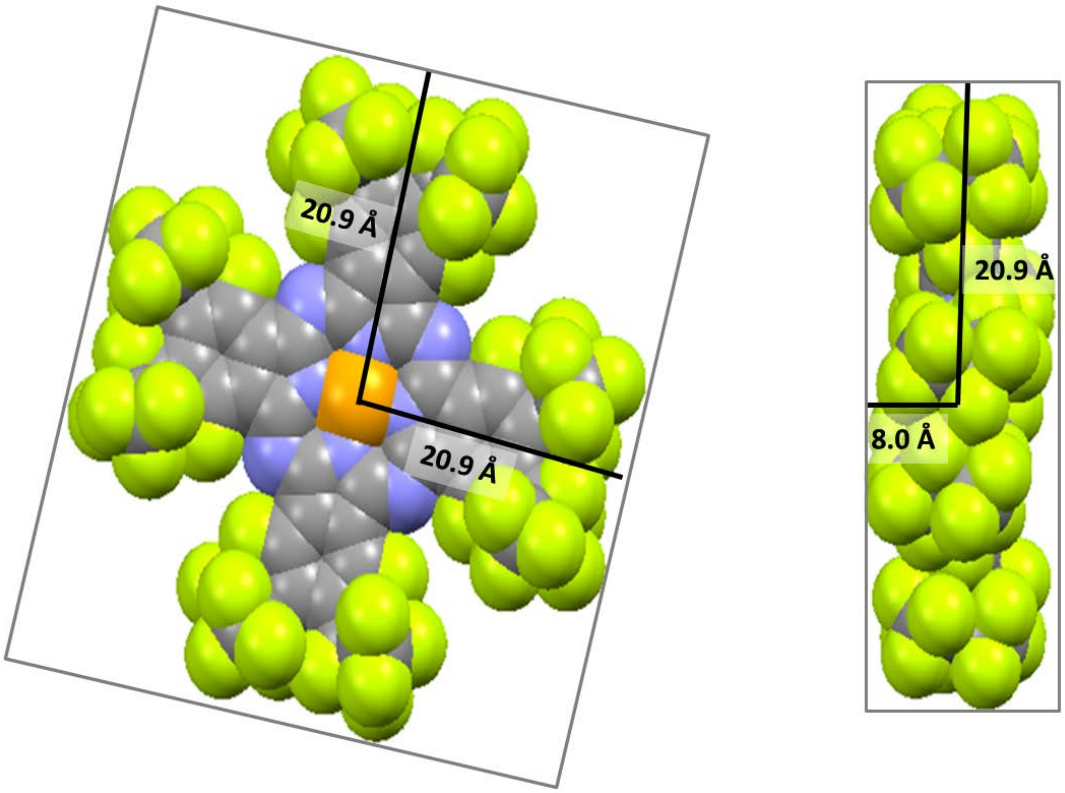

Figure 3-3: 3D Space-Filling Model of F_{64}PcZn at the 'face down' and 'on edge' orientation, demonstrating the difference in cross-section area at for each possible orientation.

Table 3-2: Cross-sectional Area and Theoretical Monolayer Coverage for Zinc Phthalocyanines at Different Orientations

	On Edge		Face Down	
	ω (Å^2/molecule)	Γ_{max} (μmol/m^2)	ω (Å^2/molecule)	Γ_{max} (μmol/m^2)
F_{16}PcZn	51	3.26	332	0.500
F_{64}PcZn	167	0.994	437	0.381

Table 3-2: Cross-sectional area (ω) and theoretical monolayer coverage (Γ_{max}) for densely packed fully symmetrical zinc phthalocyanines: F_{16}PcZn and F_{64}PcZn

Reflectance UV/Vis/NIR of the resulting solids was collected on a Varian Cary 500 (Palo Alto, CA) UV/Vis/NIR spectrometer fit with a reflectance accessory DRA-CA-5500 (Labsphere, North Sutton, NH, USA). Samples were tightly packed into a custom built quartz analysis cell

(pictured in Figure 3-21a). The data collected in the adsorbed solid state was compared to the solution state and literature to evaluate the organization of the Pcs on the solid surface. As we were collecting data for large, non-uniformly shaped porous materials, compensation for adsorption and scattering of the signal was required. Kubelka-Munk[105,106] transformations were applied to the reflectance data as follows:

$$f(R) = \frac{(1-R)^2}{2R} = \frac{k}{s} \qquad \textbf{(3 - 4)}$$

where R is the absolute reflectance of the sampled layer, *k* is the molar absorption coefficient and *s* is the scattering coefficient. We observed that SiO_2 materials were more UV/Vis transparent than Al_2O_3, limiting the linear range (*I*) under which the analysis could be used.

3.4 Results and Discussion

3.4.1 TGA Analysis of Phthalocyanines

To better understand and compare the stability of these newly synthesized materials, the materials were analyzed via decomposition by TGA under air and nitrogen. The first series included zinc phthalocyanines beginning with H_{16}PcZn and then the fluorinated F_nPcZn (n = 16, 40, 52, 64). Phthalocyanines are prone to sublimation, therefore, weight loss was attributed to both degradation and sublimation of the phthalocyanines. Theoretically, thermal degradation would occur via cleavage of C-C and C-F bonds, leaving metal residues. We therefore assumed that samples with low temperature TGA weight loss near 100% were dominated by sublimation while the lowest weight loss values would be obtained for materials with more degradation.

Figure 3-4: Thermogravimetric Analysis of Two Series of Phthalocyanines Under Nitrogen

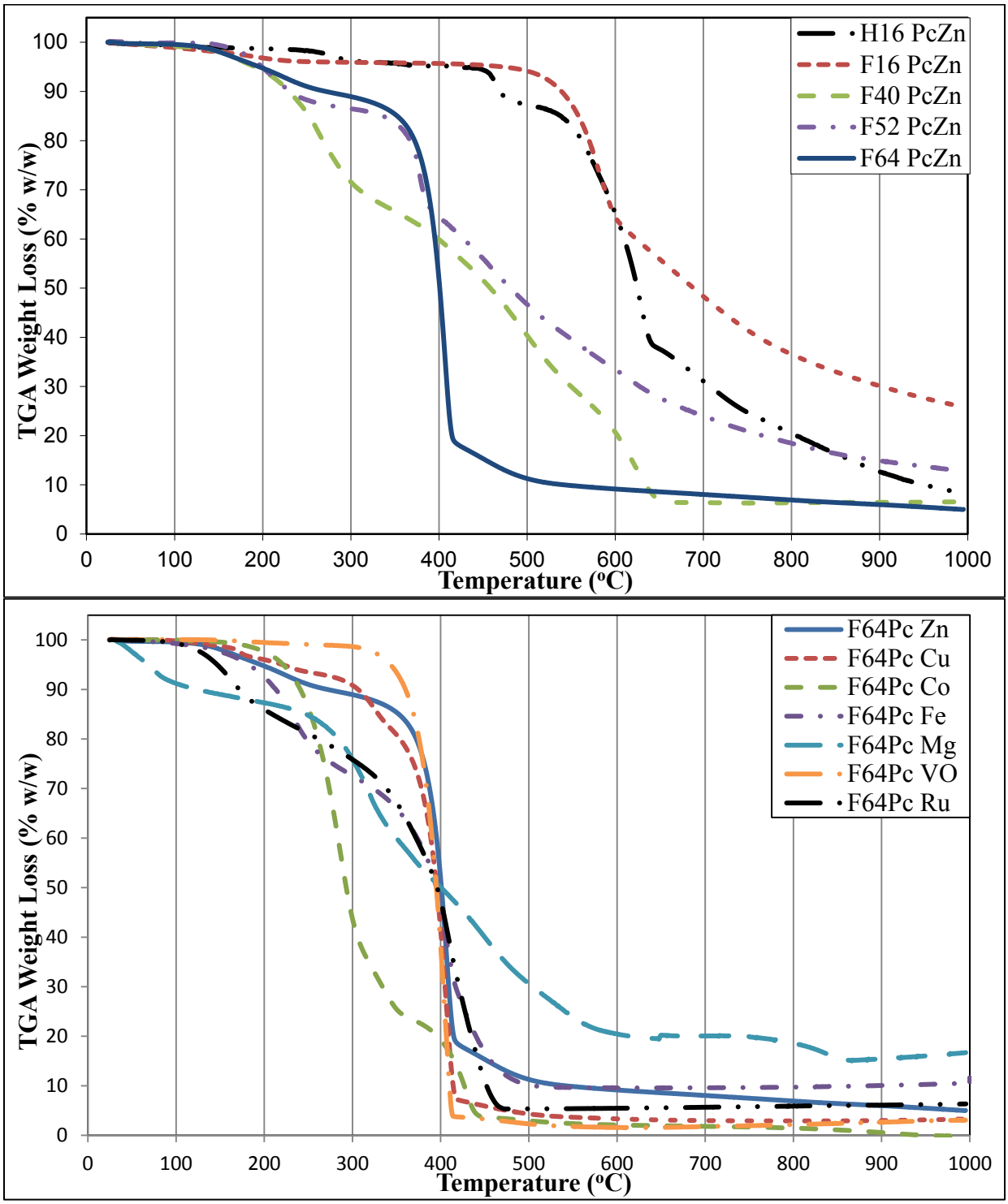

Figure 3-4: TGA weight loss curves under nitrogen for zinc phthalocyanines (top) and F_{64}PcMs (bottom). Weight loss is generally attributed to both degradation and sublimation of the phthalocyanines. Thermal stability appeared best for unsubstituted phthalocyanines, while sublimation occurred most readily for F_{64}PcM. This was likely due to the lack of bulky functional groups and a propensity for aggregation in the unsubstituted materials.

Thermal stability appeared best for unsubstituted phthalocyanines (Figure 3-4 top, Figure B-1), likely due to the lack of bulky functional groups that are more prone to thermal decomposition. We noted that F_{64}PcZn was the most susceptible to sublimation as bulky *i*-C_3F_7 groups reduce their propensity for aggregation. Solids remaining after analysis in air and N_2 had color that was consistent with ZnO, with the exception of H_{16}PcZn in air, which had the color of Zn_3N_2.

TGA weight loss curves for F_{64}PcM (M = Zn, Cu, Co, Fe, Ru, Mg, VO) were also explored. Similar to F_{64}PcZn, sublimation appeared to dominate in both air and nitrogen (sharp weight loss curve at a lower temperature), resulting in similar TGA curves in air and nitrogen for most F_{64}PcM. We also noted that the instrument was coated with the colorful phthalocyanines after analysis. Any solids remaining after analysis in both air and nitrogen had color that was consistent with metal oxides. The exception to this sublimation trend was F_{64}PcMg, which had a very high rate of degradation. The general instability of F_{64}PcMg was manifested in other aspects of our work, so it was not included in solution adsorption studies.

3.4.2 Solution Adsorption of Phthalocyanines

The goal of these adsorption experiments was to produce uniform thin films of phthalocyanines on solid surfaces. After initial screening, the impact of increasing fluorination at the periphery and a change to the central metal was explored. With this information we hoped to obtain the mechanism of the adsorption from solution for these unique materials. Initial studies probed the adsorption of F_{16}PcZn and F_{64}PcZn on metal oxides (SiO_2, TiO_2, and α-Al_2O_3), anticipating that hydrogen bonding macrocycle nitrogens or the central metal would play a role in the characteristics of adsorption from

acetone. In these initial studies, however, it was found that non-porous alumina was the only adsorbing material for the probe molecules (Figure 3-5). The studies were extended to seven days and demonstrated no change in results, with two

Figure 3-5: Adsorption of $F_{64}PcZn$ on Selected Surfaces

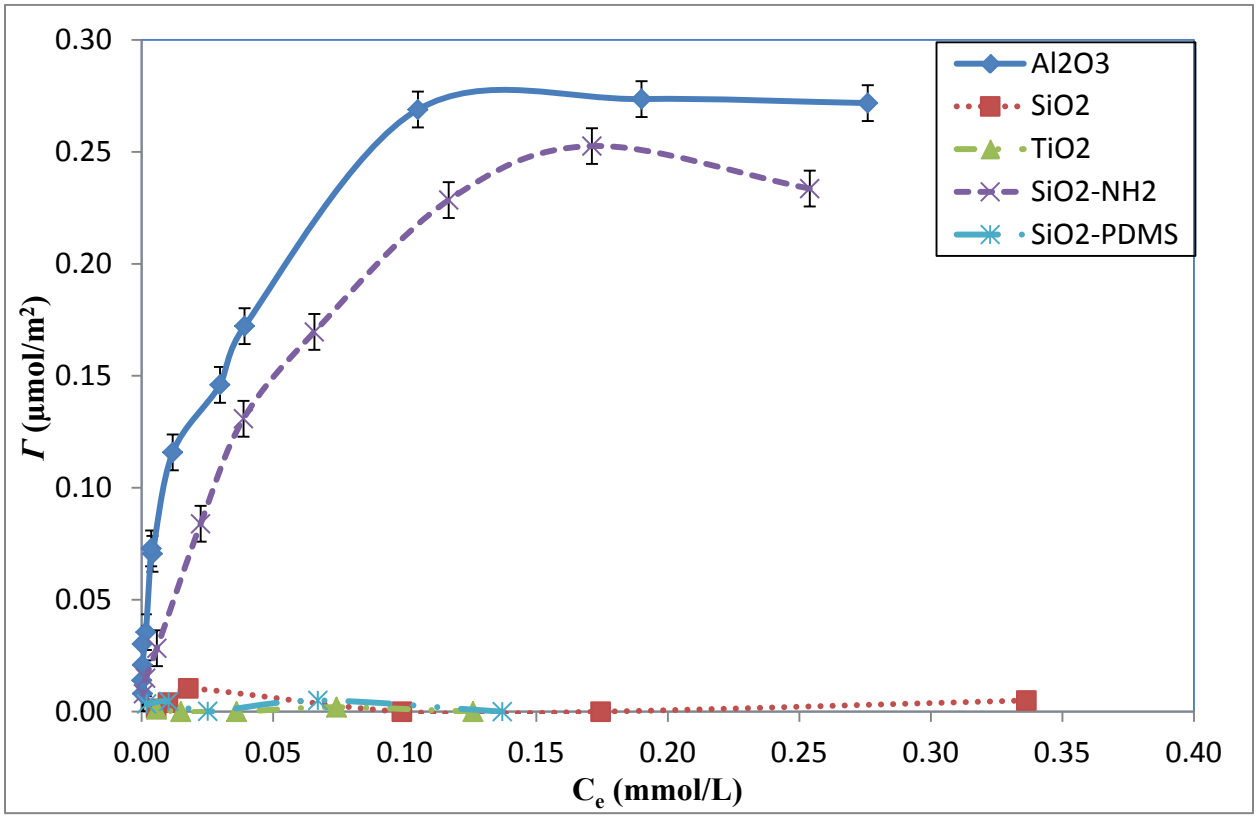

Figure 3-5: Results of the adsorption of studies for $F_{64}PcZn$ on selected surfaces. Strong, irreversible adsorption occurred for Al_2O_3 and SiO_2-NH_2. Lines were added to guide the eye. Error bars (shown only for y axis) were added to account for relative error from weighing, dilution and measurement error. (Note: Some non-adsorbing surfaces studied were excluded for the clarity of the overlay.)

days being sufficient to reach equilibrium for alumina. Beyond the surface hydroxide groups present for hydrogen bonding, one could also differentiate the metal oxides studied with respect to pH. The SiO_2[8] and TiO_2 are characterized as weakly acidic, and α-Al_2O_3 is considered amphoteric.[4] The alumina material was overall neutral, but in our studies we needed to consider that multiple

functionalities could be present at the adsorbate surface influencing the adsorption, such as acidic, basic, and charged moieties.[107]

The quantity of adsorption to Al_2O_3 was significant and was visually observed with a decrease in color of the solution and a notable coloration of the particles. Upon filtration and washing with acetone, the particles remained colored. In contrast, very careful sampling of SiO_2 (no agitation of solution prior to sampling for UV/Vis) did show evidence of very weak, reversible adsorption at low concentrations only. With only very slight agitation, the solution would return to initial concentration. Therefore, we characterized an 'adsorbing surface' as one with nearly irreversible adsorption, in which the Pc is not removed by washing. As this is an equilibrium process, we acknowledged that some desorption of the Pcs would occur if samples were given enough time to equilibrate with freshly added solvent. TGA studies were conducted to see if adsorption of the materials improved stability or hindered sublimation. We found that moisture loss interfered with interpretation of the results, so we completed studies by holding at temperatures near the sublimation and analyzed the solids by reflectance UV/Vis. The obvious color change of the materials held at temperature for 1 hour (Figure 3-6) demonstrated that sublimation was occurring at 400^{o}C, similar to the sublimation temperature of the bulk materials. This indicated only weak interactions between the Pcs and the surface.

After initial observations for metal oxides, studies were expanded to covalently attached monolayer surfaces. Porous SiO_2 (Davisil 500) was modified with different functionalities to discover any other surfaces to which these materials would adsorb (Figure 3-7). Beginning with weak hydrophobic interactions, SiO_2-PDMS was studied.

Figure 3-6: Thermal Stability of Adsorbed $F_{64}PcZn$ on Al_2O_3

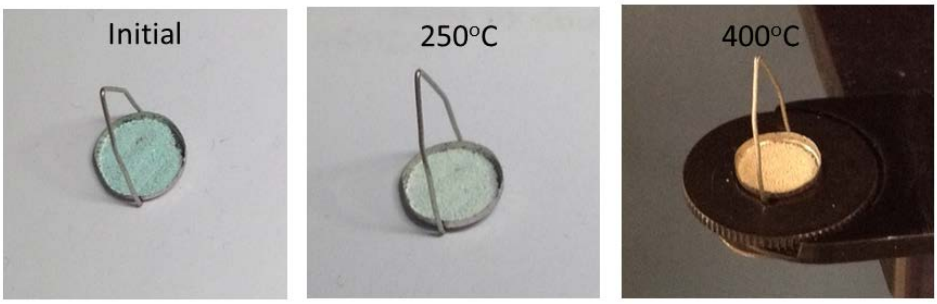

Figure 3-6: Images of Al_2O_3 samples with $F_{64}PcZn$ adsorbed to the surface prior to thermal treatment (Initial) on a TGA for 1 hour at 250°C and 400°C. Sublimation occurred at 400°C similar to the bulk material.

Fluorinated surfaces SiO_2-CF_3 and SiO_2-PFP (perfluoro phenyl groups) were also explored due to similarity to the phthalocyanines and π-stacking potential (SiO_2-PFP). Finally, propylamine functionalized Davisil (SiO_2-NH_2) was used to explore basic surfaces for potential interaction with phthalocyanines. Of these modified silica surfaces, only SiO_2-NH_2 had irreversible adsorption. The results of the adsorption studies with metal oxides and selected modified silicas are shown in Figure 3-5.

As was introduced in Chapter 1 (Figure 1-6), solute adsorption is divided into four main classes based upon the shape of the initial adsorption: S (S-shaped), L (Langmuir), H (High

affinity), and C (constant partition). Our initial observation of these isotherms was that we obtained L-type isotherms in acetone for both Al_2O_3 and SiO_2-NH_2. We could also classify the affinity of the $F_{64}PcZn$ to be higher for Al_2O_3 than SiO_2-NH_2 under the conditions studied. A

comparison of the results obtained by UV and Chemical analysis showed good agreement between the two techniques for $F_{64}PcZn$ (Table 3-4).

Figure 3-7: Functionality of Silicas Used for Adsorption Studies

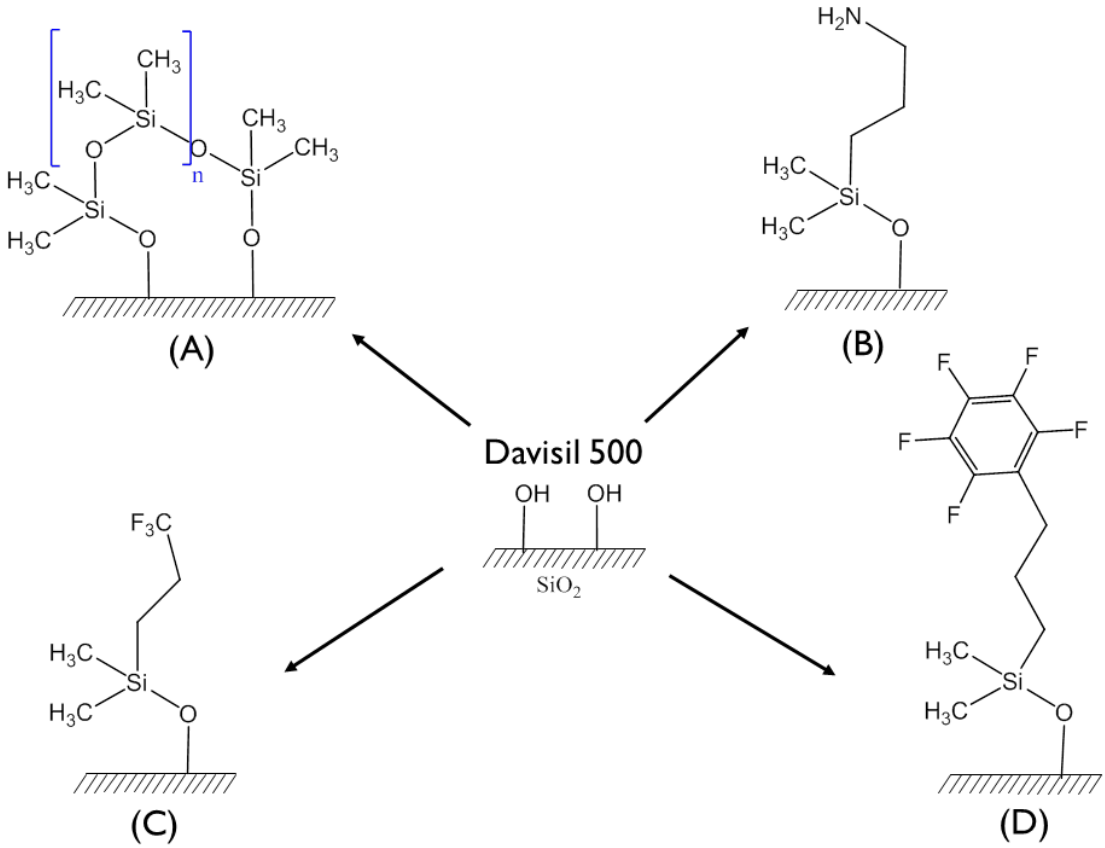

Figure 3-7: Examples of the functionality of the silica surfaces utilized in initial adsorption studies. Abbreviated names for the surfaces were: SiO_2-PDMS (A), SiO_2-NH_2 (B), SiO_2-CF_3 (C), and SiO_2-PFP (D).

Table 3-3: Data Analysis for Silica Materials

	%C (w/w)	ρ (grps/nm^2)
SiO_2-PDMS	4.54	5.24
SiO_2-CF_3	1.25	1.9
SiO_2-PFP	1.61	1.1
SiO_2-NH_2	1.73	2.7
SiO_2-Imidazole	3.25	4.4
SiO_2-Pyridine	3.03	3.4
SiO2-Aniline	2.35	3.7

3.4.3 Spectral Analysis and Quantification by UV/Vis

Phthalocyanines have strong absorbance in the visible region, giving them a distinctive blue and/or green color, hence their use as dyes and pigments. Changes to the metal center and substituents of the Pcs generally result in small shifts in the UV/Vis spectrum (Figure 3-8). Following the nomenclature established by Gouterman,[108] the sequence of generally identified peaks in order of increasing energy are Q, B, N, L, and C. Specifically, in a typical UV/Vis spectrum, a split Q-band in the 600-800 nm region is further classified by the HOMO (Q_1) and LUMO (Q_2) π-π* transitions. An additional intense band in the 300-450 nm is assigned the name B-band or occasionally, the Soret band, is owed to a second excited singlet state. Some additional unique spectral features have also been found in unsubstituted Pcs and Pcs with asymmetry in the periphery and will be discussed in more detail.

Dissolved phthalocyanines often show solvatochromic effects, such as changes to the position, intensity, or half-width of the absorbance bands. New absorption bands appear due to a charge transfer, and the absorption bands can be red or blue-shifted. The deformation of the phthalocyanine molecules due to interactions with the solvent molecules may also change the symmetry of the molecules, influencing the absorption spectra.[109] Characteristics of aggregation in solution and very poor solubility for unsubstituted phthalocyanines are well established. Specifically, cofacial dimerization of the phthalocyanine molecules at high solution concentrations can cause a (reversible) band shift.[103,108,110,111] Solvent effects and additives also play an important role in the aggregation behavior of Pcs. For example, pyridine is often used as a solvent or an additive to break up the aggregation of phthalocyanines in solution.[109]

Figure 3-8: Visible Absorbance Spectrum Comparison for Zinc Phthalocyanines

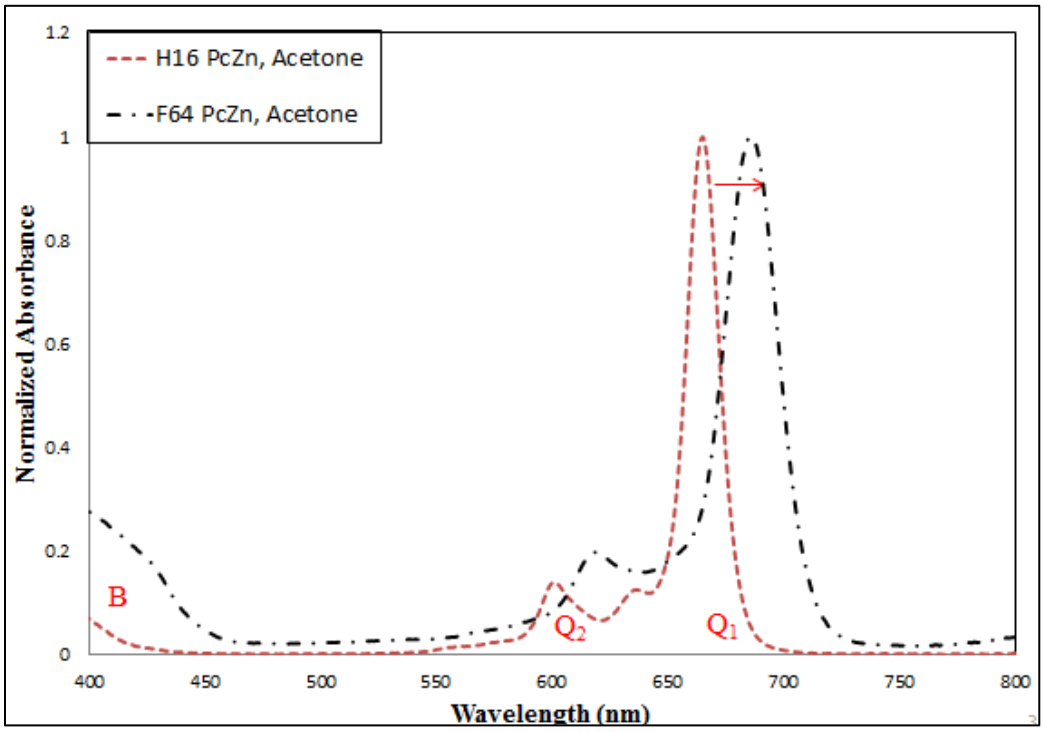

Figure 3-8: Comparison of the visible absorbance spectra for F_{16}PcZn and F_{64}PcZn, highlighting the soret band (B) and the HOMO (Q_1) and LUMO (Q_2) absorbance maxima. The addition of the electron withdrawing groups causes a shift in the molecular orbitals of the macrocycle resulting in the spectrum shift.

As expected,[112] we observed that with the addition of electron withdrawing F groups to the α and β positions to obtain F_{16}PcZn, aggregation occurred to a much greater extent than for H_{16}PcZn. The addition of bulky peripheral groups, such as *i*-C_3F_7, is a way to reduce aggregation and increase the solubility of Pcs, but aggregation was still observed to some extent for F_{40}PcZn (*cis* as major) and F_{52}PcZn (Figure 3-9). The formation of the dimers in solution added complexity to the determination of C_e and, consequently, Γ by UV/Vis spectroscopy due to spectral changes. However, during solvent studies we observed that the less polar and aprotic solvent, methylene chloride (CH_2Cl_2), effectively reduced the presence of dimers for F_{40}PcZn and F_{52}PcZn. We, therefore, diluted the samples from the acetone studies in CH_2Cl_2 to improve the accuracy

Figure 3-9: Absorbance Spectrum Comparison for $F_{40}PcZn$ in Different Solvents

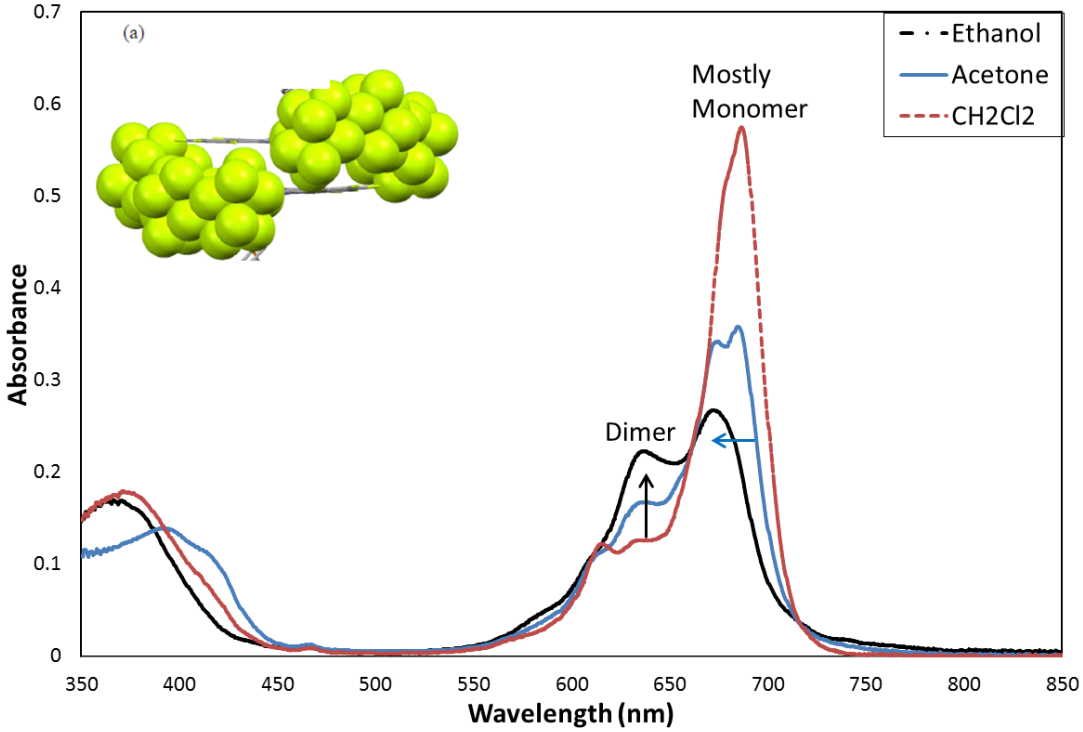

Figure 3-9: Comparison of the absorbance spectra for $F_{40}PcZn$ in ethanol, acetone, and methylene chloride. The shift in the Q-band and increase in the appearance of an additional maxima indicates formation of cofacial dimers (depicted in insert **a**[98] from X-ray data in the solid-state) in solution.

of the assay. For $F_{16}PcZn$, only dissolving samples in pyridine removed the cofacial dimers that formed in other common solvents. Similar to our previous work,[112] we observed high solubility and only a very minor aggregation in solution for $F_{64}PcM$, but the solubility and stability of these additional materials varied.

A change in the central metal will impact the catalytic activity and electronic, spectroscopic, and physical properties in a similar way as changes to the periphery.[88] However, a change in central metal had only a minor impact on the visible spectrum for $F_{64}PcM$. We did observe changes to solubility and stability that had a significant impact on the adsorption studies. To begin, we observed that phthalocyanines containing Cu, Co, and VO had spectral changes in the presence of the SiO_2-NH_2 in acetone. Further

investigation, as shown in Figure 3-10, revealed Q band quenching in the presence of the base in the order of VO >> Co > Cu. Interestingly, in the unique case of F_{64}PcFe, spectral changes occurred over time in the presence of both Al_2O_3 and SiO_2-NH_2. In this case, the Q band intensity *increased* relative to the standard, resulting in an increase in C_e and a negative Γ despite obvious adsorption of F_{64}PcFe on the surface as determined by visual observation and chemical analysis (Figure A-2). When spectral changes like these occur, chemical analysis must be relied on to directly quantify Γ and extrapolate C_e.

Figure 3-10: Spectral Changes of F_{64}PcVO in the Presence of Acid and Base

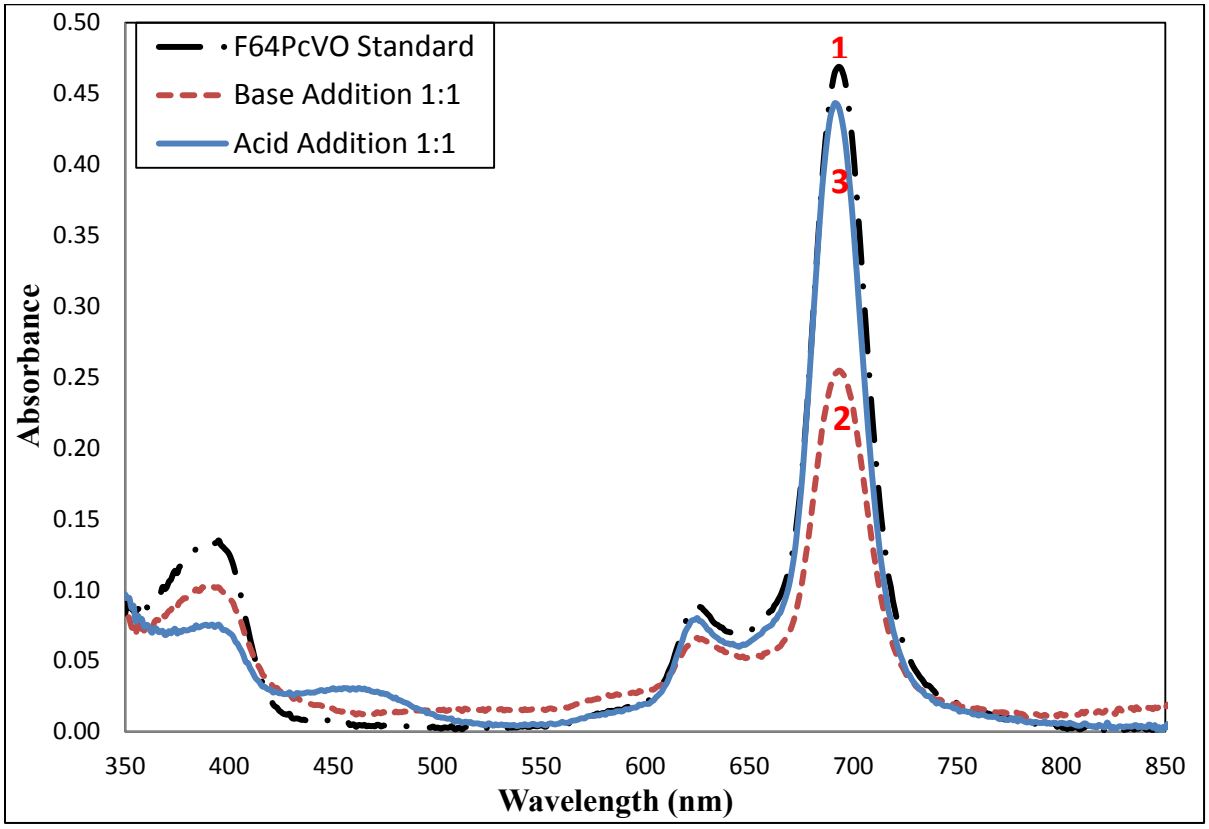

Figure 3-10: Demonstration of the spectral changes that occur for F_{64}PcVO when titrated with isopropylamine followed by 'regeneration' with dilute HCl: Initial (1), isopropyl amine at equamolar concentration (2), and HCl at an equamolar concentration to that of the added isopropylamine (3). From initial (1), quenching of Q and B bands occurs with addition of an equamolar concentration of isopropylamine (2). Partial recovery occurs for the Q band with the addition of an equamolar concentration of acid (3), but 'permanent' splitting of the B band remains.

Some of these spectral changes, however, were not observed in CH_2Cl_2 implicating possible chemical changes to acetone in the presence of the base, such as keto-enol tautomerism or immine formation, as a cause of these changes.

Table 3-4: Comparison of Quantitation Techniques for Adsorption Studies on Al_2O_3

Phthalocyanine	Γ (μmol/m^2) by UV/Vis	Γ (μmol/m^2) by %C[a]
F_{16}PcZn	0.34	0.48
F_{40}PcZn	0.35	0.39
F_{52}PcZn	0.26	0.32
F_{64}PcZn	0.23	0.22
F_{64}PcCu	0.029	0.046
F_{64}PcCo	0.041	0.043
F_{64}PcRu	0.32	0.28

[a]Determined from the chemical analysis results at specific data points.

Results obtained by UV/Vis analysis of the solutions were compared to chemical analysis of the final solids as shown in Table 3-4. Good correlation was obtained for non-aggregating materials. A change to dilution in CH_2Cl_2 and sonication for UV/Vis analysis improved the accuracy by decreasing the presence of dimers, with the exception of F_{16}PcZn (Note: Accuracy of the results for Γ_{max} are impacted by the aggregation we have discussed, but the slope of the initial curve would not be impacted as aggregation occurs similarly in both the sample and standard solutions). Good correlation was also obtained for most F_{64}PcMs with the exception of those with problems of sample degradation under the specific conditions described. Chemical analysis is accurate to +/-

0.05 %C, which corresponded to a 2-5% error relative to the high Γ values, but increased to over 20% for the lowest Γ. Additional complexity was introduced when performing chemical analysis on SiO_2-NH_2 samples due to the carbon introduced by the surface. By comparison, we determined, theoretically and empirically, that UV/Vis analysis had a 3% error based weighing, dilution and sampling for non-aggregating phthalocyanines (Note: some of this error would also be present for chemical analysis as well and was not accounted for with the standard error calculated above). Samples were rigorously dried prior to analysis to remove any residual solvents that could also contribute to the total %C, but we cannot rule out strong coordination of the solvent, particularly acetone, with the solids as was observed in previous studies. With these results, modifications and considerations, UV/Vis analysis was chosen as the preferred analysis technique for adsorption studies due to its simplicity and accuracy throughout the entire range of our studies. We continued to monitor and compare results to chemical analysis.

3.4.4 Role of the Extent of Fluorination on the Adsorption of Zinc Phthalocyanines

Moving forward from the initial results obtained for F_{16}PcZn and F_{64}PcZn, a study of adsorption from acetone onto Al_2O_3 and SiO_2-NH_2 for a series of increasingly fluorinated zinc phthalocyanines: H_{16}PcZn, F_{16}PcZn, F_{40}PcZn, F_{52}PcZn, and F_{64}PcZn was performed (Note: column purification to separate F_{28}PcZn from F_{40}PcZn was not possible at the time of these studies. Therefore, studies for F_{28}PcZn were not possible and the F_{40}PcZn utilized contained low levels of F_{28}PcZn, as confirmed by NMR). The change from H_{16}PcZn to F_{16}PcZn represented replacement of all C-H bonds with C-F (Figure 3-2). As the series moved from F_{16}PcZn to F_{64}PcZn, the β peripheral C-F bonds of each quadrant were replaced with bulky *i*-C_3F_7 groups.

The expected increase in solubility with the addition of the *i*-C_3F_7 groups was observed, with the solubility of F_{40}PcZn, F_{52}PcZn, and F_{64}PcZn being ~2 orders of magnitude higher than that of H_{16}PcZn and F_{16}PcZn. The UV-Vis spectrum, particularly π-π* Q-band maximum,[111] of F_{64}PcZn differed significantly from that of the parent, unsubstituted H_{16}PcZn material (Figure 3-8). This indicated that the electron-withdrawing properties of the peripheral substituents affected the rings' π molecular orbitals (MOs).[93] The impact of this change to the electronic structure of the macrocycle and concomitant increase in electron deficiency of the metal center was an important consideration during the adsorption studies.

The adsorption of zinc phthalocyanines on Al_2O_3 is displayed in Figure 3-11. Due to solubility differences, it was necessary to extend the adsorption studies for H_{16}PcZn and F_{16}PcZn to higher volumes than the standard 2 mLs to attempt to reach the Γ_{max} (indicated by 'knee' or point B for the curve, see **1.2.1** for detailed discussion). Even with this volume change, the Γ for H_{16}PcZn and F_{16}PcZn is significantly lower. Careful observation of the full overlay of the isotherms shows that most of the isotherms were L-type with one exception, H_{16}PcZn. The focused graph (Figure 3-11, bottom) demonstrates a sharp contrast between H_{16}PcZn (S-Type) and F_{16}PcZn (L-Type). A change from S-type to L-type adsorption indicates an increase in E_A^0. With all other factors held constant, the addition of the electron withdrawing fluorine groups seemed to cause stronger adsorption interactions at the surface of Al_2O_3. A comparison to computational studies[100] was conducted for increasingly fluorinated F_nPcZn (n = 16, 32, 48, 64) materials in which C-H in H_{16}PcZn was systematically replaced by F (F_{16}PcZn), C_2F_5 (F_{32}PcZn, F_{48}PcZn), and *i*-C_3F_7 (F_{64}PcZn). Particular attention was paid to

Figure 3-11: Adsorption of Zinc Phthalocyanines on Al_2O_3

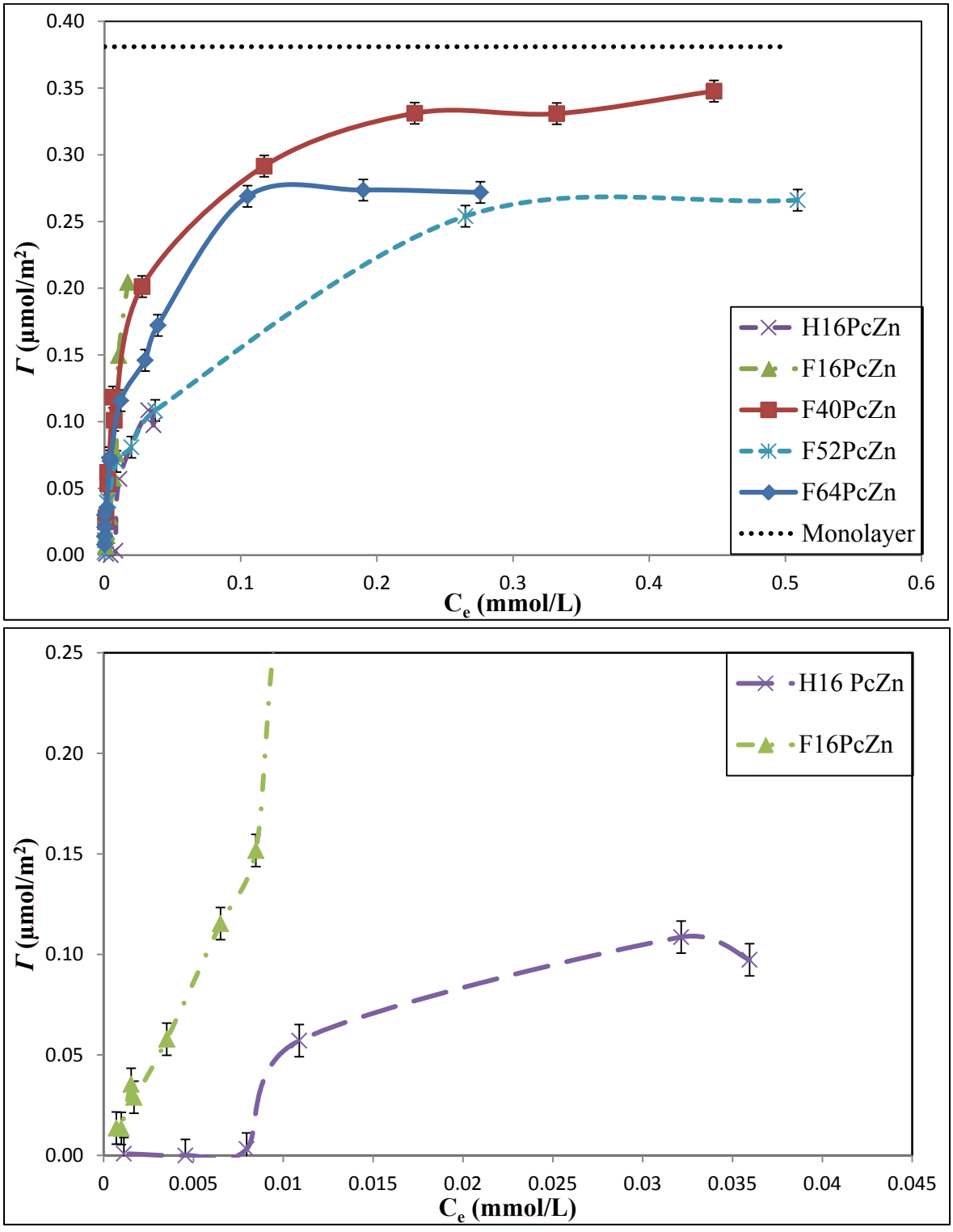

Figure 3-11: Adsorption isotherms of zinc phthalocyanines on Al_2O_3(top) and a focused overlay of H_{16}PcZn and F_{16}PcZn (bottom) showing the transition from an S-type to L-type isotherm apparently due to the increasing electron deficiency of the phthalocyanines. The theoretical monolayer for face-down oriented F_{64}PcZn is displayed for comparison to experimental results, Γ_{max} for less bulky molecules would be off-scale. The points are connected to guide the eyes.

properties that might impact the adsorption of the phthalocyanines on surfaces such as charge (Q_{Zn}), polarizability (α), and redox properties. The calculated properties are summarized in Table 3-5. Clear correlation appeared for ionization potential, electron affinity, and polarizability with increasing fluorination but some properties plateaued after F_{16}PcZn. Charge of the central metal also increased with initial replacement of C-H with F, but then leveled out for bulky group addition. This data correlated well with the adsorption data, in which we observed a dramatic change from H_{16}PcZn to F_{16}PcZn and then more minor changes to the isotherm with addition of bulky *i*-C_3F_7 groups.

A parallel study of the adsorption of zinc phthalocyanines on SiO_2-NH_2 was also completed (Figure A-1). Initial comparison of F_{64}PcZn adsorption on Al_2O_3 and SiO_2-NH_2 indicated that it had stronger interactions with the surface of Al_2O_3, though both curves were

characterized as L-type. For H_{16}PcZn, both Al_2O_3 and SiO_2-NH_2 demonstrated S-type adsorption. For F_{16}PcZn, on Al_2O_3 an L-type isotherm was obtained, but on SiO_2-NH_2 an S-type

Table 3-5: Calculated properties of Zinc Phthalocyanines

	H_{16}PcZn	F_{16}PcZn	F_{32}PcZn	F_{48}PcZn	F_{64}PcZn
Q_{Zn}, e	0.87	0.89	0.90	0.90	0.90
E_{bond}, eV	5.92	5.68	6.00	6.05	5.91
IP, eV	6.92	7.57	8.18	8.31	8.07
EA, eV	-2.56	-3.41	-4.17	-4.35	-4.22
$\alpha_{average}$, 10^{-30} esu	5.12	5.51	6.84	7.89	8.95

Table 3-5: Selection of calculated properties[100] of H_{16}PcZn and F_nPcZn (n = 16, 32, 48, 64) such as: atomic charge on Zn (Q_{Zn}), bond energy between the metal and tetrapyrrole ligand (E_{bond}), ionization potential (*IP*), electron affinity (*EA*), and polarizability.

isotherm was obtained. The transition from S-type to L-type on SiO_2-NH_2 occurred at F_{40}PcZn instead. These results were significant in that they demonstrated the effect of both the substrate surface and the electronic structure of the phthalocyanine molecule on adsorption. Computation data is not available for F_{40}PcZn, so we were not able to get an exact comparison of the change in properties from F_{16}PcZn to F_{40}PcZn

As was described in Chapter 1, it was important to note that the interactions between adsorbed molecules (solute-solute) can impact the energy of activation (E) of the system for the removal of solute. Such is specifically the case with S-type adsorption isotherms. If the solute-solute forces are significant relative to the solute-substrate forces during adsorption, then the E_A will increase with the presence of neighboring solute and 'cooperative adsorption' occurs. In this situation, E_A varies with the Γ in to a power (n) as described by equation 1-12 ($\boldsymbol{E = E_A^0 + \Delta E_A \Gamma^n - E_B - E_C}$). S-type adsorption with cooperative adsorption often indicates an 'edge on' orientation of the adsorbing molecule on the surface, yet none of the zinc phthalocyanines exceeded the theoretical Γ_{max} for densely packed molecules in the face down orientation. Phthalocyanine thin films of varied uniformity were readily produced with fluorinated zinc phthalocyanines from acetone on the surfaces of Al_2O_3 and SiO_2-NH_2. Closer study of the resulting surfaces was necessary to obtain orientation information for the adsorbed phthalocyanine species.

An additional consideration we accounted for was the solute-solvent interaction. Axial coordination of solvents to phthalocyanines, specifically acetone, has been reported and also causes changes to the electronic structure of the phthalocyanines.[93,104,113] Charge and redox potential of zinc phthalocyanines will decrease with the coordination of acetone (Table 3-6). We noted, however, that the decrease in redox properties with

Table 3-6: Calculated Properties of Fluorinated Phthalocyanines with Two Axial Acetone Ligands

	$F_{48}PcFe$	$F_{48}PcFe(L)_2$	$F_{48}PcCo$	$F_{48}PcCo(L)_2$	$F_{48}PcZn$	$F_{48}PcZn(L)_2$
$Q_{M\ (e)}$	0.88	0.80	0.70	0.69	0.67	0.65
$Q_{Ace\ (e)}$		0.22		0.16		0.13
IP, eV	8.76	7.94	8.72	8.31	8.72	8.30
EA, eV	-5.47	-4.72	-4.68	-3.87	-4.74	-4.32

Table 3-6: Summary and comparison of the calculated properties[93] of acetone-ligated and unligated $F_{48}PcMs$ (peripheral C_2F_5 groups). Properties of charge distribution (*Q*), ionization potential (*IP*), and electron affinity (*EA*) are reported.

coordination was smaller than a reduction of the fluorination in the molecule. Additionally, face down adsorption to the surface would also require displacement of axially coordinated solvent molecules. Liao *et al*[93] reported binding energy for two acetone ligands with zinc phthalocyanines of increasing fluorination. As fluorination increases, the binding energy is expected to increases. For example, predictions showed increases from 0.12 eV to 0.44 eV and 0.73 eV as the series progressed from $H_{16}PcZn$ to $F_{16}PcZn$ and $F_{48}PcZn$ (C_2F_5 groups in the β position). Thus, we expect strongest coordination and accompanying hindrance and reduced charge to impact adsorption of $F_{64}PcZn$.[97] Despite these theoretical interferences, the strongest adsorption was observed experimentally for the highly perfluorinated materials. The changes to the electronic properties with fluorination of the materials that had increased affinity for the surface dominated the adsorption.

3.4.5 Role of the Central Metal on the Adsorption of $F_{64}PcM$

A change in the central metal will impact the catalytic activity and electronic, spectroscopic, and physical properties in a similar way as changes to the periphery.[88] Therefore, adsorption studies to investigate the impact of a change in the central metal were undertaken. The uniquely higher solubility $F_{64}PcMs$ with reduced aggregation were chosen for this study. The central metals were chosen to represent materials of varied catalytic activity and *d* orbital electronic state. For example, $F_{64}PcZn$ represents a completely filled *d* orbital. Cu, Co, Fe, and Ru all have the oxidation state of 2+ with different *d* orbital filling states, which could demonstrate the impact crystal field stabilization energy. Additionally, $F_{64}PcCo$ represented material with potential Jahn-Teller distortions. $F_{64}PcRu$ is known to have different catalytic activity involving ring's macrocycle.[114] $F_{64}PcFe$ has readily modified ionic states, Fe(II) and Fe(III). Finally, $F_{64}PcVO$ has an oxidation state of 4+ and is readily available for the formation of complexes.

The results of the adsorption of $F_{64}PcM$ on Al_2O_3 are displayed in Figure 3-12. As was introduced with the UV/Vis analysis discussion, some of the $F_{64}PcMs$ studied had stability issues that impacted the analysis ($F_{64}PcFe$ was excluded from the figure due to instability previously discussed). Solubility differences between the phthalocyanines were also observed. For example, the solubility of Cu and Co phthalocyanines was nearly an order of magnitude lower than that of Zn, Fe, VO, and Ru with $F_{64}PcCu$ having the lowest solubility (~0.1 mg/mL). Interestingly, we observed that the low solubility (Cu, Co) $F_{64}PcMs$ also displayed weak S-type adsorption in acetone while the higher solubility phthalocyanines were of the stronger L-type.

Figure 3-12: Effect of the Central Metal on the Adsorption of $F_{64}PcM$ on Al_2O_3

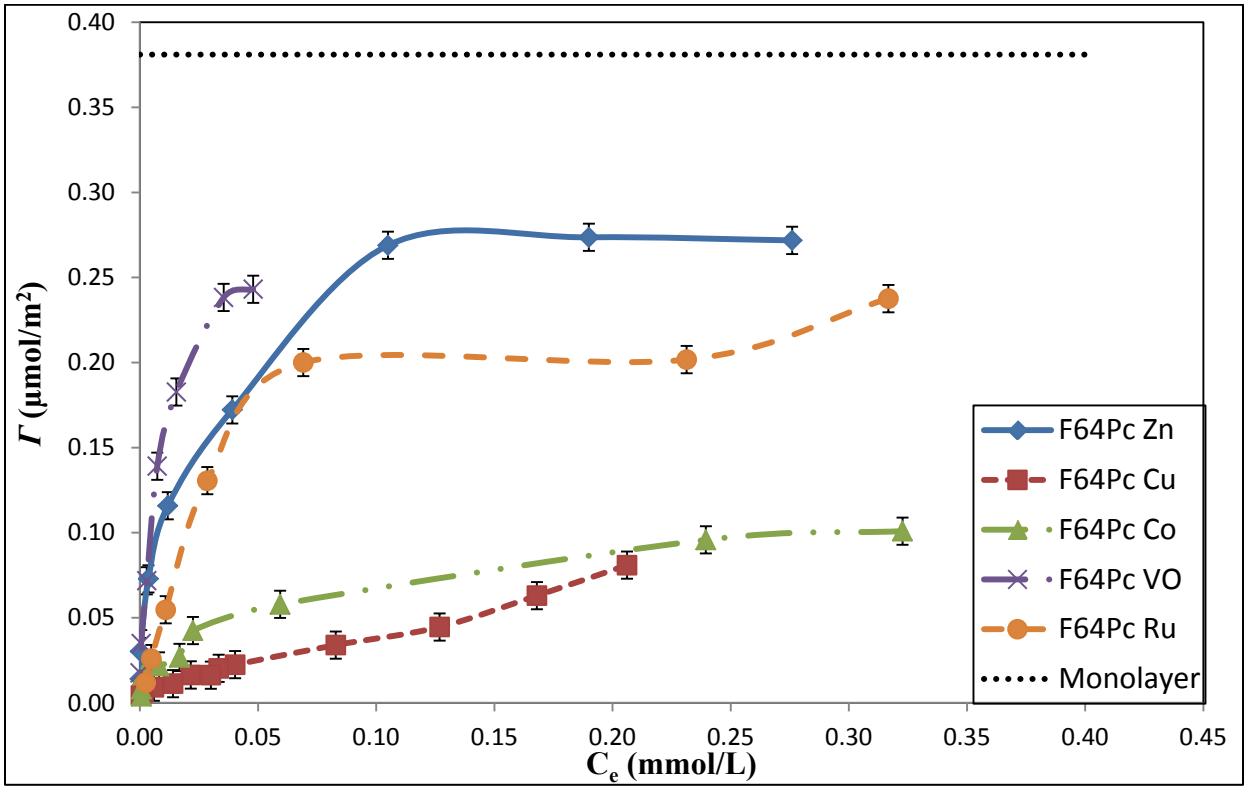

Figure 3-12: Overlay demonstrating the effect of the central metal on the adsorption of $F_{64}PcM$ on the surface of Al_2O_3. The theoretical monolayer for tightly packed, face-down $F_{64}PcM$ is included for comparison to experimental results. The points are connected to guide the eyes.

Table 3-7: Calculated Properties of $H_{16}PcM$

	M = Fe	M = Co	M = Cu	M = Zn
Q_M	0.71	0.59	0.65	0.64
$E_{bond,\ eV}$	9.81	10.49	6.96	5.66
IP, eV	6.46	6.47	6.51	6.52
EA, eV	-2.55	-3.19	-1.74	-2.16

Table 3-7: Selection of calculated properties[115] of $H_{16}PcM$ (M = Fe, Co, Cu, Zn) such as: atomic charge on M (Q_M), bond energy between the metal and tetrapyrrole ligand (E_{bond}), ionization potential (*IP*), and electron affinity (*EA*).

A comparison of the electronic properties[115] of H_{16}PcMs with various central metals is shown in Table 3-7. Direct comparison of the electronic properties of the F_{64}PcMs used in this study was not available, however, there is computational data for H_{16}PcM and F_nPcM for some of the studied metals in previous work[93,113] and the trends could easily be predicted with increasing fluorination. Specifically, Q_M, E_{bond}, IP, and EA are all expected to increase to some extent as the perfluorination increases.[93] However, analysis of these properties and our results in Figure 3-12 showed no clear correlation with electronic properties and the adsorption isotherm results for Al_2O_3. Further study is necessary to better interpret these results.

In a similar study to Al_2O_3, adsorption of the F_{64}PcMs on SiO_2-NH_2 is displayed in Figure A-3. On this surface, F_{64}PcCu and F_{64}PcCo appear to shift from S-type to L-type, however, we considered that this was, in-part, attributable to the instability of these materials in the presence of the amine as demonstrated in Figure A-2. We hoped to rely on chemical analysis results in this case, but were unable to obtain consistent values to draw a good correlation between the chemical analysis results and UV/Vis results. However, for all of these molecules, phthalocyanine thin films were produced on the surface of Al_2O_3 and SiO_2-NH_2. Comparison of the adsorption results in Figure A-3 to the properties in Table 3-7 showed only one potential correlation of the data, the electron affinity. The strength of adsorption was directly correlated with the calculated electron affinity of the material. Due the uncertainty of the results, we are unable to derive strong conclusions for these results, but the data continued to direct us toward electron donor/acceptor interactions as the major factor in the adsorption of phthalocyanines to the studied surfaces.

Similar to the zinc phthalocyanine study, coordination of solvents to the metal center may play a role in the adsorption isotherms. For these F_{64}PcM materials, the electron withdrawing nature of the *i*-C_3F_7 groups is equivalent and the difference in electronic structure can be solely attributed to the central metal. Several recent studies have highlighted the coordination of molecules, specifically acetone, to phthalocyanines containing Zn,[93,116] Co,[93] Fe[93] and Ru.[114,117,118] Analysis of results obtained by Liao *et al*[93] (Table 3-6) demonstrated that for F_{48}PcM, coordination of acetone leads to changes of different magnitudes for different metal centers. For example, the strongest coordination of acetone ligands occurred for F_{48}PcFe as well as the largest change in ionization potential. For F_{48}PcZn, the change in electron affinity with coordination was less significant than for the other metals analyzed.

Due to the differences in the adsorption isotherms for F_{64}PcMs containing various central metals, we cautiously concluded that, excluding instability and spectral changes, a change in central metal had an impact on the adsorption of F_{64}PcMs with a possible correlation to the electron affinity (Lewis acidity) of the materials on the surface of SiO_2-NH_2. This was likely due to changes to the affinity for axial coordination at the metal center for either the solvent or the surface. Extension of these studies to other metals centers will continue to expand our understanding of the ideal combination of materials and forces necessary for strong adsorption to these surfaces.

3.4.6 Mechanistic Studies of Specific Solute-Substrate Interactions

Systematic studies of the effect of the addition of electron withdrawing F and *i*-C_3F_7 groups on zinc phthalocyanines, followed by the impact of a change in central metal were undertaken. In each case, there was evidence that the mechanism of adsorption was

Table 3-8: Binding Energy Calculations for Iron (II) Phthalocyanines with Axial Ligands

L:	$H_{16}PcFe(L)_2$	$F_{16}PcFe(L)_2$	$F_{32}PcFe(L)_2$
Acetone (E_{bind}, eV)	0.22	0.58	0.83
H_2O (E_{bind}, eV)	0.26	0.52	0.73
Pyridine (E_{bind}, eV)	1.88	2.26	2.54

Table 3-8: Calculated binding energies[113] for iron (II) phthalocyanines to two axially coordinated ligands.

Figure 3-13: Schematic of the Adsorption of Phthalocyanines to the Surface of

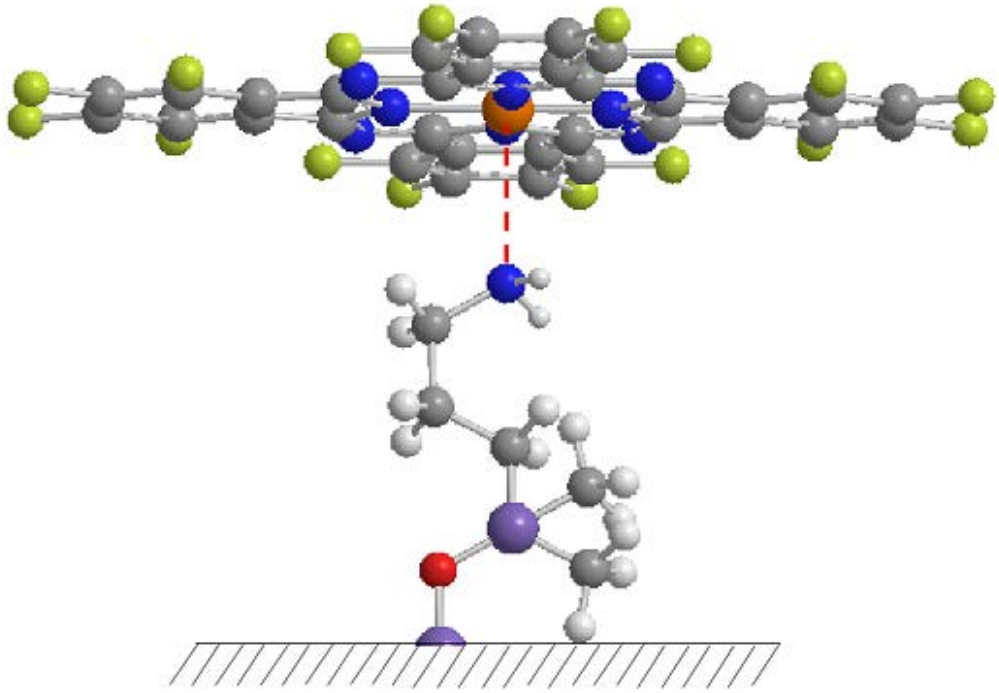

Figure 3-13: Schematic of the proposed mechanism of adsorption for phthalocyanines ($F_{16}PcZn$ pictured) to the studied surfaces (SiO_2-NH_2 pictured). The basic moiety axially coordinated to the acidic metal center of the phthalocyanine to produce a stable, reproducible modified surface.

dominated by Lewis acid-base interactions between the electron deficient central metal (as fluorination was introduced) and electron donating surfaces. This likely occurs via the axial coordination of the basic surface moieties, to the acidic central metal, similarly described in several previous works.[114] For example, imidazolyl[116,119] or pyridine[118] added to surfaces or the periphery of molecules facilitated the formation of uniform layers via axial coordination at the Pc metal center. However, to our knowledge, we are the first to report coordination of phthalocyanines with primary alkyl amines. Additionally, computational studies[93] predicted that the binding energy of axially coordinated with acetone to H_{16}PcCo was 0.16 eV, but for pyridine it was 0.77 eV. Further predictions[113] for iron phthalocyanines showed dramatic differences for the binding energy of acetone, H_2O, and pyridine as the electron deficiency of the central metal increases with fluorination (Table 3-8). We, therefore, hypothesized that the phthalocyanines adsorbed in a face down orientation to the surface by axial coordination to the surface at the central metal, as demonstrated in Figure 3-13. In a similar study, Huc *et al*[120], produced monolayers and multilayers of RuPc on pyridine-functionalized glass. They proposed a ligand exchange to first coordinate phthalocyanines to the surface and subsequent exchange at the opposite face of the phthalocyanine to facilitate multilayer formation.

To further investigate the mechanism of Lewis acid/base facilitated coordination of the Pcs to the surface, the surface of SiO_2 was modified to obtain surfaces with bases of different strengths via compounds containing aniline (pka ~4.2), pyridine (pka ~6.0), primary amine (pka ~10.4) and imidazole (pka ~11.3), as shown in Figure 3-14 (Note: if unavailable from the vendor, the pka was predicted by ACD labs using the alkoxysilane

Figure 3-14: Structure and pKa of Aminated Silicas

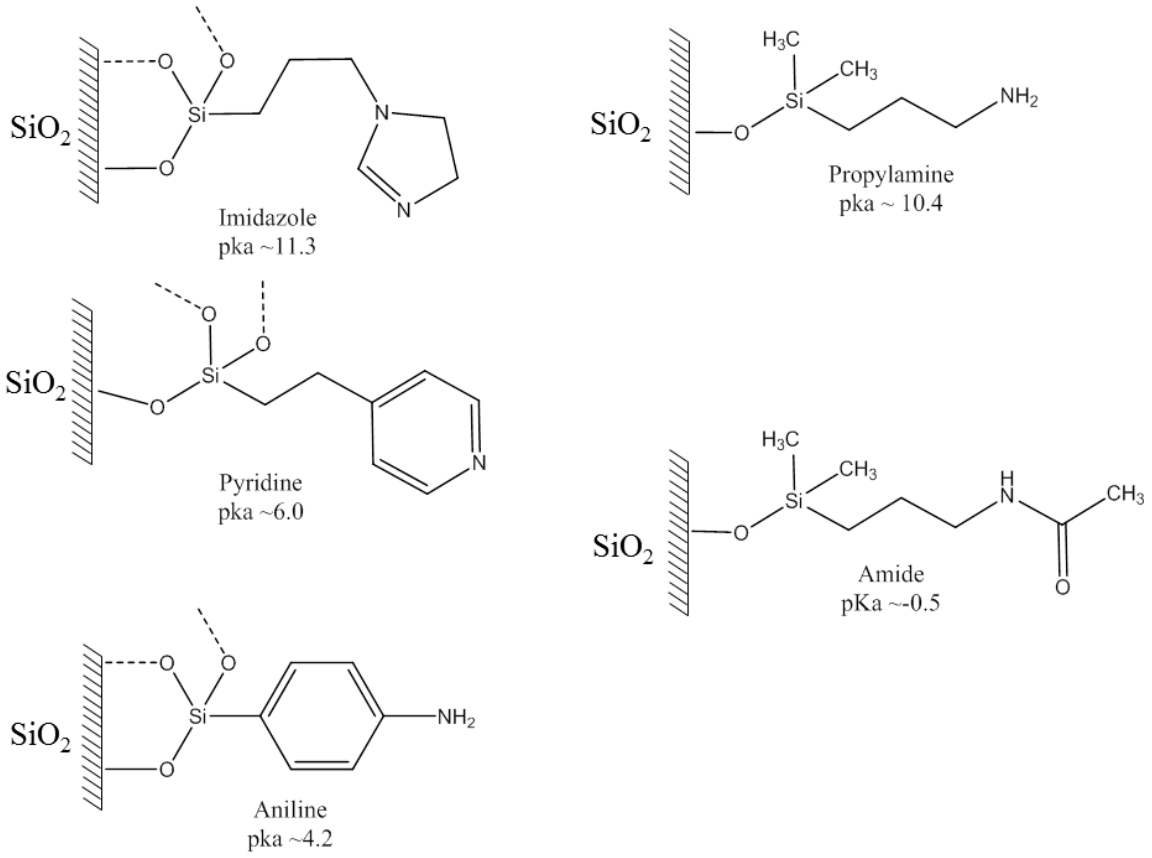

Figure 3-14: Structure and pKa of the conjugate base of additional surfaces chosen to study the effect of Lewis basicity of surfaces in the adsorption of phthalocyanines.

structure for each molecule, the pka of the conjugate base is provided). Furthermore, SiO_2-NH_2 was further reacted with acetic anhydride to form an amide (pka ~-0.5). This complemented our studies with increasingly electron deficient phthalocyanines. Grafting density (ρ, groups/nm^2) of the reaction products was compared by chemical analysis to ensure that surfaces contained an equivalent number of active functional groups. Adsorption studies for F_{64}PcZn in acetone were completed for each of the newly created surfaces. As expected, we observed an increase in the strength of adsorption with increased strength of the base, as indicated by a change from S-type to L-type curves.

Figure 3-15: Adsorption of $F_{64}PcZn$ on Various Aminated Silicas

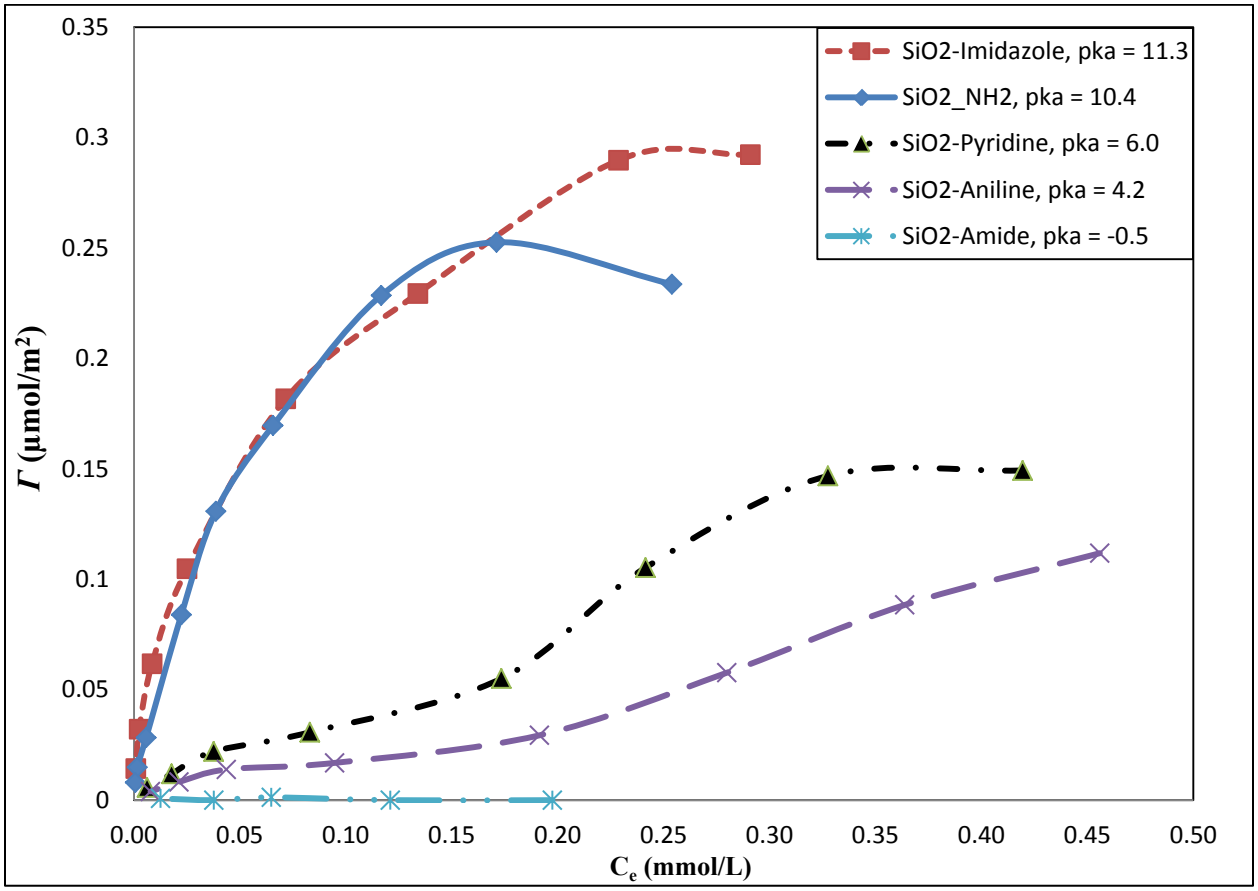

Figure 3-15: Adsorption isotherms for $F_{64}PcZn$ on silicas modified with imidazole (SiO_2-Imidazole), a primary amine (SiO_2-NH_2), pyridine (SiO_2-Pyridine), aniline (SiO_2-Aniline), and an amide (SiO_2-Amide) as displayed in Figure 3-14.

Specifically, as is shown in Figure 3-15, no adsorption occurred on SiO_2-Amide, S-type curves were obtained for SiO_2-Aniline and SiO_2-Pyridine, and L-type curves were obtained for SiO_2-NH_2 and SiO_2-Imidazole. This provided further evidence that the adsorption of phthalocyanines is dominated by Lewis acid-base interactions between the central metal and the surface.

To investigate the Lewis acid/base mechanism on the surface of alumina, acid treated (pH = 4.5, in water), alkaline treated (pH = 9.5) and neutral activated aluminas with a Brockmann activity of I were purchased. Brockman activity I aluminas represent

Figure 3-16: Effect of pH on the Adsorption of $F_{64}PcZn$ on Al_2O_3

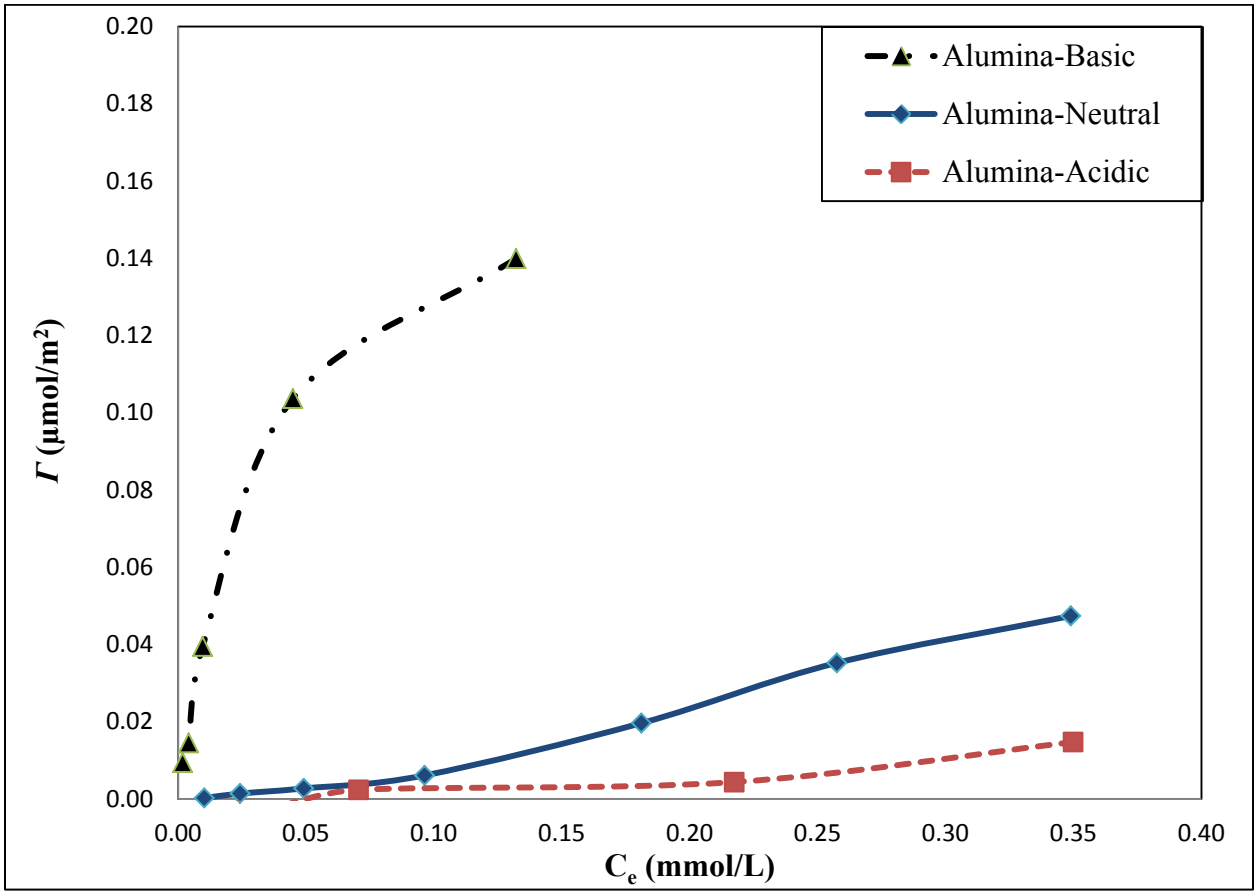

Figure 3-16: Adsorption of $F_{64}PcZn$ in acetone on pH adjusted aluminas that were acidic (pH ~4.5), neutral (pH ~7), and basic (pH ~9.5). The pH listed are the values expected in water.

the dehydrated and most active aluminas, addition of known amounts of water will decrease activity.[121] Adsorption studies for $F_{64}PcZn$ in acetone were completed for each of the materials. Further confirming the hypothesis, the strongest adsorption was observed for the basic surface and the weakest adsorption was observed for the acidic surface (Figure 3-16). It was noted that the non-porous alumina utilized in all other studies was neutral with similar water content, yet it showed stronger adsorption than the neutral activated porous alumina. This was partially attributed to pore confinement present in the activated alumina materials. Additionally, differences in the activity and

synthetic pathways for α-alumina and γ-alumina likely played a role. To our knowledge, this is the first report of the adsorption of phthalocyanines to aluminas via axial coordination from solution.

3.4.7 Role of Solvent in the Adsorption of Phthalocyanines

In the introduction it was mentioned that the factors affecting the adsorption of molecules from solution include solute-solute, solute-solvent, solute-substrate, and solvent-substrate interactions. For solute-solvent interactions, it has been well documented[93,97,113,122] that phthalocyanines often coordinate acetone, among other polar solvents, at the metal center (Table 3-6, Table 3-8). In addition to the changes to electronic properties discussed previously, this coordination (with C=O of the acetone) would contribute steric hindrance and direct competition with the adsorption of phthalocyanines to the surface and contribute to desorption (E_B) in the system ($\boldsymbol{E = E_A^0 + \Delta E_A \Gamma^n - E_B - E_C}$). Therefore, methylene chloride (CH_2Cl_2) was chosen for study because it maintained good solubility of the phthalocyanines, but lacked groups with an affinity for coordination with the phthalocyanine molecules. Studies were completed on several F_{64}PcMs and the zinc phthalocyanines with sufficient solubility in the new solvent. The solubility of the phthalocyanines was approximately 5-10 times lower in methylene chloride than acetone. The results (Figure 3-17 and Figure A-4) showed a dramatic difference in the adsorption isotherms for the phthalocyanines in methylene chloride (CH_2Cl_2) when compared to acetone.

On both Al_2O_3 and SiO_2-NH_2, the adsorption exceeded that of the theoretical monolayer for the higher solubility materials studied (Figure 3-17). We then increased the volume at the concentration of maximum solubility in order to obtain Γ_{max} in

Figure 3-17: Solvent Comparison for the Adsorption of Zinc Phthalocyanines

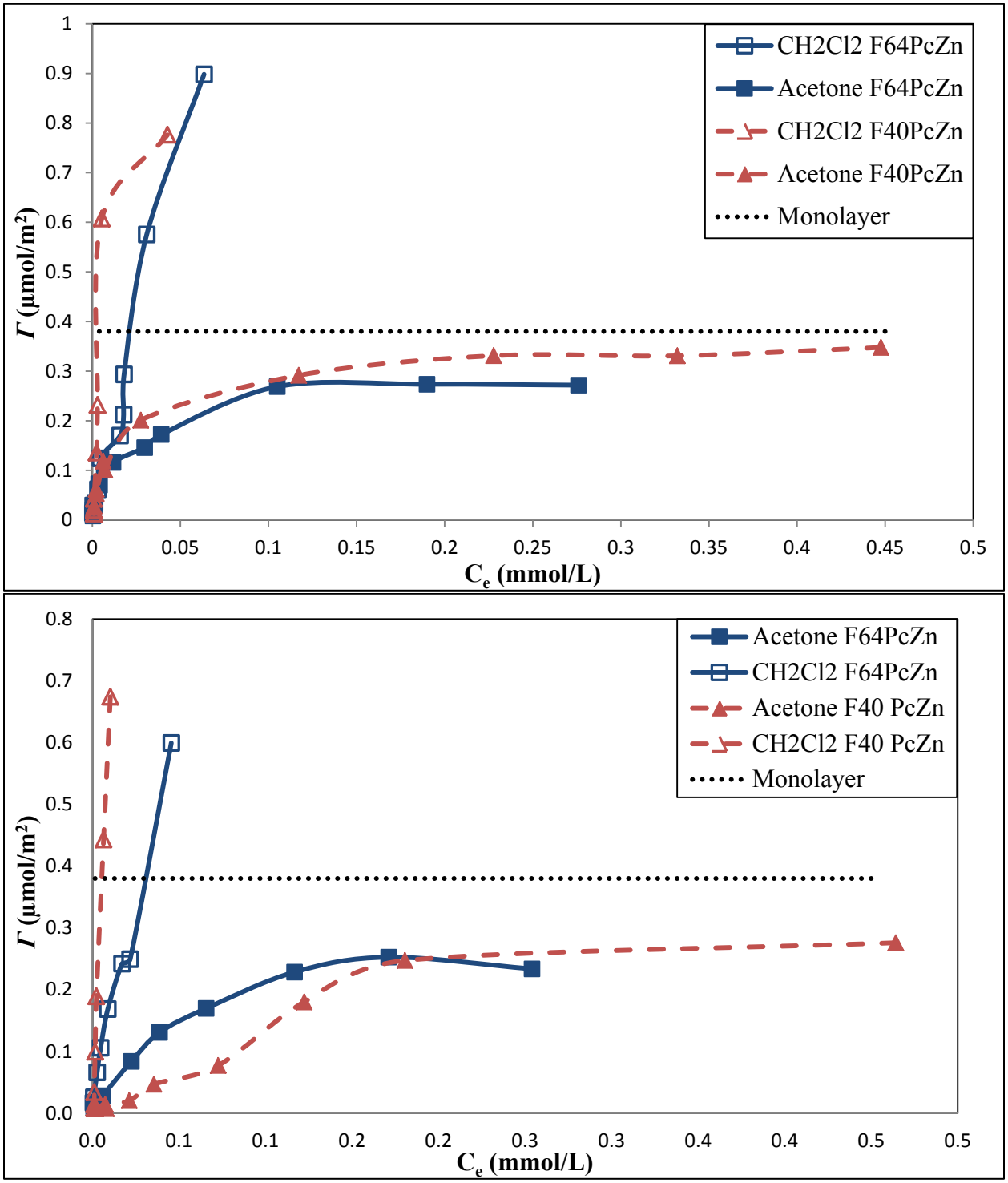

Figure 3-17: Comparison of the adsorption of zinc phthalocyanines on the surface of Al_2O_3 (Top) and SiO_2-NH_2 (Bottom) from acetone (closed symbols) and methylene chloride (open symbols). The points are connected to guide the eyes. Adsorption from methylene chloride exceeded theoretical Γ_{max} (•••• monolayer) for a densely packed face-down orientation of F_{64}PcM molecules.

methylene chloride, but it was not reached for materials under the conditions studied. Careful analysis of the CH_2Cl_2 isotherms for Al_2O_3 (Figure 3-17, top) showed that the 'knee' or point B near the Γ_{max} prior to the multilayer formation, similar to subgroup 3 of the L-type curve (Figure 1-6). This indicates that the Lewis acid-base interactions still dominate the early adsorption of the monolayer prior to multilayer formation. However, on SiO_2-NH_2, the knee is not present, in fact, the curves change from what were characterized as L-type curves to H-type (high affinity, increased E_A^0). A similar trend is observed for some (Zn, Co), but not all (Cu, Ru), F_{64}PcM (Figure A-4). In the acetone adsorption system, acetone can be coordinated to both faces of the phthalocyanine molecule (more strongly to F_{64}PcMs when compared to less perfluorinated F_nPcM[97,113,122]). Additionally, we expected more undesired chemical interactions of acetone with surface amines in the SiO_2-NH_2 system. By our proposed mechanism, at least one acetone ligand is displaced from the phthalocyanine at adsorption as well as any interfering surface-adsorbed molecules. We can assume that the second acetone ligand remains coordinated to the opposite face of the phthalocyanine, inhibiting multilayer formation to some extent. Conversely, CH_2Cl_2 is non-coordinating with $E_A^0 >> E_B$, reducing the energy necessary for displacement of the solvent during adsorption producing an L-type isotherm on Al_2O_3 and an H-type isotherm for SiO_2-NH_2. Additionally, we can conclude that E_A^0 (of the 2nd layer, equivalent for both surfaces) > E_B in the CH_2Cl_2 system, and the reduced steric hindrance contributed to the formation of multilayers.

The interactions of acetone with the surfaces should not be ignored. The difference in isotherms between Al_2O_3 (L-type to L-type subgroup 3) and SiO_2-NH_2 (L-

type to H-type subgroup 3) clearly demonstrated a difference in E_B values for each surface. We did expect weak adsorption of acetone to the surface of Al_2O_3 and SiO_2-NH_2. Furthermore, the presence of acidic and basic moieties has been shown, under certain conditions, to cause chemisorption of acetone as well as side reactions.[123] We also considered the presence of trace acid in the CH_2Cl_2 contributing to some of the changes we observed. When the contribution of E_B is reduced within the equation, the data indicates that E_A^0 is greater for SiO_2-NH_2 than Al_2O_3 (H-type versus L-type). This should be studied in more detail to gain greater understanding and provide a more detailed explanation as to why such differences were observed in the adsorption isotherms of Al_2O_3 and SiO_2-NH_2 with different solvents.

3.4.8 Solid State Characterization of Adsorbed Phthalocyanine Thin Films

Throughout the experiments in acetone, adsorption isotherms plateaued near the theoretical Γ_{max} for densely packed molecules in the face-down orientation. With this observation, it was assumed that uniform monomolecular surfaces of relatively close packing were produced. In CH_2Cl_2, multilayer formation began, which may also have represented a less ordered surface as axial coordination will not occur in the multilayer and the bulky F64PcZn produces minimal π-π stacking. Additionally, we noted that some of the less bulky zinc phthalocyanines, the molecules aggregated in solution via π-π stacking. How might this aggregation affect the order and orientation of the adsorbed molecules on the surface? To study this, UV/Vis/NIR spectra were obtained for the solids produced in the adsorption experiments. From this data we hoped to glean information about the surfaces produced by this technique.

Figure 3-18: Schematic of Phthalocyanine Polymorphs and Q-Band Shifts

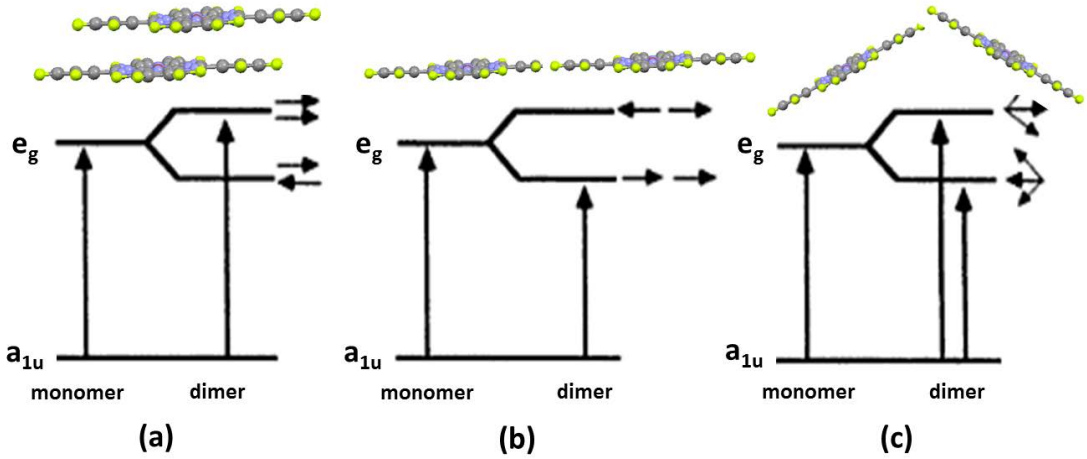

Figure 3-18: A simplified model of exciton splitting of the Q-band between two F_{16}PcM molecules in (a) cofacial, (b) edge-to-edge and (c) tilted arrangements to demonstrate the red-shift and blue-shift of each arrangement. Allowed transitions are represented by vertical single-headed arrows. Horizontal single-headed arrows represent the phase transitions.

The aggregation of phthalocyanines in the solid state has also been closely studied and divided into four classes based upon energy level splitting and emission spectra characterized by reflectance UV/Vis. For the three crystalline polymorphs, the change in energy level splitting is proportional to the magnitude of the transition moments which lie in the plane of the Pc ring and is inversely proportional to the cube of their separation, with some angular dependance.[110] The first group are cofacial dimers formed via π-π stacking in which the Q-band is blue-shifted relative to its position in the monomer spectrum (Figure 3-18). An example of cofacial aggregation, also known as the α-polymorph, was observed for F_{40}PcZn in Figure 3-9a. The second type of aggregation is edge-to-edge in the same plane yet still impacting orbitals with an expected red-shift. Edge-to-edge aggregation is considered the β-polymorph in the solid state. Finally, a much less uniform tilted aggregation will show two bands from both a red-shift and a blue-shift, this is also referred to as 'Davydov splitting.[124]' In the solid state, this tilted

aggregation is considered the χ-polymorph. The fourth class is amorphous, and is characterized by a general broadening of the Q-band in the solid state due to ring orbital distortions from neighboring molecules in several orientations, as observed with multilayers formed by vapor deposition.[124] With this system of classification, careful study of the solid state UV spectra and their complementary UV spectra could obtain information about the nature of the phthalocyanine adsorption.

Figure 3-19: Solution and Reflectance Spectral Comparison for $F_{16}PcZn$

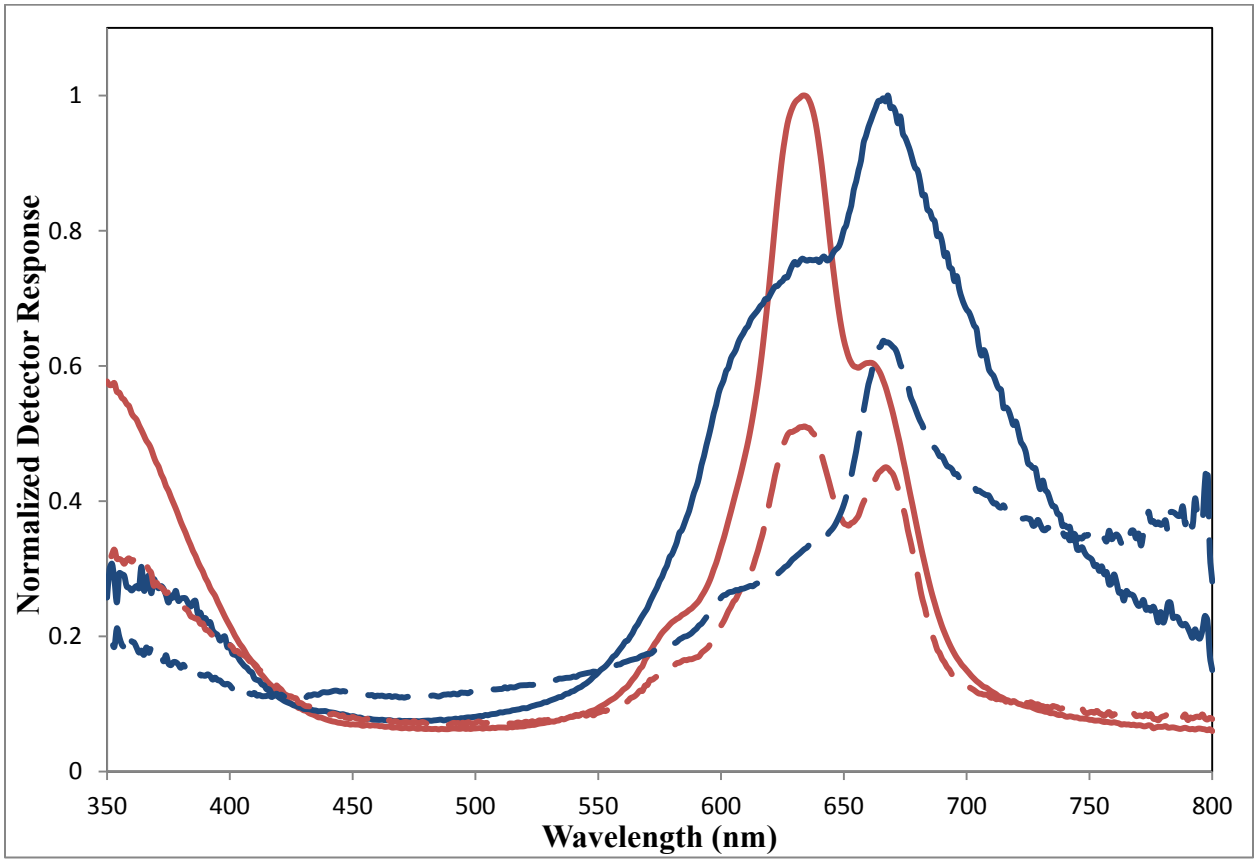

Figure 3-19: Comparison of the normalized reflectance (blue open lines) and solution (red closed lines) spectra for $F_{16}PcZn$ on SiO_2-NH_2 at the data point corresponding to a C_e of 8.5 µmol/L (solid lines) and 1.7 µmol/L (dashed lines, 3 X responses for better comparison). Q-band maxima are present for monomers (~662 nm) and cofacial dimers (~634 nm).

During the studies, we found that the linear range of the reflectance UV/Vis for these materials was limited. Only 30-40% reflectance was obtained for the packed, untreated particles. Therefore, samples with a significant quantity of adsorbed phthalocyanines could not be analyzed quantitatively. Kubelka-Munk analysis showed the linear range for multiple series to end at approximately 0.1-0.2 μmol/m^2. Additionally, peak broadening and overlapping signals led us to consider the reflectance data to be purely qualitative. Similar adsorption studies should be conducted on smooth surfaces to obtain more quantitative results.

Each data point in adsorption curve represents the equilibrium between the phthalocyanines in solution and the surface containing adsorbed phthalocyanines. Therefore, complimentary solution and solid state spectra were obtained for samples at different surface concentrations within the linear range of the reflectance UV/Vis to track changes throughout the isotherm. To begin, F_{16}PcZn, which readily aggregated in solution, had a distinct Q-band splitting in the solid state that clearly demonstrated cofacial aggregation (Figure 3-19). We noted that in solution the dimer peak (634 nm) dominated compared to the monomer peak (662 nm) at the highest concentrations, and shifted to a ratio of approximately 1:1 at lower concentrations. In the solid state, however, the monomer peak was always present at a higher level than dimer. On the surface of Al_2O_3, the ratio of monomer to dimer remained relatively consistent. Uniquely, on SiO_2-NH_2 surfaces, monomer was present at the highest level at lower concentrations, then plateaued at ratios qualitatively similar to those of Al_2O_3 at moderate to high Γ (Figure 3-19). These results were consistent with the L-type curved obtained for Al_2O_3 versus the S-type curve (cooperative adsorption only at high concentrations)

obtained on the surface of SiO_2-NH_2. The results also indicated that the cofacial dimer is partially maintained during adsorption of F_{16}PcZn on Al_2O_3, but not as consistently on SiO_2-NH_2. In a similar system in which pyridine breaks F_{16}PcZn dimers in solution,[109] adsorption to the surface of SiO_2-NH_2 might disrupt the cofacial dimers at lower Γ before cooperative adsorption at higher concentrations stabilized the phthalocyanines on the surface. Our Γ_{max} prediction for a tightly packed monolayer of face-down F_{16}PcZn was 0.500 μmol/m^2, though quantitation is difficult for these aggregating samples, our studies did not reach a distinct 'point B' due to weaker surface interactions very low solubility. We did consider that a 'monolayer' Γ_{max} of face-down cofacially stacked dimers should nearly double that of a monolayer. However, π-π stacked cofacial dimers off-set (see similar image for F_{40}PcZn in Figure 3-9a) and would inhabit a larger surface area and pack differently than our true monolayer $\Gamma_{\max}$ approximation.

Although a distinct peaks did not appear, which is often attributed to an amorphous surface, the red-shift broadening of the Q-band (>750 nm) may also be in indication of edge-to-edge packing of the already cofacially aggregated adsorbate.[124] Additionally, a blue-shift broadening appeared to overlap with the cofacial dimer peaks, coupled with the red-shift implies a tilted orientation. We assumed that edge-to-edge packing within pores, as opposed to flat surfaces, would result in observations for tilted orientation. The presence of edge-to-edge packing, tilted packing, or both implies a face-down orientation of the F_{16}PcZn molecule as opposed to the vertical orientation that is often assumed in an S-type adsorption isotherm.

Figure 3-20: Solution and Reflectance Spectral Comparison for $F_{64}PcZn$

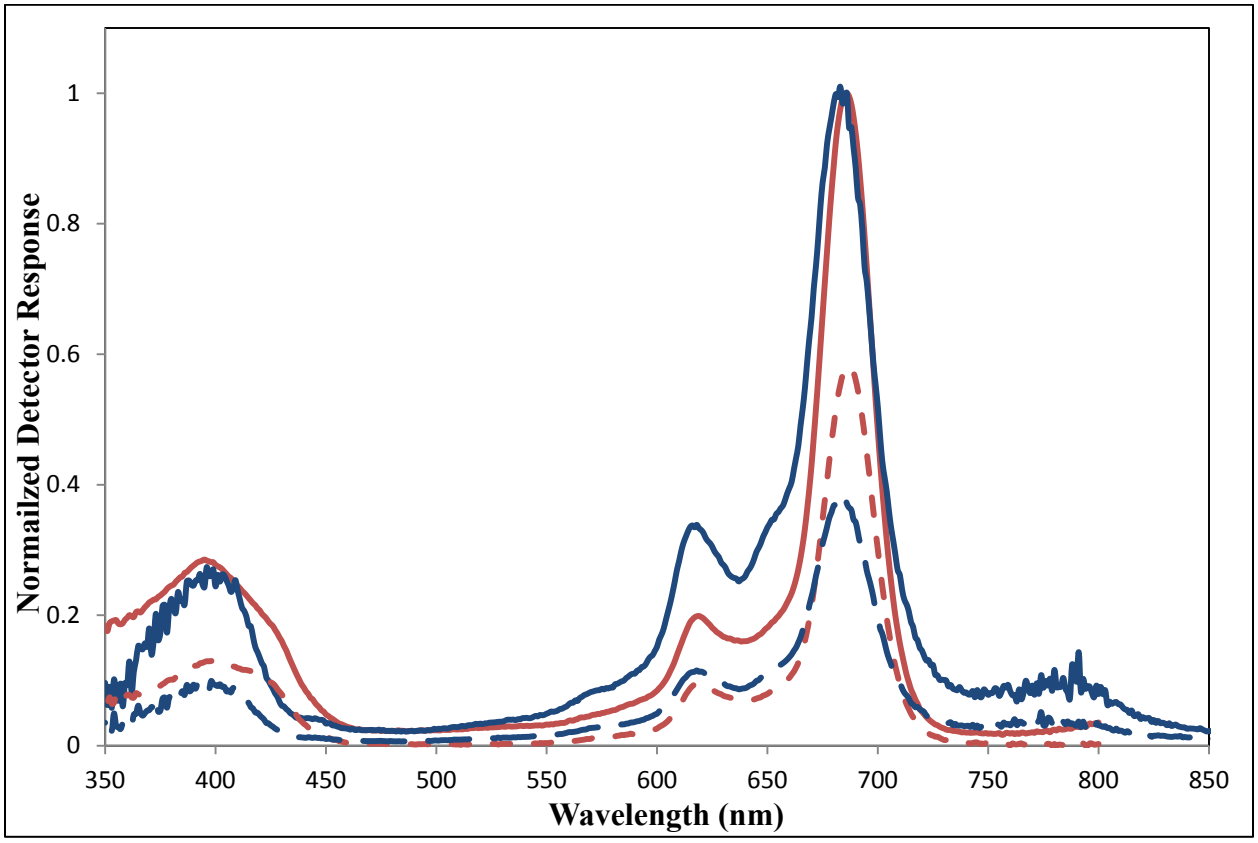

Figure 3-20: Comparison of the normalized reflectance (blue open lines) and solution (red closed lines) spectra for $F_{64}PcZn$ and Al_2O_3 at the data point corresponding to a C_e of 10.2 µmol/L (solid lines) and 2.0 µmol/L (dashed lines, 3 X responses for better comparison). Q-band maxima splitting red-shift (~785 nm) and blue-shift (~650 nm) indicate some aggregation at high Γ.

Careful analysis of the solution and solid state spectra of $F_{64}PcMs$ revealed similar results for all metals. In the solution state sharp HOMO and LUMO Q-bands are present, with the expected B-band and no obvious spectral shifts from aggregation. An overlay of the solid-state (Figure 3-20) and solution spectra for $F_{64}PcZn$ at varied concentrations were similar. However, we noted the presence of a shoulder on the Q-band at approximately 655 nm. A blue-shift could be an indication of the presence of either the α-form or the χ-form. For the α polymorph, though unlikely, the small magnitude of the shift relative to that of the $F_{16}PcZn$ is explained by the increased

separation of the cofacial dimer with the addition of the bulky CF_3 groups to the periphery. More likely, and similar to our assumptions for F_{16}PcZn, edge-to-edge aggregation (β-form) within the pores could manifest as the tilted χ-form. An additional study on a smooth, flat surface would confirm this hypothesis. Further evidence of edge-to-edge aggregation was a distinct peak at ~800 nm. A red shift such as this indicates presence of the β-polymorph. The adsorption isotherm (Figure 3-5) approached the theoretical Γ_{max} for a tightly packed monolayer in the face-down orientation, thus the edge-to-edge packing of the adsorbed molecules was manifested by the broad peak at ~800 nm. Due to the overlapping shifts that are possible, further analysis of the materials is necessary to conclusively obtain packing information. Based upon the surface concentrations near to the Γ_{max} of a face-down monolayer and evidence of edge-to-edge packing, we concluded that the F_{64}PcMs adsorbed as a uniform, closely packed monolayer in the face-down orientation.

A shift in the adsorption isotherm curves was observed when the solvent was changed from acetone to methylene chloride. Specifically, there was evidence of multilayer formation based upon the theoretical Γ_{max} for a face-down orientation, which complimented the adsorption data displayed in Figure 3-17. Accurate quantitative analysis of multilayer materials was not possible because samples with Γ greater than a monolayer were above the linear range of the reflectance UV measurements, as determined by Kubelka-Munk transformations. However, comparison of the spectra, as shown in Figure 3-21 at 0.17 μmol/m^2, demonstrated that multilayer formation occurs from CH_2Cl_2 even prior to Γ_{max} for a densely packed face-down theoretical monolayer. Broadening of the Q-band for CH_2Cl_2 materials can demonstrate random orientation on

Figure 3-21: Spectral Comparison of F_{64}PcZn Adsorption from Different Solvents

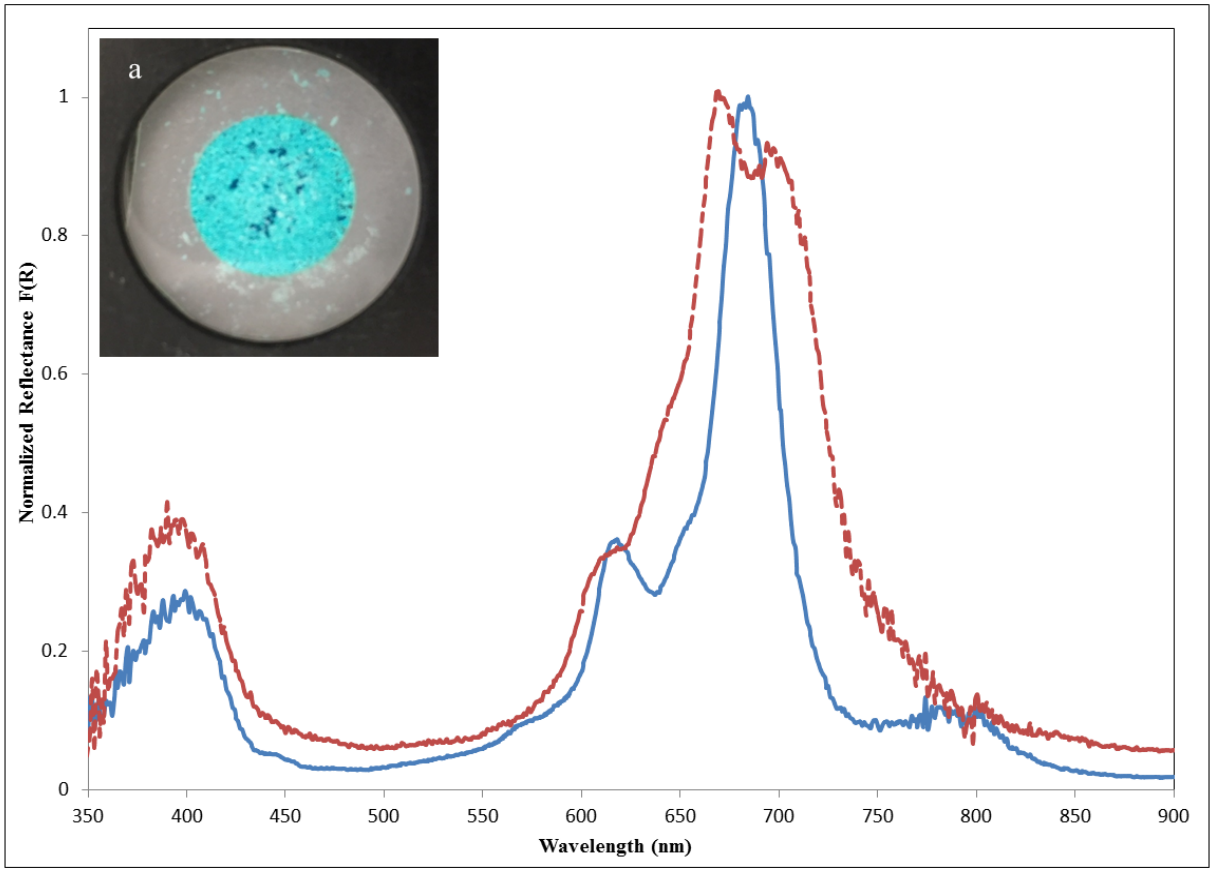

Figure 3-21: Comparison of the reflectance spectra for the adsorption of F_{64}PcZn from acetone (solid blue line) and methylene chloride (red dashes) at $\Gamma = 0.17$ μmol/m^2. General broadening and splitting of the Q band for methylene chloride relative to acetone provides evidence of multilayer formation and aggregation as demonstrated by the dark spots in the insert (a).

an amorphous surface. Red-shifted and blue-shifted maxima at ~695 and 668 nm, respectively, as well as shoulder peaks at 645 and 800 nm indicate the presence of multiple overlapping polymorphs, indicative of multilayer formation. The data clearly demonstrated that aggregation was present with adsorption from methylene chloride when compared to acetone, an indication of multilayer formation.

Unlike F_{16}PcZn and F_{64}PcZn, F_{40}PcZn and F_{52}PcZn do not have 4-fold symmetry. This resulted in splitting of the two Q-bands in the UV spectrum. In the case of *cis*-F_{40}PcZn (major component in our system), many of these peaks are not well separated

Figure 3-22: Solution and Reflectance Spectral Comparison for $F_{40}PcZn$

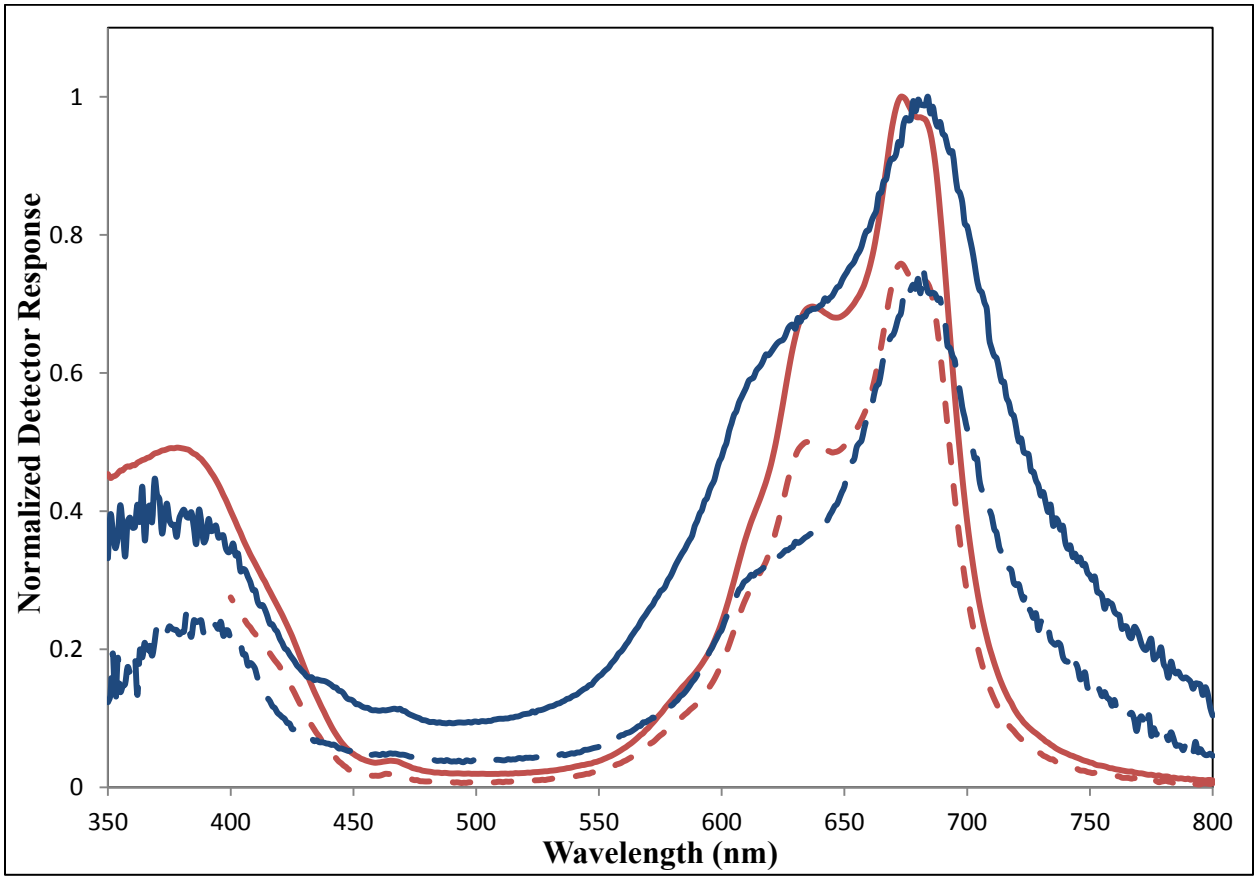

Figure 3-22: Comparison of the normalized reflectance (blue open lines) and solution (red closed lines) spectra for $F_{40}PcZn$ on Al_2O_3 at the data point corresponding to a C_e of 28.9 µmol/L (solid lines) and 6.5 µmol/L (dashed lines, 3 X responses for better comparison). Q-band maxima broadening indicated some aggregation of multiple types at all Γ, with cofacial aggregation as a constant contributing factor.

(Q_1 peaks at 678 and 687 nm in acetone), making deconvolution of the data very difficult. Additionally, we observed in solution that despite the addition of bulky i-C_3F_7 groups, some aggregation of the phthalocyanines did occur. As demonstrated in Figure 3-9, *cis*-$F_{40}PcZn$ can form off-set cofacial dimers with the i-C_3F_7 groups oriented at opposite sides of the molecules. We predict that trans-$F_{40}PcZn$ would aggregate to a lesser extent, similar to $F_{52}PcZn$. This spectral overlap was further confounded in the solid state, where distinct maxima for Q_1 peaks could not be differentiated. Unlike $F_{16}PcZn$ and $F_{64}PcZn$, we did not observe specific peaks in the reflectance spectra that indicated aggregation

beyond that of known cofacial aggregation observed in solution. However, as the surface concentration increases, the overall width of the Q-band absorption increased relative to the solution state, indicating both a red-shift and blue-shift in the solid state. We would therefore cautiously conclude, similar to F_{16}PcZn and F_{64}PcZn, that edge-to-edge packing was present in addition to the known α-form dimerization.

Similar to F_{16}PcZn, the cofacial dimerization continues to be present in the solid state (Figure 3-22). When the cofacial dimer peaks were studied, we were unable to differentiate a clear change in the ratio of monomer to dimer when adsorption on Al_2O_3 to SiO_2-NH_2 was compared (Figure A-6). This may have been due to the fact that adsorption curves for F_{40}PcZn were both characterized as L-type, unlike F_{16}PcZn. Aggregation present before adsorption will be manifested as an L-type curve as we observe with both F_{40}PcZn and F_{52}PcZn.

3.5 Conclusions

Replacement of C-H bonds in phthalocyanines with F and/or *i*-C_3F_7 groups produces catalytically active materials resistant to thermal and oxidative stress with increased solubility, reduced aggregation, and an electron deficient metal center. The solution adsorption and thermal stability of phthalocyanines with the general formula F_nPcZn when n = 16, 40, 52 and 64 and F_{64}PcM when M = Zn, Ru, Cu, Co, Fe and VO was studied on a variety of surfaces in acetone and methylene chloride. Strong, irreversible adsorption of these molecules was observed on the surface of Al_2O_3 and aminated silicas. We also reported aggregation of some of the F_nPcZn (n = 16, 40, 52) as well as an apparent pH sensitivity for some F_{64}PcM (M = VO, Fe, Co, Cu).

Careful analysis of the adsorption isotherms indicated that adsorption was dominated by Lewis acid-base interactions between the electron deficient phthalocyanine metal center and basic moieties on these surfaces. We proposed a mechanism in which the phthalocyanine adsorption occurred face-down by axial coordination of the electron deficient central metal to the electron donating surfaces. Further investigation, beyond the varied electron deficient central metal, involving surfaces of different basicity further confirmed our hypothesis.

Materials characterization by chemical analysis, solution UV/Vis, and solid-state reflectance UV/Vis demonstrated that uniform, monomolecular surfaces were produced for F_{64}PcM adsorbed from acetone. Cofacially oriented bilayers were produced with aggregating F_nPcZn molecules by adsorption from acetone. Substrate-Solvent and Solute-Solvent interactions were evaluated by studies with a coordinating solvent, acetone, and non-coordinating methylene chloride. The change to the non-coordinating solvent resulted in adsorption energies and less ordered multilayer formation. Solution adsorption of phthalocyanines was demonstrated to be an effective means of producing uniform catalytically active solid surfaces.

Appendix A: Supplemental Figures for Phthalocyanine Adsorption Studies

Figure A-1: Adsorption of Zinc Phthalocyanines on SiO_2-NH_2

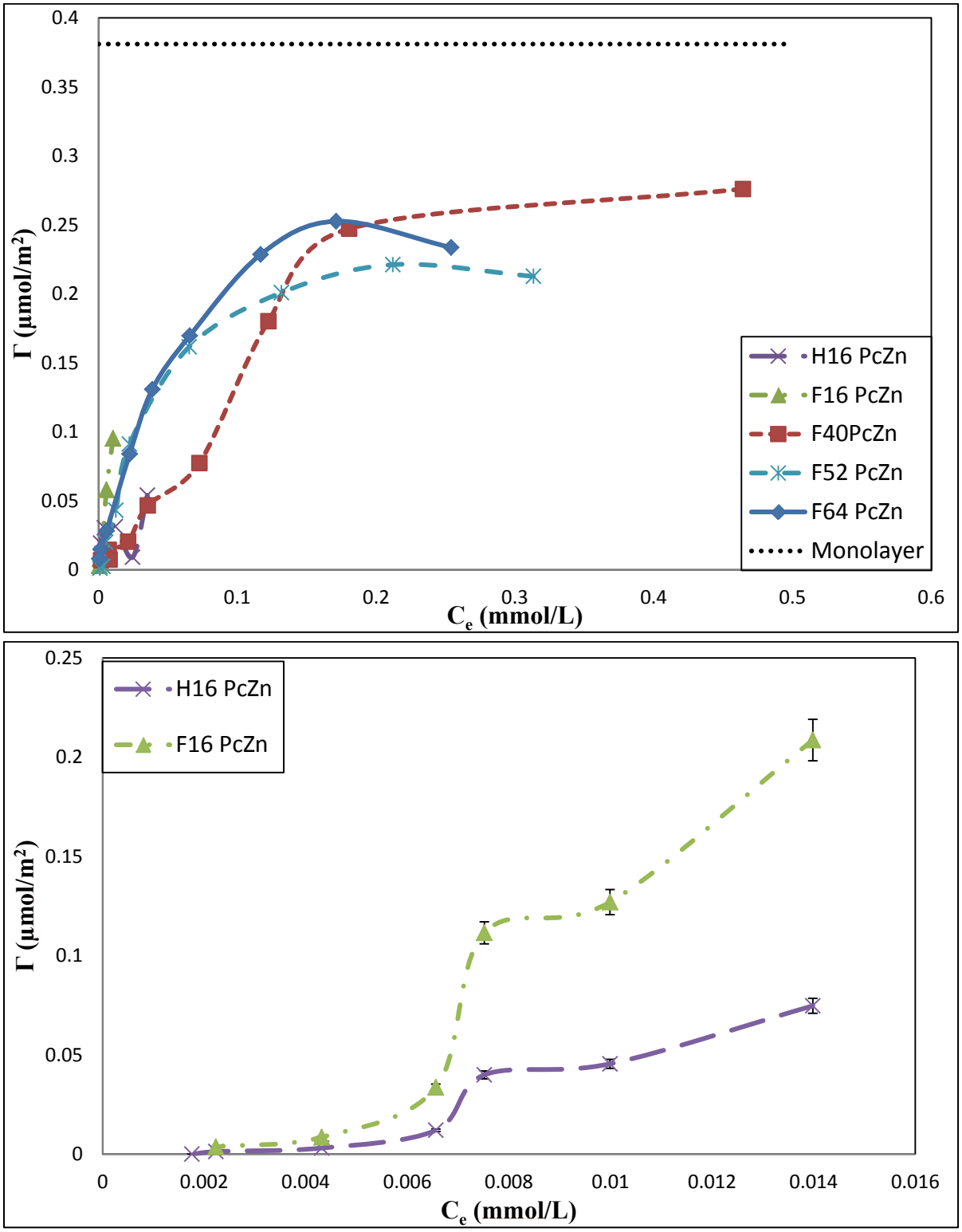

Figure A-1: Adsorption isotherms of zinc phthalocyanines on SiO_2-NH_2 from acetone (top) and a zoomed in overlay of the adsorption of H_{16}PcZn and F_{16}PcZn on SiO_2-NH_2 (bottom). The transition from S-type to L-Type occurs at F_{40}PcZn, indicating that the system adsorption energy is weaker for SiO_2-NH_2 than for Al_2O_3.

Figure A-2: Spectral Changes to $F_{64}PcMs$ in the SiO_2-NH_2/Acetone System

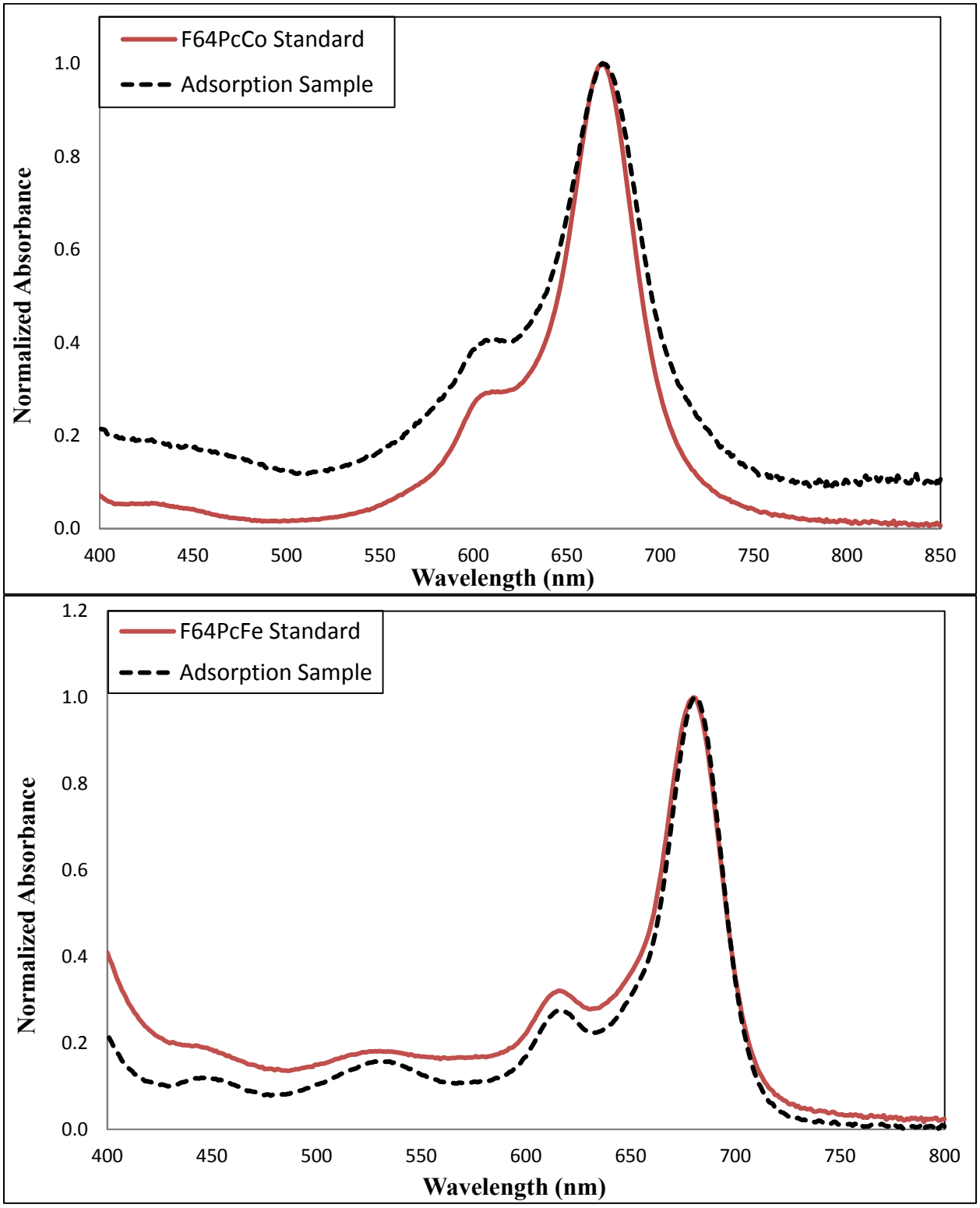

Figure A-2: Spectral changes occur for $F_{64}PcCo$ (top) and $F_{64}PcFe$ (bottom) in the presence of SiO_2-NH_2. Chemical analysis confirmed adsorption to SiO_2-NH_2 occurred for both pcs, but the accuracy of results obtained by UV/Vis was impacted by changes to the Q band in these samples relative to the standard. $F_{64}PcFe$ had an increased absorbance of the Q band while $F_{64}PcCo$ decreased

Figure A-3: Effect of the Central Metal on the Adsorption of $F_{64}PcM$ on SiO_2-NH_2

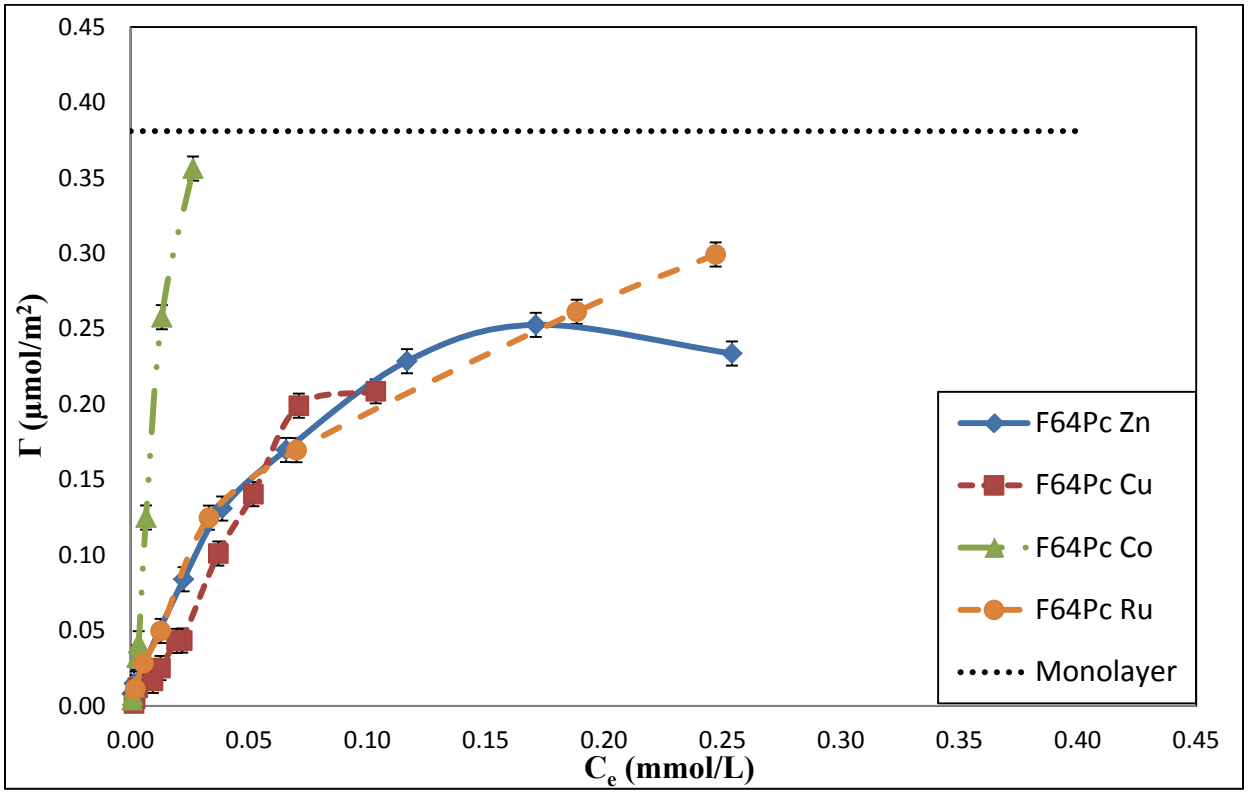

Figure A-3: Overlay demonstrating the effect of the central metal on the adsorption of $F_{64}PcM$ on the surface of SiO_2-NH_2. The points are connected to guide the eyes. Note that the presence of the basic NH_2 caused a change in the UV signal for some phthalocyanines, particularly VO (not shown), Fe (not shown), Co, and Cu. The change from and S-type isotherm with Al_2O_3 to L-type with SiO_2-NH_2 for F64PcCu and F64PcCo may be mostly attributed to spectral changes.

Figure A-4: Solvent Comparison for the Adsorption of $F_{64}PcM$

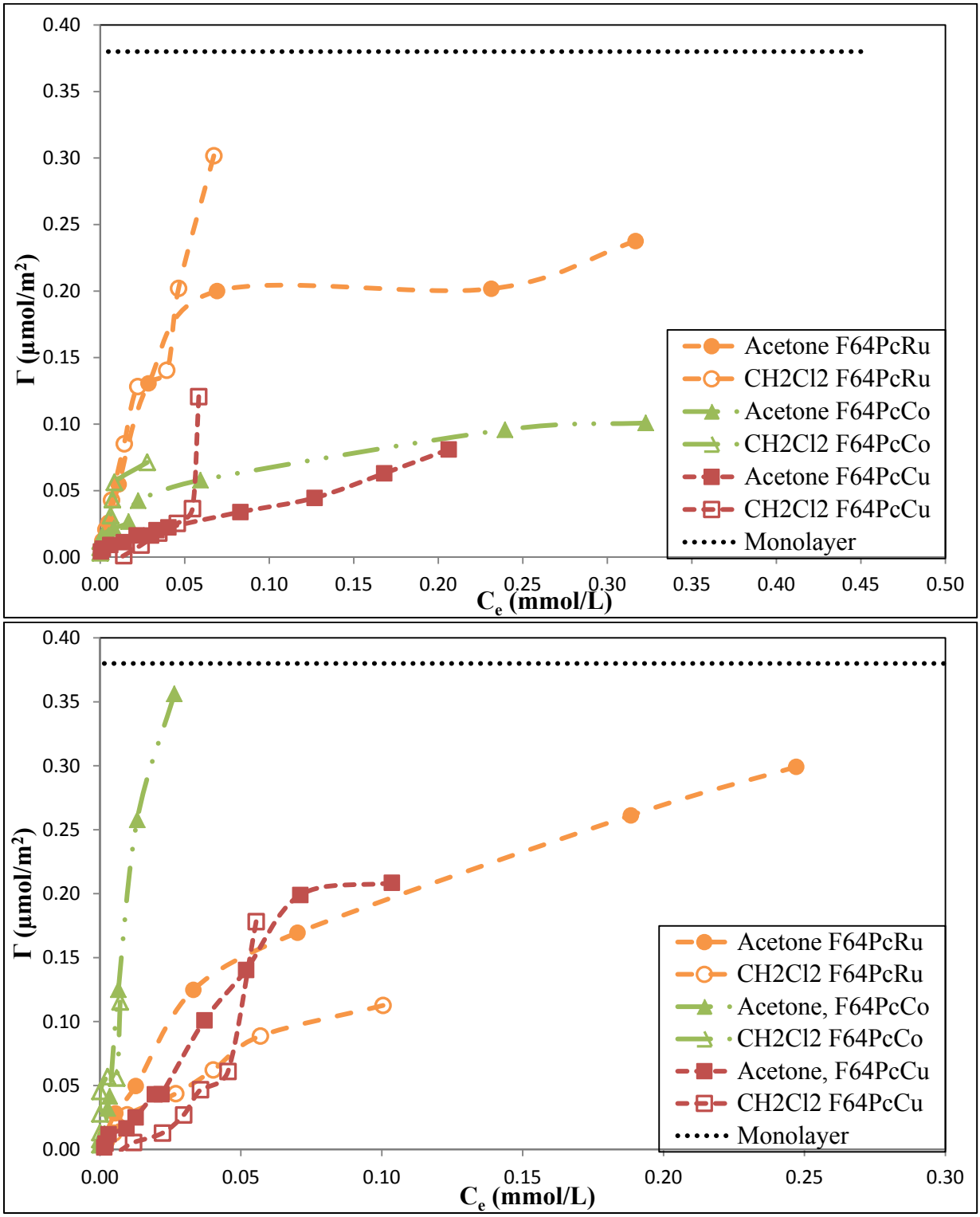

Figure A-4: Comparison of the adsorption of $F_{64}PcMs$ from acetone (closed symbols) and methylene chloride (open symbols) on the surface of Al_2O_3 (Top) and SiO_2-NH_2 (Bottom). The points are connected to guide the eyes. The theoretical Γ_{max} for a closely packed face-down $F_{64}PcM$ monolayer is included for comparison.

Figure A-5: Solution and Reflectance Spectral Comparison for $F_{40}PcZn$

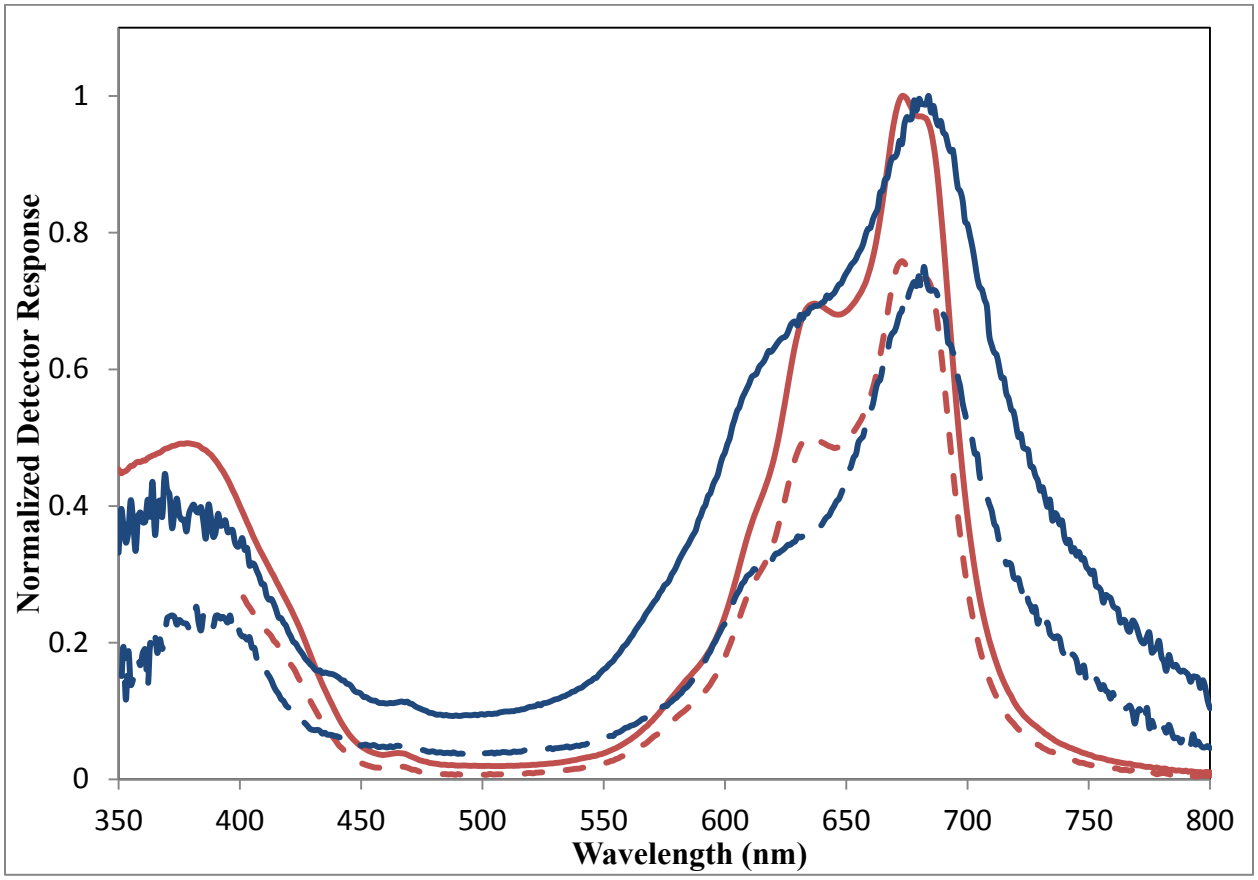

Figure A-5: Comparison of the normalized reflectance (blue double line) and solution (red single line) spectra for $F_{40}PcZn$ on Al_2O_3 at the data point corresponding to a C_e of 28.9 µmol/L (solid lines) and 6.5 µmol/L (dashed lines, 3X the actual response for better comparison). Q-band maxima broadening indicated some aggregation at all Γ, with cofacial aggregation as a contributing factor.

Figure A-6: Solid State UV/Vis Comparison of Adsorbed Phthalocyanines

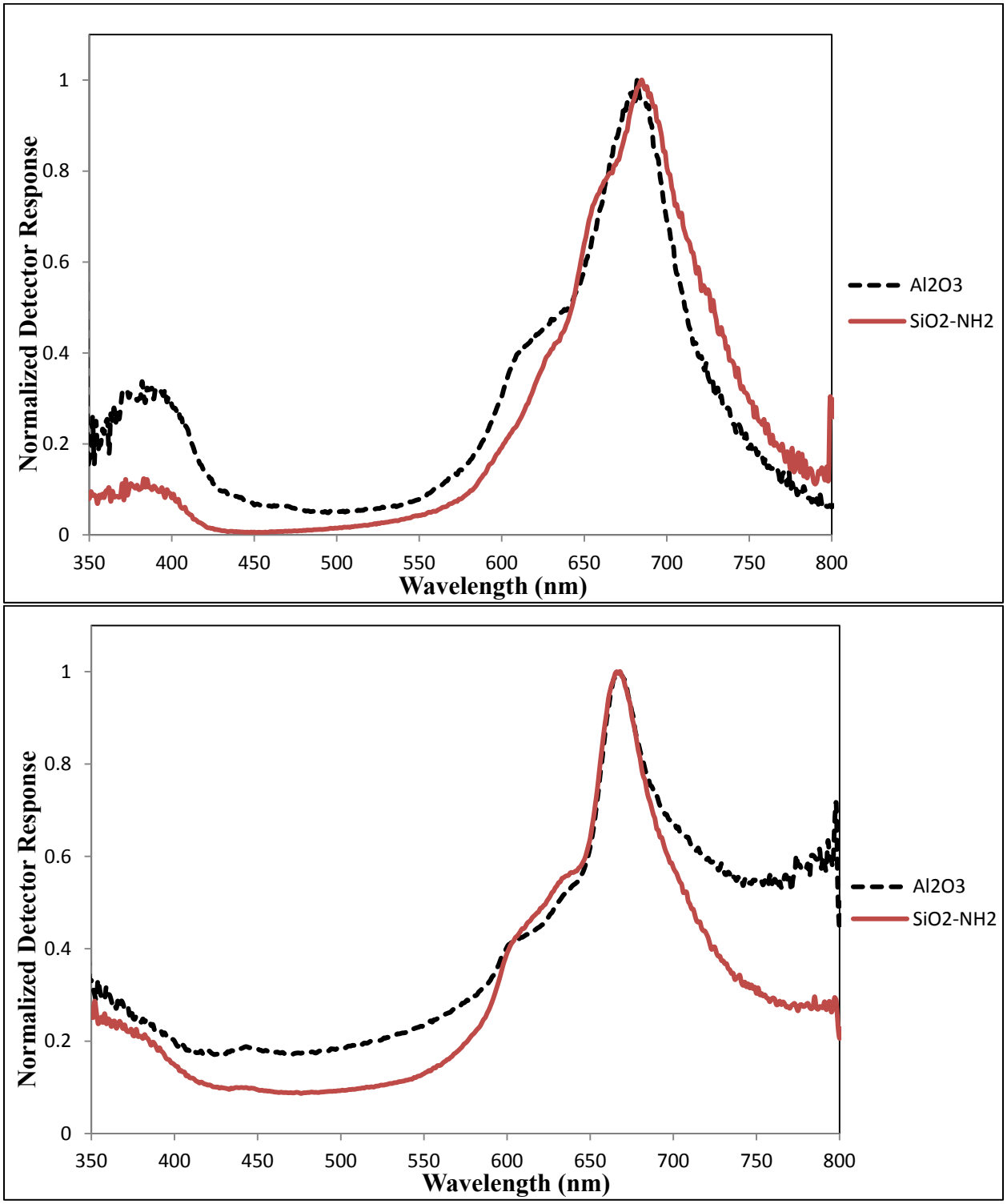

Figure A-6: Comparison of the reflectance UV/Vis spectra for $F_{40}PcZn$ at C_e ~0.008 µmol/m^2 (top) and $F_{16}PcZn$ at C_e ~0.01 µmol/m^2 (bottom) on Al_2O_3 and SiO_2-NH_2. Peak broadening and blue-shifted shoulder peaks indicate aggregation in the solid state. We observed less aggregation in the solid state at low concentrations on the surface of SiO_2-NH_2 despite the high level of dimer present in solution state at the same equilibrium point (Figure 3-19, Figure 3-22).

Appendix B: Thermogravimetric Analysis of Phthalocyanines

Figure B-1: Thermogravimetric Analysis of Zinc Phthalocyanines

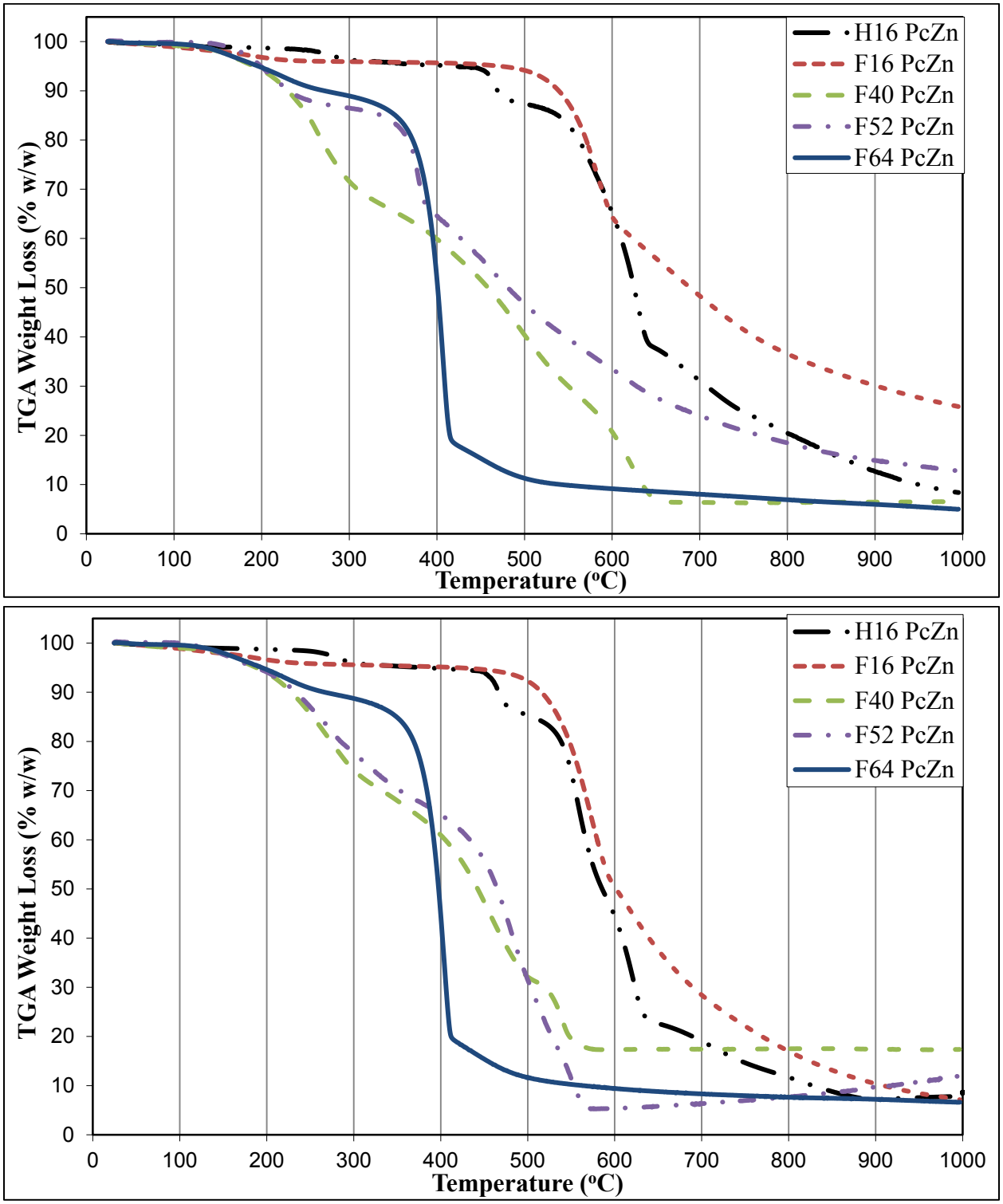

Figure B-1: TGA weight loss curves for zinc phthalocyanines with nitrogen (top) and air (bottom). Weight loss is generally attributed to both degradation and sublimation of the phthalocyanines. Thermal stability appeared best for unsubstituted phthalocyanines, likely due to the lack of bulky functional groups. We noted that F_{64}PcZn was the most susceptible to sublimation. Solids remaining after analysis had color that was consistent with ZnO, with the exception of PcZn in air, which had the color of Zn_3N_2.

Figure B-2: Thermogravimetric Analysis of $F_{64}PcM$

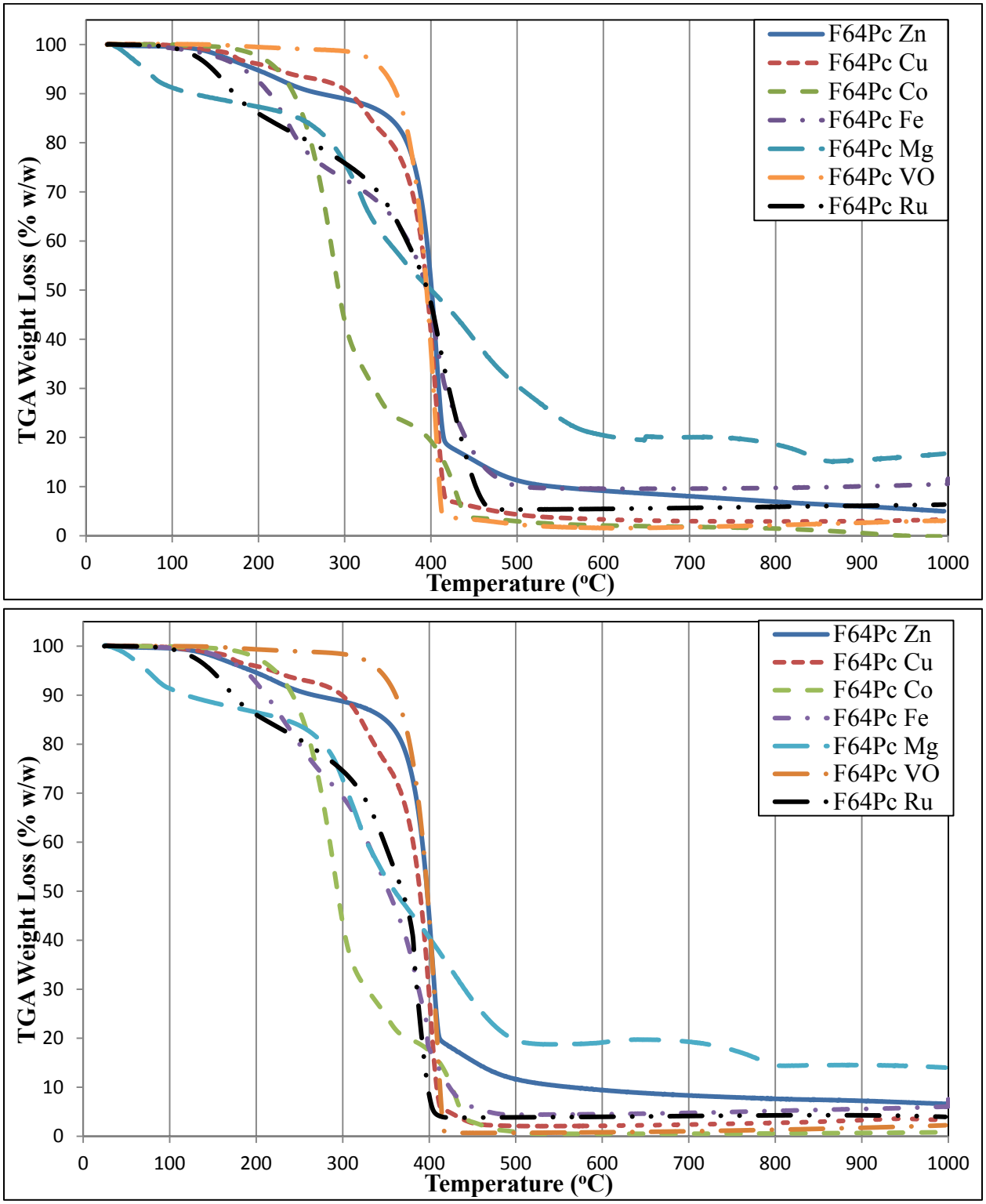

Figure B-2: TGA weight loss curves for $F_{64}PcM$ with nitrogen (top) and air (bottom). Weight loss is generally attributed to both degradation and sublimation of the phthalocyanines. Sublimation appeared to dominate, resulting in similar thermal stability in air and nitrogen for all $F_{64}PcMs$. Any solids remaining after analysis had color that was consistent with the metal oxides, even under nitrogen.

Figure B-3: Thermogravimetric Analysis of F_{16}PcM

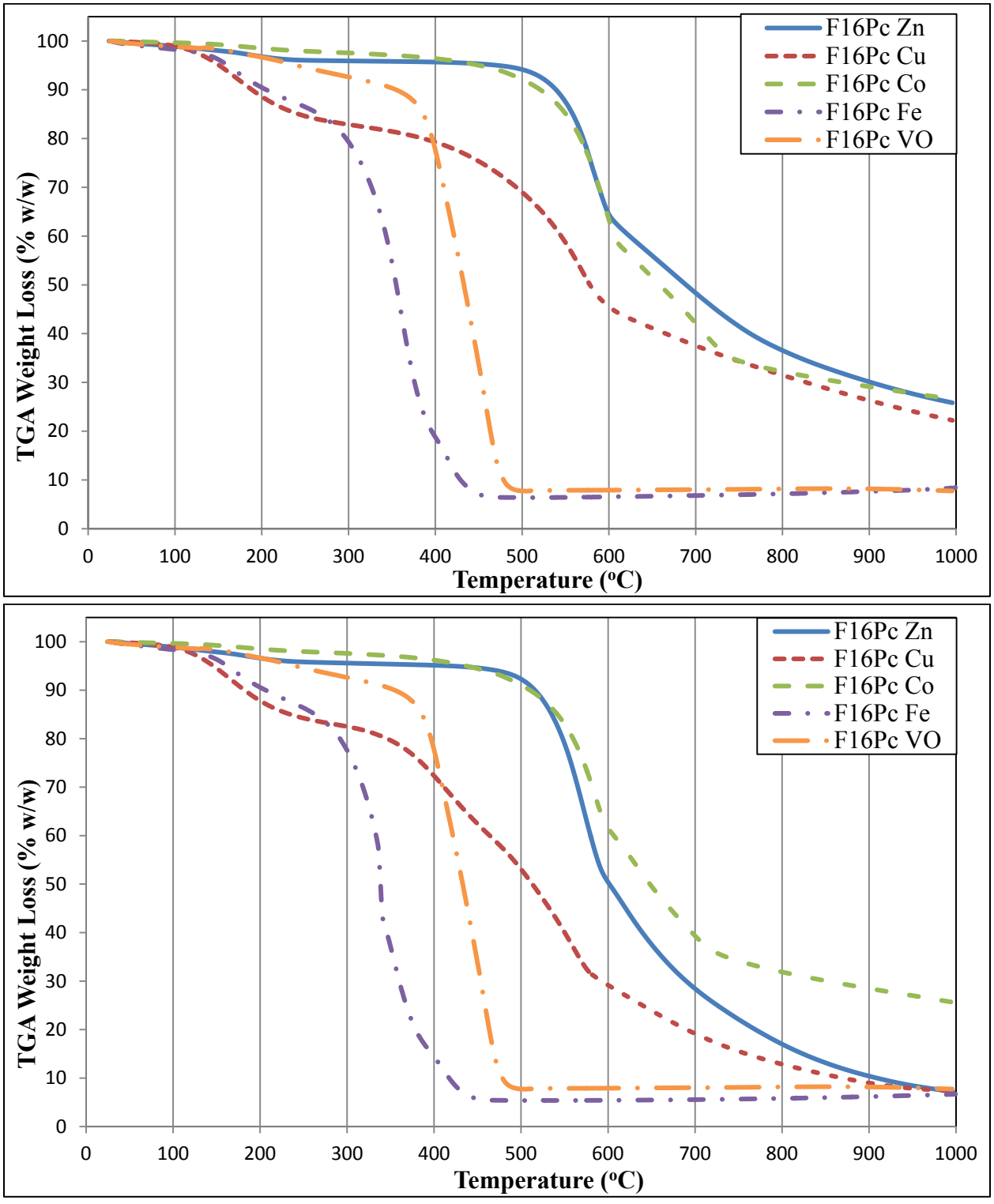

Figure B-3: TGA weight loss curves for F_{16}PcM with nitrogen (top) and air (bottom). Weight loss is generally attributed to both degradation and sublimation of the phthalocyanines. Thermal stability was best with nitrogen, with the greatest temperature change observed for F_{16}PcZn and F_{16}PcCu. Solids remaining after analysis had color that was consistent with the metal oxides, even under nitrogen.

Figure B-4: Thermogravimetric Analysis of Unsubstituted Phthalocyanines

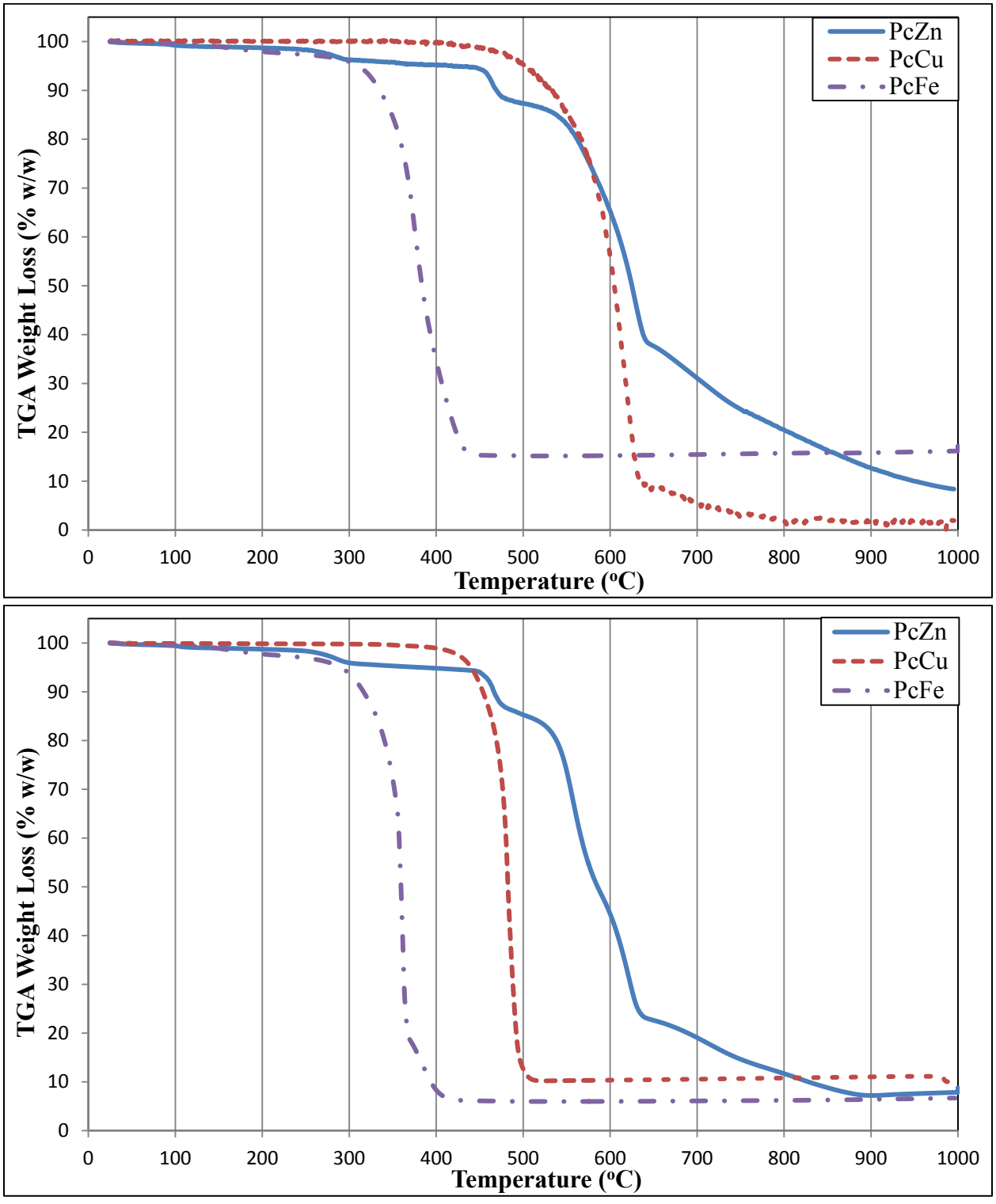

Figure B-4: TGA weight loss curves for unsubstituted phthalocyanines (H_{16}PcM) with nitrogen (top) and air (bottom). Weight loss is generally attributed to both degradation and sublimation of the phthalocyanines. Thermal stability was best with nitrogen. Solids remaining after analysis had color that was consistent with the metal oxides, with the exception of PcZn in air, which had the color of Zn_3N_2.

References

(1) Adamson, W. A.; Gast, A. P. *Physical Chemistry of Surfaces*; 6th Ed. ed.; John Wiley & Sons: New York, 1997.
(2) Housecroft, C. E.; Sharpe, A. G. In *Inorganic Chemistry*; Pearson Education Ltd.: Harlow, 2005, pp 338-381.
(3) Henrich, V. E.; Cox, P. A. *The Surface Science of Metal Oxides*; Cambridge University Press: New York, 1994.
(4) Morterra, C.; Magnacca, G. *Catalysis Today* **1996**, *27*, 497-532.
(5) Frey, N. A.; Peng, S.; Cheng, K.; Sun, S. *Chem. Soc. Rev.* **2009**, *38*, 2532-2542.
(6) Bolis, V. In *Calorimetry and Thermal Methods in Catalysis*; Auroux, A., Ed.; Springer: Berlin, 2013; Vol. 154.
(7) Rouquerol, J.; Avnir, D.; Fairbridge, C. W.; Everett, D. H.; Haynes, J. H.; Pernicone, N.; Ramsay, J. D. F.; Sing, K. S. W.; Unger, K. K. *Pure Appl. Chem.* **1994**, *66*, 1739-1758.
(8) Iler, R. K. *The Chemistry of Silica*; Wiley-Interscience: New York, 1979.
(9) Wan, Y.; Zhao, D. *Chem. Rev.* **2007**, *107*, 2821-2860.
(10) Bernardoni, F. In *Department of Chemistry and Biochemistry*; Seton Hall University: South Orange, NJ, 2010, p 191.
(11) Unger, K. K.; Gimpel, M. G. *J. Chromatogr. A.* **1979**, *180*, 93-102.
(12) Kresge, C. T.; Leonowics, M. E.; Poth, W. J.; Vortulli, J. C.; Beck, J. S. *Nature* **1992**, *359*, 710.
(13) Walcarius, A. *Chem. Soc. Rev.* **2013**, *42*, 4098-4140.
(14) Beck, J. S.; Vartuli, J. C.; Roth, W. J.; Leonowicz, M. E.; Kresge, C. T.; Schmitt, K. D.; Chu, C. T. W.; Olson, D. H.; Sheppard, E. W.; al, e. *J. Am. Chem. Soc.* **1992**, *114*, 10834-10843.
(15) Vartuli, J. C.; Schmitt, K. D.; Kresge, C. T.; Roth, W. J.; Leonowicz, M. E.; McCullen, S. B.; Hellring, S. D.; Beck, J. S.; Schlenker, J. L.; Olson, D. H.; Sheppard, E. W. *Chem. Mater.* **1994**, *6*, 2317-2326.
(16) Sayari, A.; Liu, P.; Kruk, M.; Jaroniec, M. *Chem. Mater.* **1997**, *9*, 2499-2506.
(17) Zhao, D.; Huo, Q.; Feng, J.; Chemelka, B. F.; Stucky, G. *J. Am. Chem. Soc.* **1998**, *120*, 6024-6036.
(18) Bernardoni, F.; Kouba, M.; Fadeev, A. Y. *Chem. Mater.* **2008**, *20*, 382-387.
(19) Yokoi, T.; Ogawa, K.; Lu, D.; Kondo, J. N.; Kubota, Y.; Tatsumi, T. *Chem. Mater.* **2011**, *23*, 2014-2016.
(20) Lowell, S.; Shields, J. E.; Thomas, M. A.; Thommes, M. *Characterization of Porous Solids and Powders: Surface Area, Pore Size and Density*; Springer: Dordrecht, The Netherlands, 2006.
(21) Langmuir, I. *J. Am. Chem. Soc.* **1918**, *40*, 1361-1403.
(22) Gregg, S. J.; Sing, K. S. W. *Adsorption, Surface Area and Porosity*; 2nd ed.; Academic Press: London, 1982.
(23) Brunauer, S.; Emmett, P. H.; Teller, E. *J. Am. Chem. Soc.* **1938**, *60*, 309-319.
(24) Jelinek, L.; Kovats, E. *Langmuir* **1994**, *10*, 4225-4231.
(25) Sing, K. S. W. *Adv. Colloid Interface Sci.* **1998**, *76-77*, 3-11.
(26) Barrett, E. P.; Joyner, L. G.; Halenda, P. P. *J. Am. Chem. Soc.* **1951**, *73*, 373.

(27) Naono, H.; Hakuman, M.; Tanaka, T.; Tamura, N.; Nakai, K. *J. Colloid Interface Sci.* **2000**, *225*, 411-420.
(28) Naono, H.; Hakuman, M. *J. Colloid Interface Sci.* **1991**, *145*, 405-412.
(29) Grunberg, B.; Emmler, T.; Gedat, E.; Shenderovich, I.; Findenegg, G. H.; Limbach, H. H.; Buntkowsky, G. *Chem. Eur. J.* **2004**, *10*, 5689-5696.
(30) Fadeev, A. Y. In *Encyclopedia for Surface and Colloid Science*; 2nd ed.; Somasundaran, P., Ed.; Taylor & Francis: New York, 2006; Vol. 4, p 2854.
(31) Giles, C. H.; MacEwan, T. H.; Nakhwa, S. N.; Smith, D. *J. Chem. Soc.* **1960**, 3973-3993.
(32) Langmuir, I. *Journal of the American Chemical Society* **1917**, *39*, 1848-1906.
(33) Ulman, A. *Chem. Rev.* **1996**, *96*, 1533-1554.
(34) Whitesides, G. M.; Laibinis, P. E. *Langmuir* **1990**, *6*, 87-96.
(35) Schreiber, F. *Prog. Surf. Sci.* **2000**, *65*, 151-256.
(36) Palacin, S. *Adv. Colloid Interface Sci.* **2000**, *87*, 165-181.
(37) Pujari, S. P.; Scheres, L.; Marcelis, A. T. M.; Zhuilhof, H. *Angew. Chem. Int. Ed.* **2014**, *53*, 6322-6356.
(38) Chen, W.; Fadeev, A. Y.; Hsieh, M. C.; Oner, D.; Youngblood, J.; McCarthy, T. J. *Langmuir* **1999**, *15*, 3395-3399.
(39) Fadeev, A. Y.; Kazakevich, Y. V. *Langmuir* **2002**, *18*, 2665-2672.
(40) del Pozo, C.; Corma, A.; Iglesias, M.; Sanchez, F. *Organometallics* **2010**, *29*, 4491-4498.
(41) Gandini, A.; Belgacem, M. N. In *Advances in Polymer Science*; Springer: Berlin, 2015, pp 1-38.
(42) Tripp, C. P.; Hair, M. L. *Langmuir* **1995**, *11*, 1215-1219.
(43) Thompson, M.; Royal Society of Chemistry, 2008; Vol. 29.
(44) McElwee, J.; Helmy, R.; Fadeev, A. Y. *J Collloid Interface Sci.* **2005**, *285*, 551-556.
(45) Bernardoni, F.; Fadeev, A. Y. *J. Colloid Interface Sci.* **2011**, *356*, 690-698.
(46) Kazakevich, Y. V.; Fadeev, A. Y. *Langmuir* **2002**, *18*, 3117-3122.
(47) Young, T. *Phil. Trans. R. Soc. Lond.* **1805**, *95*, 65-87.
(48) Yuan, Y.; Lee, T. R. In *Surface Science Techniques*; Bracco, B. H., B., Ed.; Springer-Verlag: Berlin, 2013; Vol. 51, pp 3-34.
(49) Cassie, A. B. D.; Baxter, S. *S. Trans. Faraday Soc.* **1944**, *40*, 546-551.
(50) Leyden, D. E. *Silanes, Surfaces, and Interfaces*; Gordon and Breach: New York, 1986.
(51) Plueddemann, E. W. *Silane Coupling Agents*; 2nd ed.; Plenum: New York, 1991.
(52) Mittal, K. L. *Silanes and Other Coupling Agents*; VSP: Utrecht, 1992.
(53) Owen, M. J. In *Adhesion Science and Engineering*; Dillard, D. A., Pocius, A. V., Eds.; Elsevier: Amsterdam, 2002; Vol. 2, pp 403-431.
(54) Park, S. E.; Prasetyanto, E. A. In *Organosilanes: Properties, Performance, and Applications*; Wyman, E. B., Skief, M. C., Eds.; Nova Science: New York, 2010, pp 101-131.
(55) Krumpfer, J. W.; Gao, L.; Fadeev, A. Y.; McCarthy, T. J. In *Advances in Silicon Science*; Dvomic, P. R., Owen, M. J., Eds.; Springer: New York, 2012; Vol. 4, pp 95-114.

(56) Shokoohi, S.; Arefazar, A.; Khosrokhavar, R. *J. Reinf. Plast. Compos.* **2008**, *27*, 473-485.
(57) Fadeev, A. Y.; McCarthy, T. J. *Langmuir* **2000**, *16*, 7268-7274.
(58) Haensch, C.; Hoeppener, S.; Schubert, U. S. **2010**, *39*, 2323-2334.
(59) Aristova, V. G.; Zimmer, I. M.; Gorbunov, A. I.; Galitskaya, O. I. *Zh. Fiz. Khim* **1974**, *48*, 134-137.
(60) Aristova, V. G.; Popkov, K. K.; Galashina, M. L. *Kolloidn. Zh.* **1974**, *36*, 123-126.
(61) Aristova, V. G.; Zimmer, I. M.; Gorbunov, A. I.; Zhilenkov, I. V.; Saushkin, V. V. *Doklady Akademii Nauk SSSR* **1980**, *255*, 131-134.
(62) Tertykh, V. A.; Pavlov, V. V. *Adsorp. Adsorb.* **1978**, *6*, 67-75.
(63) Pavlov, V. V.; Guba, G. Y.; Tertykh, V. A.; Chuiko, A. A. *Adsorp. Adsorb.* **1980**, *8*, 35-39.
(64) Li, Y.; Xia, Y.; Xu, D.; Li, G. *J. Polym. Sci., Polym. Chem. Ed.* **1981**, *19*, 3069-3079.
(65) Litvinov, V. M.; Barthel, H.; Weis, J. *Macromolecules* **2002**, *35*, 4356-4364.
(66) Krumpfer, J. W.; McCarthy, T. J. *Langmuir* **2011**, *27*, 11514-11519.
(67) Cohen-Addad, J. P.; Huchot, P.; Jost, P.; Pouchelon, A. *Polymer* **1989**, *30*, 143-146.
(68) Levresse, P.; Feke, D. L.; Manas-Zloczower, I. *Polymer* **1998**, *39*, 3919-3924.
(69) Leger, L.; Hervet, H.; Deruelle, M. In *Adsorption on Silica Surfaces*; Papirer, E., Ed.; Marcel Dekker: New York, 2000; Vol. 90, pp 597-619.
(70) Marinova, K. G.; Christova, D.; Tcholakova, S.; Efremov, E.; Denkov, N. D. *Langmuir* **2005**, *21*, 11729-11737.
(71) Sheka, E.; Natkaniec, I.; Khavryutchenko, V.; Nikitina, E.; Barthel, H.; Weis, J. *Silicon Chem.* **2000**, *1*, 261-279.
(72) Barthel, H.; Nikitina, E. *Silicon Chem.* **2004**, *1*, 261-279.
(73) Smith, J. S.; Borodin, O.; Smith, G. D.; Kober, E. M. *J. Polym. Sci., Part B: Polym. Phys.* **2007**, *45*, 1599-1615.
(74) Voronkov, M. G.; Mileshkevitch, V. P.; Yuzhelevskii, Y. A. *The Siloxane Bond*; Consultants Bureau: New York, 1978.
(75) Brandrup, J.; Immergut, E. H. *Polymer Handbook*; 3 ed.; Wiley: New York, 1989.
(76) Zhuravlev, L. T. *Colloids Surf.* **2000**, *173*, 1-38.
(77) Kozlova, S. A.; Kirik, S. D. *Microporous Mesoporous Mater.* **2010**, *133*, 124-133.
(78) Dubois, L. H.; Zegarski, B. R. *J. Am. Chem. Soc.* **1993**, *115*, 1190-1191.
(79) Grabbe, A.; Michalske, T. A.; Smith, W. L. *J. Phys. Chem.* **1995**, *99*, 4648-4654.
(80) Morrow, B. A.; Cody, I. A. *J. Phys. Chem.* **1976**, *80*, 1995-1998.
(81) Bunker, B. C.; Haaland, D. M.; Michalske, T. A.; Smith, W. L. *Surf. Sci.* **1989**, *222*, 95-118.
(82) McCrate, J. M.; Ekerdt, J. G. *Langmuir* **2013**, *29*, 11868-11875.
(83) Livingston, H. K. *J. Am. Chem. Soc.* **1944**, *66*, 569-573.
(84) Clarkson, S. J.; Semlyen, J. A. *Polymer* **1986**, *27*, 91-95.
(85) Biadasz, A.; Bursa, B.; Barszcz, B.; Bogucki, A.; Laskowska, B.; Graja, A.; Wrobel, D. *Dyes Pigments* **2011**, *89*, 86-92.

(86) Brinkmann, H.; Kelting, C.; Makarov, S.; Tsaryova, O.; Schnurpfeil, G.; Wohrle, D.; Schlettwein, D. *Phys. Status Solidi. A* **2008**, *205*, 409-420.
(87) Riede, M.; Uhrich, C.; Widmer, J.; Timmreck, R.; Wynands, D.; Schwartz, G.; Gnehr, W.-M.; Hildebrandt, D.; Weiss, A.; Jaehyung, H.; Sundarraj, S.; Erk, P.; Pfeiffer, M.; Leo, K. *Adv. Funct. Mater.* **2011**, *21*, 3019-3028.
(88) Ali, H.; van Lier, J. E. *Chem. Rev.* **1999**, *99*, 2379-2450.
(89) Zhao, J.; Huo, L.-H.; Gao, S.; Zhao, H.; Zhao, J.-G.; Li, N. *Sensor Actuat B-Chem* **2007**, *126*, 588-594.
(90) Beveridge, A. C.; Bench, B. A.; Gorun, S. M.; Diebold, G. J. *J. Phys. Chem. B* **2003**, *107*, 5138-5143.
(91) Gaffo, L.; Zucolotto, V.; Cordeiro, M. R.; Moreira, W. C.; Oliveira Jr., O. N.; Cerdeira, F.; Brasil, M. J. S. P. *Thin Solid Films* **2007**, *515*, 7307-7312.
(92) Yoon, S. M.; Song, H. J.; Hwang, I.-C.; Kim, K. S.; Choi, H. C. *Chem. Commun.* **2010**, *46*, 231-233.
(93) Liao, M.-S.; Watts, J. D.; Huang, M.-J.; Gorun, S. M.; Kar, T.; Scheiner, S. *Chem. Theory Comput.* **2005**, *1*, 1201-1210.
(94) de la Torre, G.; Claessens, C. G.; Torres, T. *Chem. Commun.* **2007**, 2000-2015.
(95) Cook, M. J. *J. Mater. Chem.* **1996**, *6*, 677-689.
(96) Nemykin, V. N.; Lukyanets, E. A. *Arkivoc* **2010**, *2010*, 136-208.
(97) Bench, B. A.; Beveridge, A. C.; Sharman, W. M.; Diebold, G. J.; van Lier, J. E.; Gorun, S. M. *Angew. Chem. Int. Edit.* **2002**, *41*, 747-750.
(98) Patel, H. H. In *Department of Chemistry and Biochemistry*; Seton Hall University: South Orange, NJ, 2015.
(99) Pellegrino, G.; Alberti, A.; Condorelli, G. G.; Giannazzo, F.; La Magna, A.; Paoletti, A. M.; Pennesi, G.; Rossi, G.; Zanotti, G. *J. Phys. Chem. C* **2013**, *117*, 11176-11185.
(100) Liao, M.-S.; Watts, J. D.; Gorun, S. M.; Scheiner, S.; Huang, M.-J. *J. Chem. Theory Comput.* **2008**, *7*, 541-563.
(101) Graffius, G.; Benardoni, F.; Fadeev, A. Y. *Langmuir* **2014**, *30*, 14797-14807.
Reprinted (adapted) with permission from Langmuir. Copyright 2014, American Chemical Society.
(102) Gorun, S. M.; Bench, B. A.; Carpenter, G.; Beggs, M. W.; Mague, J. T.; Ensley, H. E. *J. Fluorine Chem.* **1998**, *91*, 37-40.
(103) Gorun, S. M.; Loas, A. I.; Griswold, K.; Lapok, L.; Patel, H. H.; Gerdes, R. In *PCT Int. Appl.*, 2012.
(104) Dini, D.; Hanack, M. In *Phthalocyanines: Properties and Materials*; Kadish, K. M., Smith, K. M., Guilard, R., Eds.; Elsevier: New York, 2004; Vol. 17.
(105) Kubelka, P.; Munk, F. *Z. Tech. Phys.* **1931**, *12*, 593-601.
(106) DZimbeg-Malcic, V.; Barbaric-Mikocevic, Z.; Itric, K. *Technical Gazette* **2011**, *18*, 117-124.
(107) Kelber, J. A. *Surf. Sci. Rep.* **2007**, *62*, 271-303.
(108) Gouterman, M. In *The Porphyrins*; Dophin, D., Ed.; Academic Press: New York, 1978; Vol. 3, pp 1-165.
(109) Ghani, F.; Kristen, J.; Riegler, H. *J. Chem. Eng. Data* **2012**, *57*, 439-449.
(110) McKeown, N. B. *Phthalocyanine Materials: Synthesis, Structure and Function*; Cambridge University Press: New York, 1998.

(111) Leznoff, C. C.; Lever, A. B. P. In *Phthalocyanines: Properties and Applications*; Wiley-Interscience: New York, 1993; Vol. 4.
(112) Keizer, S. P.; Mack, J.; Bench, B. A.; Gorun, S. M.; Stillman, M. J. *J. Am. Chem. Soc.* **2003**, *125*, 7067-7085.
(113) Liao, M.-S.; Watts, J. D.; Gorun, S. M.; Scheiner, S.; Huang, M.-J. *J. Chem. Theory Comput.* **2008**, *7*, 541-563.
(114) Liao, M.-S.; Kar, T.; Gorun, S. M.; Scheiner, S. *Inorg. Chem.* **2004**, *43*, 7151-7161.
(115) Rawling, T.; McDonagh, A. *Coord. Chem. Rev.* **2007**, *251*, 1128-1157.
(116) Liao, M.-S.; Scheiner, S. *J Comput Chem* **2002**, *23*, 1391-1403.
(117) Kameyama, K.; Morisue, M.; Satake, A.; Kobuke, Y. *Angew. Chem. Int. Ed.* **2005**, *44*, 4763-4766.
(118) Cammidge, A. N.; Berber, G.; Chambrier, I.; Hough, P. W.; Cook, M. J. *Tetrahedron* **2005**, *61*, 4067-4074.
(119) Nazeeruddin, M. K.; Humphry-Baker, R.; M., G.; Murrer, B. A. *Chem. Commun.* **1998**, 719-720.
(120) Morisue, M.; Kobuke, Y. *Chem. Eur. J.* **2008**, *14*, 4993-5000.
(121) Huc, V.; Armand, F.; Bourgoin, J. P.; Palacin, S. *Langmuir* **2001**, *17*, 1928-1935.
(122) Aldrich; Vol. 2016.
(123) Bench, B. A.; Brennessel, W. W.; Lee, H.-J.; Gorun, S. M. *Angew. Chem. Int. Ed.* **2002**, *41*, 750-755.
(124) Zaki, M. I.; Hasan, M. A.; Al-Sagheer, F. A.; Pasupulety, L. *Langmuir* **2000**, *16*, 430-436.
(125) Schlettwein, D.; Graaf, H.; Meyer, J.-P.; Oekermann, T.; Jaeger, N. I. *J. Phys. Chem. B* **1999**, *103*, 3078-3086.

Title: Preparation of Chiral Mesoporous Materials with Helicity Perfectly Controlled

Author: Toshiyuki Yokoi, Kyohei Ogawa, Daling Lu, et al

Publication: Chemistry of Materials

Publisher: American Chemical Society

Date: Apr 1, 2011

PERMISSION/LICENSE IS GRANTED FOR YOUR ORDER AT NO CHARGE

This type of permission/license, instead of the standard Terms & Conditions, is sent to you because no fee is being charged for your order. Please note the following:

- Permission is granted for your request in both print and electronic formats, and translations.
- If figures and/or tables were requested, they may be adapted or used in part.
- Please print this page for your records and send a copy of it to your publisher/graduate school.
- Appropriate credit for the requested material should be given as follows: "Reprinted (adapted) with permission from (COMPLETE REFERENCE CITATION). Copyright (YEAR) American Chemical Society." Insert appropriate information in place of the capitalized words.
- One-time permission is granted only for the use specified in your request. No additional uses are granted (such as derivative works or other editions). For any other uses, please submit a new request.

If credit is given to another source for the material you requested, permission must be obtained from that source.

BACK | CLOSE WINDOW

Title: Wet chemical approaches to the characterization of organic surfaces: self-assembled monolayers, wetting, and the physical-organic chemistry of the solid-liquid interface

Author: George M. Whitesides, Paul E. Laibinis

Publication: Langmuir

Publisher: American Chemical Society

Date: Jan 1, 1990

PERMISSION/LICENSE IS GRANTED FOR YOUR ORDER AT NO CHARGE

This type of permission/license, instead of the standard Terms & Conditions, is sent to you because no fee is being charged for your order. Please note the following:

- Permission is granted for your request in both print and electronic formats, and translations.
- If figures and/or tables were requested, they may be adapted or used in part.
- Please print this page for your records and send a copy of it to your publisher/graduate school.
- Appropriate credit for the requested material should be given as follows: "Reprinted (adapted) with permission from (COMPLETE REFERENCE CITATION). Copyright (YEAR) American Chemical Society." Insert appropriate information in place of the capitalized words.
- One-time permission is granted only for the use specified in your request. No additional uses are granted (such as derivative works or other editions). For any other uses, please submit a new request.

If credit is given to another source for the material you requested, permission must be obtained from that source.

ELSEVIER LICENSE
TERMS AND CONDITIONS

Apr 12, 2016

This is a License Agreement between Gabriel C Graffius ("You") and Elsevier ("Elsevier") provided by Copyright Clearance Center ("CCC"). The license consists of your order details, the terms and conditions provided by Elsevier, and the payment terms and conditions.

All payments must be made in full to CCC. For payment instructions, please see information listed at the bottom of this form.

Supplier	Elsevier Limited The Boulevard,Langford Lane Kidlington,Oxford,OX5 1GB,UK
Registered Company Number	1982084
Customer name	Gabriel C Graffius
Customer address	77 Claridge Pl COLONIA, NJ 07067
License number	3846481091207
License date	Apr 12, 2016
Licensed content publisher	Elsevier
Licensed content publication	Journal of Colloid and Interface Science
Licensed content title	Adsorption and wetting characterization of hydrophobic SBA-15 silicas
Licensed content author	Frank Bernardoni,Alexander Y. Fadeev
Licensed content date	15 April 2011
Licensed content volume number	356
Licensed content issue number	2
Number of pages	9
Start Page	690
End Page	698
Type of Use	reuse in a thesis/dissertation
Intended publisher of new work	other
Portion	figures/tables/illustrations
Number of figures/tables/illustrations	3
Format	both print and electronic
Are you the author of this Elsevier article?	No
Will you be translating?	No

Original figure numbers	Figures 4, 5, 7
Title of your thesis/dissertation	Functionalization of Metal Oxide Surfaces through Chemical Reactions and Physical Adsorption
Expected completion date	Apr 2016
Estimated size (number of pages)	170
Elsevier VAT number	GB 494 6272 12
Permissions price	0.00 USD
VAT/Local Sales Tax	0.00 USD / 0.00 GBP
Total	0.00 USD
Terms and Conditions	

INTRODUCTION

1. The publisher for this copyrighted material is Elsevier. By clicking "accept" in connection with completing this licensing transaction, you agree that the following terms and conditions apply to this transaction (along with the Billing and Payment terms and conditions established by Copyright Clearance Center, Inc. ("CCC"), at the time that you opened your Rightslink account and that are available at any time at http://myaccount.copyright.com).

GENERAL TERMS

2. Elsevier hereby grants you permission to reproduce the aforementioned material subject to the terms and conditions indicated.
3. Acknowledgement: If any part of the material to be used (for example, figures) has appeared in our publication with credit or acknowledgement to another source, permission must also be sought from that source. If such permission is not obtained then that material may not be included in your publication/copies. Suitable acknowledgement to the source must be made, either as a footnote or in a reference list at the end of your publication, as follows:
"Reprinted from Publication title, Vol /edition number, Author(s), Title of article / title of chapter, Pages No., Copyright (Year), with permission from Elsevier [OR APPLICABLE SOCIETY COPYRIGHT OWNER]." Also Lancet special credit - "Reprinted from The Lancet, Vol. number, Author(s), Title of article, Pages No., Copyright (Year), with permission from Elsevier."
4. Reproduction of this material is confined to the purpose and/or media for which permission is hereby given.
5. Altering/Modifying Material: Not Permitted. However figures and illustrations may be altered/adapted minimally to serve your work. Any other abbreviations, additions, deletions and/or any other alterations shall be made only with prior written authorization of Elsevier Ltd. (Please contact Elsevier at permissions@elsevier.com)
6. If the permission fee for the requested use of our material is waived in this instance, please be advised that your future requests for Elsevier materials may attract a fee.
7. Reservation of Rights: Publisher reserves all rights not specifically granted in the combination of (i) the license details provided by you and accepted in the course of this licensing transaction, (ii) these terms and conditions and (iii) CCC's Billing and Payment terms and conditions.
8. License Contingent Upon Payment: While you may exercise the rights licensed immediately upon issuance of the license at the end of the licensing process for the transaction, provided that you have disclosed complete and accurate details of your proposed use, no license is finally effective unless and until full payment is received from you (either by publisher or by CCC) as provided in CCC's Billing and Payment terms and conditions. If

full payment is not received on a timely basis, then any license preliminarily granted shall be deemed automatically revoked and shall be void as if never granted. Further, in the event that you breach any of these terms and conditions or any of CCC's Billing and Payment terms and conditions, the license is automatically revoked and shall be void as if never granted. Use of materials as described in a revoked license, as well as any use of the materials beyond the scope of an unrevoked license, may constitute copyright infringement and publisher reserves the right to take any and all action to protect its copyright in the materials.

9. Warranties: Publisher makes no representations or warranties with respect to the licensed material.

10. Indemnity: You hereby indemnify and agree to hold harmless publisher and CCC, and their respective officers, directors, employees and agents, from and against any and all claims arising out of your use of the licensed material other than as specifically authorized pursuant to this license.

11. No Transfer of License: This license is personal to you and may not be sublicensed, assigned, or transferred by you to any other person without publisher's written permission.

12. No Amendment Except in Writing: This license may not be amended except in a writing signed by both parties (or, in the case of publisher, by CCC on publisher's behalf).

13. Objection to Contrary Terms: Publisher hereby objects to any terms contained in any purchase order, acknowledgment, check endorsement or other writing prepared by you, which terms are inconsistent with these terms and conditions or CCC's Billing and Payment terms and conditions. These terms and conditions, together with CCC's Billing and Payment terms and conditions (which are incorporated herein), comprise the entire agreement between you and publisher (and CCC) concerning this licensing transaction. In the event of any conflict between your obligations established by these terms and conditions and those established by CCC's Billing and Payment terms and conditions, these terms and conditions shall control.

14. Revocation: Elsevier or Copyright Clearance Center may deny the permissions described in this License at their sole discretion, for any reason or no reason, with a full refund payable to you. Notice of such denial will be made using the contact information provided by you. Failure to receive such notice will not alter or invalidate the denial. In no event will Elsevier or Copyright Clearance Center be responsible or liable for any costs, expenses or damage incurred by you as a result of a denial of your permission request, other than a refund of the amount(s) paid by you to Elsevier and/or Copyright Clearance Center for denied permissions.

LIMITED LICENSE

The following terms and conditions apply only to specific license types:

15. **Translation**: This permission is granted for non-exclusive world **English** rights only unless your license was granted for translation rights. If you licensed translation rights you may only translate this content into the languages you requested. A professional translator must perform all translations and reproduce the content word for word preserving the integrity of the article.

16. **Posting licensed content on any Website**: The following terms and conditions apply as follows: Licensing material from an Elsevier journal: All content posted to the web site must maintain the copyright information line on the bottom of each image; A hyper-text must be included to the Homepage of the journal from which you are licensing at http://www.sciencedirect.com/science/journal/xxxxx or the Elsevier homepage for books at http://www.elsevier.com; Central Storage: This license does not include permission for a scanned version of the material to be stored in a central repository such as that provided by Heron/XanEdu.

Licensing material from an Elsevier book: A hyper-text link must be included to the Elsevier homepage at http://www.elsevier.com . All content posted to the web site must maintain the copyright information line on the bottom of each image.

Posting licensed content on Electronic reserve: In addition to the above the following clauses are applicable: The web site must be password-protected and made available only to bona fide students registered on a relevant course. This permission is granted for 1 year only. You may obtain a new license for future website posting.

17. **For journal authors:** the following clauses are applicable in addition to the above:

Preprints:

A preprint is an author's own write-up of research results and analysis, it has not been peer-reviewed, nor has it had any other value added to it by a publisher (such as formatting, copyright, technical enhancement etc.).

Authors can share their preprints anywhere at any time. Preprints should not be added to or enhanced in any way in order to appear more like, or to substitute for, the final versions of articles however authors can update their preprints on arXiv or RePEc with their Accepted Author Manuscript (see below).

If accepted for publication, we encourage authors to link from the preprint to their formal publication via its DOI. Millions of researchers have access to the formal publications on ScienceDirect, and so links will help users to find, access, cite and use the best available version. Please note that Cell Press, The Lancet and some society-owned have different preprint policies. Information on these policies is available on the journal homepage.

Accepted Author Manuscripts: An accepted author manuscript is the manuscript of an article that has been accepted for publication and which typically includes author-incorporated changes suggested during submission, peer review and editor-author communications.

Authors can share their accepted author manuscript:

- immediately
  - via their non-commercial person homepage or blog
  - by updating a preprint in arXiv or RePEc with the accepted manuscript
  - via their research institute or institutional repository for internal institutional uses or as part of an invitation-only research collaboration work-group
  - directly by providing copies to their students or to research collaborators for their personal use
  - for private scholarly sharing as part of an invitation-only work group on commercial sites with which Elsevier has an agreement
- after the embargo period
  - via non-commercial hosting platforms such as their institutional repository
  - via commercial sites with which Elsevier has an agreement

In all cases accepted manuscripts should:

- link to the formal publication via its DOI
- bear a CC-BY-NC-ND license - this is easy to do
- if aggregated with other manuscripts, for example in a repository or other site, be shared in alignment with our hosting policy not be added to or enhanced in any way to appear more like, or to substitute for, the published journal article.

Published journal article (JPA): A published journal article (PJA) is the definitive final

record of published research that appears or will appear in the journal and embodies all value-adding publishing activities including peer review co-ordination, copy-editing, formatting, (if relevant) pagination and online enrichment.
Policies for sharing publishing journal articles differ for subscription and gold open access articles:
Subscription Articles: If you are an author, please share a link to your article rather than the full-text. Millions of researchers have access to the formal publications on ScienceDirect, and so links will help your users to find, access, cite, and use the best available version.
Theses and dissertations which contain embedded PJAs as part of the formal submission can be posted publicly by the awarding institution with DOI links back to the formal publications on ScienceDirect.
If you are affiliated with a library that subscribes to ScienceDirect you have additional private sharing rights for others' research accessed under that agreement. This includes use for classroom teaching and internal training at the institution (including use in course packs and courseware programs), and inclusion of the article for grant funding purposes.
Gold Open Access Articles: May be shared according to the author-selected end-user license and should contain a CrossMark logo, the end user license, and a DOI link to the formal publication on ScienceDirect.
Please refer to Elsevier's posting policy for further information.
18. **For book authors** the following clauses are applicable in addition to the above: Authors are permitted to place a brief summary of their work online only. You are not allowed to download and post the published electronic version of your chapter, nor may you scan the printed edition to create an electronic version. **Posting to a repository:** Authors are permitted to post a summary of their chapter only in their institution's repository.
19. **Thesis/Dissertation**: If your license is for use in a thesis/dissertation your thesis may be submitted to your institution in either print or electronic form. Should your thesis be published commercially, please reapply for permission. These requirements include permission for the Library and Archives of Canada to supply single copies, on demand, of the complete thesis and include permission for Proquest/UMI to supply single copies, on demand, of the complete thesis. Should your thesis be published commercially, please reapply for permission. Theses and dissertations which contain embedded PJAs as part of the formal submission can be posted publicly by the awarding institution with DOI links back to the formal publications on ScienceDirect.

Elsevier Open Access Terms and Conditions
You can publish open access with Elsevier in hundreds of open access journals or in nearly 2000 established subscription journals that support open access publishing. Permitted third party re-use of these open access articles is defined by the author's choice of Creative Commons user license. See our open access license policy for more information.
Terms & Conditions applicable to all Open Access articles published with Elsevier:
Any reuse of the article must not represent the author as endorsing the adaptation of the article nor should the article be modified in such a way as to damage the author's honour or reputation. If any changes have been made, such changes must be clearly indicated.
The author(s) must be appropriately credited and we ask that you include the end user license and a DOI link to the formal publication on ScienceDirect.
If any part of the material to be used (for example, figures) has appeared in our publication with credit or acknowledgement to another source it is the responsibility of the user to ensure their reuse complies with the terms and conditions determined by the rights holder.
Additional Terms & Conditions applicable to each Creative Commons user license:
CC BY: The CC-BY license allows users to copy, to create extracts, abstracts and new

works from the Article, to alter and revise the Article and to make commercial use of the Article (including reuse and/or resale of the Article by commercial entities), provided the user gives appropriate credit (with a link to the formal publication through the relevant DOI), provides a link to the license, indicates if changes were made and the licensor is not represented as endorsing the use made of the work. The full details of the license are available at http://creativecommons.org/licenses/by/4.0.

CC BY NC SA: The CC BY-NC-SA license allows users to copy, to create extracts, abstracts and new works from the Article, to alter and revise the Article, provided this is not done for commercial purposes, and that the user gives appropriate credit (with a link to the formal publication through the relevant DOI), provides a link to the license, indicates if changes were made and the licensor is not represented as endorsing the use made of the work. Further, any new works must be made available on the same conditions. The full details of the license are available at http://creativecommons.org/licenses/by-nc-sa/4.0.

CC BY NC ND: The CC BY-NC-ND license allows users to copy and distribute the Article, provided this is not done for commercial purposes and further does not permit distribution of the Article if it is changed or edited in any way, and provided the user gives appropriate credit (with a link to the formal publication through the relevant DOI), provides a link to the license, and that the licensor is not represented as endorsing the use made of the work. The full details of the license are available at http://creativecommons.org/licenses/by-nc-nd/4.0.

Any commercial reuse of Open Access articles published with a CC BY NC SA or CC BY NC ND license requires permission from Elsevier and will be subject to a fee.

Commercial reuse includes:

- Associating advertising with the full text of the Article
- Charging fees for document delivery or access
- Article aggregation
- Systematic distribution via e-mail lists or share buttons

Posting or linking by commercial companies for use by customers of those companies.

20. **Other Conditions**:

v1.8

Questions? customercare@copyright.com or +1-855-239-3415 (toll free in the US) or +1-978-646-2777.

ROYAL SOCIETY OF CHEMISTRY LICENSE TERMS AND CONDITIONS

Apr 12, 2016

This Agreement between Gabriel C Graffius ("You") and Royal Society of Chemistry ("Royal Society of Chemistry") consists of your license details and the terms and conditions provided by Royal Society of Chemistry and Copyright Clearance Center.

License Number	3846480812337
License date	Apr 12, 2016
Licensed Content Publisher	Royal Society of Chemistry
Licensed Content Publication	Journal of the Chemical Society
Licensed Content Title	786. Studies in adsorption. Part XI. A system of classification of solution adsorption isotherms, and its use in diagnosis of adsorption mechanisms and in measurement of specific surface areas of solids
Licensed Content Author	C. H. Giles,T. H. MacEwan,S. N. Nakhwa,D. Smith
Licensed Content Date	Dec 31, 1969
Licensed Content Issue Number	0
Type of Use	Thesis/Dissertation
Requestor type	academic/educational
Portion	figures/tables/images
Number of figures/tables/images	1
Format	print and electronic
Distribution quantity	5
Will you be translating?	no
Order reference number	None
Title of the thesis/dissertation	Functionalization of Metal Oxide Surfaces through Chemical Reactions and Physical Adsorption
Expected completion date	Apr 2016
Estimated size	170
Requestor Location	Gabriel C Graffius 77 Claridge Pl COLONIA, NJ 07067 United States Attn: Gabriel C Graffius
Billing Type	Invoice
Billing Address	Gabriel C Graffius 77 Claridge Pl

COLONIA, NJ 07067
United States
Attn: Gabriel C Graffius

Total 0.00 USD

Terms and Conditions

This License Agreement is between {Requestor Name} ("You") and The Royal Society of Chemistry ("RSC") provided by the Copyright Clearance Center ("CCC"). The license consists of your order details, the terms and conditions provided by the Royal Society of Chemistry, and the payment terms and conditions.

RSC / TERMS AND CONDITIONS

INTRODUCTION

The publisher for this copyrighted material is The Royal Society of Chemistry. By clicking "accept" in connection with completing this licensing transaction, you agree that the following terms and conditions apply to this transaction (along with the Billing and Payment terms and conditions established by CCC, at the time that you opened your RightsLink account and that are available at any time at .

LICENSE GRANTED

The RSC hereby grants you a non-exclusive license to use the aforementioned material anywhere in the world subject to the terms and conditions indicated herein. Reproduction of the material is confined to the purpose and/or media for which permission is hereby given.

RESERVATION OF RIGHTS

The RSC reserves all rights not specifically granted in the combination of (i) the license details provided by your and accepted in the course of this licensing transaction; (ii) these terms and conditions; and (iii) CCC's Billing and Payment terms and conditions.

REVOCATION

The RSC reserves the right to revoke this license for any reason, including, but not limited to, advertising and promotional uses of RSC content, third party usage, and incorrect source figure attribution.

THIRD-PARTY MATERIAL DISCLAIMER

If part of the material to be used (for example, a figure) has appeared in the RSC publication with credit to another source, permission must also be sought from that source. If the other source is another RSC publication these details should be included in your RightsLink request. If the other source is a third party, permission must be obtained from the third party. The RSC disclaims any responsibility for the reproduction you make of items owned by a third party.

PAYMENT OF FEE

If the permission fee for the requested material is waived in this instance, please be advised that any future requests for the reproduction of RSC materials may attract a fee.

ACKNOWLEDGEMENT

The reproduction of the licensed material must be accompanied by the following acknowledgement:

Reproduced ("Adapted" or "in part") from {Reference Citation} (or Ref XX) with permission of The Royal Society of Chemistry.

If the licensed material is being reproduced from New Journal of Chemistry (NJC), Photochemical & Photobiological Sciences (PPS) or Physical Chemistry Chemical Physics (PCCP) you must include one of the following acknowledgements:

For figures originally published in NJC:

Reproduced ("Adapted" or "in part") from {Reference Citation} (or Ref XX) with permission of The Royal Society of Chemistry (RSC) on behalf of the European Society for Photobiology, the European Photochemistry Association and the RSC.

For figures originally published in PPS:
Reproduced ("Adapted" or "in part") from {Reference Citation} (or Ref XX) with permission of The Royal Society of Chemistry (RSC) on behalf of the Centre National de la Recherche Scientifique (CNRS) and the RSC.
For figures originally published in PCCP:
Reproduced ("Adapted" or "in part") from {Reference Citation} (or Ref XX) with permission of the PCCP Owner Societies.

HYPERTEXT LINKS

With any material which is being reproduced in electronic form, you must include a hypertext link to the original RSC article on the RSC's website. The recommended form for the hyperlink is http://dx.doi.org/10.1039/DOI suffix, for example in the link http://dx.doi.org/10.1039/b110420a the DOI suffix is 'b110420a'. To find the relevant DOI suffix for the RSC article in question, go to the Journals section of the website and locate the article in the list of papers for the volume and issue of your specific journal. You will find the DOI suffix quoted there.

LICENSE CONTINGENT ON PAYMENT

While you may exercise the rights licensed immediately upon issuance of the license at the end of the licensing process for the transaction, provided that you have disclosed complete and accurate details of your proposed use, no license is finally effective unless and until full payment is received from you (by CCC) as provided in CCC's Billing and Payment terms and conditions. If full payment is not received on a timely basis, then any license preliminarily granted shall be deemed automatically revoked and shall be void as if never granted. Further, in the event that you breach any of these terms and conditions or any of CCC's Billing and Payment terms and conditions, the license is automatically revoked and shall be void as if never granted. Use of materials as described in a revoked license, as well as any use of the materials beyond the scope of an unrevoked license, may constitute copyright infringement and the RSC reserves the right to take any and all action to protect its copyright in the materials.

WARRANTIES

The RSC makes no representations or warranties with respect to the licensed material.

INDEMNITY

You hereby indemnify and agree to hold harmless the RSC and the CCC, and their respective officers, directors, trustees, employees and agents, from and against any and all claims arising out of your use of the licensed material other than as specifically authorized pursuant to this licence.

NO TRANSFER OF LICENSE

This license is personal to you or your publisher and may not be sublicensed, assigned, or transferred by you to any other person without the RSC's written permission.

NO AMENDMENT EXCEPT IN WRITING

This license may not be amended except in a writing signed by both parties (or, in the case of "Other Conditions, v1.2", by CCC on the RSC's behalf).

OBJECTION TO CONTRARY TERMS

You hereby acknowledge and agree that these terms and conditions, together with CCC's Billing and Payment terms and conditions (which are incorporated herein), comprise the entire agreement between you and the RSC (and CCC) concerning this licensing transaction, to the exclusion of all other terms and conditions, written or verbal, express or implied (including any terms contained in any purchase order, acknowledgment, check endorsement or other writing prepared by you). In the event of any conflict between your obligations established by these terms and conditions and those established by CCC's Billing and Payment terms and conditions, these terms and conditions shall control.

JURISDICTION

This license transaction shall be governed by and construed in accordance with the laws of the District of Columbia. You hereby agree to submit to the jurisdiction of the courts located in the District of Columbia for purposes of resolving any disputes that may arise in connection with this licensing transaction.

LIMITED LICENSE

The following terms and conditions apply to specific license types:

Translation

This permission is granted for non-exclusive world English rights only unless your license was granted for translation rights. If you licensed translation rights you may only translate this content into the languages you requested. A professional translator must perform all translations and reproduce the content word for word preserving the integrity of the article.

Intranet

If the licensed material is being posted on an Intranet, the Intranet is to be password-protected and made available only to bona fide students or employees only. All content posted to the Intranet must maintain the copyright information line on the bottom of each image. You must also fully reference the material and include a hypertext link as specified above.

Copies of Whole Articles

All copies of whole articles must maintain, if available, the copyright information line on the bottom of each page.

Other Conditions

v1.2

Gratis licenses (referencing $0 in the Total field) are free. Please retain this printable license for your reference. No payment is required.

If you would like to pay for this license now, please remit this license along with yourpayment made payable to "COPYRIGHT CLEARANCE CENTER" otherwise you will be invoiced within 48 hours of the license date. Payment should be in the form of a check or money order referencing your account number and this invoice number {Invoice Number}. Once you receive your invoice for this order, you may pay your invoice by credit card. Please follow instructions provided at that time.

Make Payment To:

Copyright Clearance Center

Dept 001

P.O. Box 843006

Boston, MA 02284-3006

For suggestions or comments regarding this order, contact Rightslink Customer Support: customercare@copyright.com or +1-855-239-3415 (toll free in the US) or +1-978-646-2777.

Questions? customercare@copyright.com or +1-855-239-3415 (toll free in the US) or +1-978-646-2777.

JOHN WILEY AND SONS LICENSE TERMS AND CONDITIONS

Apr 12, 2016

This Agreement between Gabriel C Graffius ("You") and John Wiley and Sons ("John Wiley and Sons") consists of your license details and the terms and conditions provided by John Wiley and Sons and Copyright Clearance Center.

License Number	3846480575783
License date	Apr 12, 2016
Licensed Content Publisher	John Wiley and Sons
Licensed Content Publication	Chemistry - A European Journal
Licensed Content Title	Hydrogen Bonding of Water Confined in Mesoporous Silica MCM-41 and SBA-15 Studied by 1H Solid-State NMR
Licensed Content Author	Bob Grünberg,Thomas Emmler,Egbert Gedat,Ilja Shenderovich,Gerhard H. Findenegg,Hans-Heinrich Limbach,Gerd Buntkowsky
Licensed Content Date	Oct 7, 2004
Pages	8
Type of use	Dissertation/Thesis
Requestor type	University/Academic
Format	Print and electronic
Portion	Figure/table
Number of figures/tables	1
Original Wiley figure/table number(s)	Figure 1
Will you be translating?	No
Title of your thesis / dissertation	Functionalization of Metal Oxide Surfaces through Chemical Reactions and Physical Adsorption
Expected completion date	Apr 2016
Expected size (number of pages)	170
Requestor Location	Gabriel C Graffius 77 Claridge Pl COLONIA, NJ 07067 United States Attn: Gabriel C Graffius
Billing Type	Invoice
Billing Address	Gabriel C Graffius 77 Claridge Pl COLONIA, NJ 07067

United States
Attn: Gabriel C Graffius

Total 0.00 USD

Terms and Conditions

TERMS AND CONDITIONS

This copyrighted material is owned by or exclusively licensed to John Wiley & Sons, Inc. or one of its group companies (each a"Wiley Company") or handled on behalf of a society with which a Wiley Company has exclusive publishing rights in relation to a particular work (collectively "WILEY"). By clicking "accept" in connection with completing this licensing transaction, you agree that the following terms and conditions apply to this transaction (along with the billing and payment terms and conditions established by the Copyright Clearance Center Inc., ("CCC's Billing and Payment terms and conditions"), at the time that you opened your RightsLink account (these are available at any time at http://myaccount.copyright.com).

Terms and Conditions

- The materials you have requested permission to reproduce or reuse (the "Wiley Materials") are protected by copyright.

- You are hereby granted a personal, non-exclusive, non-sub licensable (on a stand-alone basis), non-transferable, worldwide, limited license to reproduce the Wiley Materials for the purpose specified in the licensing process. This license, **and any CONTENT (PDF or image file) purchased as part of your order,** is for a one-time use only and limited to any maximum distribution number specified in the license. The first instance of republication or reuse granted by this license must be completed within two years of the date of the grant of this license (although copies prepared before the end date may be distributed thereafter). The Wiley Materials shall not be used in any other manner or for any other purpose, beyond what is granted in the license. Permission is granted subject to an appropriate acknowledgement given to the author, title of the material/book/journal and the publisher. You shall also duplicate the copyright notice that appears in the Wiley publication in your use of the Wiley Material. Permission is also granted on the understanding that nowhere in the text is a previously published source acknowledged for all or part of this Wiley Material. Any third party content is expressly excluded from this permission.

- With respect to the Wiley Materials, all rights are reserved. Except as expressly granted by the terms of the license, no part of the Wiley Materials may be copied, modified, adapted (except for minor reformatting required by the new Publication), translated, reproduced, transferred or distributed, in any form or by any means, and no derivative works may be made based on the Wiley Materials without the prior permission of the respective copyright owner.**For STM Signatory Publishers clearing permission under the terms of the STM Permissions Guidelines only, the terms of the license are extended to include subsequent editions and for editions in other languages, provided such editions are for the work as a whole in situ and does not involve the separate exploitation of the permitted figures or extracts,** You may not alter, remove or suppress in any manner any copyright, trademark or other notices displayed by the Wiley Materials. You may not license, rent, sell, loan, lease, pledge, offer as security, transfer or assign the Wiley Materials on a stand-alone basis, or any of the rights granted to you hereunder to any other person.

- The Wiley Materials and all of the intellectual property rights therein shall at all times remain the exclusive property of John Wiley & Sons Inc, the Wiley Companies, or their respective licensors, and your interest therein is only that of having possession of and the right to reproduce the Wiley Materials pursuant to Section 2 herein during the continuance of this Agreement. You agree that you own no right, title or interest in or to the Wiley Materials or any of the intellectual property rights therein. You shall have no rights hereunder other than the license as provided for above in Section 2. No right, license or interest to any trademark, trade name, service mark or other branding ("Marks") of WILEY or its licensors is granted hereunder, and you agree that you shall not assert any such right, license or interest with respect thereto

- NEITHER WILEY NOR ITS LICENSORS MAKES ANY WARRANTY OR REPRESENTATION OF ANY KIND TO YOU OR ANY THIRD PARTY, EXPRESS, IMPLIED OR STATUTORY, WITH RESPECT TO THE MATERIALS OR THE ACCURACY OF ANY INFORMATION CONTAINED IN THE MATERIALS, INCLUDING, WITHOUT LIMITATION, ANY IMPLIED WARRANTY OF MERCHANTABILITY, ACCURACY, SATISFACTORY QUALITY, FITNESS FOR A PARTICULAR PURPOSE, USABILITY, INTEGRATION OR NON-INFRINGEMENT AND ALL SUCH WARRANTIES ARE HEREBY EXCLUDED BY WILEY AND ITS LICENSORS AND WAIVED BY YOU.

- WILEY shall have the right to terminate this Agreement immediately upon breach of this Agreement by you.

- You shall indemnify, defend and hold harmless WILEY, its Licensors and their respective directors, officers, agents and employees, from and against any actual or threatened claims, demands, causes of action or proceedings arising from any breach of this Agreement by you.

- IN NO EVENT SHALL WILEY OR ITS LICENSORS BE LIABLE TO YOU OR ANY OTHER PARTY OR ANY OTHER PERSON OR ENTITY FOR ANY SPECIAL, CONSEQUENTIAL, INCIDENTAL, INDIRECT, EXEMPLARY OR PUNITIVE DAMAGES, HOWEVER CAUSED, ARISING OUT OF OR IN CONNECTION WITH THE DOWNLOADING, PROVISIONING, VIEWING OR USE OF THE MATERIALS REGARDLESS OF THE FORM OF ACTION, WHETHER FOR BREACH OF CONTRACT, BREACH OF WARRANTY, TORT, NEGLIGENCE, INFRINGEMENT OR OTHERWISE (INCLUDING, WITHOUT LIMITATION, DAMAGES BASED ON LOSS OF PROFITS, DATA, FILES, USE, BUSINESS OPPORTUNITY OR CLAIMS OF THIRD PARTIES), AND WHETHER OR NOT THE PARTY HAS BEEN ADVISED OF THE POSSIBILITY OF SUCH DAMAGES. THIS LIMITATION SHALL APPLY NOTWITHSTANDING ANY FAILURE OF ESSENTIAL PURPOSE OF ANY LIMITED REMEDY PROVIDED HEREIN.

- Should any provision of this Agreement be held by a court of competent jurisdiction to be illegal, invalid, or unenforceable, that provision shall be deemed amended to achieve as nearly as possible the same economic effect as the original provision, and the legality, validity and enforceability of the remaining provisions of this Agreement

shall not be affected or impaired thereby.

- The failure of either party to enforce any term or condition of this Agreement shall not constitute a waiver of either party's right to enforce each and every term and condition of this Agreement. No breach under this agreement shall be deemed waived or excused by either party unless such waiver or consent is in writing signed by the party granting such waiver or consent. The waiver by or consent of a party to a breach of any provision of this Agreement shall not operate or be construed as a waiver of or consent to any other or subsequent breach by such other party.

- This Agreement may not be assigned (including by operation of law or otherwise) by you without WILEY's prior written consent.

- Any fee required for this permission shall be non-refundable after thirty (30) days from receipt by the CCC.

- These terms and conditions together with CCC's Billing and Payment terms and conditions (which are incorporated herein) form the entire agreement between you and WILEY concerning this licensing transaction and (in the absence of fraud) supersedes all prior agreements and representations of the parties, oral or written. This Agreement may not be amended except in writing signed by both parties. This Agreement shall be binding upon and inure to the benefit of the parties' successors, legal representatives, and authorized assigns.

- In the event of any conflict between your obligations established by these terms and conditions and those established by CCC's Billing and Payment terms and conditions, these terms and conditions shall prevail.

- WILEY expressly reserves all rights not specifically granted in the combination of (i) the license details provided by you and accepted in the course of this licensing transaction, (ii) these terms and conditions and (iii) CCC's Billing and Payment terms and conditions.

- This Agreement will be void if the Type of Use, Format, Circulation, or Requestor Type was misrepresented during the licensing process.

- This Agreement shall be governed by and construed in accordance with the laws of the State of New York, USA, without regards to such state's conflict of law rules. Any legal action, suit or proceeding arising out of or relating to these Terms and Conditions or the breach thereof shall be instituted in a court of competent jurisdiction in New York County in the State of New York in the United States of America and each party hereby consents and submits to the personal jurisdiction of such court, waives any objection to venue in such court and consents to service of process by registered or certified mail, return receipt requested, at the last known address of such party.

WILEY OPEN ACCESS TERMS AND CONDITIONS

Wiley Publishes Open Access Articles in fully Open Access Journals and in Subscription journals offering Online Open. Although most of the fully Open Access journals publish open access articles under the terms of the Creative Commons Attribution (CC BY) License only, the subscription journals and a few of the Open Access Journals offer a choice of

Creative Commons Licenses. The license type is clearly identified on the article.

The Creative Commons Attribution License

The Creative Commons Attribution License (CC-BY) allows users to copy, distribute and transmit an article, adapt the article and make commercial use of the article. The CC-BY license permits commercial and non-

Creative Commons Attribution Non-Commercial License

The Creative Commons Attribution Non-Commercial (CC-BY-NC)License permits use, distribution and reproduction in any medium, provided the original work is properly cited and is not used for commercial purposes.(see below)

Creative Commons Attribution-Non-Commercial-NoDerivs License

The Creative Commons Attribution Non-Commercial-NoDerivs License (CC-BY-NC-ND) permits use, distribution and reproduction in any medium, provided the original work is properly cited, is not used for commercial purposes and no modifications or adaptations are made. (see below)

Use by commercial "for-profit" organizations

Use of Wiley Open Access articles for commercial, promotional, or marketing purposes requires further explicit permission from Wiley and will be subject to a fee.
Further details can be found on Wiley Online Library
http://olabout.wiley.com/WileyCDA/Section/id-410895.html

Other Terms and Conditions:

v1.10 Last updated September 2015

Questions? customercare@copyright.com or +1-855-239-3415 (toll free in the US) or +1-978-646-2777.

SPRINGER LICENSE
TERMS AND CONDITIONS

Apr 12, 2016

This is a License Agreement between Gabriel C Graffius ("You") and Springer ("Springer") provided by Copyright Clearance Center ("CCC"). The license consists of your order details, the terms and conditions provided by Springer, and the payment terms and conditions.

All payments must be made in full to CCC. For payment instructions, please see information listed at the bottom of this form.

License Number	3846500821536
License date	Apr 12, 2016
Licensed content publisher	Springer
Licensed content publication	Springer eBook
Licensed content title	Adsorption Mechanism
Licensed content author	S. Lowell
Licensed content date	Jan 1, 2004
Type of Use	Thesis/Dissertation
Portion	Figures/tables/illustrations
Number of figures/tables/illustrations	1
Author of this Springer article	No
Order reference number	None
Original figure numbers	Figure 4.8
Title of your thesis / dissertation	Functionalization of Metal Oxide Surfaces through Chemical Reactions and Physical Adsorption
Expected completion date	Apr 2016
Estimated size(pages)	170
Total	0.00 USD
Terms and Conditions	

Introduction

The publisher for this copyrighted material is Springer. By clicking "accept" in connection with completing this licensing transaction, you agree that the following terms and conditions apply to this transaction (along with the Billing and Payment terms and conditions established by Copyright Clearance Center, Inc. ("CCC"), at the time that you opened your Rightslink account and that are available at any time at http://myaccount.copyright.com).

Limited License

With reference to your request to reuse material on which Springer controls the copyright, permission is granted for the use indicated in your enquiry under the following conditions:

- Licenses are for one-time use only with a maximum distribution equal to the number stated in your request.

- Springer material represents original material which does not carry references to other sources. If the material in question appears with a credit to another source, this permission is not valid and authorization has to be obtained from the original copyright holder.
- This permission
• is non-exclusive
• is only valid if no personal rights, trademarks, or competitive products are infringed.
• explicitly excludes the right for derivatives.
- Springer does not supply original artwork or content.
- According to the format which you have selected, the following conditions apply accordingly:
• **Print and Electronic:** This License include use in electronic form provided it is password protected, on intranet, or CD-Rom/DVD or E-book/E-journal. It may not be republished in electronic open access.
• **Print:** This License excludes use in electronic form.
• **Electronic:** This License only pertains to use in electronic form provided it is password protected, on intranet, or CD-Rom/DVD or E-book/E-journal. It may not be republished in electronic open access.
For any electronic use not mentioned, please contact Springer at permissions.springer@spi-global.com.
- Although Springer controls the copyright to the material and is entitled to negotiate on rights, this license is only valid subject to courtesy information to the author (address is given in the article/chapter).
- If you are an STM Signatory or your work will be published by an STM Signatory and you are requesting to reuse figures/tables/illustrations or single text extracts, permission is granted according to STM Permissions Guidelines: http://www.stm-assoc.org/permissions-guidelines/
For any electronic use not mentioned in the Guidelines, please contact Springer at permissions.springer@spi-global.com. If you request to reuse more content than stipulated in the STM Permissions Guidelines, you will be charged a permission fee for the excess content.
Permission is valid upon payment of the fee as indicated in the licensing process. If permission is granted free of charge on this occasion, that does not prejudice any rights we might have to charge for reproduction of our copyrighted material in the future.
-If your request is for reuse in a Thesis, permission is granted free of charge under the following conditions:
This license is valid for one-time use only for the purpose of defending your thesis and with a maximum of 100 extra copies in paper. If the thesis is going to be published, permission needs to be reobtained.
- includes use in an electronic form, provided it is an author-created version of the thesis on his/her own website and his/her university's repository, including UMI (according to the definition on the Sherpa website: http://www.sherpa.ac.uk/romeo/);
- is subject to courtesy information to the co-author or corresponding author.
Geographic Rights: Scope
Licenses may be exercised anywhere in the world.
Altering/Modifying Material: Not Permitted
Figures, tables, and illustrations may be altered minimally to serve your work. You may not alter or modify text in any manner. Abbreviations, additions, deletions and/or any other alterations shall be made only with prior written authorization of the author(s).
Reservation of Rights
Springer reserves all rights not specifically granted in the combination of (i) the license

details provided by you and accepted in the course of this licensing transaction and (ii) these terms and conditions and (iii) CCC's Billing and Payment terms and conditions.

License Contingent on Payment

While you may exercise the rights licensed immediately upon issuance of the license at the end of the licensing process for the transaction, provided that you have disclosed complete and accurate details of your proposed use, no license is finally effective unless and until full payment is received from you (either by Springer or by CCC) as provided in CCC's Billing and Payment terms and conditions. If full payment is not received by the date due, then any license preliminarily granted shall be deemed automatically revoked and shall be void as if never granted. Further, in the event that you breach any of these terms and conditions or any of CCC's Billing and Payment terms and conditions, the license is automatically revoked and shall be void as if never granted. Use of materials as described in a revoked license, as well as any use of the materials beyond the scope of an unrevoked license, may constitute copyright infringement and Springer reserves the right to take any and all action to protect its copyright in the materials.

Copyright Notice: Disclaimer

You must include the following copyright and permission notice in connection with any reproduction of the licensed material:

"Springer book/journal title, chapter/article title, volume, year of publication, page, name(s) of author(s), (original copyright notice as given in the publication in which the material was originally published) "With permission of Springer"

In case of use of a graph or illustration, the caption of the graph or illustration must be included, as it is indicated in the original publication.

Warranties: None

Springer makes no representations or warranties with respect to the licensed material and adopts on its own behalf the limitations and disclaimers established by CCC on its behalf in its Billing and Payment terms and conditions for this licensing transaction.

Indemnity

You hereby indemnify and agree to hold harmless Springer and CCC, and their respective officers, directors, employees and agents, from and against any and all claims arising out of your use of the licensed material other than as specifically authorized pursuant to this license.

No Transfer of License

This license is personal to you and may not be sublicensed, assigned, or transferred by you without Springer's written permission.

No Amendment Except in Writing

This license may not be amended except in a writing signed by both parties (or, in the case of Springer, by CCC on Springer's behalf).

Objection to Contrary Terms

Springer hereby objects to any terms contained in any purchase order, acknowledgment, check endorsement or other writing prepared by you, which terms are inconsistent with these terms and conditions or CCC's Billing and Payment terms and conditions. These terms and conditions, together with CCC's Billing and Payment terms and conditions (which are incorporated herein), comprise the entire agreement between you and Springer (and CCC) concerning this licensing transaction. In the event of any conflict between your obligations established by these terms and conditions and those established by CCC's Billing and Payment terms and conditions, these terms and conditions shall control.

Jurisdiction

All disputes that may arise in connection with this present License, or the breach thereof, shall be settled exclusively by arbitration, to be held in the Federal Republic of Germany, in

accordance with German law.

Other conditions:

V 12AUG2015

SPRINGER LICENSE
TERMS AND CONDITIONS

Apr 12, 2016

This is a License Agreement between Gabriel C Graffius ("You") and Springer ("Springer") provided by Copyright Clearance Center ("CCC"). The license consists of your order details, the terms and conditions provided by Springer, and the payment terms and conditions.

All payments must be made in full to CCC. For payment instructions, please see information listed at the bottom of this form.

License Number	3846490543097
License date	Apr 12, 2016
Licensed content publisher	Springer
Licensed content publication	Springer eBook
Licensed content title	Adsorption Isotherms
Licensed content author	S. Lowell
Licensed content date	Jan 1, 2004
Type of Use	Thesis/Dissertation
Portion	Figures/tables/illustrations
Number of figures/tables/illustrations	1
Author of this Springer article	No
Order reference number	None
Original figure numbers	Figure 3.2
Title of your thesis / dissertation	Functionalization of Metal Oxide Surfaces through Chemical Reactions and Physical Adsorption
Expected completion date	Apr 2016
Estimated size(pages)	170
Total	0.00 USD
Terms and Conditions	

Introduction

The publisher for this copyrighted material is Springer. By clicking "accept" in connection with completing this licensing transaction, you agree that the following terms and conditions apply to this transaction (along with the Billing and Payment terms and conditions established by Copyright Clearance Center, Inc. ("CCC"), at the time that you opened your Rightslink account and that are available at any time at http://myaccount.copyright.com).

Limited License

With reference to your request to reuse material on which Springer controls the copyright, permission is granted for the use indicated in your enquiry under the following conditions:

- Licenses are for one-time use only with a maximum distribution equal to the number stated in your request.

- Springer material represents original material which does not carry references to other sources. If the material in question appears with a credit to another source, this permission is not valid and authorization has to be obtained from the original copyright holder.
- This permission
• is non-exclusive
• is only valid if no personal rights, trademarks, or competitive products are infringed.
• explicitly excludes the right for derivatives.
- Springer does not supply original artwork or content.
- According to the format which you have selected, the following conditions apply accordingly:
• **Print and Electronic:** This License include use in electronic form provided it is password protected, on intranet, or CD-Rom/DVD or E-book/E-journal. It may not be republished in electronic open access.
• **Print:** This License excludes use in electronic form.
• **Electronic:** This License only pertains to use in electronic form provided it is password protected, on intranet, or CD-Rom/DVD or E-book/E-journal. It may not be republished in electronic open access.
For any electronic use not mentioned, please contact Springer at permissions.springer@spi-global.com.
- Although Springer controls the copyright to the material and is entitled to negotiate on rights, this license is only valid subject to courtesy information to the author (address is given in the article/chapter).
- If you are an STM Signatory or your work will be published by an STM Signatory and you are requesting to reuse figures/tables/illustrations or single text extracts, permission is granted according to STM Permissions Guidelines: http://www.stm-assoc.org/permissions-guidelines/
For any electronic use not mentioned in the Guidelines, please contact Springer at permissions.springer@spi-global.com. If you request to reuse more content than stipulated in the STM Permissions Guidelines, you will be charged a permission fee for the excess content.
Permission is valid upon payment of the fee as indicated in the licensing process. If permission is granted free of charge on this occasion, that does not prejudice any rights we might have to charge for reproduction of our copyrighted material in the future.
-If your request is for reuse in a Thesis, permission is granted free of charge under the following conditions:
This license is valid for one-time use only for the purpose of defending your thesis and with a maximum of 100 extra copies in paper. If the thesis is going to be published, permission needs to be reobtained.
- includes use in an electronic form, provided it is an author-created version of the thesis on his/her own website and his/her university's repository, including UMI (according to the definition on the Sherpa website: http://www.sherpa.ac.uk/romeo/);
- is subject to courtesy information to the co-author or corresponding author.
Geographic Rights: Scope
Licenses may be exercised anywhere in the world.
Altering/Modifying Material: Not Permitted
Figures, tables, and illustrations may be altered minimally to serve your work. You may not alter or modify text in any manner. Abbreviations, additions, deletions and/or any other alterations shall be made only with prior written authorization of the author(s).
Reservation of Rights
Springer reserves all rights not specifically granted in the combination of (i) the license

details provided by you and accepted in the course of this licensing transaction and (ii) these terms and conditions and (iii) CCC's Billing and Payment terms and conditions.

License Contingent on Payment

While you may exercise the rights licensed immediately upon issuance of the license at the end of the licensing process for the transaction, provided that you have disclosed complete and accurate details of your proposed use, no license is finally effective unless and until full payment is received from you (either by Springer or by CCC) as provided in CCC's Billing and Payment terms and conditions. If full payment is not received by the date due, then any license preliminarily granted shall be deemed automatically revoked and shall be void as if never granted. Further, in the event that you breach any of these terms and conditions or any of CCC's Billing and Payment terms and conditions, the license is automatically revoked and shall be void as if never granted. Use of materials as described in a revoked license, as well as any use of the materials beyond the scope of an unrevoked license, may constitute copyright infringement and Springer reserves the right to take any and all action to protect its copyright in the materials.

Copyright Notice: Disclaimer

You must include the following copyright and permission notice in connection with any reproduction of the licensed material:

"Springer book/journal title, chapter/article title, volume, year of publication, page, name(s) of author(s), (original copyright notice as given in the publication in which the material was originally published) "With permission of Springer"

In case of use of a graph or illustration, the caption of the graph or illustration must be included, as it is indicated in the original publication.

Warranties: None

Springer makes no representations or warranties with respect to the licensed material and adopts on its own behalf the limitations and disclaimers established by CCC on its behalf in its Billing and Payment terms and conditions for this licensing transaction.

Indemnity

You hereby indemnify and agree to hold harmless Springer and CCC, and their respective officers, directors, employees and agents, from and against any and all claims arising out of your use of the licensed material other than as specifically authorized pursuant to this license.

No Transfer of License

This license is personal to you and may not be sublicensed, assigned, or transferred by you without Springer's written permission.

No Amendment Except in Writing

This license may not be amended except in a writing signed by both parties (or, in the case of Springer, by CCC on Springer's behalf).

Objection to Contrary Terms

Springer hereby objects to any terms contained in any purchase order, acknowledgment, check endorsement or other writing prepared by you, which terms are inconsistent with these terms and conditions or CCC's Billing and Payment terms and conditions. These terms and conditions, together with CCC's Billing and Payment terms and conditions (which are incorporated herein), comprise the entire agreement between you and Springer (and CCC) concerning this licensing transaction. In the event of any conflict between your obligations established by these terms and conditions and those established by CCC's Billing and Payment terms and conditions, these terms and conditions shall control.

Jurisdiction

All disputes that may arise in connection with this present License, or the breach thereof, shall be settled exclusively by arbitration, to be held in the Federal Republic of Germany, in

accordance with German law.

Other conditions:

V 12AUG2015

ROYAL SOCIETY OF CHEMISTRY LICENSE TERMS AND CONDITIONS

Apr 12, 2016

This Agreement between Gabriel C Graffius ("You") and Royal Society of Chemistry ("Royal Society of Chemistry") consists of your license details and the terms and conditions provided by Royal Society of Chemistry and Copyright Clearance Center.

License Number	3846471009746
License date	Apr 12, 2016
Licensed Content Publisher	Royal Society of Chemistry
Licensed Content Publication	Chemical Society Reviews
Licensed Content Title	Mesoporous materials and electrochemistry
Licensed Content Author	Alain Walcarius
Licensed Content Date	Jan 18, 2013
Licensed Content Volume Number	42
Licensed Content Issue Number	9
Type of Use	Thesis/Dissertation
Requestor type	academic/educational
Portion	figures/tables/images
Number of figures/tables/images	1
Format	print and electronic
Distribution quantity	5
Will you be translating?	no
Order reference number	None
Title of the thesis/dissertation	Functionalization of Metal Oxide Surfaces Through Chemical Reactions and Physical Adsorption
Expected completion date	Apr 2016
Estimated size	170
Requestor Location	Gabriel C Graffius 77 Claridge Pl COLONIA, NJ 07067 United States Attn: Gabriel C Graffius
Billing Type	Invoice
Billing Address	Gabriel C Graffius 77 Claridge Pl

COLONIA, NJ 07067
United States
Attn: Gabriel C Graffius

Total 0.00 USD

Terms and Conditions

This License Agreement is between {Requestor Name} ("You") and The Royal Society of Chemistry ("RSC") provided by the Copyright Clearance Center ("CCC"). The license consists of your order details, the terms and conditions provided by the Royal Society of Chemistry, and the payment terms and conditions.

RSC / TERMS AND CONDITIONS

INTRODUCTION

The publisher for this copyrighted material is The Royal Society of Chemistry. By clicking "accept" in connection with completing this licensing transaction, you agree that the following terms and conditions apply to this transaction (along with the Billing and Payment terms and conditions established by CCC, at the time that you opened your RightsLink account and that are available at any time at .

LICENSE GRANTED

The RSC hereby grants you a non-exclusive license to use the aforementioned material anywhere in the world subject to the terms and conditions indicated herein. Reproduction of the material is confined to the purpose and/or media for which permission is hereby given.

RESERVATION OF RIGHTS

The RSC reserves all rights not specifically granted in the combination of (i) the license details provided by your and accepted in the course of this licensing transaction; (ii) these terms and conditions; and (iii) CCC's Billing and Payment terms and conditions.

REVOCATION

The RSC reserves the right to revoke this license for any reason, including, but not limited to, advertising and promotional uses of RSC content, third party usage, and incorrect source figure attribution.

THIRD-PARTY MATERIAL DISCLAIMER

If part of the material to be used (for example, a figure) has appeared in the RSC publication with credit to another source, permission must also be sought from that source. If the other source is another RSC publication these details should be included in your RightsLink request. If the other source is a third party, permission must be obtained from the third party. The RSC disclaims any responsibility for the reproduction you make of items owned by a third party.

PAYMENT OF FEE

If the permission fee for the requested material is waived in this instance, please be advised that any future requests for the reproduction of RSC materials may attract a fee.

ACKNOWLEDGEMENT

The reproduction of the licensed material must be accompanied by the following acknowledgement:

Reproduced ("Adapted" or "in part") from {Reference Citation} (or Ref XX) with permission of The Royal Society of Chemistry.

If the licensed material is being reproduced from New Journal of Chemistry (NJC), Photochemical & Photobiological Sciences (PPS) or Physical Chemistry Chemical Physics (PCCP) you must include one of the following acknowledgements:

For figures originally published in NJC:

Reproduced ("Adapted" or "in part") from {Reference Citation} (or Ref XX) with permission of The Royal Society of Chemistry (RSC) on behalf of the European Society for Photobiology, the European Photochemistry Association and the RSC.

For figures originally published in PPS:
Reproduced ("Adapted" or "in part") from {Reference Citation} (or Ref XX) with permission of The Royal Society of Chemistry (RSC) on behalf of the Centre National de la Recherche Scientifique (CNRS) and the RSC.
For figures originally published in PCCP:
Reproduced ("Adapted" or "in part") from {Reference Citation} (or Ref XX) with permission of the PCCP Owner Societies.

HYPERTEXT LINKS

With any material which is being reproduced in electronic form, you must include a hypertext link to the original RSC article on the RSC's website. The recommended form for the hyperlink is http://dx.doi.org/10.1039/DOI suffix, for example in the link http://dx.doi.org/10.1039/b110420a the DOI suffix is 'b110420a'. To find the relevant DOI suffix for the RSC article in question, go to the Journals section of the website and locate the article in the list of papers for the volume and issue of your specific journal. You will find the DOI suffix quoted there.

LICENSE CONTINGENT ON PAYMENT

While you may exercise the rights licensed immediately upon issuance of the license at the end of the licensing process for the transaction, provided that you have disclosed complete and accurate details of your proposed use, no license is finally effective unless and until full payment is received from you (by CCC) as provided in CCC's Billing and Payment terms and conditions. If full payment is not received on a timely basis, then any license preliminarily granted shall be deemed automatically revoked and shall be void as if never granted. Further, in the event that you breach any of these terms and conditions or any of CCC's Billing and Payment terms and conditions, the license is automatically revoked and shall be void as if never granted. Use of materials as described in a revoked license, as well as any use of the materials beyond the scope of an unrevoked license, may constitute copyright infringement and the RSC reserves the right to take any and all action to protect its copyright in the materials.

WARRANTIES

The RSC makes no representations or warranties with respect to the licensed material.

INDEMNITY

You hereby indemnify and agree to hold harmless the RSC and the CCC, and their respective officers, directors, trustees, employees and agents, from and against any and all claims arising out of your use of the licensed material other than as specifically authorized pursuant to this licence.

NO TRANSFER OF LICENSE

This license is personal to you or your publisher and may not be sublicensed, assigned, or transferred by you to any other person without the RSC's written permission.

NO AMENDMENT EXCEPT IN WRITING

This license may not be amended except in a writing signed by both parties (or, in the case of "Other Conditions, v1.2", by CCC on the RSC's behalf).

OBJECTION TO CONTRARY TERMS

You hereby acknowledge and agree that these terms and conditions, together with CCC's Billing and Payment terms and conditions (which are incorporated herein), comprise the entire agreement between you and the RSC (and CCC) concerning this licensing transaction, to the exclusion of all other terms and conditions, written or verbal, express or implied (including any terms contained in any purchase order, acknowledgment, check endorsement or other writing prepared by you). In the event of any conflict between your obligations established by these terms and conditions and those established by CCC's Billing and Payment terms and conditions, these terms and conditions shall control.

JURISDICTION

This license transaction shall be governed by and construed in accordance with the laws of the District of Columbia. You hereby agree to submit to the jurisdiction of the courts located in the District of Columbia for purposes of resolving any disputes that may arise in connection with this licensing transaction.

LIMITED LICENSE

The following terms and conditions apply to specific license types:

Translation

This permission is granted for non-exclusive world English rights only unless your license was granted for translation rights. If you licensed translation rights you may only translate this content into the languages you requested. A professional translator must perform all translations and reproduce the content word for word preserving the integrity of the article.

Intranet

If the licensed material is being posted on an Intranet, the Intranet is to be password-protected and made available only to bona fide students or employees only. All content posted to the Intranet must maintain the copyright information line on the bottom of each image. You must also fully reference the material and include a hypertext link as specified above.

Copies of Whole Articles

All copies of whole articles must maintain, if available, the copyright information line on the bottom of each page.

Other Conditions

v1.2

Gratis licenses (referencing $0 in the Total field) are free. Please retain this printable license for your reference. No payment is required.

If you would like to pay for this license now, please remit this license along with yourpayment made payable to "COPYRIGHT CLEARANCE CENTER" otherwise you will be invoiced within 48 hours of the license date. Payment should be in the form of a check or money order referencing your account number and this invoice number {Invoice Number}. Once you receive your invoice for this order, you may pay your invoice by credit card. Please follow instructions provided at that time.

Make Payment To:

Copyright Clearance Center

Dept 001

P.O. Box 843006

Boston, MA 02284-3006

For suggestions or comments regarding this order, contact Rightslink Customer Support: customercare@copyright.com or +1-855-239-3415 (toll free in the US) or +1-978-646-2777.

Questions? customercare@copyright.com or +1-855-239-3415 (toll free in the US) or +1-978-646-2777.

ELSEVIER LICENSE
TERMS AND CONDITIONS

Apr 14, 2016

This is a License Agreement between Gabriel C Graffius ("You") and Elsevier ("Elsevier") provided by Copyright Clearance Center ("CCC"). The license consists of your order details, the terms and conditions provided by Elsevier, and the payment terms and conditions.

All payments must be made in full to CCC. For payment instructions, please see information listed at the bottom of this form.

Supplier	Elsevier Limited The Boulevard,Langford Lane Kidlington,Oxford,OX5 1GB,UK
Registered Company Number	1982084
Customer name	Gabriel C Graffius
Customer address	77 Claridge Pl COLONIA, NJ 07067
License number	3847731013351
License date	Apr 14, 2016
Licensed content publisher	Elsevier
Licensed content publication	Journal of Chromatography A
Licensed content title	Critical assessment of particle size analysis of porous silica microbead high-performance liquid chromatographic packings by photosedimentation
Licensed content author	K.K. Unger,M.G. Gimpel
Licensed content date	28 November 1979
Licensed content volume number	180
Licensed content issue number	1
Number of pages	10
Start Page	93
End Page	102
Type of Use	reuse in a thesis/dissertation
Portion	figures/tables/illustrations
Number of figures/tables/illustrations	1
Format	both print and electronic
Are you the author of this Elsevier article?	No
Will you be translating?	No
Original figure numbers	Figure 4

Title of your thesis/dissertation	Functionalization of Metal Oxide Surfaces through Chemical Reactions and Physical Adsorption
Expected completion date	Apr 2016
Estimated size (number of pages)	170
Elsevier VAT number	GB 494 6272 12
Permissions price	0.00 USD
VAT/Local Sales Tax	0.00 USD / 0.00 GBP
Total	0.00 USD
Terms and Conditions	

INTRODUCTION

1. The publisher for this copyrighted material is Elsevier. By clicking "accept" in connection with completing this licensing transaction, you agree that the following terms and conditions apply to this transaction (along with the Billing and Payment terms and conditions established by Copyright Clearance Center, Inc. ("CCC"), at the time that you opened your Rightslink account and that are available at any time at http://myaccount.copyright.com).

GENERAL TERMS

2. Elsevier hereby grants you permission to reproduce the aforementioned material subject to the terms and conditions indicated.
3. Acknowledgement: If any part of the material to be used (for example, figures) has appeared in our publication with credit or acknowledgement to another source, permission must also be sought from that source. If such permission is not obtained then that material may not be included in your publication/copies. Suitable acknowledgement to the source must be made, either as a footnote or in a reference list at the end of your publication, as follows:
"Reprinted from Publication title, Vol /edition number, Author(s), Title of article / title of chapter, Pages No., Copyright (Year), with permission from Elsevier [OR APPLICABLE SOCIETY COPYRIGHT OWNER]." Also Lancet special credit - "Reprinted from The Lancet, Vol. number, Author(s), Title of article, Pages No., Copyright (Year), with permission from Elsevier."
4. Reproduction of this material is confined to the purpose and/or media for which permission is hereby given.
5. Altering/Modifying Material: Not Permitted. However figures and illustrations may be altered/adapted minimally to serve your work. Any other abbreviations, additions, deletions and/or any other alterations shall be made only with prior written authorization of Elsevier Ltd. (Please contact Elsevier at permissions@elsevier.com)
6. If the permission fee for the requested use of our material is waived in this instance, please be advised that your future requests for Elsevier materials may attract a fee.
7. Reservation of Rights: Publisher reserves all rights not specifically granted in the combination of (i) the license details provided by you and accepted in the course of this licensing transaction, (ii) these terms and conditions and (iii) CCC's Billing and Payment terms and conditions.
8. License Contingent Upon Payment: While you may exercise the rights licensed immediately upon issuance of the license at the end of the licensing process for the transaction, provided that you have disclosed complete and accurate details of your proposed use, no license is finally effective unless and until full payment is received from you (either by publisher or by CCC) as provided in CCC's Billing and Payment terms and conditions. If full payment is not received on a timely basis, then any license preliminarily granted shall be

deemed automatically revoked and shall be void as if never granted. Further, in the event that you breach any of these terms and conditions or any of CCC's Billing and Payment terms and conditions, the license is automatically revoked and shall be void as if never granted. Use of materials as described in a revoked license, as well as any use of the materials beyond the scope of an unrevoked license, may constitute copyright infringement and publisher reserves the right to take any and all action to protect its copyright in the materials.

9. Warranties: Publisher makes no representations or warranties with respect to the licensed material.

10. Indemnity: You hereby indemnify and agree to hold harmless publisher and CCC, and their respective officers, directors, employees and agents, from and against any and all claims arising out of your use of the licensed material other than as specifically authorized pursuant to this license.

11. No Transfer of License: This license is personal to you and may not be sublicensed, assigned, or transferred by you to any other person without publisher's written permission.

12. No Amendment Except in Writing: This license may not be amended except in a writing signed by both parties (or, in the case of publisher, by CCC on publisher's behalf).

13. Objection to Contrary Terms: Publisher hereby objects to any terms contained in any purchase order, acknowledgment, check endorsement or other writing prepared by you, which terms are inconsistent with these terms and conditions or CCC's Billing and Payment terms and conditions. These terms and conditions, together with CCC's Billing and Payment terms and conditions (which are incorporated herein), comprise the entire agreement between you and publisher (and CCC) concerning this licensing transaction. In the event of any conflict between your obligations established by these terms and conditions and those established by CCC's Billing and Payment terms and conditions, these terms and conditions shall control.

14. Revocation: Elsevier or Copyright Clearance Center may deny the permissions described in this License at their sole discretion, for any reason or no reason, with a full refund payable to you. Notice of such denial will be made using the contact information provided by you. Failure to receive such notice will not alter or invalidate the denial. In no event will Elsevier or Copyright Clearance Center be responsible or liable for any costs, expenses or damage incurred by you as a result of a denial of your permission request, other than a refund of the amount(s) paid by you to Elsevier and/or Copyright Clearance Center for denied permissions.

LIMITED LICENSE

The following terms and conditions apply only to specific license types:

15. **Translation**: This permission is granted for non-exclusive world **English** rights only unless your license was granted for translation rights. If you licensed translation rights you may only translate this content into the languages you requested. A professional translator must perform all translations and reproduce the content word for word preserving the integrity of the article.

16. **Posting licensed content on any Website**: The following terms and conditions apply as follows: Licensing material from an Elsevier journal: All content posted to the web site must maintain the copyright information line on the bottom of each image; A hyper-text must be included to the Homepage of the journal from which you are licensing at http://www.sciencedirect.com/science/journal/xxxxx or the Elsevier homepage for books at http://www.elsevier.com; Central Storage: This license does not include permission for a scanned version of the material to be stored in a central repository such as that provided by Heron/XanEdu.

Licensing material from an Elsevier book: A hyper-text link must be included to the Elsevier

homepage at http://www.elsevier.com . All content posted to the web site must maintain the copyright information line on the bottom of each image.

Posting licensed content on Electronic reserve: In addition to the above the following clauses are applicable: The web site must be password-protected and made available only to bona fide students registered on a relevant course. This permission is granted for 1 year only. You may obtain a new license for future website posting.

17. **For journal authors:** the following clauses are applicable in addition to the above:

Preprints:

A preprint is an author's own write-up of research results and analysis, it has not been peer-reviewed, nor has it had any other value added to it by a publisher (such as formatting, copyright, technical enhancement etc.).

Authors can share their preprints anywhere at any time. Preprints should not be added to or enhanced in any way in order to appear more like, or to substitute for, the final versions of articles however authors can update their preprints on arXiv or RePEc with their Accepted Author Manuscript (see below).

If accepted for publication, we encourage authors to link from the preprint to their formal publication via its DOI. Millions of researchers have access to the formal publications on ScienceDirect, and so links will help users to find, access, cite and use the best available version. Please note that Cell Press, The Lancet and some society-owned have different preprint policies. Information on these policies is available on the journal homepage.

Accepted Author Manuscripts: An accepted author manuscript is the manuscript of an article that has been accepted for publication and which typically includes author-incorporated changes suggested during submission, peer review and editor-author communications.

Authors can share their accepted author manuscript:

- immediately
  - via their non-commercial person homepage or blog
  - by updating a preprint in arXiv or RePEc with the accepted manuscript
  - via their research institute or institutional repository for internal institutional uses or as part of an invitation-only research collaboration work-group
  - directly by providing copies to their students or to research collaborators for their personal use
  - for private scholarly sharing as part of an invitation-only work group on commercial sites with which Elsevier has an agreement
- after the embargo period
  - via non-commercial hosting platforms such as their institutional repository
  - via commercial sites with which Elsevier has an agreement

In all cases accepted manuscripts should:

- link to the formal publication via its DOI
- bear a CC-BY-NC-ND license - this is easy to do
- if aggregated with other manuscripts, for example in a repository or other site, be shared in alignment with our hosting policy not be added to or enhanced in any way to appear more like, or to substitute for, the published journal article.

Published journal article (JPA): A published journal article (PJA) is the definitive final record of published research that appears or will appear in the journal and embodies all

value-adding publishing activities including peer review co-ordination, copy-editing, formatting, (if relevant) pagination and online enrichment.
Policies for sharing publishing journal articles differ for subscription and gold open access articles:
Subscription Articles: If you are an author, please share a link to your article rather than the full-text. Millions of researchers have access to the formal publications on ScienceDirect, and so links will help your users to find, access, cite, and use the best available version.
Theses and dissertations which contain embedded PJAs as part of the formal submission can be posted publicly by the awarding institution with DOI links back to the formal publications on ScienceDirect.
If you are affiliated with a library that subscribes to ScienceDirect you have additional private sharing rights for others' research accessed under that agreement. This includes use for classroom teaching and internal training at the institution (including use in course packs and courseware programs), and inclusion of the article for grant funding purposes.
Gold Open Access Articles: May be shared according to the author-selected end-user license and should contain a CrossMark logo, the end user license, and a DOI link to the formal publication on ScienceDirect.
Please refer to Elsevier's posting policy for further information.
18. **For book authors** the following clauses are applicable in addition to the above:
Authors are permitted to place a brief summary of their work online only. You are not allowed to download and post the published electronic version of your chapter, nor may you scan the printed edition to create an electronic version. **Posting to a repository:** Authors are permitted to post a summary of their chapter only in their institution's repository.
19. **Thesis/Dissertation**: If your license is for use in a thesis/dissertation your thesis may be submitted to your institution in either print or electronic form. Should your thesis be published commercially, please reapply for permission. These requirements include permission for the Library and Archives of Canada to supply single copies, on demand, of the complete thesis and include permission for Proquest/UMI to supply single copies, on demand, of the complete thesis. Should your thesis be published commercially, please reapply for permission. Theses and dissertations which contain embedded PJAs as part of the formal submission can be posted publicly by the awarding institution with DOI links back to the formal publications on ScienceDirect.

Elsevier Open Access Terms and Conditions
You can publish open access with Elsevier in hundreds of open access journals or in nearly 2000 established subscription journals that support open access publishing. Permitted third party re-use of these open access articles is defined by the author's choice of Creative Commons user license. See our open access license policy for more information.
Terms & Conditions applicable to all Open Access articles published with Elsevier:
Any reuse of the article must not represent the author as endorsing the adaptation of the article nor should the article be modified in such a way as to damage the author's honour or reputation. If any changes have been made, such changes must be clearly indicated.
The author(s) must be appropriately credited and we ask that you include the end user license and a DOI link to the formal publication on ScienceDirect.
If any part of the material to be used (for example, figures) has appeared in our publication with credit or acknowledgement to another source it is the responsibility of the user to ensure their reuse complies with the terms and conditions determined by the rights holder.
Additional Terms & Conditions applicable to each Creative Commons user license:
CC BY: The CC-BY license allows users to copy, to create extracts, abstracts and new works from the Article, to alter and revise the Article and to make commercial use of the

Article (including reuse and/or resale of the Article by commercial entities), provided the user gives appropriate credit (with a link to the formal publication through the relevant DOI), provides a link to the license, indicates if changes were made and the licensor is not represented as endorsing the use made of the work. The full details of the license are available at http://creativecommons.org/licenses/by/4.0.

CC BY NC SA: The CC BY-NC-SA license allows users to copy, to create extracts, abstracts and new works from the Article, to alter and revise the Article, provided this is not done for commercial purposes, and that the user gives appropriate credit (with a link to the formal publication through the relevant DOI), provides a link to the license, indicates if changes were made and the licensor is not represented as endorsing the use made of the work. Further, any new works must be made available on the same conditions. The full details of the license are available at http://creativecommons.org/licenses/by-nc-sa/4.0.

CC BY NC ND: The CC BY-NC-ND license allows users to copy and distribute the Article, provided this is not done for commercial purposes and further does not permit distribution of the Article if it is changed or edited in any way, and provided the user gives appropriate credit (with a link to the formal publication through the relevant DOI), provides a link to the license, and that the licensor is not represented as endorsing the use made of the work. The full details of the license are available at http://creativecommons.org/licenses/by-nc-nd/4.0.

Any commercial reuse of Open Access articles published with a CC BY NC SA or CC BY NC ND license requires permission from Elsevier and will be subject to a fee.

Commercial reuse includes:

- Associating advertising with the full text of the Article
- Charging fees for document delivery or access
- Article aggregation
- Systematic distribution via e-mail lists or share buttons

Posting or linking by commercial companies for use by customers of those companies.

20. **Other Conditions**:

v1.8

Questions? customercare@copyright.com or +1-855-239-3415 (toll free in the US) or +1-978-646-2777.